

IDENTIFICATION OF GENETIC AND ANTIGENIC VARIATION AND EVOLUTION PATTERN
AMONG INFLUENZA A AND B VIRUSES IN THAILAND



A Dissertation Submitted in Partial Fulfillment of the Requirements
for the Degree of Doctor of Philosophy in Medical Sciences

Common Course

FACULTY OF MEDICINE

Chulalongkorn University

Academic Year 2020

Copyright of Chulalongkorn University

การศึกษาการเปลี่ยนแปลงทางด้านเจเนติกส์และแอนติเจนิค และรูปแบบการวิวัฒนาการของเชื้อ
ไวรัสไข้หวัดใหญ่สายพันธุ์เอและบีในประเทศไทย



วิทยานิพนธ์นี้เป็นส่วนหนึ่งของการศึกษาตามหลักสูตรปริญญาวิทยาศาสตรดุษฎีบัณฑิต
สาขาวิชาวิทยาศาสตร์การแพทย์ ไม่สังกัดภาควิชา/เทียบเท่า
คณะแพทยศาสตร์ จุฬาลงกรณ์มหาวิทยาลัย
ปีการศึกษา 2563
ลิขสิทธิ์ของจุฬาลงกรณ์มหาวิทยาลัย

Thesis Title	IDENTIFICATION OF GENETIC AND ANTIGENIC VARIATION AND EVOLUTION PATTERN AMONG INFLUENZA A AND B VIRUSES IN THAILAND
By	Miss Nungruthai Suntronwong
Field of Study	Medical Sciences
Thesis Advisor	Professor YONG POOVORAWAN, M.D.

Accepted by the FACULTY OF MEDICINE, Chulalongkorn University in Partial Fulfillment of the Requirement for the Doctor of Philosophy

..... Dean of the FACULTY OF MEDICINE

(Professor SUTTIPONG WACHARASINDHU, M.D.)

DISSERTATION COMMITTEE

..... Chairman

(Professor VILAI CHENTANEZ, M.D., Ph.D.)

..... Thesis Advisor

(Professor YONG POOVORAWAN, M.D.)

..... Examiner

(Associate Professor WILAI ANOMASIRI, Ph.D.)

..... Examiner

(Associate Professor SUNCHAI PAYUNGPORN, Ph.D.)

..... External Examiner

(Associate Professor Teeraporn Chinchai, Ph.D.)

จุฬาลงกรณ์มหาวิทยาลัย
CHULALONGKORN UNIVERSITY

หนึ่งฤทัย สุนทรวงค์ : การศึกษาการเปลี่ยนแปลงทางด้านเจเนติกส์และแอนติเจนิก และรูปแบบการวิวัฒนาการของเชื้อไวรัส
ไข้หวัดใหญ่สายพันธุ์เอและบีในประเทศไทย. (IDENTIFICATION OF GENETIC AND ANTIGENIC VARIATION

AND EVOLUTION PATTERN AMONG INFLUENZA A AND B VIRUSES IN THAILAND) อ.ที่ปรึกษาหลัก : ศ. นพ.ยง ภู่วรว
รณ

ไวรัสไข้หวัดใหญ่เป็นสาเหตุสำคัญในการเกิดโรคในระบบทางเดินหายใจ โดยทั่วโลกพบว่ามีอัตราการป่วยเฉลี่ย 3-5 ล้านรายต่อปี การระบาดของเชื้อไวรัสมีผลมาจากหลายปัจจัยร่วมกันได้แก่ ไวรัส,โฮสต์และปัจจัยภายนอกเช่นสภาพภูมิอากาศ ถึงแม้ว่าวัคซีนไข้หวัดใหญ่จะสามารถป้องกันและลดความรุนแรงของการติดเชื้อได้อย่างมีประสิทธิภาพ อย่างไรก็ตามไวรัสไข้หวัดใหญ่มีการเปลี่ยนแปลงอยู่ตลอดเวลา ส่งผลให้มีการเปลี่ยนสายพันธุ์ที่ใช้ในการผลิตวัคซีนในทุก ๆ ปี ดังนั้นในงานวิจัยนี้มีวัตถุประสงค์เพื่อศึกษาปัจจัยทางด้านภูมิอากาศที่ส่งผลกับการระบาดของเชื้อไวรัส,ระดับภูมิคุ้มกัน,การเปลี่ยนแปลงทางด้านเจเนติกส์และแอนติเจนิก และรูปแบบการวิวัฒนาการของเชื้อไวรัสไข้หวัดใหญ่สายพันธุ์เอและบีในประเทศไทย โดยพบว่าในปี 2010-2018 มีผู้ป่วยที่ติดเชื้อไข้หวัดใหญ่คิดเป็น21.6% ของผู้ป่วยของผู้ป่วยที่มีไข้ ประกอบด้วยเชื้อไวรัสสายพันธุ์เอ(H1N1)pdm09 34.2%,เอ(H3N2) 46% และเชื้อไข้หวัดใหญ่สายพันธุ์บี19.8% เชื้อไวรัสไข้หวัดใหญ่ในประเทศไทยมีการระบาดสูงอยู่ 2ช่วง โดยเชื้อไวรัสเอ(H1N1)pdm09 และบีจะมีการระบาดสูงในเดือนกุมภาพันธ์และสิงหาคม ในขณะที่เชื้อไวรัสสายพันธุ์เอ(H3N2) จะมีการระบาดสูงในเดือนสิงหาคมจนถึงกันยายน การเพิ่มขึ้นของการระบาดมักจะมีเกิดในฤดูฝน ในงานวิจัยนี้พบว่าการนำข้อมูลการระบาดกับข้อมูลทางภูมิอากาศได้แก่ อุณหภูมิ ความชื้น และปริมาณน้ำฝนย้อนหลังมาใช้ในโมเดล SARIMA สามารถทำนายการระบาดล่วงหน้าได้อย่างมีประสิทธิภาพ เพื่อศึกษาระดับภูมิคุ้มกันต่อเชื้อไข้หวัดใหญ่ในกลุ่มผู้สูงอายุซึ่งมีความเสี่ยงในการติดเชื้อ พบว่าสัดส่วนของผู้ที่มีแอนติบอดีถึงระดับป้องกัน (HI \geq 40) ต่อเชื้อไวรัสสายพันธุ์เอ(H1N1)pdm09(50%) และเอ(H3N2) (66%) มากกว่าเชื้อไวรัสไข้หวัดใหญ่สายพันธุ์บีซึ่งประกอบด้วยบีYamagata 2 (14%), บีYamagata 3 (21%) และบีVictoria (25%) นอกจากนี้ยังพบว่ามีเพียง 5% ของประชากรที่มีแอนติบอดีถึงระดับป้องกันการติดเชื้อในทุกสายพันธุ์ ซึ่งบ่งบอกถึงผู้สูงอายุมีระดับแอนติบอดีที่ป้องกันในวงกว้างค่อนข้างต่ำ สำหรับการศึกษาศักยภาพไวรัสที่ส่งผลต่อการระบาด เราเลือกศึกษา ยีน polymerase ประกอบด้วย PB2, PB1 และ PA ซึ่งเป็นโปรตีนเป้าหมายของยาด้านไวรัส การเกิดกลายพันธุ์ที่ยีน polymerase ยังส่งผลอย่างมีนัยสำคัญต่อการเพิ่มจำนวนไวรัส,การแพร่กระจายของเชื้อและความรุนแรงของโรค จากการศึกษาพบว่ารูปแบบวิวัฒนาการของเชื้อไข้หวัดใหญ่เอ(H3N2), บีVictoria มีการเปลี่ยนแปลงตามเวลา ในขณะที่เอ(H1N1)pdm09มีการเปลี่ยนที่ค่อนข้างคงที่และบีYamagata มีการเปลี่ยนที่ค่อนข้างเร็วในปี2017 การเปลี่ยนแปลงกรดอะมิโนในตำแหน่งยังมีความสอดคล้องกับการเพิ่มขึ้นและลดลงของรูปแบบวิวัฒนาการ และพบว่ายีน PA มีอัตราการวิวัฒนาการที่ค่อนข้างสูงเมื่อเทียบกับPB2 และ PB1 ยกเว้นเชื้อไวรัสเอ(H3N2)นอกจากนี้การศึกษาการเปลี่ยนแปลงทางด้านเจเนติกส์และแอนติเจนิกของไวรัสจากลำดับนิวคลีโอไทด์ของHA1 และคำนวณประสิทธิภาพของวัคซีนโดยใช้ $P_{epitope}$ โมเดล พบว่าเชื้อไวรัสเอ(H3N2) มีการเกิดกลุ่มย่อย 5 กลุ่มที่แตกต่างกันและเปลี่ยนแปลงไปจากวัคซีนในปี2016-17 ส่งผลให้ประสิทธิภาพของวัคซีนลดลงจาก 74%(2016) เป็น 48% (2017) และในปี2017-20 พบว่ามีการเกิด clade และsubclade ใหม่ของเชื้อเอ(H1N1)pdm09ได้แก่6B.1A1และ 6B.1A5 และเอ(H3N2)มีการระบาดร่วมกันของ 3C.2a1b, 3C.2a2 และ 3C.3a ไวรัส B/Victoria ที่มีการหายไปของกรดอะมิโน 3ตำแหน่งเริ่มระบาดในปี 2019 การเปลี่ยนแปลงกรดอะมิโนในตำแหน่งแอนติเจนิกของเอ(H1N1)pdm09มักเกิดที่เอบี โทป Sa และ Sb, เอ(H3N2) จะเกิดบนเอบี โทป A, B, D และ E และไวรัสบีมักเกิดที่ตำแหน่ง 120 loop และ 190 helix นอกจากนี้ยังพบว่าประสิทธิภาพของวัคซีนต่อเอ(H1N1)pdm09อยู่ในระดับกลาง, ประสิทธิภาพของวัคซีนต่อเอ(H3N2)ต่ำลงในปี 2019(9.17%) และปี 2020 (-18.94%) อย่างมีนัยสำคัญ ในขณะที่วัคซีนบียังคงมีประสิทธิภาพในการป้องกัน นอกจากนี้ HA, NA ก็สามารถกระตุ้นการสร้างภูมิคุ้มกันได้ในช่วงแคบในวัคซีนที่ใช้ปัจจุบันNA มักจะกระตุ้นภูมิคุ้มกันได้ค่อนข้างต่ำ จากการศึกษาพบว่าถ้าเพิ่มความยาวของ stalk โดเมนไป 30กรดอะมิโนสามารถเพิ่มแอนติบอดีต่อ NA และเพิ่มการเกิดantibody-dependent cellular cytotoxicity ในหลอดทดลองได้อย่างมีนัยสำคัญ โดยไม่ส่งผลต่อการสร้างแอนติบอดีต่อ HA นอกจากนี้ยังพบว่าการเพิ่มความยาวของstalk โดเมนของ NA สามารถเพิ่ม immunogenicityและแสดงผลในการป้องกันการติดเชื้อในหลอดทดลองได้อย่างมีนัยสำคัญ กล่าวโดยสรุปงานวิจัยนี้แสดงให้เห็นความสามารถในการพัฒนาโมเดลที่ใช้ในการทำนายการระบาดของเชื้อไข้หวัดใหญ่เพื่อวางแผนการฉีดวัคซีนซึ่งแนะนำให้ฉีดก่อนหน้าฝน การทราบถึงระดับภูมิคุ้มกันต่อเชื้อในกลุ่มประชากรมีประโยชน์ในการแนะนำเกี่ยวกับนโยบายวัคซีน การศึกษาวิจัยแสดงให้เห็นถึงวิวัฒนาการของเชื้อไข้หวัดใหญ่และการเปลี่ยนแปลงไปจากวัคซีนซึ่งสามารถช่วยในการพัฒนาวัคซีนไวรัสและการเลือกใช้สายพันธุ์วัคซีน และการต่อ stalk ของ NA สามารถช่วยในการพัฒนาประสิทธิภาพของวัคซีน

CHULALONGKORN UNIVERSITY

สาขาวิชา วิทยาศาสตร์การแพทย์

ปีการศึกษา 2563

ลายมือชื่อนิสิต

ลายมือชื่อ อ.ที่ปรึกษาหลัก

5874771530 : MAJOR MEDICAL SCIENCES

KEYWORD: INFLUENZA/HEMAGGLUTININ/POLYMERASE/VACCINE EFFECTIVENESS/VIRAL EVOLUTION/CLIMATE FACTORS/FORECASTING
MODEL/NEURAMINIDASE/SEROPROTECTION/ELDERLY

Nungruthai Suntronwong : IDENTIFICATION OF GENETIC AND ANTIGENIC VARIATION AND EVOLUTION PATTERN AMONG INFLUENZA A AND B VIRUSES IN THAILAND. Advisor: Prof. YONG POOVORAWAN, M.D.

Seasonal influenza viruses commonly cause respiratory disease and have a considerable impact on public health threats which annually estimates 3 to 5 million cases of severe illness worldwide. The triggering of the seasonal influenza epidemic results from a complex interplay between viral, host and external factors such as climate. Although vaccination is an effective tool for influenza prevention and its complications, the composition of vaccine strain has been changed every year due to influenza constantly evolving. Here, we aim to examine the association between influenza activity and local climate factors, host immunity, genetic and antigenic variation and evolution pattern among influenza A and B viruses in Thailand. During 2010-18, we found 21.6% were tested positive for the influenza virus which typing as influenza A(H1N1)pdm09 (34.2%), A(H3N2) (46.0%), and influenza B virus (19.8%). There were two seasonal waves of increased influenza activity. Peak influenza A(H1N1)pdm09 and influenza B activity occurred in February and again in August, while influenza A(H3N2) viruses were primarily detected in August and September. The SARIMA model of all influenza and climate factors including temperature, relative humidity, and rainfall are the best performed to predict influenza activity. To gain insight into host immunity to influenza, we then study the elderly who are at high risk of infection. These findings showed the proportion of seropositivity (HI titers ≥ 40) to influenza A(H1N1)pdm09 (50%), A(H3N2) (66%) were higher than influenza B viruses such as B/Yamagata 2 (14%), B/Yamagata 3 (21%) and B/Victoria (25%). Additionally, only 5% of this population presented the cross-reactive antibodies to both the influenza A and B viruses, this suggests that a low proportion of individuals provided broadly protective antibodies. For the viral factors, we study the evolution of polymerase genes included PB1, PB2, and PA proteins that are considered as a further antiviral drug target. Mutations in the polymerase gene significantly affect viral replication, transmission, and virulence. We found the pattern of evolutionary dynamics of A(H3N2) and B/Victoria have considerably changed over time, while A(H1N1)pdm09 slightly stable and B/Yamagata was increasing in 2017. Our data reveal adaptive acquired mutations relatively occur as high genetic diversity in the polymerase gene and all PA gene has shown a higher evolution rate than PB2 and PB1, except A(H3N2). Furthermore, we then quantified the genetic and antigenic variation in the nucleotide of HA1 sequences and estimated predicted VE using the $P_{epitope}$ model. Our data indicated that influenza A(H3N2) diverged from vaccine strain and formed 5 genetic groups in the 2016-2017 seasons. Such emergence of multiple subclades contributed to the declining predicted VE from 74% (2016) down to 48% (early 2017). During late 2017-2020, phylogeny revealed multiple clades/subclades of influenza A(H1N1)pdm09 (subclade: 6B.1A1 and 6B.1A5) and A(H3N2) (subclade: 3C.2a1b, 3C.2a2 and 3C.3a) were circulating simultaneously and evolved away from their vaccine strain. The B/Victoria-like lineage predominated since 2019 with an additional three AA deletions. Antigenic drift was dominantly facilitated at epitopes Sa and Sb of A(H1N1)pdm09, epitopes A, B, D, and E of A(H3N2), and the 120 loop and 190 helix of influenza B virus. Moderate predicted VE was observed in A(H1N1)pdm09. The predicted VE of A(H3N2) indicated a significant decline in 2019 (9.17%) and 2020 (-18.94%) whereas the circulating influenza B virus was antigenically similar (94.81%) with its vaccine strain. Besides HA, the NA is also targeted for immune response and showed broadly protective but current seasonal vaccines poorly induce anti-NA antibodies. Our data suggest that extending the stalk domain of the NA with the 30 amino acid can induce significantly higher anti-NA IgG responses characterized by increased *in vitro* ADCC activity, while anti-HA IgG levels were unaffected. Moreover, this recombinant virus can show a protective effect in the mouse model. In conclusion, the ability to predict a seasonal pattern of influenza may enable better public health planning and underscores the importance of annual influenza vaccination prior to the rainy season. The host immune profile cloud also helps for the guidance of influenza vaccine policy. Our findings offer insights into the viral population dynamic of polymerase genes and the genetic and antigenic divergence from vaccine strains, which could aid antiviral drug development and vaccine updating. The extended NA stalk approach may assist in the efforts towards more effective influenza virus vaccines.

Field of Study: Medical Sciences

Student's Signature

Academic Year: 2020

Advisor's Signature

ACKNOWLEDGEMENTS

First and foremost, I would like to express my deep and sincere gratitude to my research supervisor, Professor Yong Poovorawan to develop the ideas of my work, encouragement and kindness of guidance and throughout my Ph.D. life. His vision, sincerity and motivation have inspired me. It was a great honor and privilege to study and work under his guidance. I am heartfelt thanks to my committee members, Professor Vilai Chentanez, Associate Professor Wilai Anomasiri, Associate Professor Sunchai Payungporn and Associate Professor Teeraporn Chinchai for their review of my dissertation and provide a recommendation. I would also like to thank Dr. Sompong Vongpansawas for advising me throughout my research work to complete the research successfully.

Many kind people have helped me to complete these projects, and I would like to express my deepest gratitude to all of them. I would like to appreciate a Royal Golden Jubilee Ph.D. scholarship from Thailand Research Fund and Chulalongkorn University for providing the scholarship and funding supports. I would like to express my special thanks to Professor Dr. Peter Palese who gave me an opportunity to broadening international research experience and work with their research team at the Department of Microbiology, Icahn School of Medicine at Mount Sinai, New York, New York, USA, for and develop the ideas and my mentor, Dr. Felix Broecker who taught me the methodology to carry out my research and provide precious guidance and immeasurably discussion. I would like to say thanks to several members of Peter Palese's laboratory: Dr. Allen Zheng, Dr. Weina Sun and Dr. Mark J. Bailey for kind support and a cozy inviting during my aboard. Thank you very much for welcoming me as a friend.

I would like to appreciate all of the scientists and postdoctoral researchers of the center of Excellence in clinical virology, department of Pediatrics, faculty of medicine, Chulalongkorn University for their help and genuine supports throughout this research work. I am extending my heartfelt thanks to my parents, my family, and friends who always encourage me, constant support and stand beside me along the way of this journey. Finally, my thanks go to all people who have supported me, directly and indirectly, to complete this thesis successfully. My Ph.D. experience is invaluable enhanced by your tremendous love and constant supports.

จุฬาลงกรณ์มหาวิทยาลัย
CHULALONGKORN UNIVERSITY

Nungruthai Suntronwong

TABLE OF CONTENTS

	Page
ABSTRACT (THAI).....	iii
ABSTRACT (ENGLISH).....	iv
ACKNOWLEDGEMENTS.....	v
TABLE OF CONTENTS.....	vi
LIST OF TABLES.....	viii
LIST OF FIGURES.....	ix
CHAPTER I INTRODUCTION.....	1
1.1 Background and rationale.....	1
1.2 Conceptual framework.....	7
CHAPTER II LITERATURE REVIEW.....	8
2.1 Taxonomy and Classification.....	8
2.2 Influenza virus nomenclature.....	9
2.3 Epidemiology.....	10
2.4 Genome and virion structure.....	11
2.5 Protein and their major functions.....	13
2.6 Cell entry and replication cycle.....	19
2.7 Antiviral drugs treatment.....	20
2.8 Influenza vaccination.....	22
2.9 Antigenic sites on HA and receptor binding sites.....	27
2.10 Influenza evolution.....	29
2.11 Summary and significance in this study.....	31

CHAPTER III	32
Part 3.1: Climate Factors Influence Seasonal Influenza Activity in Bangkok, Thailand.	33
CHAPTER IV	51
Part 4.1: Prevalence of cross-reactive antibodies against seasonal influenza A and B viruses among the elderly in Thailand.....	52
CHAPTER V	63
Part 5.1: Identify the genetic changes and evolution pattern of polymerase complex gene among seasonal influenza viruses.	64
Part 5.2: Genetic and antigenic divergence in the influenza A(H3N2) virus circulating between 2016 and 2017 in Thailand.	80
Part 5.3: Characterizing genetic and antigenic divergence from vaccine strain of influenza A and B viruses circulating in Thailand, 2017-2020.....	94
Part 5.4: Extending the Stalk Enhances Immunogenicity of the Influenza Virus Neuraminidase.....	115
CHAPTER VI	132
Conclusion and Discussion.....	132
APPENDIX.....	136
APPENDIX A	136
APPENDIX B	168
REFERENCES	175
VITA.....	203

LIST OF TABLES

	Page
Table 1 <i>Characterization of influenza proteins and their functions.</i>	18
Table 2 Antiviral Medications Recommended for Treatment and Chemoprophylaxis	21
Table 3 The vaccine strain composition of annual influenza vaccine.....	23
Table 4 Type of influenza vaccines	25
Table 5 HA numbering of amino acid residues in defined antigenic sites and the receptor-binding site of the influenza virus.....	28
Table 6 Influenza virus-positive samples and monthly average meteorological factors.	39
Table 7 Distribution of number and percentage of laboratory-confirmed influenza- positive cases of the individual age group.	57
Table 8 The prevalence of protective antibody against seasonal influenza by hemagglutinin inhibition assay.....	59

LIST OF FIGURES

	Page
Figure 1 History of influenza outbreaks	11
Figure 2 A schematic of viral RNA segmented genome of influenza A and B virus and influenza particle structure.	13
Figure 3 A schematic replication of the life cycle of influenza	20
Figure 4 Schematic of the action of anti-Hemagglutinin and anti-Neuraminidase antibodies.....	24
Figure 5 Monthly distribution of influenza activity from 2010 to 2018.....	40
Figure 6 Incidence of influenza virus relative to meteorological factors.....	41
Figure 7 Yearly influenza incidence and the periodic fluctuation of climate factors..	43
Figure 8 Association between meteorological factors and influenza virus.....	45
Figure 9 Seasonal ARIMA (p,d,q)(P, D, Q) ₁₂ fitted time series analysis.....	47
Figure 10 Comparison of the antibody titers (GMT) among influenza (subtype).....	58
Figure 11 Seroprevalence of protective antibody against seasonal influenza virus. ..	59
Figure 12 Schematic represents the number of influenza (sub)type presented seropositivity (HI titer ≥40) for individual.....	60
Figure 13 Time scale tree and population dynamic diversity in the polymerase gene of circulating influenza A(H1N1)pdm09 (2009-2019) in Thailand.....	71
Figure 14 Time scale tree and population dynamic diversity in the polymerase gene of circulating influenza A(H3N2) (2006-2019) in Thailand.	72
Figure 15 Time scale tree and population dynamic diversity in the polymerase gene of circulating influenza B/Victoria lineages (2004-2019) in Thailand.....	74
Figure 16 Time scale tree and population dynamic diversity in the polymerase gene of circulating influenza B/Yamagata lineages (2003-2017) in Thailand.	75

Figure 17 Schematic diagrams showing the comparison of the nucleotide substitution rate of PB2, PB1, and PA gene for individual influenza (sub)type.....	77
Figure 18 Distribution of influenza A(H3N2) virus between January 2016 and June 2017.....	84
Figure 19 Phylogeny of the nucleotide sequences of the HA coding region of A(H3N2).	86
Figure 20 The defining residue substitutions placed on the HA protein structure of A(H3N2).	88
Figure 21 Calculated quarterly VE between January 2016 and June 2017.....	90
Figure 22 Monthly distribution of influenza A and B viruses from July 2017 to March 2020 (n = 17,480).....	100
Figure 23 Phylogenetic analysis of the entire HA gene of A(H1N1)pdm09.	102
Figure 24 Phylogenetic analysis of the HA gene of A(H3N2).	104
Figure 25 Phylogenetic analyses of the nucleotide sequences of the HA coding region of the influenza B virus.....	106
Figure 26 Placement of residue changes identified in influenza virus strains in this study.....	108
Figure 27 Estimation of the trend of predicted VE between July 2017 and March 2020.....	110
Figure 28 Design and rescue of influenza viruses with extended N1 neuraminidase stalk domains.	125
Figure 29 The extended stalk domain enhances IgG responses to the N1 neuraminidase.....	127
Figure 30 The extended stalk domain enhances ADCC active antibody responses to the N1 neuraminidase.	128

CHAPTER I

INTRODUCTION

1.1 Background and rationale

Seasonal influenza viruses are the most common cause of human respiratory disease and they are a major cause of morbidity and mortality worldwide. The effect of influenza seasonal epidemics causes a severe illness globally each year resulting in three to five million cases, 290,000 to 650,000 cases of influenza-associated death worldwide. Currently, the seasonal influenza virus consisted of two subtypes of influenza A virus: A(H1N1)pdm09, A(H3N2), and two lineages of influenza B virus: B/Victoria B/Yamagata lineages. The young children and elderly are at high risk of influenza infection. The influenza vaccine is an effective way to prevent influenza infection and reduce the risk of severe influenza-associated complications. Antiviral agents are used for prophylaxis and therapy of illness. However, influenza typically evolves undergone antigenic shift and antigenic drift mechanism. Such constantly evolving, the viral variants were produced leading to escape the pre-existing immunity against the previously circulating strains. To date, the composition of vaccine strain has been reformulated every year. Amino acid changes in significant positions can lead the virus to resist the antiviral drug treatment and enhance viral replication, transmission, and virulence. Due to these viruses constantly changing over time, the surveillance of influenza infection and monitoring the genetic and antigenic variation should be performed.

The triggering of the seasonal influenza epidemic was result from a complex interplay between external factors such as weather and social lifestyle, host factors and viral factors. For climate factors, in the temperate regions, influenza activity peaks during the cold winter months unlike tropical regions such as Thailand, different patterns of influenza activity vary depending on the regional climates and geographical location. Several reports indicated the fluctuating of climate factors included sun exposure, temperature, wind speed, relative humidity, rainfalls, and absolute humidity may influence the seasonality of influenza activity. We will examine which climate factors influence the pattern of influenza activity and use these findings to design the potential forecasting models for influenza activity by using time series analysis. For host factors, the lack of pre-existing immunity or cross-reactive antibodies to influenza virus likely contributed to the high attack rate and related to increase influenza

epidemic. For the viral factors, the constantly evolving influenza virus also affects the increase of influenza activity both non-antigenic and antigenic genes. The influenza virus polymerase complex has also known as non-antigenic genes and received considerable attention as a target for developing antiviral agents. The mutations at the significant sites in the polymerase gene might be related to enhancing viral replication, transmission, and virulence. While the hemagglutinin gene has known as a major target of influenza vaccination which continues changes under selective pressure such as immune response. The mutations in the antigenic sites of HA can produce the new variant strain that escapes the pre-existing immunity and reduce the vaccine effectiveness (VE). However, the effectiveness of the vaccine depends on the type of vaccines, the host immune profile, and the closely antigenic between vaccine strains and circulating strains. Thus, monitoring the genetic and antigenic divergence of HA sequences are significant in the selective process of vaccine compositions.

To better understanding, we will perform temporal dynamic and evolution analysis to demonstrate the evolution pattern and substitution rates in the polymerase gene among seasonal influenza A and B viruses. This knowledge can help to probably identify the significant point mutations of influenza proteins and predict evolution patterns that may affect the re-emergence in the future. For the success of the influenza vaccine approach, we will monitor the viral diversity which affects the vaccine effectiveness and pre-existing host immunity, particularly in high-risk group populations. This study provides a better understanding of the incidence, genetic and antigenic and evolution pattern of circulating strains of influenza virus and will be critical for the successful implementation of new strategies of annual influenza vaccine and prediction of the re-emergence of new strains.

Thus, the hypothesized of this study are described as follows:

- (i) Biannual influenza activity was observed in Thailand and significantly associate with climate factors comprise of rainfall, relative humidity, and temperature. The impact of climate factors o influenza activity can use to design the accurate forecasting model for influenza outbreaks.
- (ii) The proportion of individual who has seropositive to influenza A is higher than the influenza B virus. The prevalence of broadly protective antibodies to both influenza A and B virus is low in the elderly.
- (iii) Characterization of the long-term genetic changes and determine the evolution analysis of polymerase gene complex among influenza A(H3N2), A(H1N1)pdm09 and influenza B viruses are critical to identifying the amino

acid involved in the viral population diversity. Quantifying the genetic and antigenic characteristics and assessing the vaccine effectiveness of Thailand strain against vaccine strain is critical for select the optimal strain that includes in vaccine strain. Extending the stalk domain of the NA could render it more immunogenic on virus particles and showed the effective effect of prophylaxis and recovery from influenza infection in the mouse model.



Part I: Climate Factors Influence Seasonal Influenza Activity in Bangkok, Thailand

Research questions:

1. What is the incidence of the multi-year incidence of influenza virus infection between 2010 and 2018?
2. How were different influenza virus (sub)types associated with the monthly climate factors included temperature, relative humidity, and rainfall?
3. Is the time series analysis that used the previous data of influenza incidence and climate factors able to predict the influenza incidence in the next season?
4. Which one of the forecasting models between all influenza viruses and individual influenza (sub)type provides better performance for prediction?

Research objective:

1. To investigate the multi-year incidence of influenza virus infection and identify predominant influenza (sub)type between 2010 and 2018 in Thailand.
2. To demonstrate the relationship between different influenza virus (sub)types and the monthly climate factors included temperature, relative humidity, and rainfall.
3. To generate the forecasting model by using time series analysis and the previous data of influenza incidence and climate factors.
4. To compare the performance of the forecasting model between all influenza viruses and individual influenza (sub)type.

Part II: Prevalence of cross-reactive antibodies against seasonal influenza A and B viruses among the elderly in Thailand

Research question:

1. What are the prevalence of cross-reactive antibodies to influenza A(H1N1)pdm09, A(H3N2), and influenza B viruses among the elderly population in Thailand?

Research objective:

1. To investigate the prevalence of cross-reactive antibodies to influenza A(H3N2), A(H1N1)pdm09, and influenza B viruses among the elderly population in Thailand; a cross-sectional study.



Part III: Identify the adaptive genetic changes and evolution pattern of polymerase complex gene, quantify genetic and antigenic characterization of influenza A and B viruses for assessing the divergence of the vaccine strain.

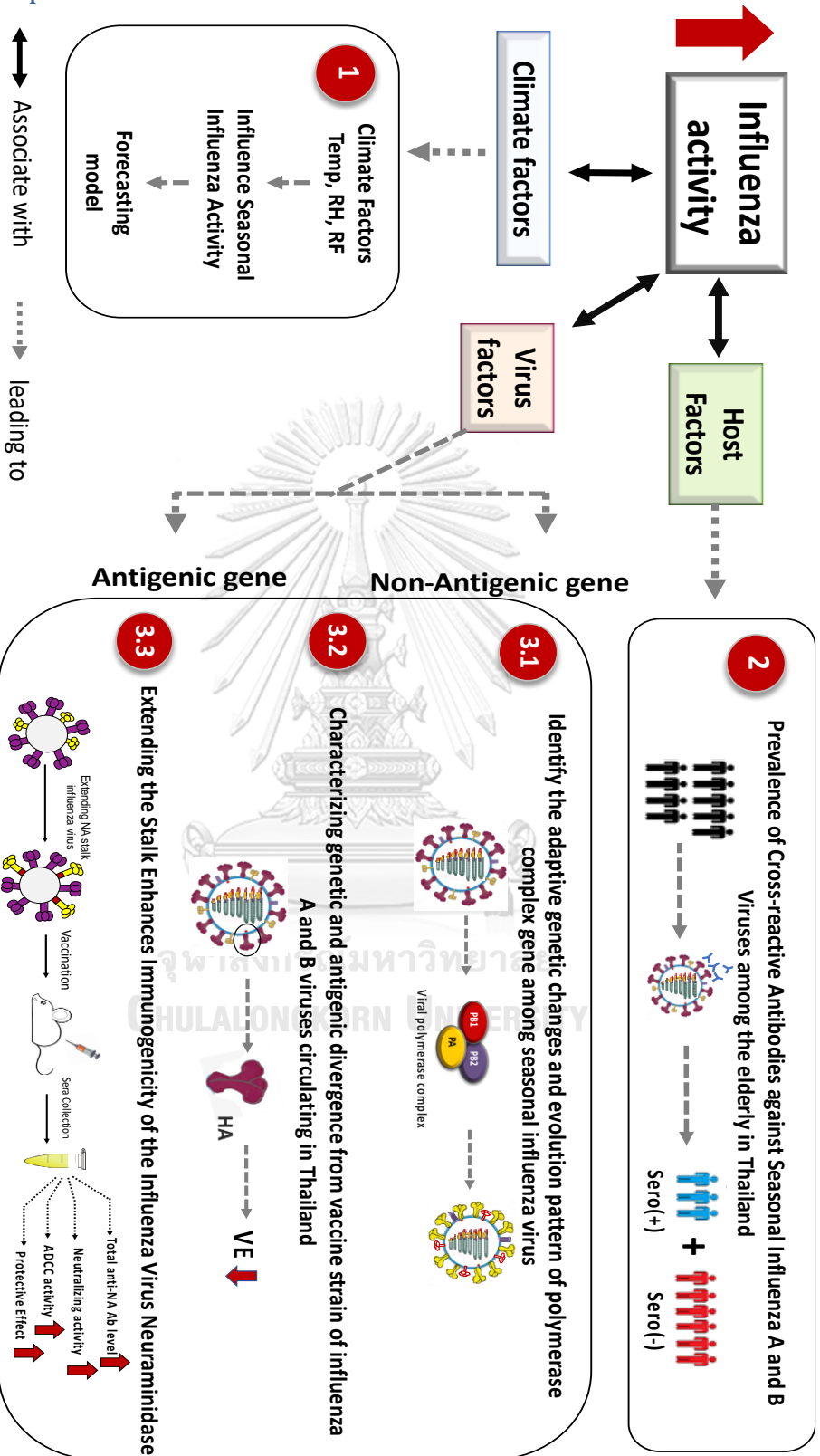
Research questions:

1. Do the genetic changes occur in polymerase gene among seasonal influenza viruses and involves the viral population dynamic?
2. Do the genetic and antigenic variation of the influenza virus diverge from their influenza vaccine?
3. Could extending the stalk domain of the NA render it more immunogenic on virus particles and showed the productive effect of prophylaxis and recovery from influenza infection in the mouse model?

Research objectives:

1. To examine the long-term genetic changes and evolution analysis of polymerase gene complex among influenza A(H3N2), A(H1N1)pdm09 and influenza B viruses.
2. To demonstrate the genetic and antigenic variation and natural selection of influenza circulating strains and assess the number of amino acid changes in the antigenic sites of HA1 using the P_{epitope} model provided the predicted VE.
3. To investigate extending the stalk domain of the NA recombinant virus could render it more immunogenic and determine the productive effect of prophylaxis and recovery from influenza infection in the mouse model.

1.2 Conceptual framework



CHAPTER II LITERATURE REVIEW

Influenza (mostly referred to as “flu”) is known as a contagious viral infection. Influenza viruses are identified as the respiratory causative pathogens which contributed to causing a public health significance worldwide. It annually recurrent epidemic outbreaks also known as seasonal influenza that leading to globally estimate 3 to 5 million of severe illness and 290,000 to 650,000 deaths [1]. High incidence of influenza infection most likely found in young children who seem to be the main human transmitters for influenza virus infection while the most case of influenza-associated deaths was found in elderly who aged ≥ 75 years of aged [1, 2]. In humans, the influenza virus can be transmitted from infected people to other individuals by three routes; direct transmission which is primarily transmitted by sneezing and coughing via large-particle droplets, aerosol transmission and contact with contaminated surfaces containing respiratory secretion [3]. Influenza virus shedding typically begins in the first 24 to 48 hours after infection and peaks before the illness begins [4]. The onset of symptoms is about 2 days (range from 1 to 4 days) and clinical features of influenza infection most vary from mild to severe and deaths. A mild respiratory symptom most commonly appears in the upper respiratory tract and is characterized by sore throat, a runny nose, a sudden onset of fever (>38 °C), cough (typically dry), chills, muscle and joint pain, headache and fatigue which are also known as the influenza-like illness (ILI) [5]. The severe symptom of infection was typically caused by a secondary bacterial infection in the lower respiratory tract leading to lethal pneumonia and some reports found that influenza complications might affect the heart, nervous system and other organs [6, 7]. The severity most occurs mainly among high-risk groups while healthy people can resolve from fever and other symptoms within 1-2 weeks without requiring medical attention [5].

2.1 Taxonomy and Classification

Influenza virus belonging to the *Orthomyxoviridae* family is an enveloped virus that contained a negative-sense, single strand RNA segmented genome. The *Orthomyxoviridae* family includes seven genera: *Alphainfluenzavirus* (influenza A virus), *Betainfluenzavirus* (influenza B virus), *Gammainfluenzavirus* (influenza C virus), *Deltainfluenzavirus* (influenza D virus), *Isavirus*, *Thogotovirus* and *Quaranjavirus* [4]. The first four genera are identified to cause influenza infection. Influenza A virus has eight segmented genomes and circulated in a wide range of hosts including avian,

domestic animals, humans and other mammalian species [8]. Influenza B virus also has eight segmented genomes and commonly infects humans, but there have been some reports of influenza B infection in horses and seals [9]. In contrast, influenza C and D contain only seven segmented genomes and rarely cause substantial respiratory disease in humans. However, the influenza C virus can cause respiratory illness especially in children [10] while the influenza D virus has not been reported infected in humans [11].

Currently, Influenza A virus can classify into subtypes according to the combination of surface glycoprotein HA and NA and then further divided by strains. To date, there are 18 HA and 11 NA subtypes. Newly, HA17-18 and NA10-11 have been discovered from the bat that showed phylogenetically close to influenza A virus but the reassortment events within influenza A virus have not been reported [12-14]. However, there has limited subtypes of seasonal human influenza virus comprise of H1, H2, H3 and N1 and N2 such as H1N1, H2N2, and H3N2 that significant to cause the epidemic outbreaks; as defined by widespread and person-to-person transmission [15]. In contrast, the Influenza B virus is not divided into different subtypes but are recently diverged into two lineages depend on antigenically differences of HA glycoprotein since the 1970s, resulting in B/Victoria (B/Victoria/2/1987-like) and B/Yamagata (B/Yamagata/16/1988-like) lineages [16, 17]. The B/Victoria lineage most predominated in the 1980s, while B/Yamagata lineage most globally predominated during the 1990s [16].

2.2 Influenza virus nomenclature

The criteria of influenza virus nomenclature has been established by WHO since 1980 [18]. The name of viral isolation comprised of the letter that defined as a type of influenza virus either A, B, C or D, followed by species of a host which was collected influenza virus (in case of isolation has not been isolate from human), the geographic region at which the virus was isolated, the number and the year of isolation. In the case of the influenza A viruses, the protein antigenic type, the haemagglutinin (HA) and neuraminidase (NA) subtype, are typically indicated after the name of isolation. For illustration, influenza A/Turkey/England/50/91(H5N1) virus is an influenza type A, isolated firstly from a turkey in England in 1991 and the isolate number is 50. The protein antigenic type of viral isolation was hemagglutinin (HA) subtype 5 and neuraminidase (NA) subtype 1.

2.3 Epidemiology

Currently, the influenza disease burden is caused by the seasonal influenza virus consisted of two subtypes of influenza A virus: A(H1N1)pdm09, A(H3N2) and two lineages of influenza B virus: B/Victoria B/Yamagata. Seasonal influenza viruses are co-circulated in humans result in an annual epidemic outbreak. Influenza A virus is clinically severe more than the influenza B virus due to the genetic and antigenic variation including antigenic shift and antigenic drift that lead the virus to evade the existing immunity result on the cause of recurrent influenza annual epidemic. To date, the only influenza A virus has been reported to cause a pandemic outbreak.

Influenza A virus has a significant risk of zoonotic infection and a host switch that causes the high incidence epidemic and pandemic outbreak globally. Nevertheless, this virus can jump from animals to humans lead to more crush disasters on a global scale. There are four pandemics have been occurred in the past one hundred years. In 1918, the first case of deadly influenza infection which reported in Spain cause 20 million to 50 million deaths by a strain of A(H1N1) and the conclusive evidence of the origin is still unknown [19]. After that, 1957 Asian flu was emerged thought out the combination of human A(H2N2) and mutant strain in ducks that killed 2 million people. Since 1968, the first pandemic of A(H3N2) also known as Hong Kong flu, this strain cause around 1 million deaths particularly the elderly aged more than 65 years old. The recent influenza pandemic was “swine flu in 2009” that first isolated in Mexico (Figure 1). It is a novel strain generate from triple reassortment which mixed segmented genes among bird, swine and human. So far, influenza A(H1N1) seasonal which annually causes the seasonal epidemic strain has been replaced by influenza A(H1N1)pdm09 [20, 21].

The evidence of influenza A(H3N2) global migration indicated that the new variants firstly emerged in tropical regions such as southeast Asia and eastern Asia and then act as local persistence for seeding seasonal epidemics to the rest of the world [22]. The temperate regions were seeded from the tropic annually which first reached Oceania, North America, Europe and later South America. However, some studies indicated the virus migration from the multiple different geographical regions can cause the global permanent of viral population and further seeded in temperate regions for seasonal epidemics in a given year [23]. The influenza activities are different depending on the geographic region. In temperate region, the influenza epidemic outbreak typically occurs in the cold and dry season (winter month) while the peak of influenza activities in tropical regions are very diverse and most typically related to the humid – rainy season in some regions [24]. The seasonal influenza virus causes an attraction

rate to estimate 5-10% in adults and 20-30 % in children [25]. The seasonal influenza incidence estimated during 2010–2016 was approximately 8% (ranging from 3-11%) among all ages in the United States [26]. Besides, seasonal influenza epidemics were associated with an estimated 140 000–960 000 hospitalizations in the United States during 2010–2018 [27]. Seasonal influenza-associated respiratory deaths were recently estimated 291 243–645 832 occur annually worldwide [1] Furthermore, each influenza season has considerable financial consequences from hospital and treatment costs so the monitoring of influenza infection and predicting the vaccine strain is necessary to perform.

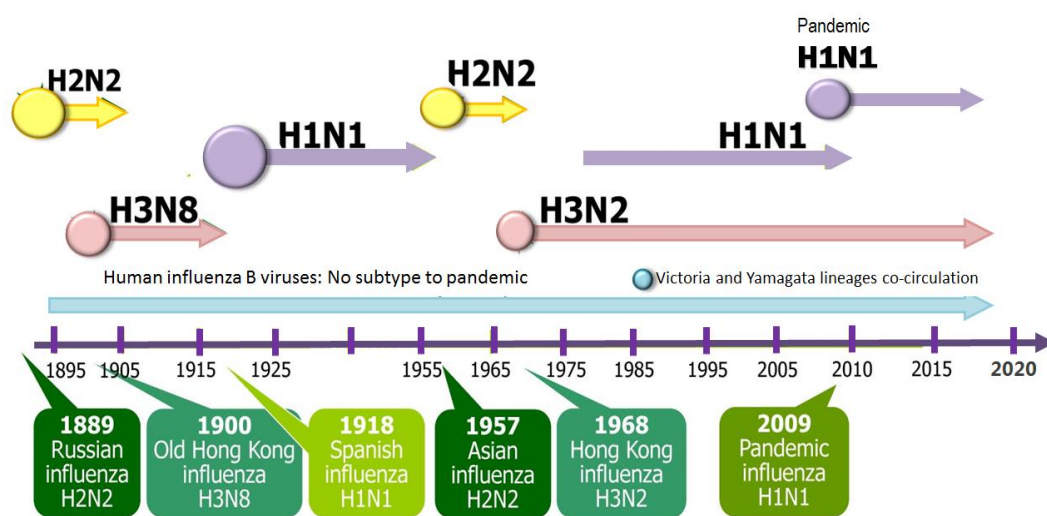


Figure 1 History of influenza outbreaks.

Comprise of the Spanish influenza H1N1 virus in 1918, the Asian influenza H2N2 virus in 1957, the Hong Kong influenza H3N2 virus in 1968, and the Swine flu H1N1 virus in 2009. To date, influenza A(H3N2), A(H1N1)pdm09 and influenza B viruses are significant to cause the epidemic outbreaks (Modified from Nicoll A et al., 2010) [20].

2.4 Genome and virion structure

Influenza A and B viral genome is estimated 13 kb contained the eight gene segments of negative-sense, single-strand RNA which including polymerase basic 2 (PB2), polymerase basic 1 (PB1), polymerase acidic (PA), hemagglutinin (HA), nucleoprotein (NP), neuraminidase (NA), matrix (MP) and a non-structural protein (NS) [28]. The gene segments are ranging from 2.3 to 0.9 kb. The individual gene segment forms a helical nucleocapsid also known as viral ribonucleoprotein (vRNP) which the viral RNA was wrapped by nucleoprotein and then bound with polymerase complex (RNA-dependent RNA polymerase, RdRp). These viral genomes can encode up to 11

proteins. The three largest segments (PB2, PB1 and PA) are typically translated into the three subunits of viral RNA-dependent RNA polymerase proteins involving the replication and transcription process. In the case of the influenza A virus, the PB1 and PA gene can encode at least two proteins. The HA, NA and NP encode a single protein by individual gene segments. The nucleoprotein (NP) by each gene segment. The M and NS genes typically translate into more than one protein; M gene encodes the matrix (M1) protein and membrane (M2) protein and NS gene encode two non-structural proteins (NS1 and NEP). Nevertheless, the influenza virus can also express the additional accessory proteins such as PB1-F2, PB1-N40, PA-X, PA-N155, PA-182 (Figure 2A).

The morphology of the influenza virus is either spherical with approximately 100 nm in diameter or occasionally filamentous form which reaches more than 20 μm in length [29]. The viral envelop surface which is the host cell-derived lipid membrane contains the integral membrane protein (M2) and displays the two glycoproteins as spikes that extending about 10-14 nm from the surface. The bridge between viral envelop and nucleocapsid are formed by matrix protein (M1). The individual gene segment is wrapped by multiple nucleoproteins (NP) and bound with polymerase complex (PB2, PB1 and PA) to form the viral ribonucleoprotein (vRNP) (Figure 2B). RNPs are playing a critical role in transcribed and produce positive sense mRNA. During influenza infection, these proteins are moved to the nucleus of the host cell in the area that RNA viral transcribed [30].

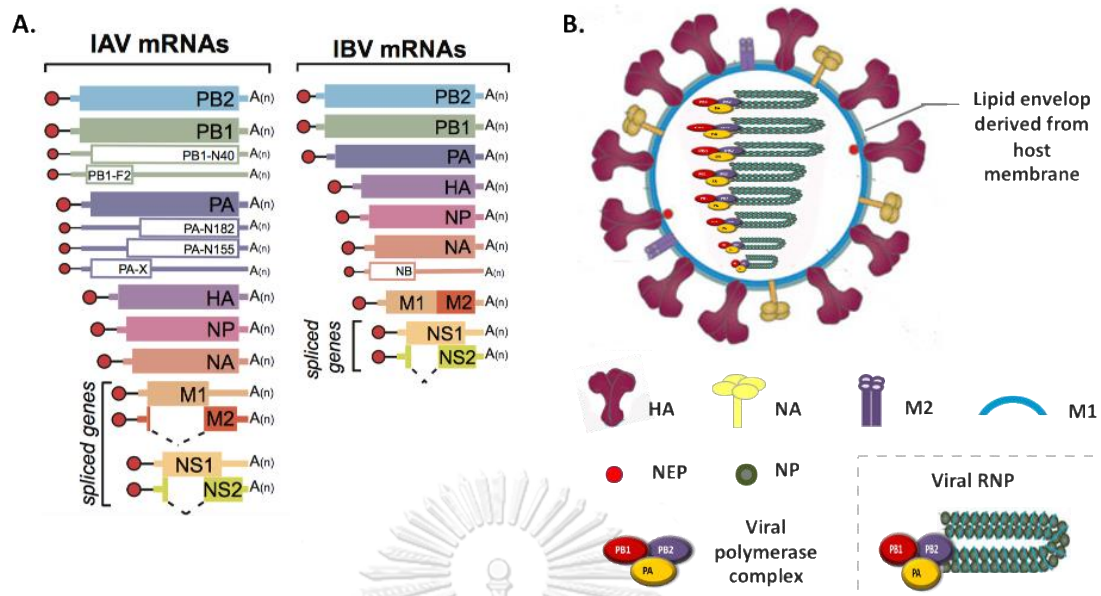


Figure 2 A schematic of viral RNA segmented genome of influenza A and B virus and influenza particle structure.

(A) Diagram of the eight viral RNA (vRNA) gene segments comprised of PB2, PB1, PA, HA, NP, NA, M and NS and their transcribed of influenza A virus (left) and influenza B virus (right). The encoded viral gene product (box) and the alternative splicing (dash line) are shown. Red circle defined as the M7pppG cap and A(n) indicated the poly-A tail (Modified from Dan Dou et al., 2018) [31]. (B) Diagram of influenza virion structure and their protein includes the viral membrane which contained HA, NA and M2 channel, the viral capsid structure supported by matrix M1 protein, the eight segments of viral ribonucleoprotein (vRNP). Each viral RNP formed the scaffold of viral RNA and NP proteins which bound to polymerase complex (PB2, PB1, PA) (Modified from Mediana et al., 2011) [32].

2.5 Protein and their major functions

Influenza virus can encode up to 11 proteins which include the complex of RNA-dependent RNA polymerase (RdRp, ~ 250 kDa in size) proteins (PB1, PB2 and PA proteins assemble to form the complex), two glycoproteins as spikes (HA and NA), nucleoprotein, two non-structural protein, M1, M2 and the additional accessory proteins which have recently been identified (Table 1).

2.5.1 Polymerase basic 2 (PB2) and mutations

PB2 gene encodes polymerase basic 2 protein which is a subunit of influenza polymerase proteins that involves a process called “cap-snatching” through binding

of the 5'-cap of pre-mRNA in the host cell and lead to begin the viral mRNA synthesis [33].

Amino acid substitution at E627K residue in PB2 is significant to increase virulence that helps the virus to adapt to body temperature constraints. Briefly, E627 can help replicate in avian (41°C) while K627 help virus to replicate in human URT (33°C) [34]. Mutation at D701N residue has been found to expand host ranges and help to increase virulence by enhancement of PB2 transported into the nucleus [35]. Amino acid substitutions in PB2- M631L and PB2-E712D have been found to strongly up-regulate the viral RNA polymerase and therefore disease severity. A recent study reported both PB2-Q591K and G590S were related to enhancing the pathogenicity in the mammalian host [36]. Amino acid substitutions at T271A, V661A and V683T/A684S in PB2 were identified to contribute to the increasing activity and relate to enhancing the polymerase activity in low temperature [37].

2.5.2 Polymerase basic 1 (PB1) and mutations

PB1 gene can translate several proteins underlying the leaky ribosomal scanning and translation termination-reinitiating mechanism including PB1 protein, PB1-F2 and PB1-N40 [38, 39]. PB1 subunit contains a catalytically active that are responsible for the mRNA elongation that acquired the viral RNA as a template [40]. Nevertheless, PB1 gene also encodes PB1-F2 which is responsible for antagonist host interferon (IFN) and pro-apoptotic activity.

Amino acid substitution at N66S in PB1-F2 plays a crucial role in the high virulence of this virus by suppressing the production of interferon (IFN) that is responsible for host innate immune response [41]. Furthermore, PB1-T296R substitution was identified to enhance polymerase activity [42].

2.5.3 Polymerase acidic (PA) and mutations

PA gene encodes the PA protein which is a subunit of influenza polymerase protein and a newly PA-X protein which is a result of the plus one ribosomal frame shifting [43, 44]. For cap snatching, the endonuclease domain in PA subunit typically cleaves 10-13 nucleotides downstream of the 5' cap to generate the capped primer [45]. Moreover, PA gene encodes PA-X protein which is a newly identified protein responsible for suppressing the cellular gene expression leading to regulate and modulate the host cell response [35].

Currently, PA gene has now been identified to encode the novel interesting proteins including PA-N155 and PA-N182 which involve in viral replication [46]. Furthermore, PA had I94V and T97I mutations which were identified acting as an

accessory molecule to enhance virulence. Both PA-E31K and PA-K356R have shown the ability to increase the viral replication property by enhancing the activity of the polymerase enzyme. PA-L336M was required to modulate the severity of influenza infection.

2.5.4 Hemagglutinin (HA) and mutations.

HA gene encodes hemagglutinin protein which is a transmembrane glycoprotein protein and plays a critical role in viral attachment and penetration. The HA spike is synthesized as a homotrimer protein contained head and stalk regions. The stalk region extends from the viral membrane while the head region extends from the stalk and carries the receptor binding site that binds to the host cell receptor (sialic acid) to lead the virus enters the host cell [47]. During the fusion process, many influenza virus HA proteins are cleaved by extracellular trypsin-like proteases that can limit the viral replication that occurs at the specific site either respiratory tract or gastrointestinal tract. However, some influenza virus, high pathogenic influenza virus (HPAIV), can be cleaved by furin-like protease when moving through the ER, thus the virus is not limited at the site but capable to cause the multiorgan infection. Also, HA proteins are high immunogenicity that plays a critical role in induced host neutralizing antibodies [48].

Amino acid substitutions in this protein can involve in cellular host range and tissue tropism which may affect the virulence of the influenza virus. A recent study shows that H5N1 virus which has amino acid substitution in HA can help to increase the ability to bind with human sialic acid receptors. Moreover, the amino acid positions that are adjacent or located in receptor binding sites which describe in Table 4 and potential N- glycosylation in 154-156 residues can influence the binding preference, pathogenesis and virulence. The substitutions at S137A and S227R residues in HA and potential glycosylation at position A160T site are determined for influence to enhance the ability for human- receptor binding.

2.5.5 Nucleoprotein (NP) and mutations

The nucleoprotein protein (NP) typically wraps the viral RNA to form helical nucleocapsids. This protein is responsible for the process of after synthesis and phosphorylated post-translation in the cytoplasm. It is transported into the host nucleus to bind with the newly viral RNA after the RNA synthesis process [49]. It provides a structure of RNP complex by interacting with the viral matrix proteins (M1) and polymerase proteins (PB1 and PB2). This protein is also a major target of cytotoxic

T lymphocytes which cross-reactivity of non-specific NP of all influenza virus subtype [50].

The mutation at N319K in NP which shown to enhance the interaction of monomeric NP with human importin- α 1. Moreover, the combined mutations at Q236H (PB2), E627K (PB2), and N309K (NP) or Q591K (PB2) and S50G (NP) mutations which has a synergistic effect in viral replication [51]. NP-D375N was identified to enhance the replication kinetics.

2.5.6 Neuraminidase (NA) and mutations

NA gene encodes neuraminidase protein which is a transmembrane glycoprotein and primarily functions as a receptor-destroying enzyme that acts on the last step of the viral replication process. Neuraminidase (NA) protein forms homo-tetramers and extends from the viral membrane.

The tetrameric head region contains an enzymatic domain that can cleave the sialic acid of the host cell surface and allows the new virion releasing from the infected cell [52]. NA protein also plays a critical role in removing mucins and facilitating virus access to host epithelial cells [53].

Amino acid substitution at K110E residue has been found to significantly promote NA enzymatic activity. This protein has known to be the target of the second anti-viral drug approved against influenza infection such as oseltamivir, zanamivir and peramivir. The amino acids located in the enzyme active site of the neuraminidase inhibitor comprise of R118, D151, R152, R224, E276, R292, R371, and Y406 – N2 numbering which in the catalytic core and E119, R156, W178, S179, D/N198, I222, E227, H274, E277, D293, and E425 which located in active site pocket. The amino acid substitutions that acquired for neuraminidase inhibitor drug resistance consist of E119V, Q136K, N142S, G320E and I222V+S331R for A(H3N2) and Q136K/R, D198E, I222K/R/T, S246N, H274Y, R292K, and N294S for A(H1N1)pdm09 [54].

2.5.7 Matrix (MP) and mutations

the matrix one (M1) protein is translated from MP gene without the splicing process. Moreover, it also has three splices demonstrated to result in matrix protein two (M2), mRNA3, and M2 related variant (M42) depend on alternative splicing of overlapping reading frames [55]. M1 protein is a structural protein that functions as a bridge between and virion envelope and nucleocapsid. The interaction between M1 and nucleocapsids are depended on the pH value. Their interactions are disrupted at low pH to facilitate the uncoating mechanism which allows the nucleocapsid

transported to the nucleus (the viral replication site) while the neutral pH supports the binding between M1 and nucleocapsid to facilitate the virion assembly.

M2 protein (~ 97 aa in length) is an integral membrane protein that is produced from MP gene, but the M2 mRNA is spliced. This protein is responsible for acid activate ion channel which functions as a proton transporter. During the viral entry, the acidic endosome can trigger the uncoating process by transporting protons to the interior of the virion and allow the viral RNP complex moving into the host cytoplasm [55]. M2 ion channel protein is also known as the adamantanes derivatives drug against influenza infection. The amino acid substitutions in M2 transmembrane domain which are acquired to adamantanes resistance comprise of L26F, V27A, A30T/V, S31N, and G34E. These mutations lead to an increase in pore size, destabilization and hydrophilicity of channel conformation [56].

2.5.8 Nonstructural (NS) and mutations

The NS gene can encode two nonstructural proteins- NS1 and NS2 depending on the differential RNA splicing. The NS1 protein can be classified into two different functional domains.

Briefly, the RNA-binding domain (RBD) is responsible for binding with low affinity against RNA sequence and the effector domain is responsible for mediate interacted with several host cellular proteins and remains the stability of RNA-binding domain. NS1 functions include inhibiting the cellular mRNA release and splicing. In addition, NS1 protein disrupts the host immune response by inhibiting the interferon pathway and also influence maturation and migration of host antigen-presenting cell result in dysfunction of T cell and cytokine production [57]. NS2/NEP protein or nuclear export protein encodes from an NS alternatively splicing. This protein is responsible for incorporating the viral RNA and transporting viral RNP complexes from the nucleus to the cytoplasm [58].

Unspliced NS gene encodes the non-structural protein (NS1) and a spliced transcribed encodes the non-structural protein two (NEP/NS2) and NS3 [59]. NS1 is a virulence molecule responsible for limiting interferon (IFN) and proinflammatory cytokines response. A recent study shows that the deletion from 263-277 of NS1 and D92E can help the virus replicate in the presence of interferon (IFN) and increase viral virulence. NS1-D92Y can induce the virus to lack the ability to inhibit RIG-I ubiquitination [60]. NS1-G139D and NS1-S151T were identified to increase the pathogenicity of the influenza virus [61]. A recent study shows that E55K, L90I, I123V,

E125D, K131E, and N205S substitutions in NS1 protein promote viral strain to inhibit host gene expression result in reducing the level of pro-inflammatory cytokines [62].

Table 1 *Characterization of influenza proteins and their functions.*

Gene ID Ref.	Segments	Proteins	Functions
1	PB2	PB2	component of RNA polymerase: cap recognition [43, 63]
2	PB1	PB1	RNA polymerase: elongation [63]
		PB1-F2	pro-apoptotic activity; IFN antagonist [43]
		PB1 N40	viral life cycle [32]
3	PA	PA	RNA polymerase: protease [63]
		PA-X	RNA endonuclease activity [34, 44]
		PA-N155	Increase replication kinetics and pathogenicity but less effect on polymerase activity [64]
		PA-N182	Effect the viral replication but less effect on polymerase activity [64]
4	HA	HA	receptor binding site, fusion activity, major antigen, assembly and budding [64]
5	NP	NP	RNA binding RNA synthesis, RNP nuclear import [48]
6	NA	NA	neuraminidase activity [50]
7	M	M1	interaction with RNPs and glycoproteins, RNP nuclear export, assembly and budding [35]
		M2	membrane protein ion channel activity assembly and budding [35]
		M42	Alternative ion channel in influenza M2 deficient strain [55]
8	NS	NS1	Inhibit cellular mRNA releasing and splicing, IFN antagonist activity [52]
		NEP/NS2	RNP nuclear export regulation of RNA synthesis [53]

2.6 Cell entry and replication cycle

The influenza infection starts with the attachment between the viral receptor (HA protein) and the sialic acid receptor on the host cell surface. Influenza virus can infect by recognized two types of sialic acid depend on the viral preference such as α 2,6 sialic acid which found in the epithelial cell of the human upper respiratory tract and α 2,3 sialic acid which found in the epithelial cell of the avian intestine and the epithelial cell of the human lower respiratory tract [65]. Following the attachment, virions can enter the host cell through a receptor mediate- endocytosis mechanism. In the fusion and uncoating, endosomal vesicles with low pH can induce virion to change the conformational structure of HA to expose its fusion domain. HA is cleaved by a proteolytic enzyme such as trypsin-like protease and furin-like protease which results in the dimerization of the head region (HA1) and stalk region (HA2). The stalk domain (HA2) is responsible for mediated fusion with the endosomal membrane [66]. While M2 ion channel also allows the influx of proton ions to move into the viral particle and induce dissociation of M1 from viral RNP to release eight segmented viral RNP complexes into the cytoplasm. The viral RNP complexes are imported to the host nucleus by the nuclear localization signal and initiated viral mRNAs synthesis. Nowadays, the replication also occurs that leads to producing positive sense RNA which is a replicative intermediate template to generate the viral RNA. The mRNA is transported to the cytoplasm where they translate into viral protein by using host cell machinery. Some viral proteins move back to the nucleus where the viral RNP complex production and others pass the post-translation process such as glycosylation [67]. The newly formed nucleocapsids migrate into the cytoplasm. After the assembly of the viral genome and protein, they are cleaved by the NA protein which has an enzyme activity to release of newly virion from an infected cell (Figure 3) [46].

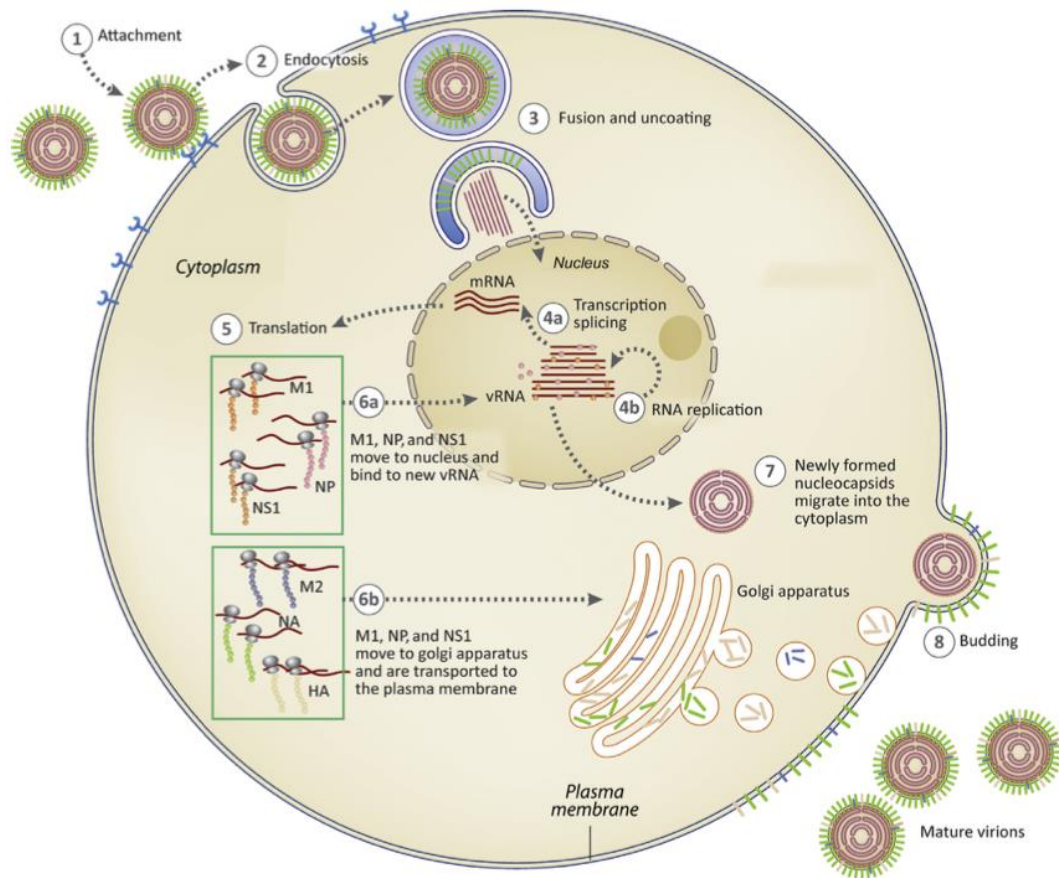


Figure 3 A schematic replication of the life cycle of influenza

The replication cycle of the influenza virus consists of multiple processes; viral attachment, entry by endocytosis, fusion and uncoating, genome replication and transcription, translation, packaging and budding from the infected cell (Payne S et al., 2017) [68].

2.7 Antiviral drugs treatment

Food and Drug Administration (FDA) approved several antiviral agents for treatment and chemo-prophylaxis include M2 inhibitors, neuraminidase inhibitors, cap-dependent endonuclease inhibitor [69]. The antiviral drug can be used as treatment and some can be used as chemoprophylaxis to prevent influenza infection. The M2 inhibitors which consist of amantadine and rimantadine can block the uncoating step of influenza A virus through occluding the ion channel but not the influenza B virus. In addition, the M2 inhibitors also have side effects and generate influenza that resistant strain recently spreading worldwide, thus, FDAs have not recommended these drugs for influenza treatment recently [70]. Only four influenza antiviral medications were currently approved by the U.S. FDA for influenza treatment (Table 2). The first three agents are neuraminidase inhibitors (NAIs) which are classified into oseltamivir,

zanamivir and peramivir according to the route of treatment. This antiviral agent can block the release of the newly formed virions from the infected cells by inhibition of neuraminidase enzyme. However, the influenza H1N1 virus which is an oseltamivir-resistant strain was occurred and spread worldwide since 2007 [71]. The ribavirin is an inhibitor of inosine 5'-monophosphate dehydrogenase which enzyme is significant in viral RNA synthesis but not currently approved by the FDA for influenza treatment [72]. The fourth agent is baloxavir marboxil which is a cap-dependent endonuclease inhibitor by disrupting the viral mRNA synthesis and viral replication [73]. This agent has shown antiviral activity against both influenza A and B virus and the circulating strains that resist neuraminidase inhibitor. Baloxavir can reduce the viral load within 1 day after drug treatment in a patient with uncomplicated influenza. In one randomized controlled trial, baloxavir had greater efficacy than oseltamivir on adolescents and adults with influenza B infection [74].

Table 2 Antiviral Medications Recommended for Treatment and Chemoprophylaxis of Influenza [72].

Antiviral Drug (Route)	Trade name – Manufacturer	Use	Recommended for	Not recommended for use in	Adverse Events
Oseltamivir (Oral)	Tamiflu, Roach	Treatment (5 days)	Any age	N/A	nausea, vomiting, headache. Post marketing reports of serious skin reactions and sporadic, transient neuropsychiatric events
		Chemo-prophylaxis (7 days)	3 mos and older	N/A	
Zanamivir (Inhaled)	Relenza, GlaxoSmithKline	Treatment (5 days) Chemo-prophylaxis (7 days)	7 yrs and older 5 yrs and older	people with underlying respiratory disease (e.g., asthma, COPD)	risk of bronchospasm, especially in the setting of underlying airways disease; sinusitis, and dizziness. Post marketing reports of serious skin reactions and sporadic,

					transient neuropsychiatric events
Peramivir (Intravenous)	Rapivab, BioCryst Pharmaceuticals	Treatment (1 days)	2 yrs and older	N/A	Diarrhea, vomiting, nausea, and neutrophil count decreased
		Chemo-prophylaxis	Not recommended	N/A	
Baloxavir (Oral)	Xofluza	Treatment (1 days)	12 yrs and older	N/A	none more common than placebo in clinical trials
		Chemo-prophylaxis	Not recommended	N/A	

Abbreviations: N/A = not applicable, COPD = chronic obstructive pulmonary disease.

2.8 Influenza vaccination

The influenza vaccine is an effective way to prevent influenza infection. Nowadays, influenza vaccine is available for the seasonal trivalent vaccine (TIV) which generates from either inactivated influenza antigens or lives attenuated influenza viruses that are derived from two influenzas A strains and one of influenza B strain. Additionally, the quadrivalent influenza vaccine (QIV) formulation is currently available which contains the influenza A and B strains similar to the trivalent vaccine but adds more influenza B strain result in two influenzas A strains and two influenza B strains. Undergoing the rapid evolution of influenza viruses, global influenza surveillance was performed to select the best match vaccine strain against circulating strains (Table 3). Moreover, influenza vaccine production has been provided for both temporal regions including the northern hemisphere (consideration the clinical isolation from October to January) and the southern hemisphere (consideration the clinical isolation between March and August) [75]. In Thailand, the southern hemisphere vaccine has been recommended base on the location, percentage of humidity, temperature and influenza activity (Table 3) [76].

Table 3 The vaccine strain composition of annual influenza vaccine for southern hemisphere that recommended by World Health Organization (WHO) between 2004 and 2020 [75].

Year	Southern hemisphere vaccine			
	A(H1N)	A(H3N2)	Influenza B virus (TIV)	Influenza B virus (QIV)
2004	A/New Caledonia/20/99	A/Fujian/411/2002	B/Hong Kong/330/2001	
2005	A/New Caledonia/20/99	A/Wellington/1/2004	B/Shanghai/361/2002	
2006	A/New Caledonia/20/99	A/California/7/2004	B/Malaysia/2506/2004	
2007	A/New Caledonia/20/99	A/Wisconsin/67/2005	B/Malaysia/2506/2004	
2008	A/Solomon Islands/3/2006	A/Brisbane/10/2007	B/Florida/4/2006	
2009	A/Brisbane/59/2007	A/Brisbane/10/2007	B/Florida/4/2006	
2010	A/California/7/2009	A/Perth/16/2009	B/Brisbane/60/2008	
2011	A/California/7/2009	A/Perth/16/2009	B/Brisbane/60/2008	
2012	A/California/7/2009	A/Perth/16/2009	B/Brisbane/60/2008	
2013	A/California/7/2009	A/Victoria/361/2011	B/Wisconsin/1/2010	B/Brisbane/60/2008
2014	A/California/7/2009	A/Texas/50/2012	B/Massachusetts/2/2012	B/Brisbane/60/2008
2015	A/California/7/2009	A/Switzerland/9715293/2013	B/Phuket/3073/2013	B/Brisbane/60/2008
2016	A/California/7/2009	A/Hong Kong/4801/2014	B/Brisbane/60/2008	B/Phuket/3073/2013
2017	A/Michigan/45/2015	A/Hong Kong/4801/2014	B/Brisbane/60/2008	B/Phuket/3073/2013
2018	A/Michigan/45/2015	A/Singapore/INFIMH-16-0019/2016	B/Phuket/3073/2013	B/Brisbane/60/2008
2019	A/Michigan/45/2015	A/Switzerland/8060/2017	B/Colorado/06/2017	B/Phuket/3073/2013
2020	A/Brisbane/02/2018	A/South Australia/34/2019	B/Washington/02/2019	B/Phuket/3073/2013

Nevertheless, the influenza vaccine for the influenza pandemic and the high pathogenic infection have been developed. These vaccines elicit antibodies specific to the main surface glycoprotein such as hemagglutinin (HA) and neuraminidase (NA). Particularly, hemagglutinin protein is a major protein that induces the host immune response to produce neutralizing antibodies. The action of anti-hemagglutinin antibody and anti-neuraminidase antibody have been shown in Figure 4. Antibodies against HA head domain typically inhibit the step of viral attachment by blocking the interaction

between HA receptors and sialic acid and inhibit the viral egress from the infected cell. While antibodies against the stalk HA can inhibit the fusion and uncoating machinery by disrupting the rearrangement of HA conformation. Besides, stalk HA antibodies may inhibit HA maturation and viral egress. The NA-specific antibodies action on trapping the virus once they come to contact the mucosal surface and binding NA to prevent the viral shedding process. Moreover, both stalk HA and NA-specific antibodies probably able to induce the ADCC and complementary pathway (Krammer F et al., 2015) [77].

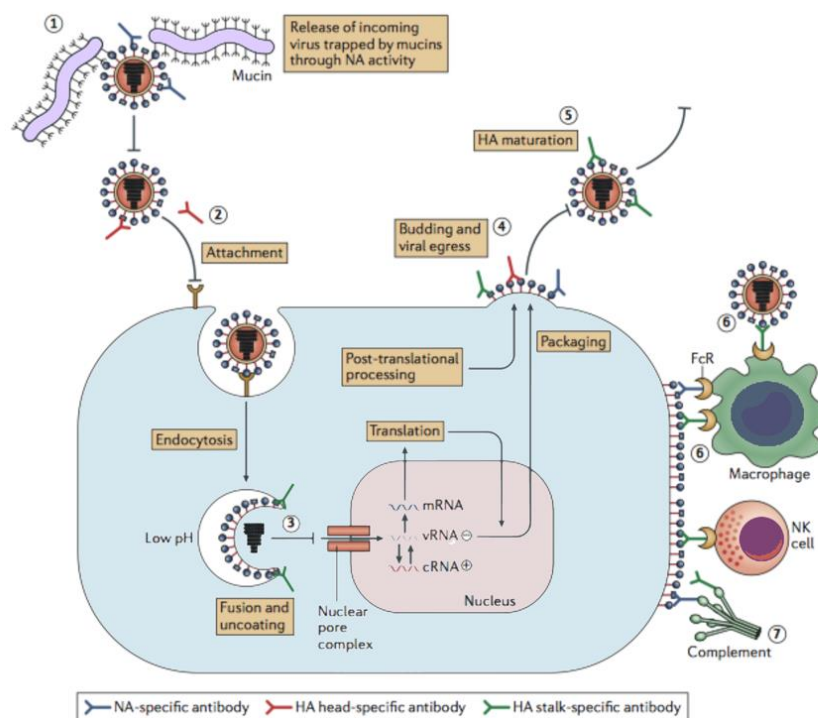


Figure 4 Schematic of the action of anti-Hemagglutinin and anti-Neuraminidase antibodies.

Antibodies directed against the haemagglutinin (HA) globular head domain (red) and the stalk domain (green) or neuraminidase (NA) (blue) may confer protection via several mechanisms. cRNA, complementary RNA; FcR, Fc receptor; NK, natural killer; vRNA, viral RNA (Modified from Krammer F et al., 2015) [77].

Several factors affect the influenza vaccine effectiveness including the type of vaccine administered, host factors such as the health and age of the vaccinated individual, host pre-existing immunity, and the degree of similarity between circulating strain and vaccine strain (CDC VE measure). The type of influenza vaccine currently in the market includes inactivated influenza vaccine (IIV) which is comprised of whole inactivated virus, split virion and virosomal or subunit antigen, live-attenuated influenza vaccine (LAIV) and recombinant influenza vaccine (RIV) (Table 4). Moreover,

many novel types of influenza vaccines still under development such as viral vector, peptide and DNA [78].

Table 4 Type of influenza vaccines

(Grohskopf LA et al., 2020, FDA Thailand) [79].

Type of vaccine	Trade name (Manufacturer)	Age indication	HA (IIVs and RIV4)/dose or Virus count (LAIV4)/dose
IIV4	Afluria Quadrivalent (Seqirus)	6 mos-36 mos	7.5 µg/0.25 mL
		3 yrs- 64 yrs	15 µg/0.5 mL
	Fluarix Quadrivalent* (split virion) (GlaxoSmithKline)	6 mos-36 mos	7.5 µg/0.25 mL
		3 yrs- 64 yrs	15 µg/0.5 mL
	FluLaval Quadrivalent (GlaxoSmithKline)	6 mos-36 mos	7.5 µg/0.25 mL
		3 yrs- 64 yrs	15 µg/0.5 mL
	INFLUENZA VACCINE* (split virion) (GPO-MBP)	6 mos-36 mos	7.5 µg/0.25 mL
		3 yrs- 64 yrs	15 µg/0.5 mL
	INFLUVAC* (split virion) (Abbot Laboratories)	6 mos-36 mos	7.5 µg/0.25 mL
		3 yrs- 64 yrs	15 µg/0.5 mL
	INTANZA (split virion) (Sanofi Pasteur)	6 mos-36 mos	7.5 µg/0.25 mL
		3 yrs- 64 yrs	15 µg/0.5 mL
	Fluzone Quadrivalent* (split virion) (Sanofi Pasteur)	6 mos-36 mos	7.5 µg/0.25 mL
		3 yrs- 64 yrs	15 µg/0.5 mL
FluQuadri Quadrivalent* (split virion) (Sanofi Pasteur)	6 mos-36 mos	7.5 µg/0.25 mL	
	3 yrs- 64 yrs	15 µg/0.5 mL	

ccIV4	Flucelvax Quadrivalent (Seqirus)	≥ 4 mos	15 µg/0.5 mL
	Fluzone-High-Dose Quadrivalent (Sanofi Pasteur)	≥ 65 yrs	60 µg/0.7 mL
alIV4 (MF59 for Adjuvant)	Fluad Quadrivalent * (subunit vaccine) (Biogenetech)	≥ 65 yrs	15 µg/0.5 mL
alIV3	Fluad (subunit vaccine)* (Biogenetech)	≥ 65 yrs	15 µg/0.5 mL
RIV4	Flublok Quadrivalent (Sanofi Pasteur)	≥ 18 yrs	45 µg/0.5 mL
LAIV4	FluMist Quadrivalent (AstraZeneca)	2-49 yrs	10 ^{6.5-7.5} fluorescent focus units/0.2 mL

IIV3 = egg based inactivated trivalent influenza vaccine; IIV4 = egg based inactivated quadrivalent influenza vaccine; cclIV4 = cell culture based inactivated quadrivalent influenza vaccine; LAIV4 = live attenuated quadrivalent influenza vaccine; RIV4 = recombinant quadrivalent influenza vaccine; allV3 = inactivated trivalent influenza vaccine with MF59 as adjuvant; alIV4 = inactivated quadrivalent influenza vaccine with MF59 as adjuvant. Asterisk indicated the influenza vaccines available in Thailand.

Due to antigenic drift, accumulated mutation typically occurs and leads the virus to evade the existing immunity result in necessary reformulating the vaccine strains every year. Nevertheless, the current influenza vaccine still has some limitations including limited efficacy in the aging population, lack of cross-protective immune response and poor immunogenicity of the antigen. Several of these issues lead to improve the seasonal influenza vaccine.

2.8.1 High-Risk group

According to the Advisory Committee on Immunization Practices (ACIP) recommendation, the annual influenza vaccine is recommended for all people aged more than 6 months who do not have contraindications[80]. However, the influenza vaccination should be emphasized to vaccinate in the high-risk groups who at risk of infection and might be vulnerable to medical complications which attribute to

influenza-associated severity. In Thailand, the Ministry of Public Health (MoPH) has provided the influenza vaccine for risk groups and start for the vain nation to patients in April annually since 2004 [81]. The high-risk groups are indicated as follows. Young children aged 6 through 59 months who have not been exposed to the influenza virus are moderately susceptible to influenza infection and can cause a sudden high fever with moderate to severe symptoms. The young children are seen to be the human transmitter that generally contagious large number of viral particles to other individuals, vaccinated influenza vaccine can also reduce the rate of transmission. Older adult, the persons who have chronic pulmonary (including asthma), cardiovascular (excluding isolated hypertension), renal, hepatic, neurologic, hematologic, or metabolic disorders (including diabetes mellitus), immunocompromising condition, and the individual who are extremely obese (body mass index ≥ 40 for adults) are also recognized at increased risk of severe influenza disease and influenza-associated complications. Pregnant women are also considered at risk factors for severe illness after infection because of the effect of pregnancy on the immune system and raised cardiopulmonary demands. In addition, the elderly who aged greater than 65 years are considered vulnerable populations because of the decline in systemic immunity, which is typically known as immunosenescence, that can reduce the vaccine effectiveness and also lead the aging individual to develop influenza associated complications. To improving the vaccine efficacy in the elderly, several strategies were applied including a high-dose vaccine which increasing the amount of HA per strain from the standard dose 15 μg to 60 μg , adding adjuvants such as water emulsion (MF59) and changing the route delivery such as intradermal immunization [82].

CHULALONGKORN UNIVERSITY

2.9 Antigenic sites on HA and receptor binding sites

Hemagglutinin (HA) protein

Native HA is synthesized as a single polypeptide (HA0) that is cleavage by furin proteolytic enzyme results in HA1 and HA2 [66]. Influenza virus HA has two significant biological roles in (i) HA1 facilitate viral attachment by binding host cell sialic acid-containing receptors and (ii) HA2 mediate fusion between the viral membrane and the endosomal membrane during viral uncoating leading to release of the viral RNP complex into the cytoplasm of the infected cell. In addition, HA1 is a major target of neutralizing antibodies that also under constant immune selection pressure. Thus, the virulence of the influenza virus can be affected by an amino acid mutation on receptor binding site or amino acid that close proximately to the primary receptor-binding site

on HA1 protein. Therefore, the accumulated point mutations in HA by antigenic drift mechanism, particularly in HA1 can allow the virus to escape neutralizing antibodies [68]. The antigenic site of influenza epitopes (HA1) defines as amino acid residues of the antigen which was contacted with amino acid residues of influenza neutralizing antibody. One neutralizing antibody does not have the ability to bind the whole amino acid residues in the antigenic site but the epitopes in the same antigenic sites may be overlapping therefore one amino acid residues within the antigenic site can affect the ability for binding several antibodies. According to the previous study, A(H1N1)pdm09-HA has four major antigenic sites, which were identified by studies using A/Puerto Rico/8/34 (H1N1) and can define four classical antigenic sites (Ca 1/2, Cb, Sa and Sb) and influenza A(H3N2) virus has identified into five clusters of antigenic sites comprise of A-E [83]. In addition, the recent study identifies the antigenic site of A(H1N1)pdm09 base on influenza A(H3N2) and can divide five clusters like A(H3N2), these five clusters (A-E) of the antigenic site are also overlapped the classical antigenic sites of influenza A(H1N1)pdm09. Antigenic site of influenza B virus also identifies into four major epitopes on the membrane-distal globular domain of influenza B virus HA: the 120-loop, the 150-loop, the 160-loop and the 190-helix and their respective surrounding regions and shown in following (Table 5).

Table 5 HA numbering of amino acid residues in defined antigenic sites and the receptor-binding site of the influenza virus.

The amino acid positions on antigenic sites and receptor binding sites of both influenza A(H1N1)pdm09 and A(H3N2) were based on the H1 numbering. While the amino acid positions on epitopes and receptor binding sites of the influenza B virus were shown as HA numbering.

Subtype	Functions		HA numbering amino acid residues	Ref
A(H1N1)	Antigenic sites	Ca	137,138,139,140,141,142,166,167,168,169,170,203,204,205,221,222,235,236,237	[83, 84]
		Cb	70,71,72,73,74,75	
		Sa	124,125,153,154,155,156,157,159,160,161,162,163,164	
		Sb	184,185,186,187,188,189,190,191,192,193,194,195	
	Receptor binding site		94,131,133,150,152,180,187,190,191,223,225	[85]
A(H3N2)	Antigenic sites	A	122,124,126,130,131,132,133,135,137,138,140,142,143,144,145,146,150,152,168	[86, 87]
		B	128,129,155,156,157,158,159,160,163,164,165,186,187,188,189,190,192,193,194,196,197,198	
		C	44,45,46,47,48,50,51,53,54,273,275,276,278,279,280,294,297,299,300,304,305,307,308,309,310,311,312	

	Receptor binding site	D E	96,102,103,117,121,167,170,171,172,173,174,175,176,177, 179,182,201,203,207,208,209,212,213,214,215,216,217,218, 219,226,227,228,229,230,238,240,242,244,246,247,248 57,59,62,63,67,75,78,80,81,82,83,86,87,88,91,92,94, 109,260,261,262,265 98,134,135,136,137,138,153,155,183,190,194, 195,224,225,226,227,228	[66]
Influenza B virus*	Antigenic sites	120-loop 150-loop 160-loop 190-helix	75, 77, 116,118,122,129,137 141, 144,145,146,147,148,149,150,151 162,163,164,165,167 194,195,196,197, 198, 199,200, 201, 201,202, 238	[88]
	Receptor binding site**		95, 136, 137, 138, 139, 140, 141,142, 150, 158, 159, 160, 190, 191, 192, 193, 194,195, 196, 197, 200, 201, 237, 238, 239, 240, 241	[89]

* Residues of antigenic of influenza B virus base on HA numbering of B/Hong Kong/8/1973 (B/HK/73)

** receptor binding site of influenza B virus base on HA numbering of B/Yamanashi/98

2.10 Influenza evolution

Influenza viruses are evolutionarily dynamic pathogens that can evolve rapidly due to genetic variation lead to accumulating mutations on the eight segmented genome particularly surface glycoprotein HA and NA. The accumulated genetic changes occur because the viral RNA-dependent RNA polymerase (RdRp) lacks proofreading function. The rate of faulty nucleotides during viral replication estimate 10^{-3} to 10^{-4} [90]. Undergoing the evolution changes among the influenza virus, the three mechanisms have been identified including point mutations (antigenic drift), reassortment (antigenic shift) and recombination (rarely occur among influenza virus).

The point mutations occur when the viral replication due to the error-prone of polymerase enzyme resulting in accumulation of mutation especially in the antigenic site which is also known as “antigenic drift” [91]. The significant substitutions in the epitopes of HA and/or NA of the new virion resulting from continuing points mutations which lead the antigenic properties to migrate from the wild type. The new variants continually produce during viral replication result in mixing populations with several variants, some of them acquire the beneficial mutations that lead them to become predominate circulating under the selection pressure. As consequence, pre-existing immunity in the population is unable to detect the new variants anymore. Furthermore, some mutations in the NA gene can promote the resistance of commonly antiviral drugs such as oseltamivir [92]. Therefore, fast-evolving viruses like the

influenza virus should be tracked in real-time to understand their evolution dynamics and monitor when the new variants outbreak. Although the number of faulty nucleotides would represent the rate of mutations per unit time, it was difficult to determine because it required more experiments of viral replication. There is a biological computational tool for the alternative way that is used to estimate the rate of nucleotide substitutions. The Bayesian Evolution Analysis by Sampling Trees (BEAST) software has become a primary tool used for time scale trees, phylodynamic and evolution analysis which provide the rate of viral nucleotide substitutions [93]. The nucleotide substitutions rate in DNA sequences is defined as the number of nucleotide substitutions per site per unit time (commonly years). Moreover, the point mutations accumulated in the non-antigenic gene are also associated with increasing the virulence of virus, pathogenicity, transmission rate and drug resistance [94].

Influenza virus can be able to exchange their segmented genome between intra or inter influenza subtype through co-infection in the same cells which this mechanism has been well recognized as re-assortment. The re-assortment can achieve the new antigenic pattern by exchange HA and NA gene which is known as “antigenic shift” that could generate the new strain and/or subtype and often associated with the pandemic of the influenza virus outbreak. There is evidence confirming that three major pandemics in human-caused by re-assortment between human influenza A virus and other host species including the H2N2 in 1957, H3N2 in 1968 and H1N1 in 2009. The HA, NA and PB1 gene of the H2N2 pandemic strain in 1957 and HA and PB1 segmented of the H3N2 pandemic strain in 1968 acquired from avian influenza virus, and reassorted the remaining gene segment with human influenza virus in 1918. While the H1N1 pandemic2009 acquired the triple re-assortment between the European H1N1 swine influenza virus (NA, M), North American H1N2 swine influenza virus (PB2, PA), influenza A(H3N2) (PB1) and classic swine influenza virus (HA, NP, NS) [95]. The proofreading errors of viral RNA polymerase, immune pressure, antiviral drug pressure, the novel environment of host were identified as the cause of these modifications [96].

Besides, recombination is another mechanism relatively with viral evolution but rarely occurs among influenza viruses. The evidence reveals that the genetic recombinant is one of the initial processes to generate the genetic diversity upon which natural reaction acts. There are two main mechanisms of influenza virus recombination comprise of non-homologous recombination that appeared between two distinct RNA segments and controversial homologous recombination that occur during the template-switching process while polymerase acts on viral replication [97].

2.11 Summary and significance in this study

To date, the influenza virus remains a global problem in all parts of the world. Apart from continuous monitoring influenza epidemic, development of universal influenza vaccine and effective antiviral agents as well as effective management and strategy are required to control the currently circulating strains and further new variant of influenza virus outbreak. It is necessary to study epidemiology, what environmental factors affect the influenza epidemic, the molecular genetics and evolution analysis of influenza virus that might explain how they escape the pre-existing immunity and what adaptive genetic changes. Deep knowledge may lead to a better understanding of viral pathogenesis and the development of new therapeutic approaches for treatment and prevention. Continued monitoring of influenza infection is necessary for assisting awareness and facilitating disease management and effective intervention.



CHAPTER III

CLIMATE FACTORS INFLUENCE SEASONAL INFLUENZA ACTIVITY IN BANGKOK, THAILAND

(Published in: PLoS ONE. 2020 Sep; 15(9): e0239729.

DOI: <https://doi.org/10.1371/journal.pone.0239729>)

Nungruthai Suntronwong¹, Sirapa Klinfueng¹, Sumeth Korkong¹, Preeyaporn
Vichaiwattana¹, Thanunrat Thongmee¹, Sompong Vongpunsawad¹, Yong Poovorawan¹

¹Center of Excellence in Clinical Virology, Faculty of Medicine, Chulalongkorn
University, Bangkok, Thailand 10330

จุฬาลงกรณ์มหาวิทยาลัย
CHULALONGKORN UNIVERSITY

CHAPTER III

Part 3.1: Climate Factors Influence Seasonal Influenza Activity in Bangkok, Thailand.

Summary

Yearly increase in influenza activity is associated with cold and dry winter in the temperate regions, while influenza patterns in tropical countries vary significantly by regional climates and geographic locations. To examine the association between influenza activity in Thailand and local climate factors including temperature, relative humidity, and rainfall, we analyzed the influenza surveillance data from January 2010 to December 2018 obtained from a large private hospital in Bangkok. We found that approximately one in five influenza-like illness samples (21.6% or 6,678/30,852) tested positive for influenza virus. Influenza virus typing showed that 34.2% were influenza A(H1N1)pdm09, 46.0% were influenza A(H3N2), and 19.8% were influenza B virus. There were two seasonal waves of increased influenza activity. Peak influenza A(H1N1)pdm09 activity occurred in February and again in August with lesser to extend of influenza B virus, while influenza A(H3N2) viruses were primarily detected in August and September. Time series analysis suggests that increased relative humidity was significantly associated with increased influenza activity in Bangkok. Months with peak influenza activity generally followed the most humid months of the year. We performed the seasonal autoregressive integrated moving average (SARIMA) multivariate analysis of all influenza activity on the 2011 to 2017 data to predict the influenza activity for 2018. The resulting model closely resembled the actual observed overall influenza detected that year. Consequently, the ability to predict seasonal pattern of influenza in a large tropical city such as Bangkok may enable better public health planning and underscores the importance of annual influenza vaccination prior to the rainy season.

Introduction

Influenza virus infection is a major cause of acute respiratory disease and contributes to significant morbidity and mortality each year [98]. Seasonal pattern of influenza varies throughout the temperate, tropical and sub-tropical regions of the world [99]. In the temperate regions of both northern and southern hemisphere, influenza activity peaks during the cold winter months and is linked to increased person-to-person transmission in indoor close-contact settings and low absolute humidity [100-105]. In tropical regions, different patterns of influenza activity are observed [106, 107]. Inter-tropical belt region shows highly heterogeneous timing of influenza epidemics in which some countries have an annual peak coinciding with rainy season, biannual peaks of influenza activity, or no distinct seasonality at all.

Previous studies have examined the meteorological factors conducive to influenza transmission in different parts of the world. In temperate regions, a study in the U.K. suggests that both influenza A and B viruses preferred low temperatures and dew points [108], while a study in Canada observed that increased influenza A virus detection was associated with increased relative humidity and low temperature [109]. Results from studies in tropical regions, however, are inconsistent depending on the location and the study period. In the tropical Republic of Côte d'Ivoire, rainfall was a good predictor of influenza activity [110], while in Uganda, influenza A(H1N1) but not influenza A(H3N2) and B activity was associated with lower precipitation [111]. In Central America, the overall influenza activity was consistently associated with increased specific humidity, but temperature and the amount of rainfall were associated with influenza activity in only certain locations [112].

Influenza pattern in tropical Southeast Asia has been less well-studied compared to that in industrialized countries. Although influenza outbreaks fluctuate seasonally, major influenza activity often coincides with the rainy season in Cambodia, Laos PDR, Myanmar and the Philippines [113-116]. Thailand experiences primary influenza activity during the rainy season, with an additional secondary peak of less magnitude at the beginning of the year [117]. Meanwhile, some studies in Indonesia, Singapore, and Vietnam reported no consistent pattern of influenza peak [114, 118, 119]. Circulating influenza virus strains in Southeast Asia have mostly been A(H1N1)pdm09, A(H3N2), and influenza B virus [120]. Yet, few studies have examined in-depth the seasonality of influenza with local climates. It was reported that increasing temperature and humidity has been linked to increased influenza activity in the Philippines and Vietnam [99, 121]. However, neither temperature nor humidity was

positively associated with influenza A and B virus in Singapore [122].

In Thailand, data from suspected influenza cases suggest that temperature and relative humidity, but not rainfall, correlated with the overall influenza activity in central Thailand[123]. In that study, information regarding individual influenza virus (sub)types were not available, and the prediction models for influenza activity differed depending on geographical regions. It was possible that the diversity of regional climates, such as in the higher elevations of the north, the sea-bound southern peninsula, and the low elevation of the central plain, may also complicate the generalization of climate influence on influenza activity within the country. Bangkok is situated in central Thailand adjacent to the Gulf of Thailand where the prevailing hot and humid weather is disrupted by the cooler and drier air from the north a few weeks each year (typically between December and February)[124]. Since fluctuating climate factors may influence the seasonality of influenza activity in and around metropolitan Bangkok, we examined the multi-year incidence of influenza virus infection and how different influenza virus (sub)types were associated with the monthly meteorological factors of temperature, relative humidity, and rainfall. Using time series analysis, we examined potential forecasting models for influenza activity. Improved understanding of the seasonal pattern of influenza virus infection for a large urban area may guide public health policies on the optimal timing of influenza vaccination in the country.



Materials and Methods

Ethical approval

The study was approved by the Institutional Review Board of the Faculty of Medicine of Chulalongkorn University (IRB No. 127/61). Consent was not obtained because the data were analyzed anonymously.

Laboratory testing of influenza virus

From January 2010 to December 2018, 30,852 nasopharyngeal or throat swab samples from patients with influenza-like illness (ILI) from Bangkok 9 International Hospital (latitude 13.75 °N and 100.55 °E longitude) in Bangkok were analyzed as part of an ongoing influenza surveillance [120, 125]. We defined ILI as fever >38 °C accompanied by cough and/or sore throat. Respiratory specimens arrived with limited patient information and included only age and gender. Samples were tested by using real-time reverse-transcription polymerase chain reaction to identify influenza A(H1N1)pdm09, A(H3N2) and influenza B virus as previously described [126].

Meteorological data

Data on the monthly average temperature (°C), rainfall (cm³), and relative humidity (%) from January 2010 to December 2018 were available from Wolfram Alpha database [124]. They were recorded at VTBD (Don Mueang International Airport) in Bangkok (latitude 13.91°N and 100.6 °E longitude).

Data analysis

Monthly incidence of influenza was compiled based on the sample collection date. Percentages of monthly influenza virus-positive samples relative to all ILI samples each month were determined. Univariate analysis of the meteorological variables including average temperature, relative humidity and rainfall was done on data between influenza-active months and months without influenza activity using Mann-Whitney U test. An influenza-active month was defined as a month in which the proportion of the confirmed influenza cases was equal to or greater than a fixed threshold of 10% [107, 127]. This was calculated by dividing the monthly confirmed influenza cases by each year's total number of influenza virus-positive samples [24].

To examine the seasonality of influenza, we applied a generalized linear model (GLM) with Gaussian and Poisson distribution on the monthly values of climate variables and laboratory-confirmed influenza cases, respectively [128]. A seasonal model in the waveform with a period of 12 months was then established with the estimated parameters from the GLM [108, 129].

Cross-correlation analysis and forecasting model

We initially examined the relationships between each influenza virus (sub)type and all influenza activity with respect to meteorological variables. The monthly confirmed cases of influenza A(H1N1)pdm09, influenza A(H3N2), influenza B, and all influenza viruses were considered as dependent variables. Monthly values of mean temperature, relative humidity, and accumulated rainfalls were considered as independent variables. Cross-correlation analysis was conducted to assess the relationship between virus incidence and various meteorological factors, and for relationships among influenza A(H1N1)pdm09, influenza A(H3N2), and influenza B virus with different lag times (defined as the difference between time of maximum climate factor values and time of maximum influenza incidence) of between 1 to 4 months [123].

We considered four forecast models for individual and all influenza viruses using dependent variables from influenza A(H1N1)pdm09 (model 1), influenza A(H3N2) (model 2), influenza B (model 3), and all influenza viruses (model 4). For each model, we also considered potential association among different influenza viruses. Climate factors were considered as independent variables or proxy predictors in forecasting future influenza activity. Time series analysis was conducted to identify the best-fit model for each influenza (sub)type and for all influenza viruses in two ways. A univariate time series used past data as dependent variables to predict the future, while multivariate time series used the combined data from dependent and independent variables for prediction. The forecast model used data from January 2011 to December 2017 to calibrate and estimate the parameters. The last 12 months of data were used to test the forecasting ability. Data from 2010 were excluded due to bias from the influenza pandemic of 2009.

The Auto-Regressive Integrated Moving Average (ARIMA) (p,d,q) model was used in this study. The parameter p represents maximum lag in the auto-regression (AR). The non-seasonal differencing (d) is the order of integration (I) and represents the number of differences required to make the series stationary. The parameter q of the moving average (MA) represents the linear regression of the output value on the time series when compared with the current and previous terms[130]. Additionally, seasonal autoregressive integrated moving average model SARIMA $(p,d,q)(P,D,Q)_s$ was also used. The parameters P , D , Q , and s represent the order of seasonal AR, the degree of seasonal differencing, the seasonal moving average, and the season's length, respectively[131].

Forecasting incidence by using ARIMA model involved four steps. First, we used the augmented Dickey-Fuller (ADF) and the Kwiatkowski-Phillips Schmidt-Shin (KPSS) tests to assess whether the individual time series was stationary. The log-transformation and/or differencing was applied to render the data stationary when necessary. Second, autocorrelation function (ACF) and partial autocorrelation function (PACF) were applied to estimate p and q based on the cutoff time lag. The P and Q order was obtained from ACF and PACF peak at time s lags. Third, residual diagnosis and Ljung-Box (modified Box-Pierce) test was used to identify the possibility of the model and to diagnose white-noise. Finally, the Ljung-Box portmanteau test was applied to determine whether there was a lack-of-fit of the residuals of the time series. The null hypothesis was that the model does not exhibit lack-of-fit. It was expected that the test failed to reject the null hypothesis and that the residuals series showed white noise ($p\text{-value} > 0.5$)[132].

The model goodness-of-fit was taken into account the root-mean square error (RMSE), the mean absolute percentage error (MAPE), and the corrected Akaike's Information Criterion (AICc). The lowest parameter values suggest the optimal model [133]. For multivariate model, only climate variables that provided significant lagged effect and presented the highest correlation coefficient among lag 1 up to lag 4 were considered [123, 134]. All statistical analysis was performed in SPSS version 23 (SPSS Inc., USA) and R version 3.6.0 (R Foundation, Vienna, Austria)[135]. Alpha of 0.05 denotes statistical significance.

Results

Influenza surveillance

In this study period, 6,678 (21.6%) of the ILI samples tested positive for influenza virus (Table 6). Of these, 80.2% (5,357/6,678) were influenza A virus and 19.8% (1,321/6,678) were influenza B virus. Influenza A virus subtypes identified were 34.2% A(H1N1)pdm09 and 46.0% A(H3N2). From 2010 to 2018, overall influenza cases generally peaked in and around August to September, which coincided with the rainy season (Figure 5). Biannual frequency of predominantly influenza A(H1N1)pdm09 virus was more apparent than that of influenza B virus.

Table 6 Influenza virus-positive samples and monthly average meteorological factors.

	Positives (%)	Mean (SD) ^b
All influenza virus	6,678 (21.6) ^a	18.93 (10.20)
A(H1N1)pdm09	2,282 (34.2) ^c	5.8 (7.19)
A/H3N2	3,075 (46.0) ^c	9.13 (8.11)
B	1,321 (19.8) ^c	4 (4.26)
Meteorological factors		
Temperature (°C)	-	28.73 (1.71)
Relative humidity (%)	-	73.32 (4.96)
Rainfall (cm ³)	-	9.11 (9.46)

^a All influenza virus-positive samples divided by all ILI samples submitted.

^b Mean and standard deviation (SD) were calculated from the monthly percentage of influenza positives relative to all monthly ILI samples.

^c The number of specific influenza virus divided by all influenza virus-positive samples.

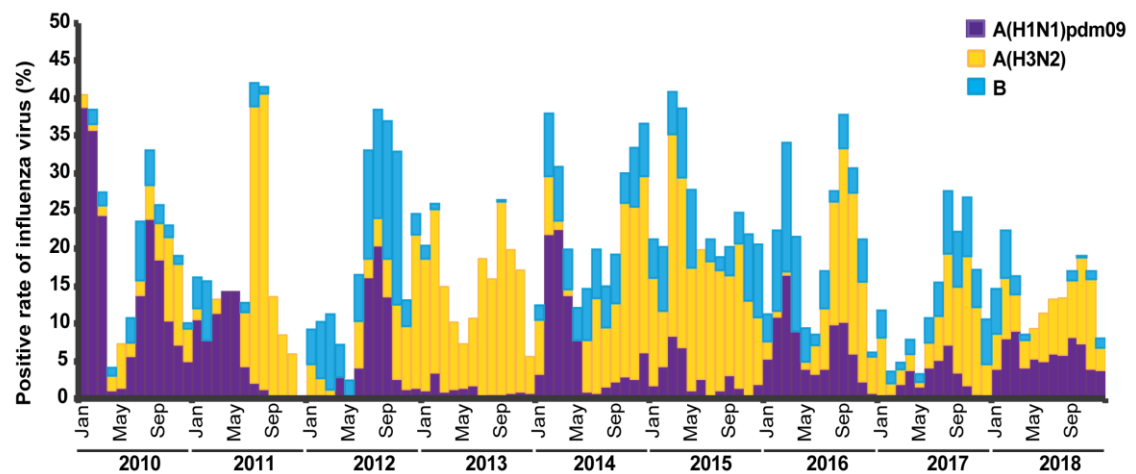


Figure 5 Monthly distribution of influenza activity from 2010 to 2018.

Bar graph represents the proportion of ILI samples tested positive for seasonal influenza A(H1N1) (purple), influenza A(H3N2) (yellow), and influenza B (blue) virus each month.

Climate factors and influenza activity

We hypothesized that certain climate factors were associated with increased influenza activity, therefore we examined monthly variations in the average temperature, relative humidity, and rainfall with respect to the monthly number of confirmed influenza virus infection. Average monthly temperature was typically highest from April to May (29-33 °C) and lowest in January (23-28 °C) (Fig 6A). January was also the least humid month (65-73%), while the period from September to October experienced the highest relative humidity (76-82%) and coincided with the rainy season in Bangkok (Fig 6B). Increases in the relative humidity concurred with increases in confirmed influenza A(H3N2) virus. Although the amount of rainfall varied throughout the study period, most rainfall occurred in September (10-40 cm³) (Fig 6C). However, the amount of rainfall did not correlate with the fluctuations of any influenza virus. When we evaluated the influence of climate factors in the months with and without substantial influenza activity, we found that only relative humidity significantly correlated with influenza virus (Table S1).

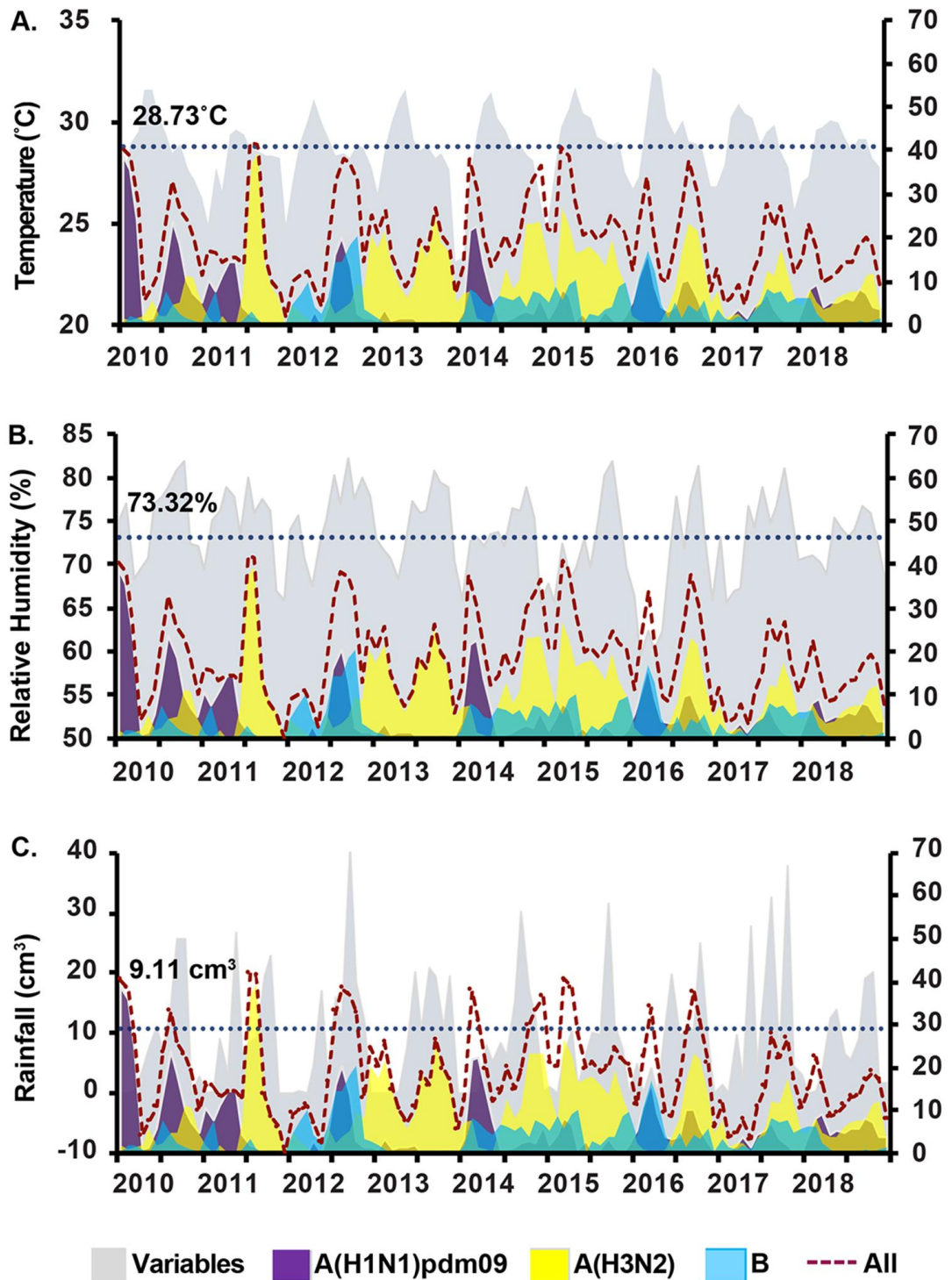


Figure 6 Incidence of influenza virus relative to meteorological factors.

Monthly mean temperature (A), relative humidity (B), or rainfall (C) (shaded gray) are shown with the confirmed cases of influenza A(H1N1)pdm09 virus (purple), influenza A(H3N2) virus (yellow), influenza B virus (blue), and all influenza viruses (dashed line). Scale on the right Y-axis denotes the percentage of the influenza virus-positive

samples each month. Dotted horizontal line indicates the overall average temperature (28.73 °C), relative humidity (73.32%), and rainfall (9.11 cm³) over nine years (left Y-axis).

Analysis by GLM suggests that increased influenza activity occurred twice a year (Figure 7). The first and smaller wave of increased influenza activity was in February, which corresponds to the beginning of hot and dry weather. The second and larger influenza wave occurred between August and September, which coincides with the second half the rainy season. Both periods represented increased influenza A(H1N1)pdm09 and influenza B virus activity. Meanwhile, influenza A(H3N2) activity was only associated with the second wave, which coincided with higher relative humidity and rainfall and occurred approximately 5 months after the first influenza A(H1N1)pdm09 peaked. As expected, GLM showed no association between influenza activity and temperature.

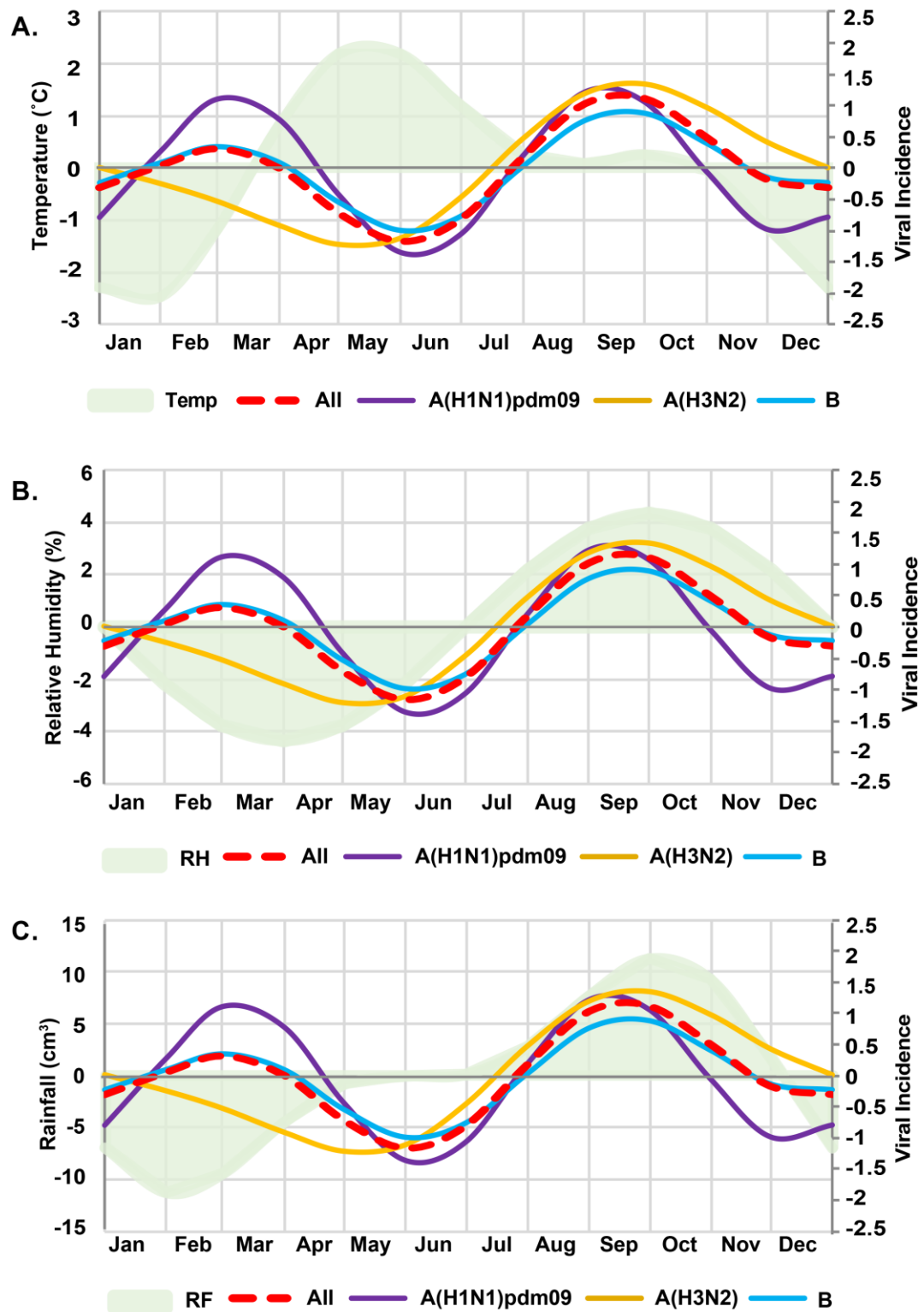


Figure 7 Yearly influenza incidence and the periodic fluctuation of climate factors.

Generalized linear models depict the incidence of influenza virus each month (colored waves) relative to the monthly mean values of climate factors (shaded). The left Y-axis represents the z-score of the (A) mean temperature (Temp), (B) relative

humidity (RH), and (C) rainfall (RF). The right Y-axis represents the differences in the viral incidence for all influenza viruses (red dashed line), influenza A(H1N1)pdm09 virus (purple line), influenza A(H3N2) virus (yellow line), or influenza B virus (blue line). The highest point on the wave indicates the time of year influenza virus detection peaked.

Identifying the ARIMA(X) model

We next examined the time delay in the association between climate factors and the incidence of influenza. This was defined as the time difference in months between the peak of a climate factor and the peak of an influenza virus activity (e.g., lag 1 represents 1 month difference). We found that there was no significant association between influenza A(H1N1)pdm09 activity with any meteorological variables (Fig 8A). Influenza A(H3N2) showed a moderately positive correlation with the mean temperature of lag 4 ($r = 0.65$, $p < 0.001$), and with relative humidity and rainfall of lag 1 ($r = 0.47$ and $r = 0.44$, respectively) ($p < 0.001$) (Fig 8B). Additionally, influenza B was positively correlated with temperature at lag 4 ($r = 0.37$, $p < 0.05$) (Fig 8C). To determine the correlation among influenza (sub)types, weakly negative correlation was found between influenza A(H1N1)pdm09 and influenza A(H3N2) at lag 4 ($r = -0.26$, $p < 0.05$). In contrast, influenza A(H1N1)pdm09 showed strongly positive correlation with influenza B virus ($r = 0.63$, $p < 0.001$). All influenza activity showed positive correlation with the mean temperature at lag 4 ($r = 0.62$, $p < 0.001$), and relative humidity and rainfall at lag 1 ($r = 0.32$ and $r = 0.3$, respectively) ($p < 0.05$) (Fig 8D).

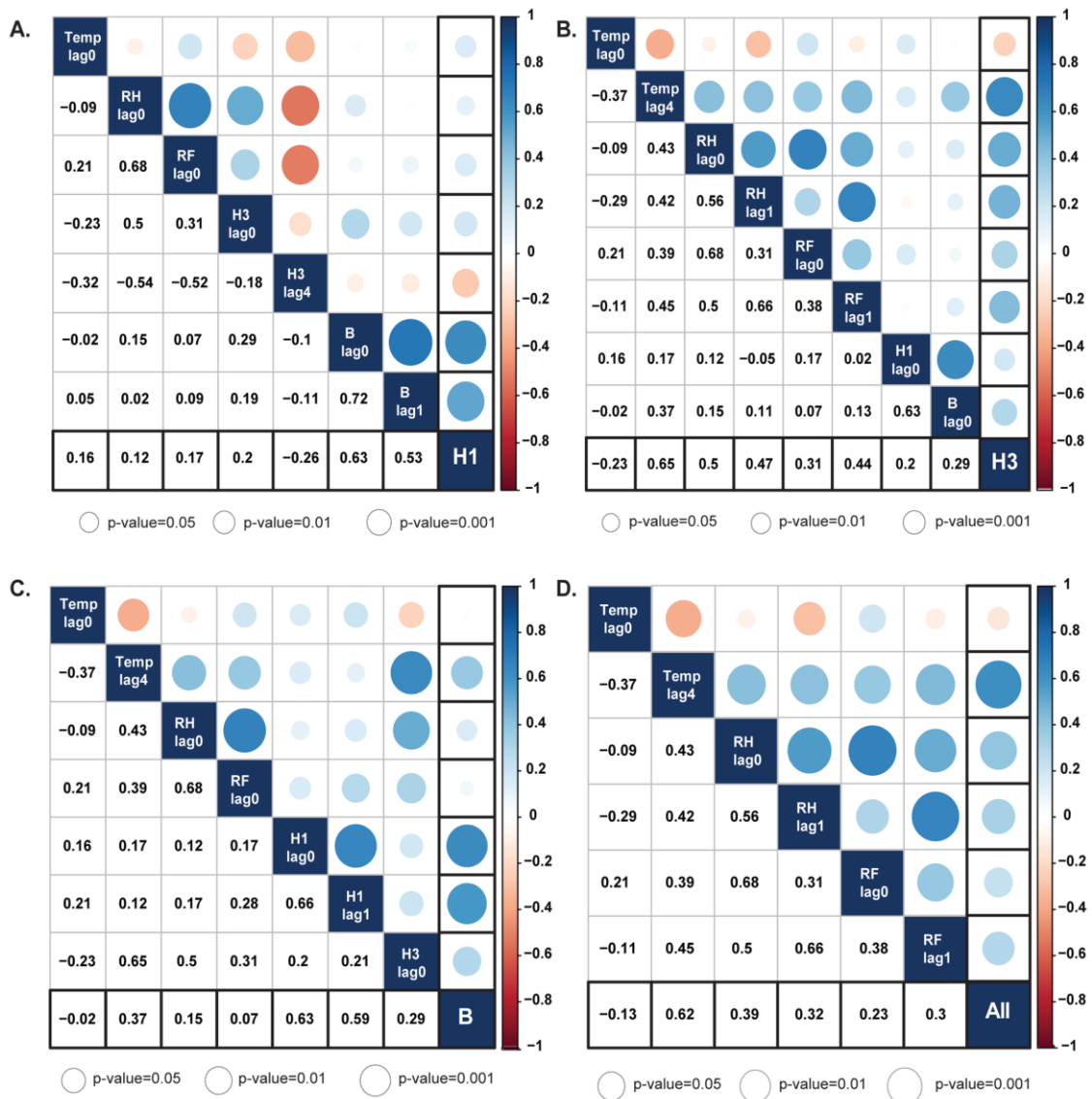


Figure 8 Association between meteorological factors and influenza virus.

Correlation analysis of (A) influenza A(H1N1)pdm09 virus, (B) influenza A(H3N2) virus, (C) influenza B virus, and (D) all influenza viruses against climate variables and in the presence of co-circulating viruses at different lag times. Spearman's rank cross-correlation coefficients ranged from -1 to 1. Negative value equates to negative association as indicated by red circles, and positive value equate to positive association as indicated by blue circles. Circle size represents the magnitude of the p-value. Color intensity represents the strength and weakness of the correlation (right scale). Temp, mean temperature; RH, relative humidity; RF, rainfall.

To identify the best-fitting model for the observed values, we performed the \log_{10} transformation on the dependent variables to obtain a stationary time series

(Figure S1). We then computed the suitable univariate and multivariate ARIMA models. For multivariate model, variables which provided significant correlation were selected as predictors (Table S2). The appropriate ARIMA models for individual influenza (sub)type and all influenza viruses were established (Figure S2 and S3) by comparing the AICc values between the univariate and multivariate time series. We found that multivariate ARIMA model using both influenza incidence and climate factors provided better goodness of fit than the univariate ARIMA model, which used only influenza incidence (Table S3). It also performed better and had reduced errors (RMSE and MAPE) than the univariate model. For influenza A(H1N1)pdm09, the SARIMA(2,1,1)(0,1,1)₁₂ of multivariate time series gave a better forecast (RMSE = 0.89, MAPE = 22.99%), while the SARIMA(1,0,2)(1,1,0)₁₂ model combined with all climate factors for influenza A(H3N2) provided lowest forecasting error (RMSE = 0.77, MAPE = 22.47%). In addition, the multivariate ARIMA(3,0,3)₁₂ fitted well for influenza B when combined with temperature and influenza A(H1N1)pdm09 (RMSE = 1.14, MAPE = 46.09%). The SARIMA(2,0,1)(1,0,0)₁₂ with the mean temperature at lag 4, relative humidity at lag 1, and rainfalls at lag 1 was the selected multivariate model with the best forecast value, which took into account all influenza and climate factors (RMSE = 0.15, MAPE = 2.81%). Fitted graphs derived from the univariate and multivariate analysis of the time series (Figure 9) showed that the multivariate models were better able to capture the observed influenza activity during 2018 than the univariate models. Overall, the forecast model using all influenza activity and all climate factors performed better than the forecast model of individual (sub)type.

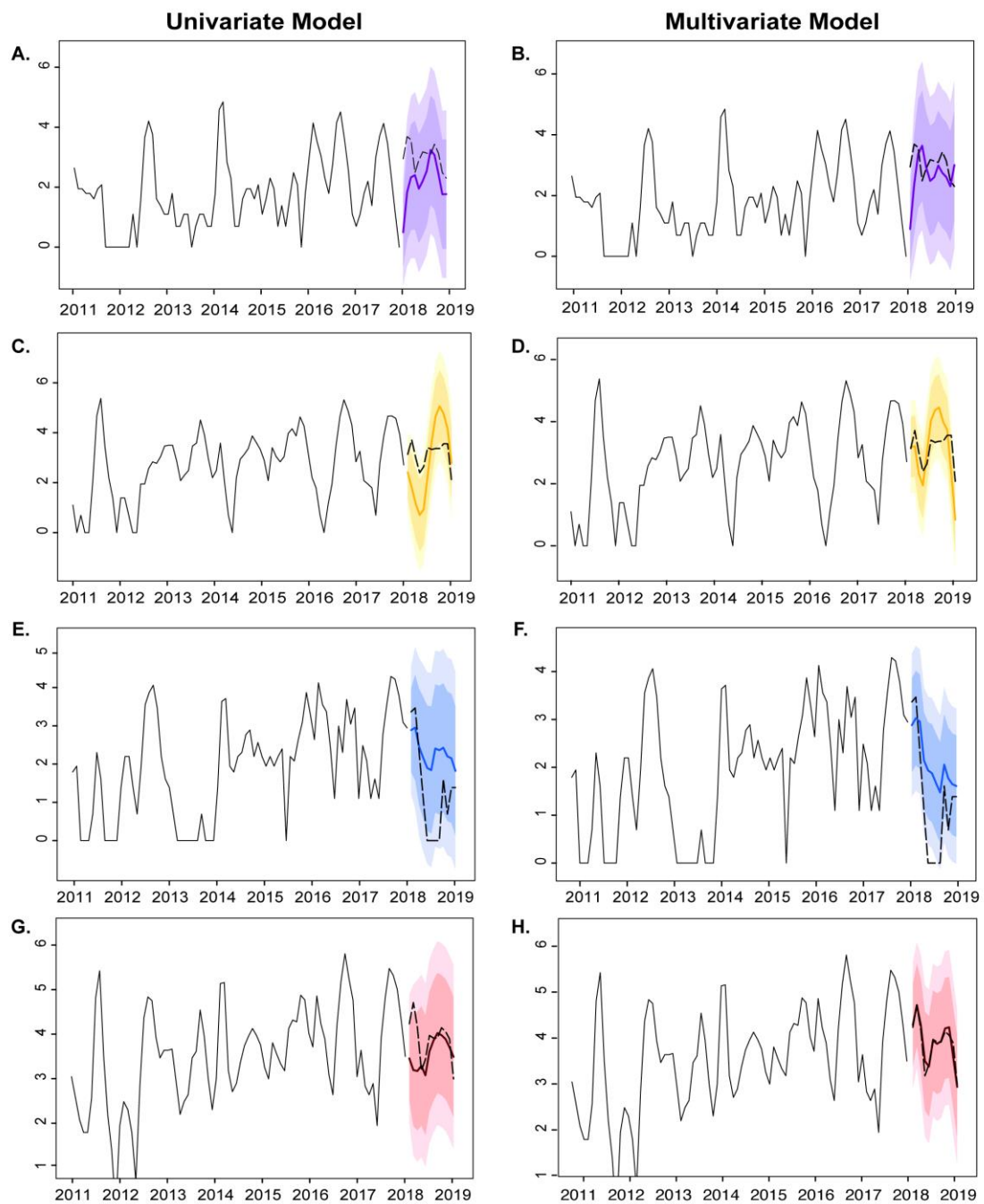


Figure 9 Seasonal $ARIMA(p,d,q)(P,D,Q)_{12}$ fitted time series analysis

for individual influenza (sub)type and all influenza virus activity in the different forecasting models. Time series for influenza A(H1N1)pdm09 (A, B), influenza A(H3N2) (C, D), influenza B (E, F), and all influenza virus (G, H) activities are shown in black (January 2011 to December 2017) and dashed (January 2018 to December 2018) lines. Colored lines represent the predicted seasonality trends for 2018 using univariate (left panels) or multivariate (right panels) analysis with the 90% (darker shade) and 95% (lighter shade) confidence intervals shown.

Discussion

Influenza is prevalent throughout the year in some countries with tropical climate [103]. In Thailand, increased influenza activity appears biannually typically in the rainy (June-August) and cool (December-February) seasons [117, 120, 125]. Our multi-year study confirmed the substantial decrease in influenza activity following the relatively hot and dry month of May, which precedes the rainy season and coincides with the yearly recommended influenza vaccination period in Thailand [76, 136]. We found that the first wave of influenza activity in a typical year involves A(H1N1)pdm09, and to a lesser extent influenza B virus, both of which peaked in February and again in August-September. The second and major wave of influenza activity occurs around August-September in which all influenza viruses co-circulate. The observation that influenza A(H1N1)pdm09 activity increases during the periods of low (February-May) and high (August-October) relative humidity has previously been reported and suggests that humidity extremes along with temperatures influence influenza virus survival and/or transmission in a complex way [101, 137-139].

Our findings add to the accumulating evidence that climate factors do affect the incidence of influenza in Southeast Asia. Our study showed that overall influenza positively correlated with relative humidity (up to lag 1) and rainfall (lag 1) similar to an earlier report in the tropics including a previous Thai study with data from 2009-2014 [110, 123]. One of the most significant findings from this study was that temperature, relative humidity, and rainfall were all associated with influenza A(H3N2) activity in Bangkok. Moreover, temperature was positively correlated with overall influenza activity at 4 months lag, which happens to coincide with the period of increased rainfall and humidity. Previous studies in Cambodia, the Philippines and Vietnam have linked rainfall to increased overall influenza [105, 140]. In another Philippines study, temperature and specific humidity were positive indicators for both influenza A and B viruses [99]. On the contrary, Singapore identified negative correlations between relative humidity and both influenza A and B viruses [122]. Despite differences in conclusions, we believe that findings from each of these studies are valid for their respective study sites due to intrinsic differences in geography among these countries. Seemingly contradictory results further underscore the complexity of climatic drivers on individual (sub)type of influenza, and it has been proposed that future regional data are warranted especially for relatively large and dispersed countries such as the Philippines and Indonesia [106].

The association between climate factors such as temperature with the onset of influenza epidemic in some countries may be dependent on the latitudes [137]. It has been suggested that influenza activity in countries located at low latitudes or in the tropics significantly correlated with rainfall [105]. Influenza incidence may be linked to the latitude gradients whereby countries located between 10 and 30 degrees north latitude tend to experience influenza A activity from June to November and year-round sporadic influenza B activity [99, 141]. It was postulated that the observed increase in influenza activity in the tropics during the humid and rainy season may be indirectly linked to over-crowding in the community and virus stability on fomites [142, 143]. Our observation of low overall influenza activity during hot and dry periods is consistent with the notion that increase temperature may limit aerosol transmission in tropical regions [102].

Using ARIMA model, the relationship between all influenza incidence and meteorological variables enabled a forecast model with significant prediction. The analyzed forecasts for individual influenza A(H1N1)pdm09, A(H3N2), and influenza B virus, however, were not as robust. Although factoring in the average temperature, relative humidity, and rainfalls can increase the accuracy of the forecasting model, each influenza (sub)type was affected by specific climate factors and presented forecasting challenges. Better prediction result from overall influenza activity might have been due to the increased sample size of the combined data for all three (sub)types of influenza viruses. Interestingly, we found that influenza A(H1N1)pdm09 did not always co-circulate with influenza A(H3N2) virus like it did with influenza B virus at up to 1 month lag. We also did not observe the inverse correlation between influenza A(H3N2) and influenza B virus previously identified in the tropical Uganda [111]. Again, there are probably unaccounted differences in geographical factors in addition to the fact that we did not have weekly climate data, which would have been more useful for our calculations. Finally, our time series analysis showed that the best-fit model resulted when incorporating the climate factor parameters.

This study had several limitations. Influenza surveillance was derived from one major hospital in western Bangkok and may not have represented the influenza activity of the entire city. Our surveillance was passive in nature because samples were submitted to us rather than actively sought, therefore we did not use the time of viral exposure for analysis. The overwhelming majority of the samples came from in-patient settings, so nosocomial influenza was not considered. Although we had influenza data prior to 2011, these were excluded due to fewer sample size and possible bias from the influenza pandemic of 2009. From our experience, we presumed that only

influenza A(H1N1)pdm09 and A(H3N2) viruses comprised the overwhelming majority of influenza A virus in circulation, but it is possible that other less frequent subtypes were missed. Due to latitude and climate differences, influenza incidence in northern and southern Thailand may be different and this would benefit from future studies. In addition, daily or weekly climate factor values, when available, would be more useful in improving modeling accuracy. Despite these limitations, our results suggest that certain climate factors do influence influenza activity and further support the existing schedule for influenza vaccination prior to the rainy season. The time series analysis of influenza virus could potentially supplement a more accurate forecasting of future seasonal influenza activity when combined with an active epidemiological surveillance. Countries lacking the latter but share similar geographical and climatological factors may benefit from the model-based disease predictions. This and other time series analysis, especially when performed on the daily climate factors, could potentially improve the foundation for enhanced modeling of disease seasonality.

CHAPTER IV

PREVALENCE OF CROSS-REACTIVE ANTIBODIES AGAINST SEASONAL INFLUENZA A AND B VIRUSES AMONG THE ELDERLY IN THAILAND

(In preparation before submission)

Nungruthai Suntronwong¹, Sirapa Klinfueng¹, Sumeth Korkong¹, Preeyaporn
Vichaiwattana¹, Thanunrat Thongmee¹, Sompong Vongpunsawad¹, Yong Poovorawan¹

¹Center of Excellence in Clinical Virology, Faculty of Medicine, Chulalongkorn
University, Bangkok, Thailand 10330

จุฬาลงกรณ์มหาวิทยาลัย
CHULALONGKORN UNIVERSITY

CHAPTER IV

Part 4.1: Prevalence of cross-reactive antibodies against seasonal influenza A and B viruses among the elderly in Thailand

Summary

Influenza infection commonly cause a respiratory disease that associated the annually epidemic outbreak. Elderly population still found a significant risk of infection even though the vaccine was available. Because they have never been received the vaccine or they cannot generate well of immune response or their immunity was waived. To gain insight into influenza immunity among elderly in Thailand, we aim to determine the seroprevalence of cross-protective antibodies against individual influenza viruses among the older persons more than 60 years of age. Serum sample were collected during a cross-sectional population-based study which was performed in Khon Khan province, Thailand in 2015. Here, 176 sera samples were obtained from the elderly 60 to 95 year of age. Representative influenza A/H1N1, A/H3N2, B/Victoria and B/Yamagata viruses which circulated in Thailand between 2017 and 2020 that closed to the next vaccine strain were selected. Hemagglutination inhibition was conducted to determine the antibody titers against influenza A and B virus. Our findings show that antibody titer against influenza A virus significantly higher than influenza B virus. The proportion of the study subject who has a seropositivity (HI titers ≥ 40) against A(H1N1)pdm09, A(H3N2) were account for 50% and 66% whereas the prevalence of antibodies against influenza B virus was lower than influenza A virus. The seroprevalence to influenza B virus was account for 14%, 21% and 25% for B/Yamagata2, B/Yamagata3 and B/Victoria, respectively. Additionally, we found only 5% of this population presented the antibodies against both the influenza A and B viruses, this suggests that a low proportion of individuals provided broadly protective antibody against seasonal influenza virus. These findings may have inform the maker for health care planning and guide control measure which concerning a vaccine policy.

Introduction

Influenza virus is a significant pathogen that causes respiratory tract infection result in substantial morbidity and mortality during the annual influenza epidemic, particularly among elderly persons. A previous report indicated that the influenza-associated death was estimated globally at 290,000 to 650,000 individuals each year [144]. Influenza vaccination is a primary tool to effectively prevent influenza infection and beneficial to reduce the serious influenza related sequelae [145]. The severity of influenza infection depends on multiple factors such as the virulence of virus, the decline of immune response, the level of pre-existing immunity. Advisory Committee on Immunization Practices (ACIP) recommended influenza vaccination for the high-risk population who can develop serious complications including pregnant women, young children (6 months to 5 years), elderly persons (≥ 65 years), people with chronic medical conditions, and health care personnel (MMWR) [146].

Among the high-risk group, the elderly are at risk of infection because they have been vaccinated or they never completely immunized or their immunity has been declined due to aging (immunosenescence) [82]. Thus, this population is most probably afflicted by significant comorbidities and vulnerable to serious influenza-related complications such as pneumonia that might lead to hospitalized and die [144, 147]. The high mortality rate typically occurs among people older than 65 years of aged (2.9 to 44 per 100,000 individuals for persons aged 65-74 years and 17.9 to 223.5 per 100,000 individuals for people aged more than 75 years) [1]. With advanced age, the meta-analysis indicated that vaccine effectiveness (VE) against influenza-like illness (ILI) and laboratory-confirm influenza were poor among elderly persons which estimate approximately 39% and 49%, respectively [148]. However, the elderly receiving the influenza vaccine might have a lower risk of influenza infection (from 6% to 2.4%) when compared with an individual who has not been vaccinated [149]. Therefore, monitoring the immunity status influenza viruses should be considered in the elderly population.

In Thailand, the aging population has grown rapidly that increase seven-fold or 16% from 1960 (1.5 million) to 2015 (10.7 million) [150]. To prevent the high rate of influenza-associated hospitalization and death of the elderly. Serological surveillance was typically conducted to assess the immunity level in the population [151]. The vaccination of the annual influenza vaccine in older aged more than 65 has been recommended since 2008 [152, 153]. Several reports indicate the seroprevalence among a high-risk group such as young children, health care workers, chronic medical

conditions [154]. However, the seroprevalence data of the elderly population are lacking. Thus, we here aim to assess the seropositivity (HAI \geq 1:40) against seasonal influenza A(H1N1)pdm09, A(H3N2), and B viruses among the elderly over 60 years of age as well as determine the seasonal influenza incidence by detection virus from nasopharyngeal swab specimen. Data of seroprevalence is useful in the pandemic scenarios, helps to determine pre-existing immunity, and reflects on the vaccine coverage. Thus, the evaluation of the prevalence of antibodies in the elderly population might provide valuable data and even guide prioritize intervention actions for public health strategy and support the decision-making on vaccine policy.



Material and methods

Source of nasopharyngeal swab and influenza testing

In this study, the Chumphae district in Khon Kaen province was chosen as a site to study influenza surveillance. A total of 7,758 nasopharyngeal swabs were collected from influenza-like illness patients who have a fever ($\geq 38^{\circ}\text{C}$), sore throat, cough, and symptoms of respiratory tract infection at Chumphae hospital between 2010 and 2015. All specimen was stored at 4°C during transportation to the Center of Excellence in Clinical Virology as part of influenza surveillance. All nasopharyngeal swab were subjected to RNA extraction accordant with the manufacturer's instructions. The real-time RT PCR method was conducted to identify the positive test against influenza A(H1N1)pdm09, A(H3N2) and influenza B virus according to the previous study [126].

Serum samples

Serum samples were obtained during a cross-sectional descriptive study which was performed in the Khon Kaen, Thailand from October to November 2015 to evaluate the seroprevalence against diphtheria, tetanus and pertussis (15). For this objective, 430 serum samples were collected from older persons aged ≥ 60 years. In our study, 176 serum samples (a remaining volume $\geq 200\ \mu\text{l}$) were obtained and used for serological testing against influenza A(H1N1)pdm09, A(H3N2) and influenza B viruses. Data regarding the date of vaccination and the date of the previous infection were not recorded. The study protocol was approved by the Institutional Review Board of the Faculty of Medicine, Chulalongkorn University (IRB No. 127/61). All samples were analyzed anonymously.

Representative influenza viruses

To test for antibodies that cross-reactive with influenza viruses in the late influenza season, the representative of influenza A(H1N1)pdm09, A(H3N2), B/Victoria and B/Yamagata that circulated in the 2017-2020 influenza season were selected. The test positive samples for influenza A(H1N1)pdm09 and A(H3N2) were propagated in 80% confluent of Madin-Darby canine kidney (MDCK) cell and incubated at 37°C for 3-5 days while influenza B virus was grown and incubated at 33°C for 3 days. The supernatant was harvested and cleared by centrifugation. All viruses were performed on conventional PCR and sequencing. The nucleotide sequences of the propagated virus were compared to the sequence of original samples and constructed the phylogenetic with reference and vaccine strain.

Hemagglutinin Inhibition assay

All sera were stored at -20°C and brought to room temperature before testing. Serum samples were quantitatively the antibody titer in duplicate by using hemagglutinin inhibition assay which reports as previous described [155]. Briefly, individual serum was pre-treated with the receptor-destroying enzyme (RDE; Denka Seiken, Tokyo, Japan) as a dilution 1:4 and incubated at 37°C overnight to remove nonspecific inhibitors of hemagglutinin. Serum samples were further incubated at 56°C to inactivate the process and follow by adding phosphate-buffered saline (PBS) to perform a dilution 1:10. RDE- treated sera were tested nonspecific HA activity by using 0.5% TRBCs. If agglutinin appears, adsorption of sera with TRBCs should be performed by incubating the packed RBCs and RDE treated serum at 4°C for 1 h. The hemagglutination inhibition method was tested in two-fold serial dilution by starting at 1:10 dilution and subsequently incubated with 4 hemagglutination units of the tested virus at room temperature for 30 min. The hemagglutination titer can read after adding a 0.05% turkey red blood cell and incubated at 4°C for 1 h. Serum sample collected from individual who received influenza vaccination was used as the positive control. The highest reciprocal of the serum dilution that expressed completely inhibits hemagglutination was recorded as the endpoint titer. HAI titer more than or equal to 40 were considered protective against the tested virus [156, 157]. To comparative the antibody level, HAI titer less than 10 was assigned a value of 5 to calculate the geometric mean titer (GMT) as previous studies [158, 159].

Statistical analysis

Influenza incidence was calculated as the proportion of number laboratory confirm- positive influenza virus and the number of influenza-like illness (ILI). Data are presented in bar graphs showing the seroprevalence against influenza virus among differentiated age groups in elderly. Comparison the different in titer (GMT) among individual influenza (sub)type was evaluated using the Kruskal-Wallis test. The prevalence of protective antibody (considered only HI titer ≥ 40) estimates among influenza (sub)type are shown as number, percentage and 95% confidence intervals (95% CI). The statistical significance was considered as p-value less than 0.05. All statistical analysis was performed in SPSS version 23 (SPSS Inc., USA) and GraphPad Prism version 8.0.0 (GraphPad Software, San Diego, California USA).

Results

Detection influenza incidence among different aged groups

To identify the influenza incidence, individuals were classified into 7 groups including 0-2 year (infant and toddler), 3-4 year (pre-school age), 5-11 (school age), 12-17 (adolescent), 18-39 year (young adult), 40-59 year (older adults) and ≥ 60 years of aged (elderly). The number of influenza-like illnesses and the percentage of positive samples for each year between 2010 and 2015 were shown (Table 7). We found the average percentage of influenza-positive cases in this region was 8.7% (672/7,758). The highest percentage was 15.8% (54/660) which found in adolescent (12-17 year of aged) and the lowest influenza incidence was 4.7% (112/2400) that found in the infant (0-2 year of aged), while the incidence of influenza in elderly (≥ 60 years of age) was 6% (33/553) in this region. To exploring the circulating strains that infected in elderly, most predominant circulating strain was influenza A(H3N2) which was account for 54.5% (18/33), and then influenza A(H1N1)pdm09 and influenza B virus which was estimated as 30.3% and 15.2 %, respectively (S4 Figure).

Table 7 Distribution of number and percentage of laboratory-confirmed influenza-positive cases of the individual age group.

Age groups	Year			2010			2011			2012			2013			2014			2015			Total		
	ILI	No. Pos	%Pos	ILI	No. Pos	%Pos	ILI	No. Pos	%Pos	ILI	No. Pos	%Pos	ILI	No. Pos	%Pos	ILI	No. Pos	%Pos	ILI	No. Pos	%Pos	ILI	No. Pos	%Pos
0 to 2 (infant & toddler)	330	26	7.9	381	25	6.6	404	9	2.2	399	10	2.5	453	22	4.9	433	20	4.6	2400	112	4.7			
3 to 4 (preschool age)	154	29	18.8	173	13	7.5	148	3	2.0	157	12	7.6	172	20	11.6	218	12	5.5	1022	89	8.7			
5 to 11 (school age)	219	58	26.5	260	22	8.5	278	16	5.8	287	21	7.3	363	70	19.3	314	25	8.0	1721	212	12.3			
12 to 17 (adolescent)	67	18	26.9	76	6	7.9	68	6	8.8	193	30	15.5	146	27	18.5	94	15	16.0	644	102	15.8			
18 to 39 (young adults)	66	16	24.2	8	1	12.5	2	0	0.0	231	18	7.8	269	29	10.8	182	6	3.3	758	70	9.2			
40 to 59 (older adults)	41	8	19.5	8	0	0.0	0	0	0.0	130	18	13.8	243	26	10.7	238	2	0.8	660	54	8.2			
≥ 60 (elderly)	77	6	7.8	31	2	6.5	25	2	8.0	94	11	11.7	119	9	7.6	207	3	1.4	553	33	6.0			
Total	954	161	16.9	937	69	7.4	925	36	3.9	1491	120	8.0	1765	203	11.5	1686	83	4.9	7758	672	8.7			

Protective antibody titer among individual influenza (sub)types

A total of 176 sera samples were tested by using hemagglutination inhibition assay (Table S4). The tested virus was A/Thailand/CU-CN364/2017 (clade 6B.1) for A(H1N1)pdm09 and A/Thailand/CU-B36461/2018 (clade 3C.3a) for A(H3N2). The B/Thailand/CU-B31196/2019, B/Massachusetts/02/2012 and B/Thailand/CU-B26097/2018 were chosen for B/Victoria clade 1A, B/Yamagata clade 2, B/Yamagata clade 3, respectively. The clade of the selected virus for individual influenza (sub)type was corresponding with the clade of the southern hemisphere vaccine in 2015 and circulating strain during 2017-20 (Figure S5). Analysis of antibody level (GMT) among influenza (sub)type in the elderly, we observed the highest antibody titer was 47.8 (95% CI: 40.6 – 56.2) which was detected against influenza A(H3N2) and showed a

significant titer higher than A(H1N1)pdm09 and influenza B viruses (Figure 10). The antibody titer of influenza A(H1N1)pdm09 was account for 23.1 (95% CI: 19 – 28.2) follow by B/Victoria (19.6, 95% CI: 17.4 – 22.1), B/Yamagata 3 (17.9, 95% CI: 15.9 – 20.1) and the lowest titer was B/Yamagata 2 which presented geometric mean titers as 10.7 (95% CI: 9.4 -12.1) (Table 8). Influenza A(H1N1)pdm09 shown a significant titer higher than both B/Victoria and B/Yamagata 2. Among influenza B virus, we observed the antibody titer against B/Yamagata 2 was significantly lower than both B/Victoria and B/Yamagata 3. Furthermore, we observed the antibody titer of influenza A virus was slightly higher than influenza B virus in the studied population.

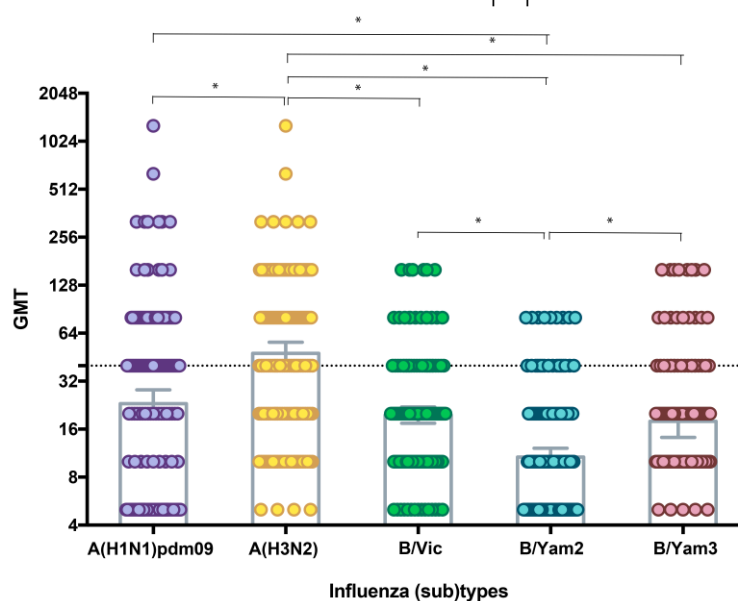


Figure 10 Comparison of the antibody titers (GMT) among influenza (subtype).

The colored circle was defined as influenza virus A) A(H1N1)pdm09 (A/Thailand/CU-CN364/2017, purple), B) A(H3N2) (A/Thailand/CU-B36461/2018, yellow), C) B/Victoria (B/Thailand/CU-B31196/2019, green), D) B/Yamagata 2 (B/Massachusetts/02/2012, blue) and E) B/Yamagata 3 (B/Thailand/CU-B26097/2018, pink). Y-axis indicated the geometric mean titer and the X-axis showed influenza (sub)types. Error bars indicated geometric mean titer with 95% confidence intervals (95% CI). The asterisk refers to the significant level <0.0001 (Kruskal-Wallis test).

Seropositivity (HAI titers ≥ 40) against influenza virus

Assessing the seroprevalence of protective antibody in each influenza (sub)type, our study showed that the highest prevalence of seropositivity was detected for A(H3N2), corresponding with 65.91% (116/176) and the followed influenza (sub)type was A(H1N1)pdm09 which estimated as 50% (88/176). The proportion of individuals

who presented seroprotective to influenza B viruses of the B/Yamagata 1 and the B/Victoria lineage were discriminated against. The seroprevalence of protective antibody against B/Victoria, B/Yamagata 2 and B/Yamagata 3 were account for 25% (44/176), 14.2% (25/176) and 21% (37/176), respectively in elderly (Table 8).

Table 8 The prevalence of protective antibody against seasonal influenza by hemagglutinin inhibition assay.

(HI titer ≥ 40) and geometric means titers (GMT) among the elderly population.

Virus	HI titer ≥ 40		GMT		
	Number/ Total	%	Mean	Lower 95% CI	Upper 95% CI
A(H1N1)Pdm09	88/176	50.00	23.14	18.99	28.19
A(H3N2)	116/176	65.91	47.76	40.56	56.23
B/Victoria	44/176	25.00	19.61	17.42	22.08
B/Yamagata 2	25/176	14.20	10.69	9.422	12.13
B/Yamagata 3	37/176	21.02	17.91	15.94	20.13

We then identify the seroprevalence of protective antibodies by different age groups among the elderly, aged were classified into three groups 60 -69, 70-79 and ≥ 80 years (Figure 11). The higher percentage of seroprevalence to A(H1N1)pdm09 and B/Yamagata 2 were seen in 60-69 year of aged. The seropositive individuals to A(H3N2) and B/Victoria were higher in an older person aged more than 80 years while the high seroprotective against B/Yamagata 3 was noticed in 70-79 year. However, the seropositivity was not significantly different among aged groups. (Table S5).

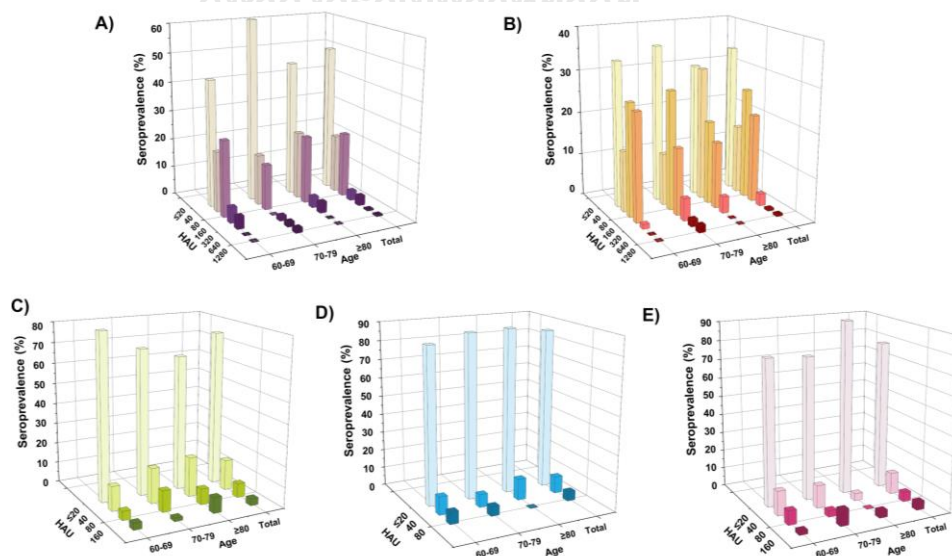


Figure 11 Seroprevalence of protective antibody against seasonal influenza virus.

Colored bars were defined as influenza virus A) A(H1N1)pdm09 (A/Thailand/CU-CN364/2017, purple), B) A(H3N2) (A/Thailand/CU-B36461/2018, yellow), C) B/Victoria (B/Thailand/CU-B31196/2019, green), D) B/Yamagata 2 (B/Massachusetts/02/2012, blue) and E) B/Yamagata 3 (B/Thailand/CU-B26097/2018, pink). The X-axis showed the 2-fold of HI titers. Y-axis indicated the different aged groups and Z-axis showed the percentage of seroprevalence. The intensity of color bars indicated the more HAI titer.

Furthermore, the prevalence of protective antibody for each influenza (sub)type was used to determine the proportion of individuals with seropositivity at least one influenza (sub)type. Overall, 89% (156/176) of the elderly most present the seropositive at least one influenza (sub)type and 11% (20/176) was assessed for the seronegative individuals. Only 5% of this population was observed seropositivity for all influenza viruses while most elderly (42%) showed the seropositivity to one influenza (sub)type (Figure 12). This suggests that a low proportion of individuals provided broadly protective antibodies to all seasonal influenza viruses.

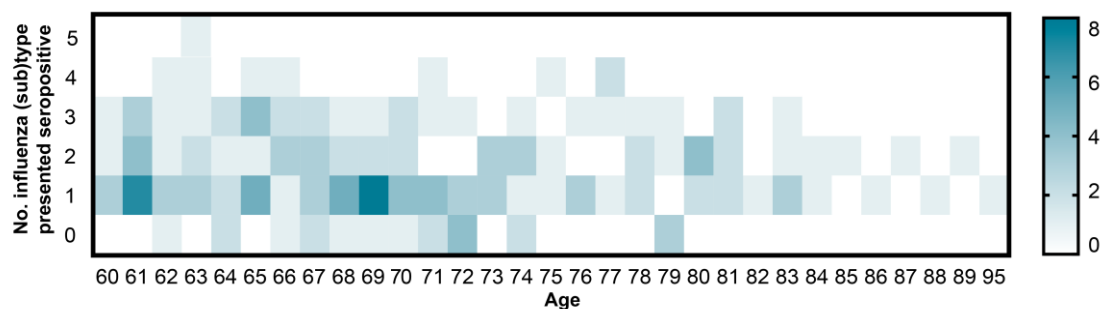


Figure 12 Schematic represents the number of influenza (sub)type presented seropositivity (HI titer ≥ 40) for individual.

X axis indicated the aged range of elderly and Y axis showed the number of seropositive influenza (sub)type. Colored intensity indicated the number of individuals.

Discussion

In this study, we assess the seroprevalence of the protective antibody to the influenza virus that circulated in the late influenza season among the elderly population by using the sera sample that was collected in 2015, Khon Kaen province, Thailand. Overall, the seroprevalence of antibodies against influenza A/H3N2 viruses was higher than the seroprevalence of antibodies against influenza A/H1N1 or B viruses. This was corresponding with surveillance data from Thailand which found influenza A(H3N2) was predominant during 2015 [159]. For influenza B virus, the seroprevalence to B/Yamagata clade 3 was higher than the seroprevalence to B/Victoria and B/Yamagata clade 2. This finding was in accordance with the evidence of lineages shift of influenza B virus that showed the predominant strain was B/Yamagata clade 3 [160]. During influenza seasons in this period, antibodies to influenza A/H3N2 viruses were and the high proportion of individuals with seropositive at least one influenza (sub)type. The proportion of elderly had broad protection to all seasonal influenza viruses was low.

Antibody titer of influenza A virus among the elderly was significantly higher, compatible with the influenza B virus that was related to the predominant of circulating influenza A virus in the previous season. The immunity status of the elderly might be changed over time due to the newly emerged influenza virus and the decline of an immune response (immunosenescence). The evolution rate of hemagglutinin, which is a main antigenic determinant protein, of influenza A virus substantially higher than influenza B virus [161]. The genetic and antigenic of the influenza virus typically changing over time, the newly antigenic drift virus was introduced result in causing an elevated influenza incidence. Furthermore, this finding was in accordance with the predominant influenza of influenza A virus particularly A(H3N2) in 2015 influenza season in Thailand (June to August)[159]. Influenza B virus quite sporadic circulating activity [120]. The low level of seroprevalence to influenza B virus in the elderly might occur because influenza B antibody was less persistent than influenza A virus [162]. A cross-protective antibody was found in all adults but less in the elderly due to immunosenescence.

Influenza vaccine post-introduction evaluated in Thailand suggests that the number of purchase vaccines was raised by 25%[163]. Although the previous report estimates the vaccine coverage increase among the elderly from 12% (2010) to 20% (2016), the low proportion of individuals showed broad protection to all influenza (sub)type (5.1%) remain observed in this study [163, 164]. A low proportion of all

populations had broad protection to all seasonal influenza viruses, thus suggesting low vaccine uptake and the need for intervention and recommendations on preventive measures.

There are some limitations to this study. First, lacking information regarding the previous influenza infection and the date of individual vaccination. It is limited to interpret the source of influenza immunity due to immunization or natural infection. Even though hemagglutination inhibition assay is a gold standard method for serological study of influenza virus, the seropositivity indicated by HAI titer ≥ 40 does not represent the total protective antibody such as anti-hemagglutinin stalk antibody, anti-neuraminidase antibody. Moreover, the functional measures of antibody did not perform such as neutralization and ELISA methods which methods are better to reflect the protective antibody to influenza infection. The tested for cellular immunity is not determined in this study, although it is also associated with the protection. Furthermore, the tested viruses used in this study lacked A(H3N2) clade 3C.2a which was the predominant circulating strain since 2016. So, we likely underestimate the cross-reactivity against A(H3N2).

As Thailand continues to increase the immunity to influenza in the high-risk group [152, 153]. This finding is important to guide the vaccine policy and highlight to increase broad influenza protection. However, further study needs to evaluate the seroprevalence to other high-risk groups such as young children because these individuals play a critical role in human transmitters of influenza virus, as previous report indicated that vaccination of children reduces the incidence of severe influenza virus infections in elderly individuals [165]. The seroprevalence study of the high-risk individuals will be important to evaluate the progress of vaccine implements and reflect the intervention action to the influenza virus. So, the need for improved prevention and control recognizes as a priority should be a concern.

CHAPTER V

IDENTIFY THE GENETIC CHANGES AND EVOLUTION PATTERN OF POLYMERASE COMPLEX GENE AMONG SEASONAL INFLUENZA VIRUSES

(Part 5.1)

(In preparation before submission)

Nungruthai Suntronwong¹, Sirapa Klinfueng¹, Sumeth Korkong¹, Preeyaporn
Vichaiwattana¹, Thanunrat Thongmee¹, Sompong Vongpunsawad¹, Yong Poovorawan¹

¹Center of Excellence in Clinical Virology, Faculty of Medicine, Chulalongkorn
University, Bangkok, Thailand 10330

CHAPTER V

Part 5.1: Identify the genetic changes and evolution pattern of polymerase complex gene among seasonal influenza viruses.

Summary

Seasonal influenza virus is an important respiratory pathogen and has a considerable impact on the public health threats which typically estimates 3 to 5 million cases of severe illness worldwide. The genomic of the influenza virus does evolve. Such evolution can occur through the acquisition of point mutations that raising via polymerase error leading to generate the newly virus strain. The viral polymerase complex consists of PB1, PB2, and PA proteins that assembly and responsible for viral replication. Mutations in the polymerase gene showed a significant relation with the efficacy of viral replication, transmission, and virulence. To determine the genetic changes and evolution pattern of the polymerase gene of the seasonal influenza virus, we characterize the amino acid changes of PB2, PB1 and PA gene among influenza A and B virus between 2010-2019 and further estimate the evolution rate, phylodynamic to explored the genetic fluctuation over time. The result suggests that the pattern of evolutionary dynamics of A(H3N2), B/Victoria and B/Yamagata have considerably changed, exhibiting an overall increase in genetic diversity. These results suggest that the polymerase gene of the recent influenza A(H3N2), B/Victoria and B/Yamagata are evolving at a faster rate than in the previous decades. Our data reveal novel adaptive mutations acquired in a relevant influenza virus evolution in humans. Our data suggest that the continual fluctuation of genetic diversity in the polymerase gene of the influenza virus highlighted the monitoring of developing antiviral agents.

Introduction

Seasonal influenza virus is an important respiratory pathogen and has a considerable impact on the public health threats which typically estimates 3 to 5 million cases of severe illness worldwide [27]. Influenza viruses cause epidemic seasonal infections, resulting in ~500,000 deaths annually worldwide and the most recently calculated estimates being 291,243–645,832 deaths per year during the 1999–2015 period [1]. Globally, seasonal influenza viruses are comprised of influenza A(H1N1)pdm09, A(H3N2) and influenza B virus (B/Victoria and B/Yamagata lineages) have co-circulated since 1977. Seasonal influenza virus-associated deaths in the United States range from 5,000 to 52,000 people per year, depending on the year [147]. The genomic of the influenza virus does evolve over time. Such evolution can occur through the acquisition of point mutations that are raising via polymerase error which typically occur at approximately 1 in 10,000 bases for individual replication cycle [8]. Basically, the replication errors lead to generating the viral population with more variants. An understanding of how influenza viruses accumulate the genetic change can inform public health preparedness.

The main influenza proteins involving genetic changes are polymerase. The viral polymerase complex, composed of subunits PB1, PB2, and PA that assembly with additional viral nucleoprotein (NP) and genomic RNA to mediate the viral genome replication and transcription [34, 94]. A few mutations in polymerase protein that might enhance the virulence and affect the replication machinery. For illustrated the changes glutamic acid residue at 627 in PB2 subunit to lysine that found to enhance the efficiency on polymerase activity in the human cell and also increase virulence by helping the virus grow at low temperature [37]. M631L (PB2) and E712D (PB2) had found to strongly up-regulate the viral RNA polymerase and therefore disease severity while Q591K (PB2) and G590S (PB2) were related to enhance the pathogenicity (Reeves AB 2016). PB1-F2 and PB1-N40 are responsible for antagonist host interferon (IFN) and pro-apoptotic activity [38, 39]. Furthermore, the substitution at PB1-375S and PB1-T296R showed a relevance with all three human pandemics (Taubenberger JK 2005). The combined mutations at Q236H (PB2), E627K (PB2), and N309K (NP) or Q591K (PB2) and S50G (NP) mutations which have a synergistic effect in viral replication [51]. Amino acid changes at PB2-701, PB2-714 and PA-615 have correlated the high pathogenicity in both. Mice and human [35]. E31K (PA), I94V (PA), L336M (PA), K356R(PA) and T97I (PA) mutations were identified to enhance virulence and severity of influenza infection. Although the polymerase genes are non-antigenic property, a few amino acid changes

in some positions might affect the replication, transmission, pathogenicity and virulence of the influenza virus. Nevertheless, the data of characterized genetic and evolution analysis among seasonal influenza remain unless. Thus, monitoring the evolution rate and characterized the genetic changes should be performed.

Although clinically approved neuraminidase inhibitors (NAIs) for influenza treatment and typically use in several, it was a single class of antiviral drug which raising concern the emergence of NAI resistant variants[92]. The further antiviral drug most focuses on the polymerase gene complex. Currently, the endonuclease inhibitor, a new antiviral drug, was approved (Baloxavir Marboxil; BXA). However, I38T substitutions in PA was found to be a major pathway for reduced susceptibility to BXA [166]. Although the residue reduces the antiviral drug PA and further antiviral drug polymerase are identified, the continual evolution of the polymerase gene still occurs. So, the profile of the genetic changes of the polymerase gene in human hosts should be performed to tracking the viral fitness and monitor the drug-resistant in the circulating strain. Here we identify amino acid changes that are characteristic of the evolution pattern of polymerase in humans. The findings will help in the understanding of the evolution pattern and human-adaptive genetic changes on the polymerase gene which is a target for an antiviral drug. Continue monitoring the genetic changes and antiviral susceptibility is critical to strengthen public health endeavors aimed at pandemic preparedness and influenza interventions.



Materials and methods

Ethical consideration

This study protocol was approved by the Institutional Review Board (IRB) of the Faculty of Medicine at Chulalongkorn University (IRB No. 127/61). The IRB waived the need for consent because the clinical samples were deidentified and anonymous before analyzed at the Center of Excellence in Clinical Virology at King Chulalongkorn Memorial Hospital as part of the routine influenza surveillance program.

Laboratory influenza testing

From January 2010 to December 2019, 46,015 respiratory samples from patients with influenza-like illness (ILI) were collected from Bangpakok 9 International Hospital, King Chulalongkorn Hospital and Chumpare Hospital, Khon Kean. To identify the positive samples for influenza infection, the viral RNA was extracted directly from clinical samples by using commercially Viral Nucleic Acid Extraction Kit (Ribospin vRD II, GeneAll Biotechnology, Seoul, Korea) according to the manufacturer's instructions. Real-time reverse-transcription quantitative polymerase chain reaction (RT-qPCR) was used to identify A(H1N1pdm09), A(H3N2), and the influenza B virus by detection of the matrix (M) and hemagglutinin (HA) gene as previously described [126]. Laboratory-confirmed influenza B-positive samples were subjected to cDNA synthesis with specific primer Flu B (5'-AGCAGAAGCA-3') and ImProm-II Reverse Transcription System (Promega, Madison, WI, USA), followed by multiplex PCR and melting curve analysis to identify the influenza B lineages [167].

Polymerase gene amplification and sequencing

A total of 9,416 samples were found to be positive for influenza infection between January 2010 and December 2019. We further performed nucleotide sequencing of PB2, PB1 and PA by randomly selecting 2 positive samples per month for individual influenza (sub)type comprised of A(H1N1)pdm09 (n= 138), A(H3N2) (n=147) and influenza B virus (n=103) for representative circulating strain based on the lowest Ct value. The PB2, PB1 and PA segments of individual influenza (sub)type were amplified using conventional polymerase chain reaction with the primer sets of influenza A and B virus as described in S1 Table. Briefly, the cDNA of influenza A(H1N1)pdm09 and A(H3N2) were synthesized using primer Uni12 (5'-AGCAAAAGCAGG-3') while influenza B virus was subjected to cDNA synthesis by using specific primer Flu B. PCR mixture of 25 μ L contained 5 μ L of AccuStart II GelTrack PCR SuperMix (Quantabio, Beverly, MA, USA), 0.25 mM MgCl₂, 0.5 μ M each of forward and reverse primers, and 3 μ L of cDNA template. The primer name and nucleotide sequences for

PB2, PB1, and PA of influenza A(H1N1)pdm09, A(H3N2) and influenza B virus were described as Table S6, S7 and S8, respectively. Amplification conditions were 94°C for 3 mins, 40 cycles of 30 s at 94°C, 30 s at 55°C, 90 s at 72°C, followed by 7 mins of final extension at 72°C. Amplicons were agarose gel-purified and subjected to Sanger sequencing. PB2, PB1 and PA nucleotide sequences of A(H1N1)pdm09 (2010) and influenza B virus (2010-2014) have been submitted in the GenBank database as the previous studies [125, 168]. The nucleotide sequences generated in this study, A(H1N1)pdm09 (2011-2019), A(H3N2) (2010-2019) and influenza B virus (2015-2019), have been assembled using SeqMan Pro (DNASTAR, Madison, WI, USA) and deposited in the GenBank database under the accession number as described in the Table S9.

Estimate evolution rate and time scale tree

The nucleotide sequences of PB2 (n= 295), PB1(n=305) and PA (n=305) genes obtained from this study were combined with the others Thai strains and reference which was available from the National Center for Biotechnology Information (www.ncbi.nlm.nih.gov) and the Global Initiative for Sharing All Influenza Data (GISAID) (<http://platform.gisaid.org>) database. The duration time for individual sequences was calculated to depend on the collection date by using an Excel program. All nucleotide sequences were further aligned using MUSCLE. The phylogenetic trees were constructed for each gene segment for individual influenza (sub)type. A total of 905 nucleotide sequences (PB2(n= 295, PB1(n=305) and PA (n=305)) of influenza A(H1N1)pdm09, were used to construct the timescale tree with the Bayesian method which implemented by BEAST v1.10.4 [93].

The aligned sequences for each gene and individual influenza subtype were further identified as the best-fit nucleotide substitution model by jModelTest v2.1.3. The Bayesian Information Criterion (BIC) indicated a general-time reversible (GTR) model with Gamma and Invariant sites (GTR+G+I) and also combined with strict clock were identified as a nucleotide for nucleotide substitution model and molecular clock model, respectively. It was used to generate a time scale tree and determine the population dynamic and evolution rate. The Bayesian Markov Chain Monte Carlo (BMCMC) algorithm setting was 100 million chains for all genes datasets. The constructed tree was sampling every 10,000 taxa and discarding 10% of the chain as burn-in. The chain convergence and the effective sample size (ESS) from BEAST software were analyzed by Tracer v1.7.1. The acceptable ESS value should be greater than 200. The rate of nucleotide substitution with 95% highest posterior density and means value was determined. The time scale time was constructed by using TreeAnnotator V.1.4 and visualized by FigTree v1.4.4. The genetic diversity was

represented by the temporal dynamic which was analyzed by the Bayesian skyline plot model (BSP).

Observed amino acid substitution sites among influenza proteins

All nucleotide sequences for each segment will be translated into amino acid sequences and the amino acid changed residues will be observed using Bio edit software.

Statistical Analysis

All statistical analyses were analyzed by using SPSS software for Windows 22.0 (SPSS Inc., Chicago, IL) and Graph Pad Prism version 5.0. The chi-square test was applied to compare the substitution rate for each gene and each subtype. All statistical significance was considered as a p-value of less than 0.05.



Results

Long-term Fluctuations of polymerase gene (PB2, PB1 and PA)

A(H1N1)pdm09

Estimation of substitution in relative genetic diversity constructed by the Bayesian skyline plot showed that the highest levels of relative genetic diversity of A(H1N1)pdm09 occur in 2010 after the sharp decline of the population in 2009 (Figure 13). We found a continuous since then and both PB1 and PA gene exhibited a trough in genetic diversity from late 2015 to 2016. The phylogeny showed that following the period 2015-2016 when the relative genetic diversity was low, amino acid substitution in PB2 (V267I), PB1 (G175D) and PA (A343T) occurred. For PB2, the population with amino acid substitution V267I has diverged into two subgroups, the first was not achieved and the second is accomplished with replaced by the I267V. Both viral strains with G154D mutation in PB1 and A434T mutation in PA were not successful and disappeared in 2017. Although the recent relative genetic diversity of all polymerase gene remain unchangeably fluctuation since 2017, amino acid substitution has found in circulating strain during 2018-2109 including PB2(T81I, G225S, V667I), PB1(V200I, K386R) and PA(F105L, S225C and I505V).

A(H3N2)

Demonstrate of changes in relative genetic diversity of A(H3N2) showed that the rapid increase in genetic diversity of three polymerase genes ($>10^1$) with a peak observed in late 2011 and 2017 (Figure 14). The phylogeny indicated that the polymerase gene of A(H3N2) continually evolve and has diverged into multiple co-circulating subgroups. The highest relative genetic diversity in 2011 was consistent with the emergence of contemporaneous amino acid substitutions in PB2 (T613A), PB1(A587T) and PA(N409S, D396E). While following the period 2018, the relative genetic diversity was a rapid increase, these were associated with the amino acid substitutions in PB2 (S107N, K340R, V444I and M410V) and PA(K158R, V41I, K716N). Among influenza A virus, the population dynamic polymerase gene of influenza A(H3N2) was more frequently fluctuated than influenza A(H1N1)pdm09.

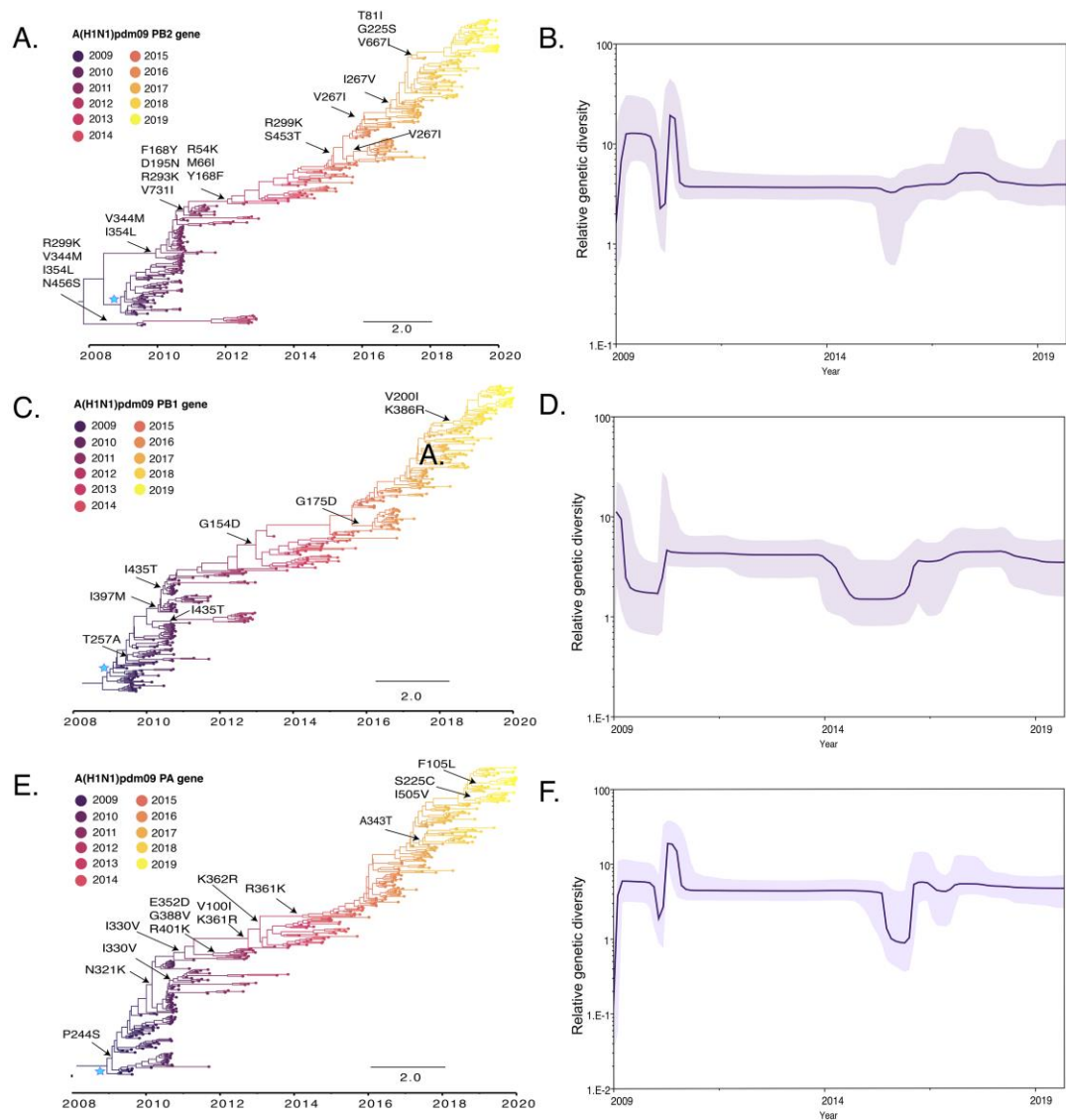


Figure 13 Time scale tree and population dynamic diversity in the polymerase gene of circulating influenza A(H1N1)pdm09 (2009-2019) in Thailand.

Temporal phylogeny and relative genetic diversity of PB2 (A and B), PB1 (C and D) and PA (E and F). Phylogenetic trees were constructed using a strict clock model with branches colored by year of virus isolation. For individual phylogeny, the main amino acid substitutions are mapped at the backbone of each tree. The viral population dynamic of polymerase genes was generated using the Bayesian skyline plot (BSP). Solid lines indicated the mean of relative genetic diversity, while the shaded area represented the 95% HPD intervals.

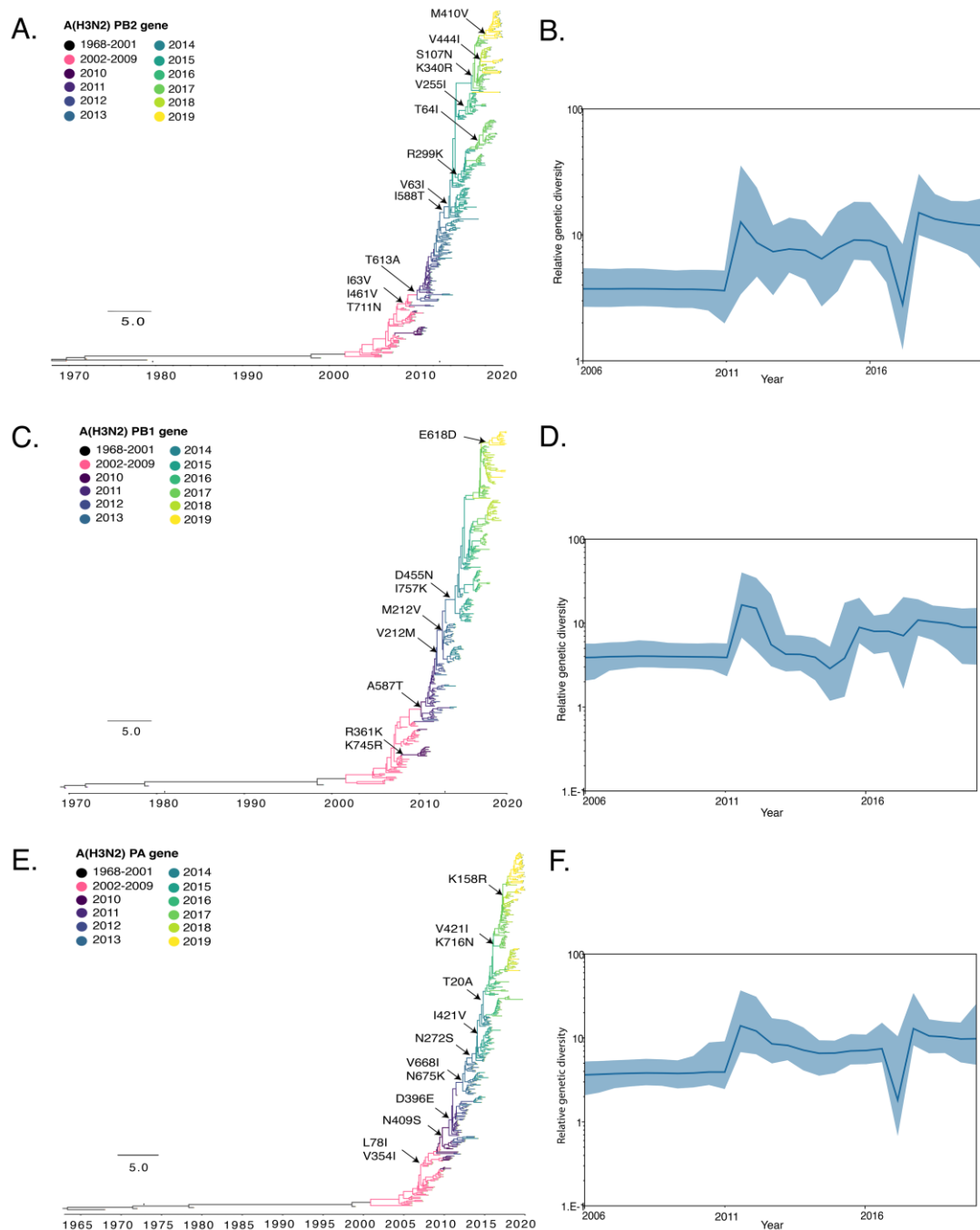


Figure 14 Time scale tree and population dynamic diversity in the polymerase gene of circulating influenza A(H3N2) (2006-2019) in Thailand.

Temporal phylogeny and relative genetic diversity of PB2 (A and B), PB1 (C and D) and PA (E and F). Phylogenetic trees were constructed using a strict clock model with branches colored by year of virus isolation. For individual phylogeny, the main amino acid substitutions are mapped at the backbone of each tree. The viral population dynamic of polymerase genes was generated using the Bayesian skyline plot (BSP).

Solid lines indicated the mean of relative genetic diversity, while the shaded area represented the 95% HPD intervals.

B/Victoria

Determine of substitution in relative genetic diversity constructed by the Bayesian skyline plot showed that the highest levels of relative genetic diversity of B/Victoria occur in 2018 ($>10^1$) (Figure 15). We observed three peaks in PB2 and PB1 during 2009, 2015 and 2018, two peaks in PA during 2015 and 2018. The constructed tree indicated that the highest relative genetic diversity of B/Victoria during 2014-15 is proceeded by the amino acid substitution in PB1 (S371P), PA (T352A, I723V and Y387C). Although the high genetic diversity fluctuated with high relative genetic diversity in 2018, we were not found the amino acid substitutions in the polymerase gene that related during their population emerged.

B/Yamagata

Although the genetic diversity in B/Yamagata has not changed since 2011, the rapid increase in genetic diversity of three polymerase genes was observed with a peak in early 2018 and remained stable with high genetic diversity (10^2) since then (Figure 16). The phylogeny showed that B/Yamagata are experienced selective selection and diverged into two major branches, the lower branch of PB2 (K73E), PB1 (T457A) and PA (L294M, I326M, and S530L) is corresponding with the polymerase gene of reference strains which belonged to B/Yamagata clade 2 while the higher branches have corresponded with B/Yamagata clade 3. Amino acid distribution in polymerase gene showed that following the period 2011 -2017 when the relative genetic diversity was highest, one amino acid substitution was presented in PB2 (Q354H), PB1(A591S), PA (S547G) and quick succession in circulating in human.

These findings suggest that the pattern of population diversity of A(H3N2) and B/Victoria have considerably changed over time, while A(H1N1)pdm09 slightly stable and B/Yamagata was increasing in 2017. All polymerase genes included PB2, PB1 and PA exhibited in a similar pattern within the individual (sub)type. The polymerase gene of influenza A(H3N2), B/Victoria, and B/Yamagata since 2017 have been evolved at a faster rate than in the previous decades. Our data reveal adaptive acquired mutations relatively occur as high genetic diversity in the polymerase gene and all PA gene has shown a higher evolution rate than PB2 and PB1, except A(H3N2).

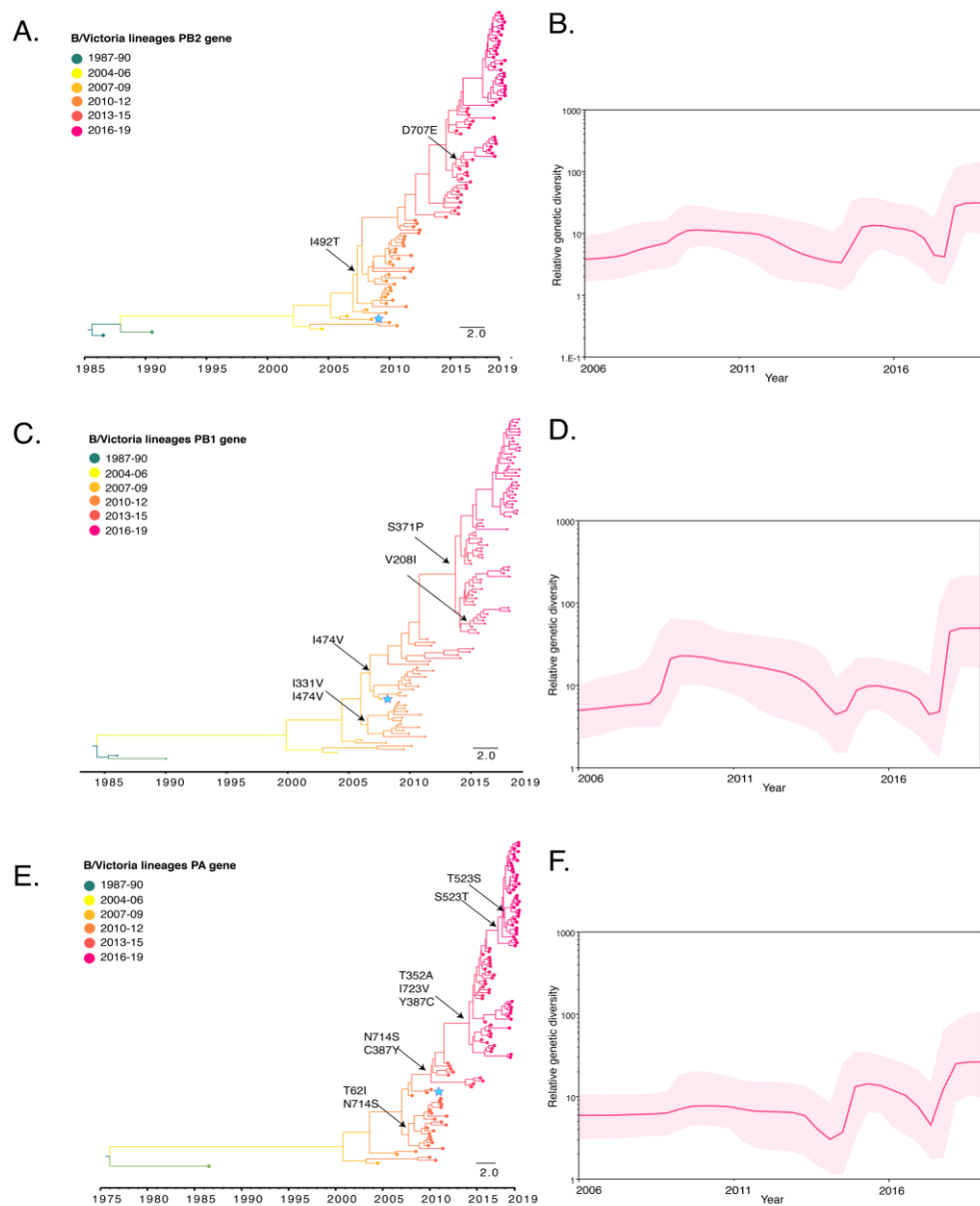


Figure 15 Time scale tree and population dynamic diversity in the polymerase gene of circulating influenza B/Victoria lineages (2004-2019) in Thailand.

Temporal phylogeny and relative genetic diversity of PB2 (A and B), PB1 (C and D) and PA (E and F). Phylogenetic trees were constructed using a strict clock model with branches colored by year of virus isolation. For individual phylogeny, the main amino acid substitutions are mapped at the backbone of each tree. The viral population dynamic of polymerase genes was generated using the Bayesian skyline plot (BSP). Solid lines indicated the mean of relative genetic diversity, while the shaded area represented the 95% HPD intervals.

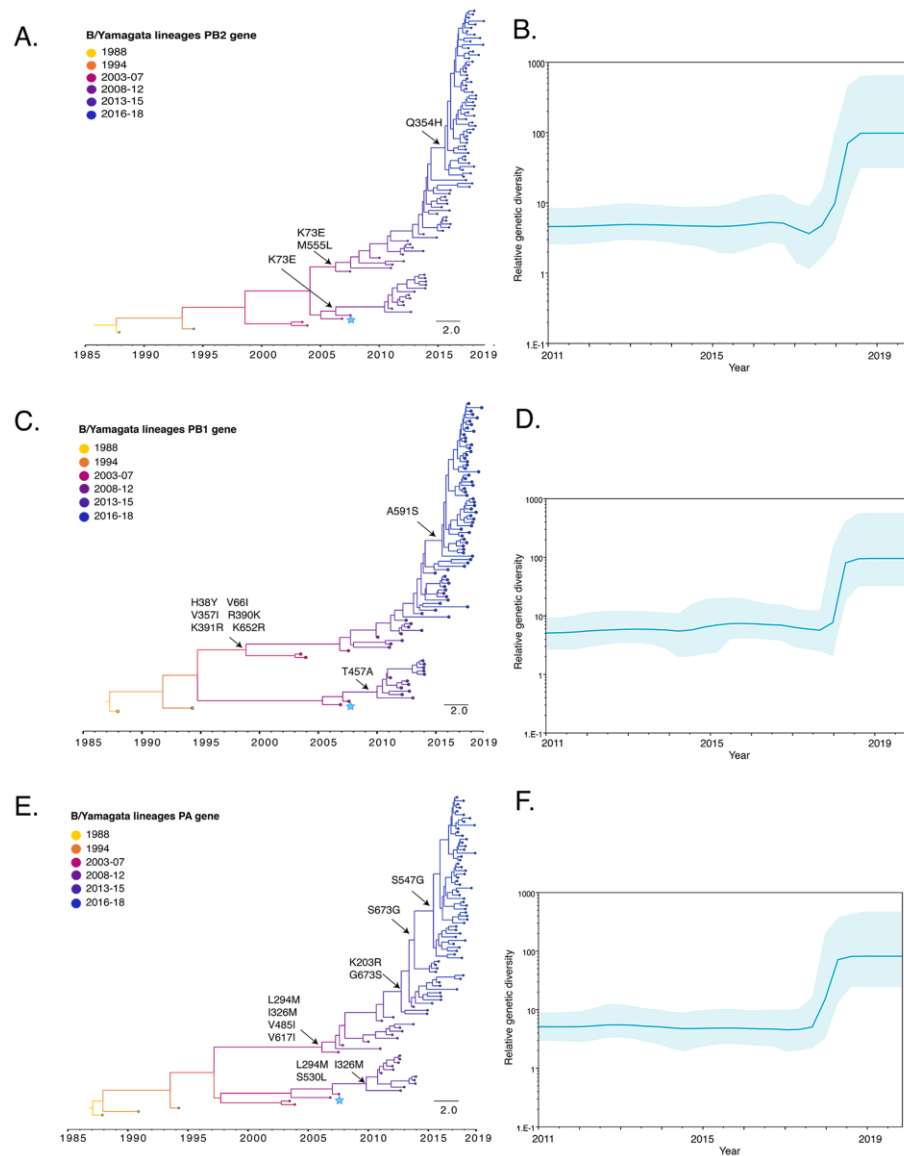


Figure 16 Time scale tree and population dynamic diversity in the polymerase gene of circulating influenza B/Yamagata lineages (2003-2017) in Thailand. Temporal phylogeny and relative genetic diversity of PB2 (A and B), PB1 (C and D) and PA (E and F). Phylogenetic trees were constructed using a strict clock model with branches colored by year of virus isolation. For individual phylogeny, the main amino acid substitutions are mapped at the backbone of each tree. The viral population dynamic of polymerase genes was generated using the Bayesian skyline plot (BSP). Solid lines indicated the mean of relative genetic diversity, while the shaded area represented the 95% HPD intervals.

Comparison evolution rate among polymerase gene

The changes of nucleotide levels are described as genetic adaptive and provide phylogenetically informative while changes in amino acid levels are critical for replication machinery, transmission, virulence and drug resistance. Influenza polymerase proteins are important for an antiviral drug target. A comparison evolution rate among polymerase could help to identify the appropriate antiviral drug that should be less evolve and more stable. Amino acid substitutions on PB2, PB1 and PA were characterized and modeled by using the set of trees obtained through our analysis of nucleotide data. Unsurprisingly, the PB2 had a higher amino acid substitution rate than PB1 and PA. According to the result from posterior probabilities, marginal likelihoods, Bayes factor and convergence in terms of ESS values, the best-fit model for PB2, PB1 and PA are strict clock model with constant population size. Based on this models, the rate of nucleotide substitution for PB2 of A(H1N1)pdm09 (2.99×10^{-3} substitutions/ site/year) and A(H3N2) (2.69×10^{-3} substitutions/ site/year) were higher than B/Victoria (1.16×10^{-3} substitutions/ site/year) and B/Yamagata lineage (1.38×10^{-3} substitutions/ site/year). Estimating evolution rate of PB1 at nucleotide level showed the higher rate was found in A(H1N1)pdm09 (2.79×10^{-3} substitutions/ site/year) as follow A(H3N2) (2.62×10^{-3} substitutions/ site/year) and the low evolution rate was observed in B/Victoria (1.13×10^{-3} substitutions/ site/year) and B/Yamagata lineages (1.43×10^{-3} substitutions/ site/year), respectively. Based on the evolution rate of PA, both influenza A (sub)type, A(H1N1)pdm09 (3.53×10^{-3} substitutions/ site/year) was higher than A(H3N2) (2.33×10^{-3} substitutions/ site/year) were presented the higher than both influenza B lineage, B/Victoria and B/Yamagata (1.36×10^{-3} and 1.59×10^{-3} substitutions/ site/year, respectively). Comparison the evolution rate of these three genes among influenza (sub)type, we found the evolution of PA was higher than PB2 and PB1 when observed among A(H1N1)pdm09, B/Victoria and B/Yamagata that showed a high evolution rate in PB1 gene except A(H3N2) (Figure 17).

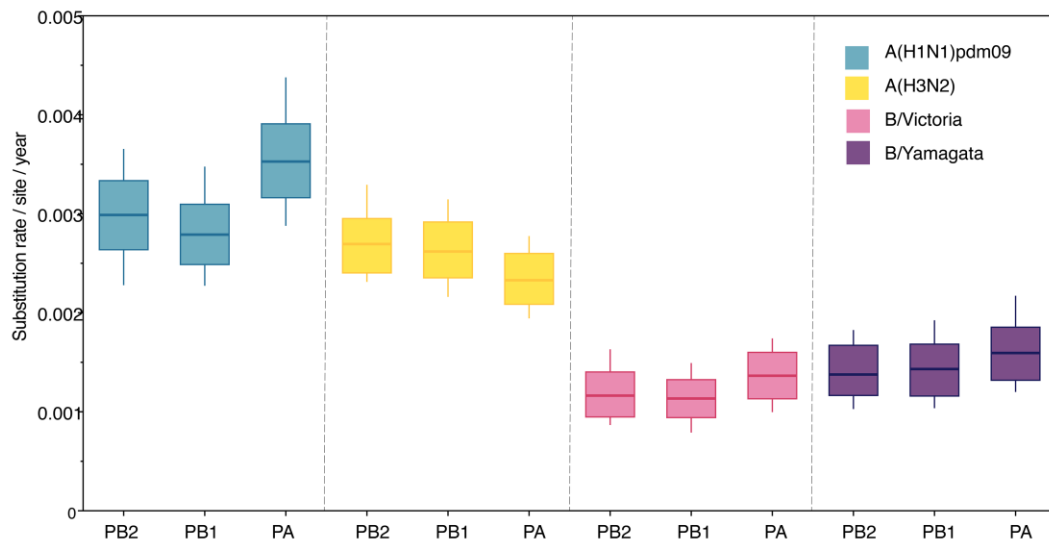


Figure 17 Schematic diagrams showing the comparison of the nucleotide substitution rate of PB2, PB1, and PA gene for individual influenza (sub)type. Box plot indicates the mean evolution rate with 95% confidence intervals. Colored box plots denote different gene segments.

Discussion

In this study, we found the evolution rate of nucleotide substitution in polymerase genes was higher for A(H1N1)pdm09, A(H3N2) virus than influenza B virus, both B/Victoria and B/Yamagata lineages with similar to the previous study [169]. There is evidence indicated the nucleotide evolution rate of polymerase gene including PB2 (1.82×10^{-3} substitutions/site/year), PB1 (0.87×10^{-3} substitutions/site/year), PA (1.32×10^{-3} substitutions/site/year) for human influenza A virus that circulating before 1968 were lower than our findings [8]. Besides, our data showed that B/Yamagata lineage was faster evolved than B/Victoria lineage. This result was consistent with the recent study that indicated the B/Yamagata substitution rate of PB2, PB1 and PA were 2.03×10^{-3} , 2.17×10^{-3} , and 2.40×10^{-3} substitutions/site/year, respectively. While 1.79×10^{-3} , 1.77×10^{-3} and 1.81×10^{-3} substitutions/site/year were nucleotide substitution rate of B/Victoria that found in PB2, PB1 and PA, respectively [170]. Among overall influenza (sub)type, genetically variable PA proteins were demonstrated higher variability than the PB2 and PB1 which was consistent with the previous report [171].

As we have known, the high evolution rate was typically found in surface glycoproteins such as hemagglutinin (HA) and neuraminidase (NA) due to the selective pressure of immune response [172]. The neuraminidase was also known as the target of currently antiviral agents, neuraminidase inhibitor. The evolution analysis of neuraminidase (NA) in Thailand indicated the mean substitution rate of A(H1N1)pdm09 (2009-2015) was 3.18×10^{-3} substitutions/site/year and A (H3N2) (2004-2015) was 3.49×10^{-3} substitutions/site/year and influenza B virus (20002-2015 with unidentified lineages) was 1.61×10^{-3} substitutions/site/year [92]. Furthermore, the previous evidence indicates the evolution rate of B/Yamagata in the NA gene was account for 2.82×10^{-3} substitutions/site/year and B/Victoria was 2.41×10^{-3} substitutions/site/year [172]. Comparing the evolution rate between neuraminidase and polymerase gene, the polymerase gene showed a slower evolve than neuraminidase although the evolution of polymerase gene is constantly evolving. In conclusion, this finding observed the evidence for the ongoing evolution of polymerase gene including the amino acid changes that are probably associated with the fluctuation of viral population diversity and provide the nucleotide substitution rate. Continual monitoring of genetic changes and evolution dynamics of polymerase gene included PB2, PB1 and PA segments will assist the development of further antiviral agents.

CHAPTER V

GENETIC AND ANTIGENIC DIVERGENCE IN THE INFLUENZA A(H3N2) VIRUS
CIRCULATING BETWEEN 2016 AND 2017 IN THAILAND

(Part 5.2)

(Published in: PloS one. 2017 Dec;12(12):e0189511.

DOI: <https://doi.org/10.1371/journal.pone.0189511>)

Nungruthai Suntronwong¹, Sirapa Klinfueng¹, Sumeth Korkong¹, Preeyaporn
Vichaiwattana¹, Thanunrat Thongmee¹, Sompong Vongpunsawad¹, Yong Poovorawan¹

จุฬาลงกรณ์มหาวิทยาลัย

¹Center of Excellence in Clinical Virology, Faculty of Medicine, Chulalongkorn
University, Bangkok, Thailand 10330

CHAPTER V

Part 5.2: Genetic and antigenic divergence in the influenza A(H3N2) virus circulating between 2016 and 2017 in Thailand.

Summary

Influenza virus evolves rapidly due to the accumulated genetic variations on the viral sequence. Unlike in North America and Europe, influenza season in the tropical Southeast Asia spans both the rainy and cool seasons. Thus, influenza epidemiology and viral evolution sometimes differ from other regions, which affect the ever-changing efficacy of the vaccine. To monitor the current circulating influenza viruses in this region, we determined the predominant influenza virus strains circulating in Thailand between January 2016 and June 2017 by screening 7,228 samples from patients with influenza-like illness. During this time, influenza A(H3N2) virus was the predominant influenza virus detected. We then phylogenetically compared the hemagglutinin (HA) gene from a subset of these A(H3N2) strains (n = 62) to the reference sequences and evaluated amino acid changes in the dominant antigenic epitopes on the HA protein structure. The divergence of the circulating A(H3N2) from the A/Hong Kong/4801/2014 vaccine strain formed 5 genetic groups (designated I to V) within the 3C.2a clade. Our results suggest a marked drift of the current circulating A(H3N2) strains in Thailand, which collectively contributed to the declining predicted vaccine effectiveness (VE) from 74% in 2016 down to 48% in 2017.

Introduction

Influenza A virus is an important respiratory pathogen responsible for the annual influenza outbreak and considerable socio-economic burden on the public healthcare system [173]. The multivalent influenza virus vaccine administered annually can reduce the risk of morbidity and mortality, but it is dependent on how well the chosen strains included in the vaccine match the strains in circulation [174]. The commonly circulating seasonal influenza A subtypes are A(H1N1)pdm09 and A(H3N2), of which the latter is reportedly associated with a high rate of hospitalization and mortality in the United States in the 2016-2017 flu season [175].

The hemagglutinin (HA) surface glycoprotein of A(H3N2) possesses defined antigenic and receptor-binding sites [85, 176]. The HA diversity resulting from accumulated mutations facilitates viral escape from the host immune response [177, 178]. The HA protein is proteolytically processed into two subunits (HA1 and HA2) [179]. The globular HA1 domain contains five antigenic sites (A through E) [180-182], while the HA2 stem domain mediates fusion and viral uncoating [66, 183]. Sequence drifts on the HA from accumulated mutations are observed more frequently in the A(H3N2) than A(H1N1), which often lead to the gradual reduction of the vaccine effectiveness (VE) over time [184-186]. As a result, influenza virus strains most suitable for vaccine production are carefully evaluated each year [187, 188].

Timely analysis of the genetic variations on the HA1 sequence of the circulating influenza virus strains is crucial for the prediction of VE. We therefore determined whether A(H3N2) was regionally predominant in the current influenza season and compared the genetic composition of the circulating A(H3N2) to the current vaccine strain A/Hong Kong/4801/2014.

Materials and Methods

Ethical approval

Respiratory samples from patients with influenza-like illness were analyzed in the Center of Excellence in Clinical Virology at King Chulalongkorn Memorial Hospital as part of the routine influenza surveillance program. This study was approved by the Institutional Review Board (IRB) of the Faculty of Medicine at Chulalongkorn University (IRB No. 377/57). The IRB waived the need for consent because the samples were de-identified and anonymous.

Samples and HA gene amplification

A total of 7,228 samples obtained between January 2016 and June 2017 in Bangkok and Khon Kaen province were collected from patients with fever $>38^{\circ}\text{C}$ and respiratory symptoms such as sore throat, nasal congestion, cough and runny nose. These individuals sought medical care at King Chulalongkorn Memorial Hospital, Bangpakok 9 International Hospital, and Chum Phae Hospital. Samples were subjected to viral RNA extraction (GeneAll Biotechnology, Seoul, Korea) according to the manufacturer's instructions. We used a previously described real-time reverse-transcription polymerase chain reaction (RT-PCR) to identify influenza virus A(H1N1pdm09), A(H3N2), and influenza B virus [126]. Influenza B virus-positive samples were subjected to cDNA synthesis using ImProm-II reverse transcription system (Promega, Madison, WI) and primer FluB (5'-AGCAGAAGCA-3') [189], followed by lineage determination using multiplex PCR and melting curve analysis [167, 190]. Among A(H3N2)-positive samples, 62 strains (approximately 4 strains per month) were randomly selected for cDNA synthesis using primer Uni12 (5'-AGCAAAGCAGG-3') [191] and the entire HA gene amplified using published primer sets [186]. Briefly, the reaction mixture consisted of 5 μl PRIME MasterMix (5Prime, Hamburg, Germany), 0.25 mM of MgCl_2 , 0.5 μM each of forward and reverse primers, 2 μl of cDNA template, and nuclease-free water to a final volume of 25 μl . Amplification in a thermal cycler was performed under the following conditions: initial denaturation for 3 minutes at 94°C , followed by 40 cycles of 30 seconds at 94°C for denaturation, primer annealing for 30 seconds at 55°C , 90 seconds at 72°C for extension, and 7 minutes of final extension at 72°C . Amplicons were agarose gel-purified using Expin Combo GP kit (GeneAll Biotechnology, Seoul, Korea) and the HA gene sequenced. A(H3N2) nucleotide sequences were assembled using the SeqMan Pro software (DNASTAR, Madison, WI) and deposited in the GenBank database under the accession numbers (MF673231-MF673292) (Table S10).

Phylogenetic analysis

A total of 91 A(H3N2) HA nucleotide sequences, 62 obtained from this study and an additional 29 sequences identified in Thailand publicly available from the NCBI (<http://www.ncbi.nlm.nih.gov>) and GISAID (<http://platform.gisaid.org>) databases, were aligned using ClustalW and translated into amino acid residues using BioEdit Software version 7.0.9.1 (Table S11). Phylogenetic analysis was performed using the maximum likelihood method and HKY+G model implemented in MEGA 6 [192]. Bootstrapping was done in 1,000 replicates and values >70% were shown. Potential N-linked glycosylation sites on the HA was determined using the NetNGlyc 1.0 server with the threshold value of >0.5 for the mean potential score[193]. The selective pressure or the proportion between nonsynonymous to synonymous substitutions (dN/dS , defined as ω) observed on all HA sequences were analyzed using the single likelihood ancestor counting (SLAC), fixed effects likelihood (FEL), and mixed effects model of evolution (MEME) algorithms implemented in the HYPHY software[194]. Positively selected codon was considered significant at P -value of 0.1. Amino acid residue numbering was based on the HA1 of the A(H3N2) vaccine strain A/Hong Kong/4801/2014 unless otherwise indicated. Residues different from those of the A/Hong Kong/4801/2014 were placed on a three-dimensional HA protein structure (A/Aichi/2/1968; Protein Data Bank accession number 1HGE) using VMD 1.9.2 [195].

Estimates of vaccine effectiveness

The predicted vaccine effectiveness (VE) was estimated using the P_{epitope} model, which characterizes the antigenic distance between the A(H3N2) vaccine and circulating strains. Antigenic distance defined by the P_{epitope} was calculated from the fraction of substituted amino acid residues in the dominant HA epitope [196]. For A(H3N2), the association between the VE and the P_{epitope} is given by $E = -2.47 \times P_{\text{epitope}} + 0.47$ in which VE is 47% when $P_{\text{epitope}} = 0$.

Statistical Analysis

Statistical analyses were performed using the Statistical Package for Social Sciences version 22.0 (SPSS Inc., Chicago, USA). The one-way ANOVA test was used to analyze VE divergence, and $p < 0.05$ was considered statistically significant.

Results

In all, 15.1% of the samples (1,091/7,228) tested positive for influenza viruses, of which 78.6% (857/1,091) were influenza A virus and 21.4% (234/1,091) were influenza B virus (Figure 18). As expected, an increase in the number of influenza virus-positive samples occurred in the rainier months (August to November). Among influenza A virus-positive samples, 62.8% (538/857) were A(H3N2) and 37.2% (319/857) were A(H1N1pdm09). Influenza B virus lineages were found to be 57.7% (135/234) B/Victoria and 42.3% (99/234) B/Yamagata. Thus, A(H3N2) represented a majority of the influenza virus during this study period.

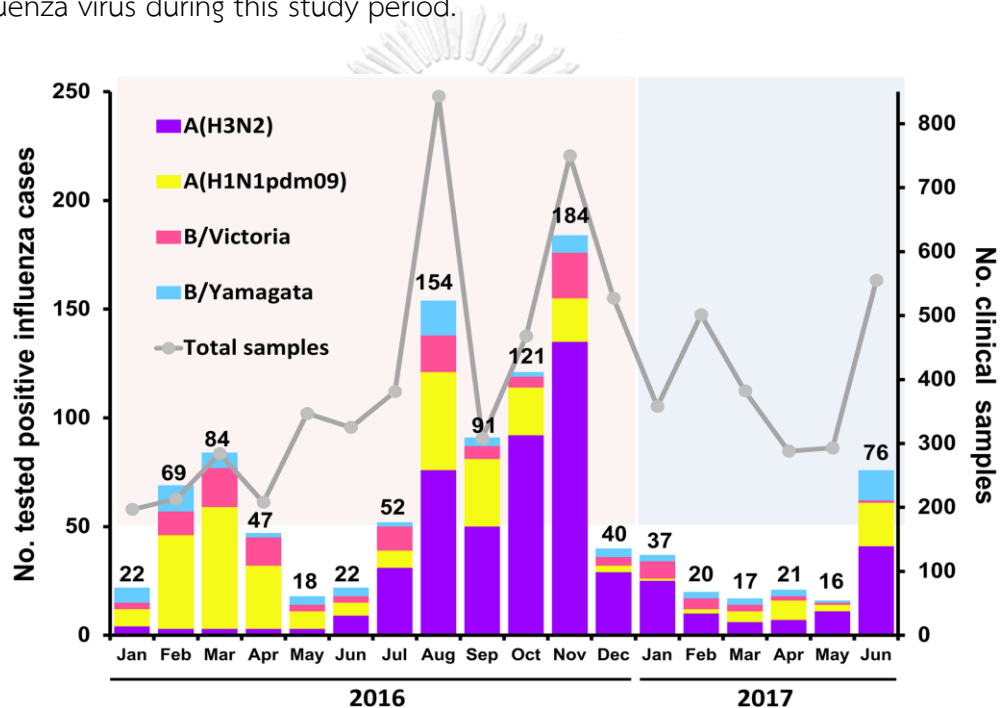


Figure 18 Distribution of influenza A(H3N2) virus between January 2016 and June 2017.

Total number of clinical samples evaluated (Y-axis on the right) and different influenza virus-positive samples are shown (Y-axis on the left). Numbers above the bar graphs denote influenza virus-positive samples identified each month.

Analysis of the HA gene sequence

Ninety-one complete coding sequences of the HA gene showed between 98.5-99.6% nucleotide sequence identity (98.1-99.8% amino acid sequence identity) to the A/Hong Kong/4801/2014 vaccine strain for A(H3N2). Among these, the vast majority diverged from the A/Hong Kong/4801/2014 (Figure 19). Most belonged to the 3C.2a

clade, which possessed distinct variations in amino acid patterns (designated group I to V). Their divergence was associated with sequential overlapping time of circulation. For example, group I strains (20/91) circulated in January to October 2016, while group II strains (20/91) circulated in November 2016 to March 2017. Group III strains (16/91) circulated between January and June 2017. Group IV strains (22/91) circulated between September 2016 and March 2017 and were most closely related to the A(H3N2) strains identified during 2016-2017 influenza season from several countries in the northern hemisphere (A/Denmark/107/2016, A/Israel/B6014/2016, and A/London/15/2017) [197, 198]. Interestingly, several novel A(H3N2) strains (4/91) circulating between January and April 2017 possessed sufficient residue variations in addition to what were previously described to warrant a separate cluster (group V).



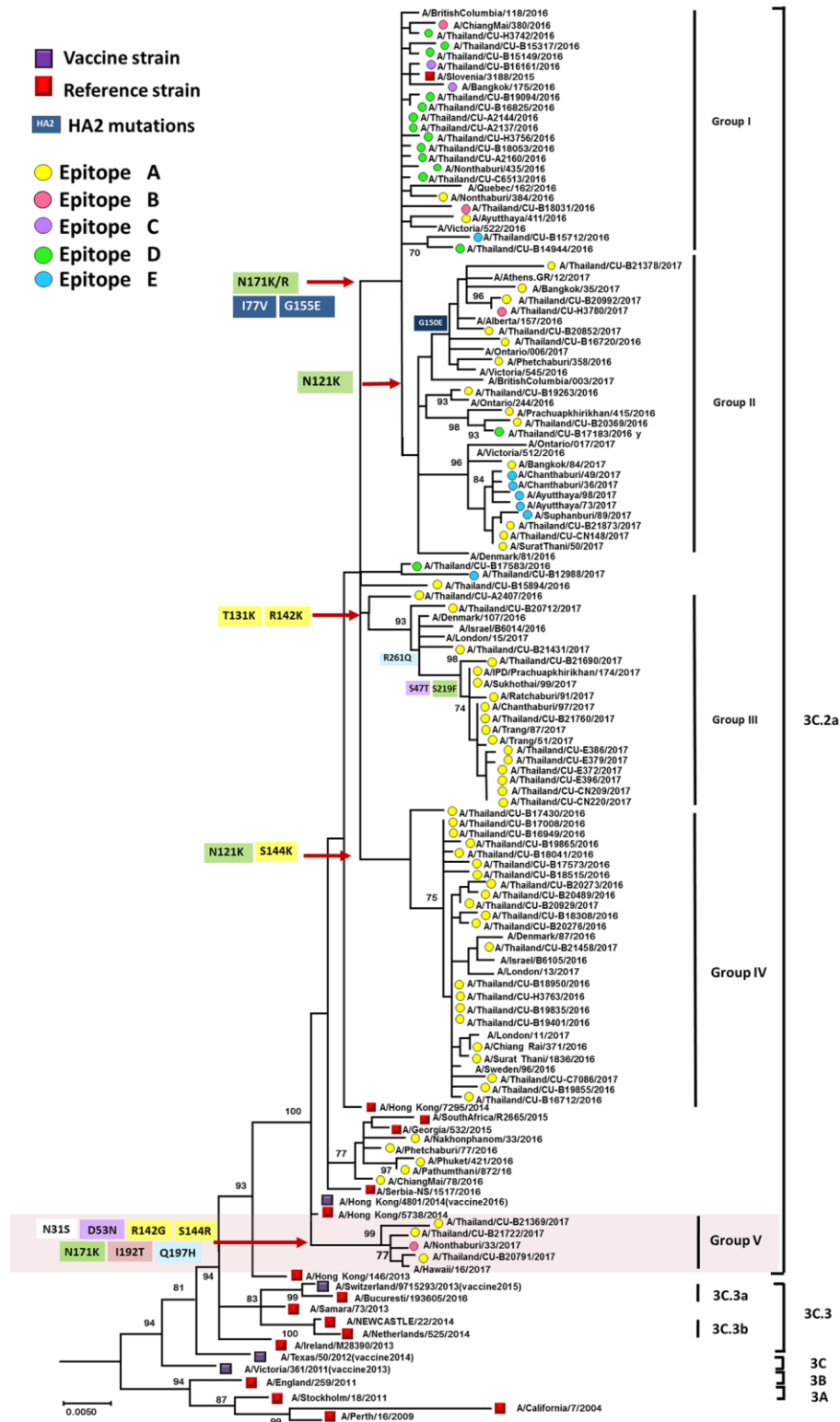


Figure 19 Phylogeny of the nucleotide sequences of the HA coding region of A(H3N2). Sequences of randomly selected samples from this study ($n = 62$) (designated A/Thailand/CU and denoted in colored dots) and those identified in Thailand from the databases during 2016-2017 ($n=29$) were compared to the A(H3N2) vaccine and

reference strains of known clades reported by the WHO and others (squares). The phylogenetic tree was constructed using the maximum likelihood method and HKY+G model with 1,000 bootstrap replicates implemented in MEGA (version 6). Branch values of >70% are indicated at the nodes. Dominant epitope (A-E) determined for each sequence are marked with different colored dots (A=yellow, B=pink, C=purple, D=green, and E=blue). The signature amino acid substitutions (colored) occurring on the antigenic epitopes are also shown. Scale bar represents approximately 0.5% nucleotide difference between close relatives. Residue numbers are specific for HA1 (color-coded by epitope) and HA2 (dark blue). The vaccine strain A/Hong Kong/4801/2014 belonged to 3C.2a clade. Shaded area (Group V) highlights strains of interest.

Residue variations on the HA affecting antigenic epitopes, receptor-binding site, and potential glycosylation

Comparison of the deduced amino acid sequences to that of A/Hong Kong/4801/2014 showed that group I differed from the vaccine strain by residues N171K and I77V+G155E(HA2), and group II by N121K+N171K/R and I77V+G155E(HA2). Some strains in group II also possessed additional residue variants K92R+H311Q (6/11), or Q75H and G150E (HA2) (5/11) (Figure S6). Group III strains were defined by residue pattern S47T+T131K+R142K+S219F+R261Q. Meanwhile, group IV strains differed from the vaccine strain by N121K+S144K. Most interestingly, the novel group V formed by strains identified in this study possessed a unique constellation of residue variations N31S+D53N+R142G+S144R+N171K+I192T+Q197H (Figure 20).

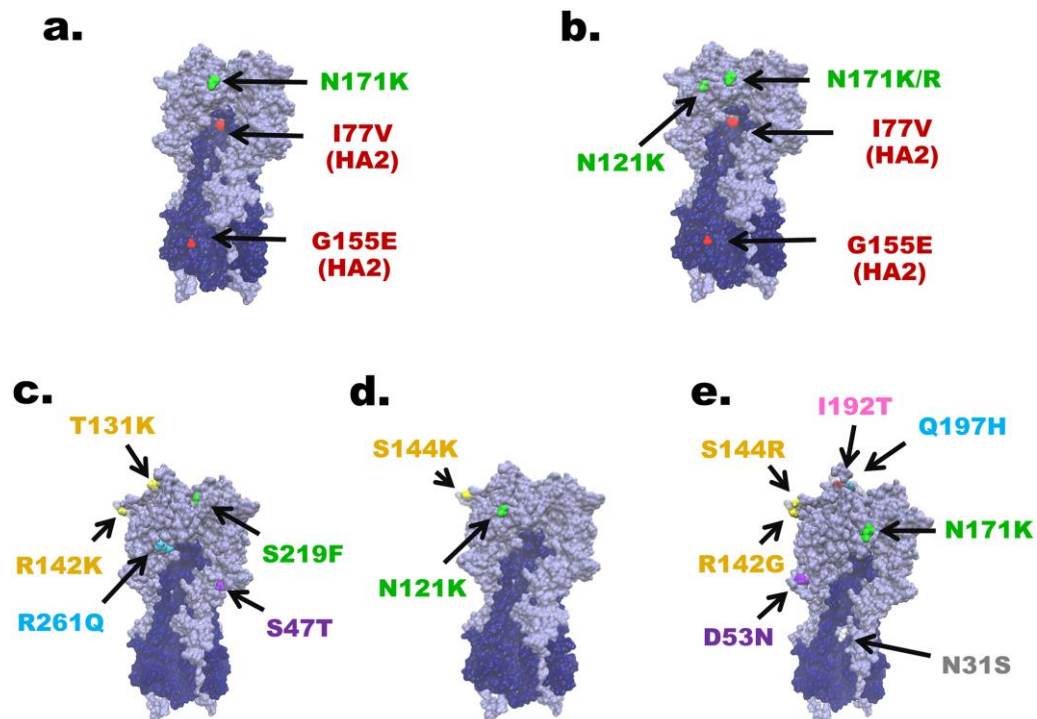


Figure 20 The defining residue substitutions placed on the HA protein structure of A(H3N2).

Differences between A(H3N2) strains in this study and A/Hong Kong/4801/2014 were visualized on the homotrimeric HA structure of A/Aichi/2/1968 (Protein Data Bank accession number: 1HGE). (a) to (e) correspond to groups I to V, respectively.

Residues on the five antigenic sites are color-coded: A (yellow), B (pink), C (purple), D (green) and E (blue). Mutation not located within the antigenic site (white) and mutations in HA2 (red) are also noted.

A(H3N2) strains circulating in Thailand collectively showed a total of 37 residue substitutions in the antigenic epitopes. Some of the strains possessed as many as seven amino acid changes. Among 53 sequenced strains from 2016, those identified at the beginning of the year were epitope D dominant as characterized by N121K, N171K/, and S219Y/F. Sequence shift to mostly epitope A were observed by the end of 2016 as characterized by N122D, T131K , T135K, R142K/G and S144K/R. Not surprisingly, A(H3N2) strains identified in the first-half of 2017 (n = 38) continued to show dominance in epitope A. Among the potential N-linked glycosylation sites on the HA (at residues 8, 22, 38, 45, 63,122, 126, 133, 158, 165, 246, 285 and 483 on the A/Hong Kong/4801/2014 vaccine strain) (15), substitutions at N122D (1/91) and S124N (2/91) found in some strains in this study eliminated the potential glycosylation site at residue 122 (Figure S6). Additionally, there was a loss of potential glycosylation site at

residue 126 due to N126S substitution (1/91), at residue 133 due to T135K (9/91), and at residue 158 due to N158K (3/91) and T160K (2/91) substitutions.

The receptor-binding sites of A(H3N2) are highly conserved at positions 98, 136, 153, 183, 190, 194, 195 and 228 on HA1 (13). We observed T135K residue change adjacent to the receptor-binding region for all 3C.2a group II strains. Evolutionary selective pressure on the entire HA amino acid sequence analyzed using the dN/dS ratio showed an average of 0.305 (SLAC algorithm) among the A(H3N2) strains in this study, suggesting no positively selected site. Meanwhile, the FEL method revealed that residues 142, 171, 261 and 406 (HA numbering) were under positive selection pressure. Moreover, the MEME method indicated five positively selected sites (131, 144, 171, 261 and 416). Therefore, these data provided strong evidence of positively selected sites within epitope A (131, 142 and 144), D (171) and E (261) (Table S12).

Predicted vaccine effectiveness

The average P_{epitope} value was 0.049 ($n = 53$) for all of the A(H3N2) strains identified in 2016, suggesting a predicted worst-case VE against the virus of 74.17%. Meanwhile, the average P_{epitope} was 0.099 ($n = 38$) for strains identified in 2017, suggesting a predicted worst-case VE against the virus of 47.87% (Table S13). Although the predicted VE between the strains identified in this study and the A/Hong Kong/4801/2014 vaccine strain ranged between 17.02 and 87.18%, there was an overall decline in predicted VE each quarter (Figure 21). These results suggest that the A(H3N2) strains circulating in Thailand drifted from the vaccine strain and effectively reduced the VE.

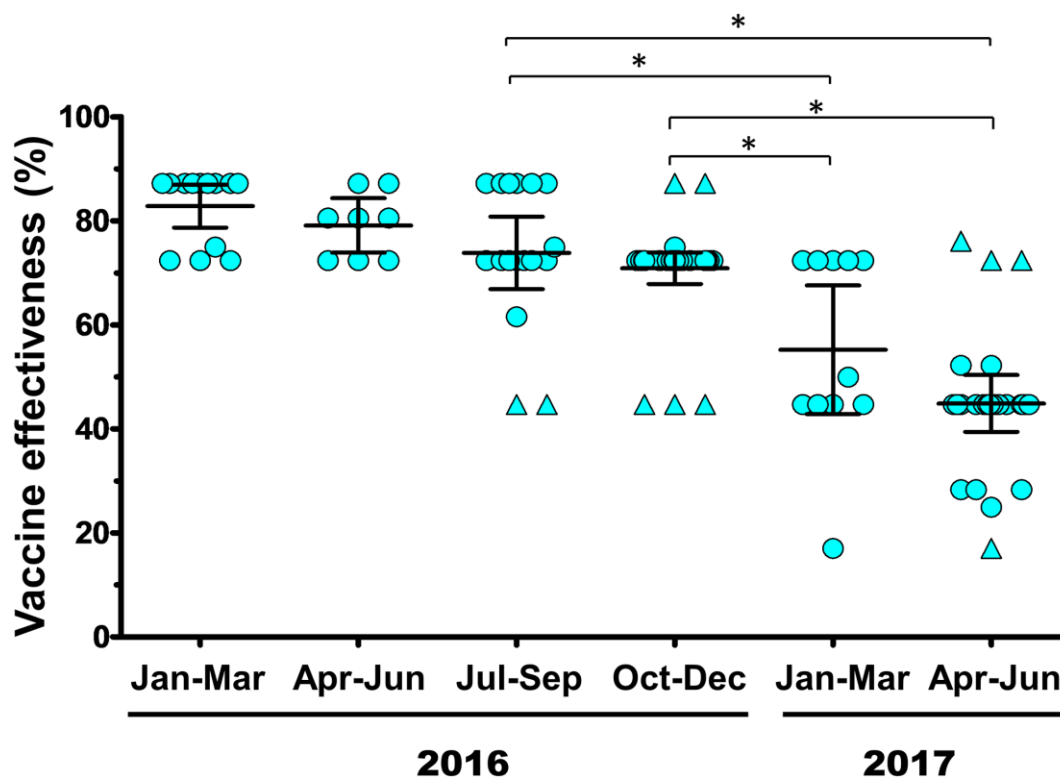


Figure 21 Calculated quarterly VE between January 2016 and June 2017.

Vaccine effectiveness (VE) was derived using the $P_{epitope}$ model by comparing the A(H3N2) sequences identified in this study to that of the vaccine strain A/Hong Kong/4801/2014. Circles represent the predicted VE percentage for each strain analyzed, while triangles represent statistical outliers. For each quarter, the middle bar represents the mean value, while the upper and lower bars denote interquartile range. Asterisks indicate statistically significant differences ($P < 0.01$).

Discussion

In this study, we aimed to characterize the circulating A(H3N2) in Thailand beginning in 2016 by determining clade designation and identifying mutations in the antigenic sites impacting the predicted VE. We categorized the strains identified in this study and those reported elsewhere between 2016 and 2017 using the HA sequences. Due to evolving genetic variations of A(H3N2) and the lagging nomenclature standard, we attempted to reconcile the most recent 3C.2a strains identified to date. Group I and II strains in this study collectively represented clade 3C.2a1 designated by the WHO. Group III strains in this study comprised some newer Israel strains and the proposed 3C.2a1 cluster III from the U.K., while group IV described additional Israel strains and the proposed 3C.2a2 clade (29,30). Additionally, newly emergent A(H3N2) strains identified in this study necessitated further subdivision into a separate group V according to a number of significant variance from the A/Hong Kong/4801/2014 vaccine strain and other previously described variants. Members of group V were characterized by seven amino acid substitutions at N31S, D53N, R142G, S144R, N171K, I192T and Q197H. These residue variants have a number of implications including alterations of the antigenic epitopes and immune escape. For example, residue 144 in antigenic site A is adjacent to residue S145 implicated in receptor-binding [199].

New antigenic variants emerge when at least one substitution occurred in the antigenic sites [182, 200]. Several strains circulating in Thailand (5/74) belonging to group II and IV demonstrated F193S change located in epitope B, which is one of seven mutation sites representing a major antigenic transition cluster [85]. Both N122D and N126S in some A(H3N2) strains resulted in the loss of N-linked glycosylation, an important observation to consider since the gain or loss of N-linked glycosylation can affect influenza virus virulence and recognition by neutralizing antibody [201]. T135K located adjacent to the receptor-binding site in epitope A has also been identified in other studies and is implicated in decreasing vaccine effectiveness [202, 203]. Taken together, these variations underscore the rapid evolution of A(H3N2) influenza virus in circulation.

Southeast Asian countries use the influenza vaccine formulated for the southern hemisphere, which for some years have different inclusion strains in the vaccine than those formulated for the northern hemisphere. A/Hong Kong/4801/2014 belonging to clade 3C.2a (characterized by N121K) is a component in both northern and southern hemispheres since 2016. This vaccine strain was well-matched for the circulating A(H3N2) in Thailand that first season (predicted VE of approximately

80%)[159]. Since then, A(H3N2) strains circulating in Europe and Canada have genetically drifted away from the vaccine strain consistent with the observed antigenic drift and decreasing predicted VE we found in this study for each quarterly period beginning in 2016 [204-206]. As a result, A/Hong Kong/4801/2014 may not be as effective in eliciting immunity against future circulating A(H3N2) in the next influenza season despite the decision to include it in the 2017-2018 vaccine for northern hemisphere [75].

This study had several limitations. We were unable to ascertain the vaccination status of the individuals in which the samples were derived, which would have improved the evaluation of the predicted VE. The scope of this study did not allow us to determine additional evolutionary relationships among the strains identified in different countries, which would have required additional nucleotide sequences from around the world not yet deposited in the databases and a longer study time frame. The antigenic drift and predicted VE were estimated from the accumulated mutations on the antigenic epitopes and would benefit from additional antigenic characterization such as hemagglutination inhibition assay. Finally, immunity against the neuraminidase contributing to the antigenic drift was not assessed in this study. Nevertheless, any genetic surveillance of influenza viruses will continue to be an important component in influenza prevention and vaccine improvement.



CHAPTER V

CHARACTERIZING GENETIC AND ANTIGENIC DIVERGENCE FROM VACCINE
STRAIN OF INFLUENZA A AND B VIRUSES CIRCULATING IN THAILAND,
2017-2020

(Part 5.3)

(Submission in Journal Scientific Reports)

Nungruthai Suntronwong¹, Sirapa Klinfueng¹, Sumeth Korkong¹, Preeyaporn
Vichaiwattana¹, Thanunrat Thongmee¹, Sompong Vongpunsawad¹, Yong Poovorawan¹

จุฬาลงกรณ์มหาวิทยาลัย

Chulalongkorn University

¹Center of Excellence in Clinical Virology, Faculty of Medicine, Chulalongkorn
University, Bangkok, Thailand 10330

CHAPTER V

Part 5.3: Characterizing genetic and antigenic divergence from vaccine strain of influenza A and B viruses circulating in Thailand, 2017-2020.

Summary

We monitored the circulating strains and genetic variation among seasonal influenza A and B viruses in Thailand between July 2017 and March 2020. The hemagglutinin gene was amplified and sequenced. We identified amino acid (AA) changes and estimated predicted vaccine effectiveness (VE) using the P_{epitope} model. Phylogenetic analyses revealed multiple clades/subclades of influenza A(H1N1)pdm09 and A(H3N2) were circulating simultaneously and evolved away from their vaccine strain, but not the influenza B virus. The predominant circulating strains of A(H1N1)pdm09 belonged to 6B.1A1 (2017–18) and 6B.1A5 (2019–20) with additional AA substitutions. Clade 3C.2a1b and 3C.2a2 viruses co-circulated in A(H3N2) and clade 3C.3a virus was found in 2020. The B/Victoria-like lineage predominated since 2019 with an additional three AA deletions. Antigenic drift was dominantly facilitated at epitopes Sa and Sb of A(H1N1)pdm09, epitopes A, B, D and E of A(H3N2), and the 120 loop and 190 helix of influenza B virus. Moderate predicted VE was observed in A(H1N1)pdm09. The predicted VE of A(H3N2) indicated a significant decline in 2019 (9.17%) and 2020 (–18.94%) whereas the circulating influenza B virus was antigenically similar (94.81%) with its vaccine strain. Our findings offer insights into the genetic divergence from vaccine strains, which could aid vaccine updating.

Introduction

Influenza A and B virus infection remains a common cause of respiratory disease worldwide [207]. The majority of seasonal influenza viruses in circulation are influenza A(H1N1)pdm09, A(H3N2), and two lineages of the influenza B virus (B/Yamagata-like lineage and B/Victoria-like lineage) [208]. Annual influenza vaccination can reduce the risk of morbidity and mortality in infected individuals, but in some years the influenza vaccine offers lower than expected efficacy due to antigenic differences against the strains circulating in the community [209]. Recently, several new subclades of A(H3N2) have emerged, which have contributed to the reduction of the effectiveness of the vaccine [210, 211]. Although influenza A(H1N1)pdm09 evolved at a slower rate than A(H3N2), newly emerging genetic groups have been reported [212]. In addition, B/Victoria-like lineage strains with deletions are also increasingly prevalent [213].

The hemagglutinin (HA) protein is an important surface glycoprotein, which possesses the antigenic and receptor-binding sites (RBSs) and elicits the host immune response [214, 215]. The HA protein is divided into the globular head domain (HA1) and the stem domain (HA2). There are proposed antigenic sites on the HA1 of A(H1N1)pdm09 (Sa, Sb, Ca1, Ca2, and Cb) and on the HA1 of A(H3N2) (A through E) [84, 182, 214]. Meanwhile, there are four major HA antigenic sites for influenza B virus (120 loop, 150 loop, 160 loop, and 190 helix) [88]. Accumulation of mutations in the HA protein, particularly on the antigenic sites, RBSs and the surrounding region, has enabled the continuous evolution and the emergence of new influenza virus strains [85, 178, 182], which escape the existing neutralizing antibodies [216]. As a result, the influenza virus strains to be included in the annual vaccine composition are carefully evaluated each year [213].

Although influenza activity in Thailand occurs throughout the year, it is often bimodal¹⁷. Most influenza infection occur in the rainy season (August to November), but frequent infection can also occur in the cooler and drier months of January to March [114, 120]. Thailand is geographically located in the northern hemisphere, but uses the vaccine formulation for the southern hemisphere based on the seasonal influenza virus infection data. Typically, the vaccine composition for the southern hemisphere is determined many months before the actual influenza season begins in order to allow time for production and distribution [217, 218]. Occasionally, the selected strains to be included in the vaccine are not well-matched (antigenically dissimilar) with the actual circulating strains and subsequently resulted in the poor

vaccine effectiveness (VE) [219] as happened during the 2014-15 and 2016-17 influenza seasons [120, 159].

Periodic monitoring of the influenza virus strains circulating in the region is important for antigenic characterization and improved vaccine design. Here, we examined the influenza incidence from July 2017 and March 2020 from samples submitted for routine diagnostics from three hospitals in Thailand. We characterized the genetic and antigenic variations of the HA gene on 90 strains of influenza A(H1N1)pdm09, 90 strains of influenza A(H3N2), and 81 strains of influenza B virus sampled monthly over the study period. Deduced amino acid changes were mapped on the HA three-dimensional structures, and the predicted VE was analyzed for each influenza (sub)types.



Materials and methods

Ethical approval of the study protocol

The study was approved by the Institutional Review Board of Faculty of Medicine of Chulalongkorn University (No. 127/ 61). All clinical specimens were de-identified and analyzed anonymously. Findings in this work were intended to be public health surveillance of influenza in Thailand. For these reasons, it did not require informed consent.

Sample collection and testing

Respiratory specimens comprising of nasopharyngeal swabs were submitted for testing as part of the routine influenza surveillance from July 2017 to March 2020 from patients with influenza-like illness (ILI). ILI was defined as fever (body temperature $>38^{\circ}\text{C}$) combined with respiratory symptoms (cough, nasal congestion, runny nose, sore throat). A total of 17,480 samples from Bangpakok 9 International Hospital ($n = 14,743$), King Chulalongkorn Memorial Hospital ($n = 266$), and Chum Phae Hospital ($n = 2,471$) were tested. Viral RNA was extracted directly from clinical samples by using Ribospin vRD II according to the manufacturer's instructions (GeneAll Biotechnology, Seoul, Korea). Real-time reverse-transcription quantitative polymerase chain reaction (RT-qPCR) was used to identify A(H1N1pdm09), A(H3N2), and the influenza B virus as previously described [126]. Laboratory-confirmed influenza B-positive samples were subjected to cDNA synthesis with primer FluB (5'-AGCAGAAGCA-3') and ImProm-II Reverse Transcription System (Promega, Madison, WI, USA), followed by multiplex PCR and melting-curve analysis [167].

Amplification of the hemagglutinin gene

Samples positive for influenza A(H1N1)pdm09 ($n = 90$), influenza A(H3N2) ($n = 90$), or influenza B virus ($n = 81$) sampled monthly throughout the study period were subjected to conventional RT-PCR to amplify the entire HA gene and Sanger sequencing. Influenza A(H1N1)pdm09 and A(H3N2) were subjected to cDNA synthesis using primer Uni12 (5'-AGCAAAAGCAGG-3'). The primer sets for both influenza A and B viruses have been described elsewhere [125, 186]. PCR mixture of 25 μL contained 5 μL of AccuStart II GelTrack PCR SuperMix (Quantabio, Beverly, MA, USA), 0.25 mM MgCl_2 , 0.5 μM each of forward and reverse primers, and 3 μL of cDNA template. Amplification conditions were 94°C for 3 min, 40 cycles of 30 s at 94°C , 30 s at 55°C , 90 s at 72°C , followed by 7 min of final extension at 72°C . Amplicons were agarose gel-purified and subjected to Sanger sequencing. Nucleotide sequences were assembled using SeqMan Pro (DNASTAR, Madison, WI, USA) and deposited in the GenBank

database under the accession numbers MT803149-MT803238 for A(H1N1)pdm09, MT803239-MT803328 for A(H3N2) and MT803397-MT803477 for influenza B viruses (Table S14).

Genetic characterization

Phylogenetic trees for each influenza virus were generated using the nucleotide sequences obtained from this study and additional HA sequences from other Thai strains previously identified and available from the National Center for Biotechnology Information (www.ncbi.nlm.nih.gov) and the Global Initiative for Sharing All Influenza Data (GISAID) (<http://platform.gisaid.org>) database. A total of 183 nucleotide sequences of influenza A(H1N1)pdm09, 232 nucleotide sequences of influenza A(H3N2), and 177 nucleotide sequences of the influenza B virus were aligned with the reference and vaccine strains for each influenza virus using MUSCLE. Nucleotide substitution models for the HA gene of influenza A(H1N1)pdm09 (TN93+G), influenza A(H3N2) (HKY+G+I) and influenza B (HKY+G) were implemented in MEGA X [220]. Trees were constructed using the maximum-likelihood method and bootstrapping of 1,000 replicates. Deduced amino acid sequences were compared to the reference and vaccine strains to identify substitutions, which were noted at each branch node on the phylogenetic trees. Potential N-linked glycosylation sites on the HA gene was analyzed using the NetNGlyc 1.0 server and a threshold value of >0.5 [193].

Visualization of amino acid residue changes on the HA structure

Publicly available three-dimensional crystal structures of influenza virus HA of influenza virus strains A(H1N1)pdm09 (A/California/04/2009, Protein Data Bank accession number 3LZG), A(H3N2) (A/Victoria/361/2011, accession number 4WE9), B/Victoria (B/Brisbane/60/2008, accession number 4FQM) and B/Yamagata (B/Yamanashi/166/98, accession number 4M44) were used to illustrate approximate residue position and changes on the HA. Identification of residues in the structure was performed using PyMOL Molecular Graphics System v1.3 (Schrödinger; www.schrodinger.com). Amino acid single-letter code preceding the numerical position represents residue in the vaccine strains, while amino acid single-letter code following the numerical position represents that found in this study. Vaccine strains were A(H1N1)pdm09 (A/Michigan/45/2015), A(H3N2) clade 3C.2a (A/Hong Kong/4801/2014), A(H3N2) clade 3C.3a (A/Switzerland/9715293/2013), B/Victoria-like lineage (B/Brisbane/60/2008), and B/Yamagata-like lineage (B/Phuket/3073/2013).

Determination of selection pressure

The ratio of non-synonymous/synonymous substitutions (dN/dS) was considered when evaluating codon under selective pressure. dN/dS was analyzed using

the mixed-effects model of evolution (MEME) and the fixed effects likelihood (FEL) methods. Both algorithms were in the HYPHY software implemented in the Datamonkey webserver (<https://www.datamonkey.org/>) [194]. Positively selected residue was considered significant at $P = 0.1$.

Prediction of VE

The predicted influenza VE was estimated using the P_{epitope} model, which took into account the distinct antigenic sites between circulating strains and the vaccine strain by considering the epitope sites. The P_{epitope} model was calculated by using the number of amino-acid substitutions in the dominant epitope and the total number of amino acids in that dominant epitope. The association between the P_{epitope} model and VE was determined by a mathematical formula. For A(H1N1)pdm09, $VE = -1.19 \times P_{\text{epitope}} + 0.53$ in which VE is 53% when the $P_{\text{epitope}} = 0$ [221]. For A(H3N2), the association between the VE and P_{epitope} is given by $VE = -2.47 \times P_{\text{epitope}} + 0.47$ in which VE is 47% when $P_{\text{epitope}} = 0$ [196]. For the influenza B virus, $VE = -0.864 \times P_{\text{epitope}} + 0.6824$ in which VE is 68.24% when $P_{\text{epitope}} = 0$ [222]. The trend of predicted VE was computed using R v3.6.0 (R Foundation for Statistical Computing, Vienna, Austria). The difference among annually predicted VE was calculated using one-way ANOVA ($P < 0.05$ was considered statistically significant). Statistical analysis was done using Prism 8.0 (GraphPad, San Diego, CA, USA).

Results

In this study, 20.90% (3,654/17,480) of the nasopharyngeal swabs from ILI patients tested positive for influenza virus, of which 74.2% (2,711/3,654) were influenza A virus and 25.8% (943/3,654) were influenza B virus. Typical monthly influenza activity peaked between August and November, and again in January to March (Figure 22). Among influenza A virus-positive samples, 52.2% (1,415/2,711) were A(H3N2) and 47.8% (1,296/2,711) were A(H1N1)pdm09). Influenza B virus of the B/Yamagata lineage predominated during the 2017-18 season and accounted for 48.4% (456/943) over the study period. In comparison, influenza B/Victoria accounted for 51.6% (487/943) and was most predominant in the 2019-20 season.

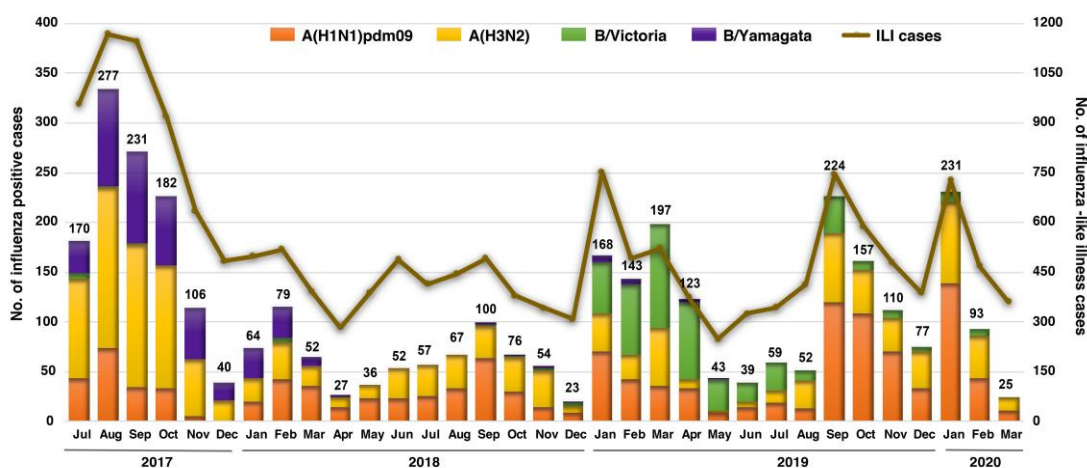


Figure 22 Monthly distribution of influenza A and B viruses from July 2017 to March 2020 ($n = 17,480$).

Numbers above the bar graph indicate the monthly number of influenza virus-positive samples (left Y-axis) with respect to the monthly ILI samples (right Y-axis).

Characterization of the clades/subclades based on HA sequences and their divergence from the vaccine strain

A(H1N1)pdm09

To better understand the genetic changes among the recently circulating influenza strains in Thailand, we selected representative influenza samples for genetic characterization (Table S1). We analyzed the phylogenetic tree of 183 HA sequences of influenza A(H1N1)pdm09 comprising the Thai strains identified in this study and

previously elsewhere in Thailand, along with the vaccine and reference strains. Compared to A/Michigan/45/2015, the vaccine strain for the southern hemisphere from 2017 and 2019, all of the A(H1N1)pdm09 Thai strains belonged to clade 6B.1 and 89.6% (164/183) further clustered into subclade 6B.1A, which possessed changes of amino acid residue S74R, S164T, and I295V (Figure 23). Since 2018, circulating Thai strains further diverged to form subclades 6B.1A1, 6B.1A5 and 6B.1A6 which all carried the S183P mutation (Figure S7). Strains in the subclade 6B.1A5A (characterized by N129D, T185I, D235E, and D260N on HA1, and A193V on HA2) predominated in the 2019-20 season. Interestingly, a subset of 6B.1A5A Thai strains possessed additional D187A and Q189E changes and clustered with the 2020-2021 season northern hemisphere vaccine strain A/Guangdong-Maonan/SWL1536/2019. The most divergent among the 6B.1A5A subclade was a cluster of strains possessing N156K, K130N, L161I, V250A (HA1) and E179D (HA2). Taken together, these data suggest that the existing A(H1N1)pdm09 strains circulating in recent years have genetically drifted from the A/Brisbane/02/2018, which was introduced as the 2020 southern hemisphere vaccine strain (Figure S8).

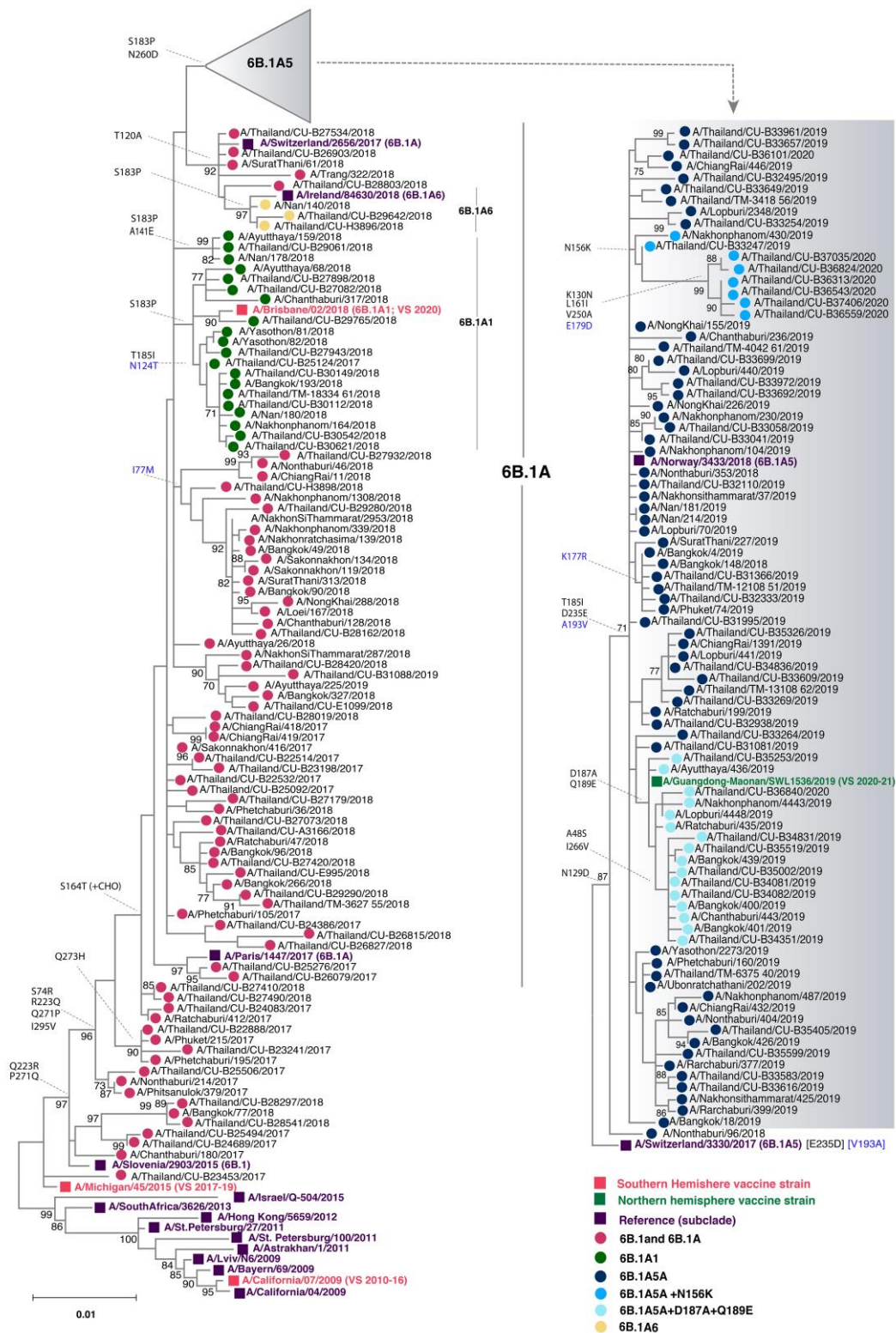


Figure 23 Phylogenetic analysis of the entire HA gene of A(H1N1)pdm09.

Sequences from 90 A/Thailand/CU strains and 93 other Thai strains available from the database were compared with the A(H1N1)pdm09 vaccine and reference strains of known clades. Phylogenetic tree was constructed using the maximum-likelihood

method using the TN93+G model with 1,000 bootstrap replicates implemented in MEGAX. Branch values of >70% are indicated at the nodes, along with the characteristic residues defining these branches. Residue changes in HA1 are denoted in black; changes in HA2 are in blue. Gain (+CHO) and loss (-CHO) potential glycosylation sites were indicated. Southern hemisphere vaccine strains (magenta squares), the 2020-21 northern hemisphere vaccine (green squares) and the reference strains (purple squares) are indicated. Colored circles indicate the clade and subclade of A(H1N1)pdm09 circulating strains. VS defined as vaccine strain.

A(H3N2)

Phylogenetic analysis of 232 HA sequences of influenza A(H3N2) comprising the Thai strains identified in this study and previously elsewhere in Thailand, along with the vaccine and reference strains, showed that 98.7% (229/232) belonged to clade 3C.2a (the remaining three Thai strains were 3C.3a, all identified in 2020) (Figure 24). These Thai strains diverged into subclades 3C.2a1 (defined by N121K, R142G, and N171K on HA1, and I77V and G155E on HA2) and 3C.2a2 (defined by T131K, R142K, and R261Q on HA1) (Figure S7). Further divergence into 3C.2a1b was marked by E62G, K92R, and H311Q on HA1, and E150G on HA2. Strains identified circulating during 2017-2018 are the 3C.2a1b with addition of T135K that circulated together with 3C.2a2 virus. Most circulating strains in 2019 were 3C.2a1b with T131K, which diverged from the 2019 season southern hemisphere vaccine strain A/Switzerland/8060/2017 (3C.2a2). Co-circulation of 3C.2a1b (with additional T135K and T128A) and 3C.3a virus was identified in the first three months of 2020. The additional residue changes in subclade 3C.2a1b at positions 128 and 135 resulted in a loss of potential glycosylation at these sites. The 3C.3a virus was characterized by S91N, N144K, F193S on HA1, and I149M and D160N on HA2 (by comparison with B/Switzerland/9715293/2013), which were genetically similar to the 2019-2020 season northern hemisphere vaccine strain A/Kansas/14/2017. From our data, A/South Australia/34/2019 chosen for the 2020 A(H3N2) southern hemisphere vaccine strain will not expect a good match since 60% of the currently circulating strains are from 3C.2a1 with T135K and T128A, while 30% are 3C.3a in 2020 (Figure S8).

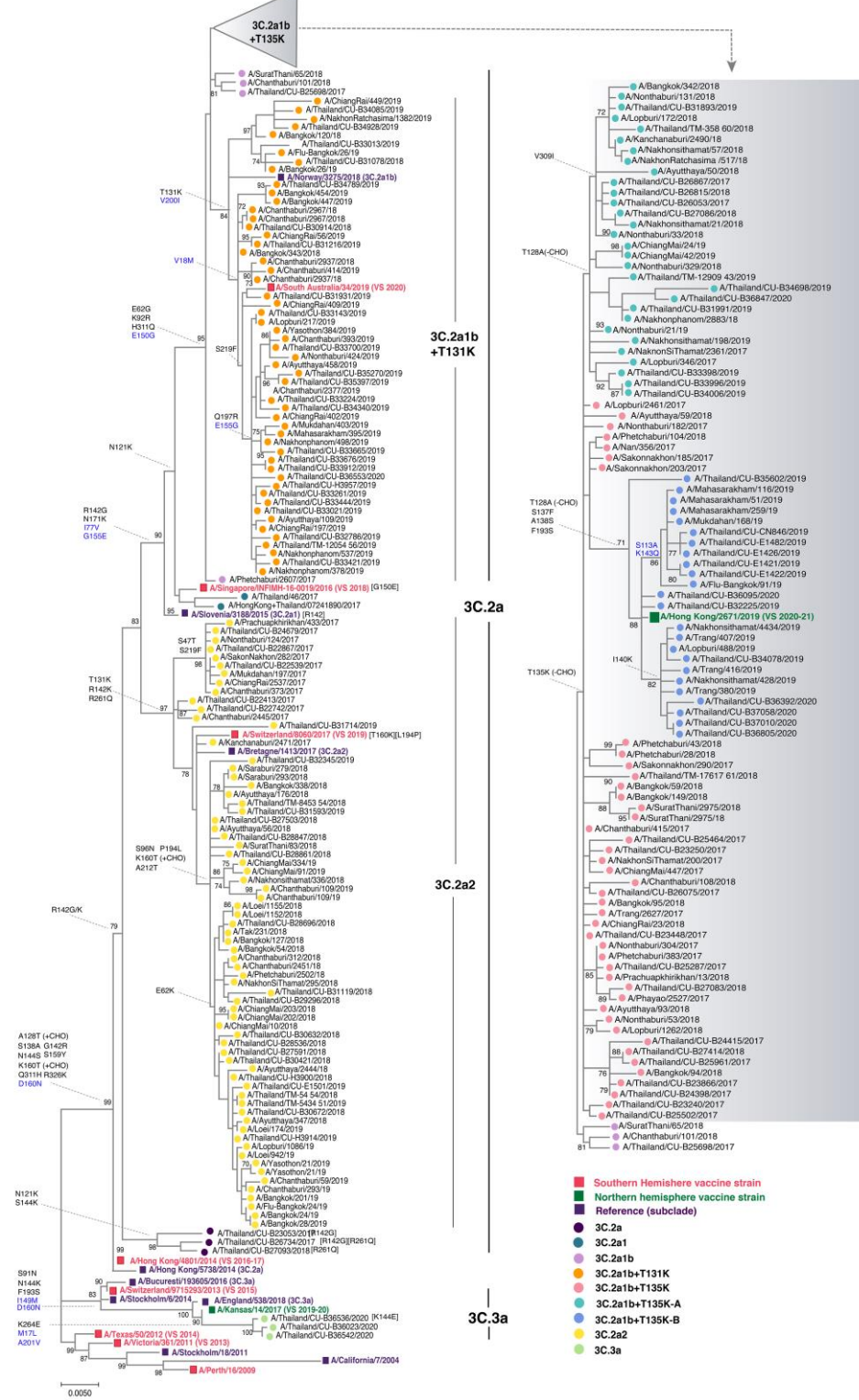


Figure 24 Phylogenetic analysis of the HA gene of A(H3N2).

Sequences from 90 A/Thailand/CU strains and 142 other Thai strains available from the database were compared with the A(H3N2) vaccine and reference strains of known clades. Phylogenetic tree was constructed using the maximum-likelihood

method using the HKY+G+I model with 1,000 bootstrap replicates implemented in MEGAX. Branch values of >70% are indicated at the nodes, along with the characteristic residues defining these branches. Residue changes in HA1 are denoted in black; changes in HA2 are in blue. Gain (+CHO) and loss (-CHO) potential glycosylation sites were indicated. Southern hemisphere vaccine strains (magenta squares), the 2019-21 northern hemisphere vaccine (green squares) and the reference strains (purple squares) are indicated. Colored circles denote the clade and subclade of A(H3N2) circulating strains. VS defined as vaccine strain.

Influenza B virus

From the analysis of 177 HA sequences, the circulating B/Yamagata strains were belonged to clade 3 and experience very little change (L172Q and M251V) compared to the B/Phuket/3073/2013, which served as the southern hemisphere vaccine strain since 2015 (Figure 25). Our B/Victoria strains belonged to clade 1A and grouped with B/Brisbane/60/2008, which was the vaccine strain prior to 2019. These strains possessed either 162-163 double deletions with I180V, or 162-164 triple deletions with I180T or K136E in HA1. From 2019 onward, however, strains with triple deletions and K136E predominated (68/77), which clustered with the 2020 southern hemisphere vaccine strain B/Washington/02/2019.

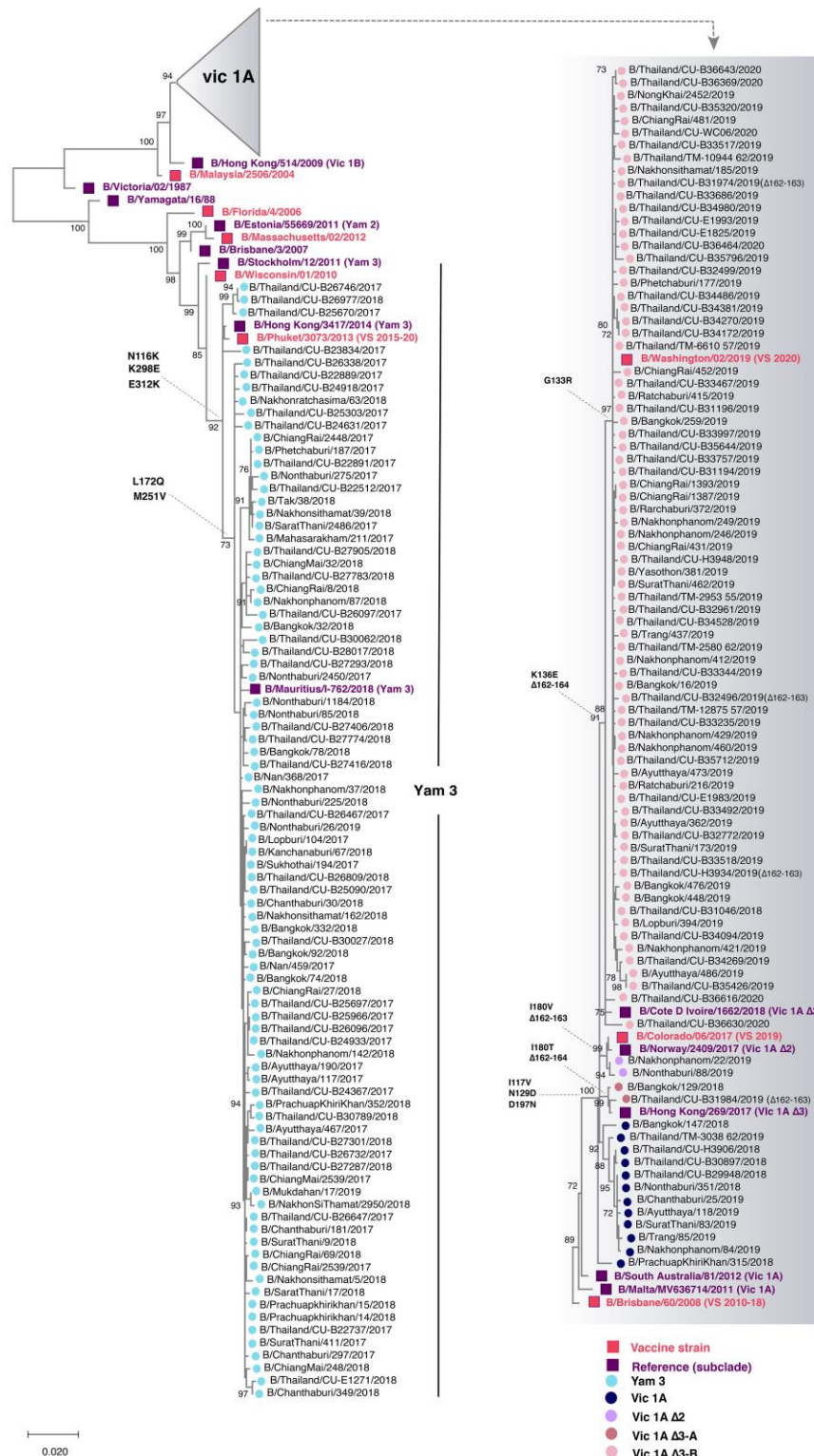


Figure 25 Phylogenetic analyses of the nucleotide sequences of the HA coding region of the influenza B virus.

Eighty-one nucleotide sequences from this study (designated A/Thailand/CU) and other Thai strains available from the database during July 2017-March 2020 (n = 96)

were compared with the influenza B vaccine and reference strains of known clades (magenta and purple squared, respectively). Phylogenetic tree was constructed using the maximum-likelihood method and the HKY+G model with 1,000 bootstrap replicates implemented in MEGAX. Branch values of >70% are indicated at nodes. Colored circles denote the clade and subclade of the circulating influenza B virus strains. VS defined as vaccine strain.

Deduced amino acid changes mapped onto the receptor binding and antigenic sites of HA

To visualize how amino acid changes present among the Thai strains in this study may affect important domains on the HA, we used publicly available influenza A and B virus HA structures to project amino acid differences between the vaccine and the Thai strains. Comparing the circulating influenza A(H1N1)pdm09 with A/Michigan/45/2015 (vaccine strain since 2017), we identified N156K, L161I and S164T substitutions on the Sa antigenic site (Figure 26A), which often drives A(H1N1)pdm09 evolution, particularly at residue 156 [85]. We found that T185I, D187A, and Q189E mapped to the Sb antigenic site and overlapped the RBS, while S74R is on epitope Cb. No residue changes appeared on epitopes Ca1 nor Ca2.

Using A/Hong Kong/4801/2014 as a representative A(H3N2) vaccine strain for subclade 3C.2a, five residue changes mapped to antigenic epitope A (T131K, T135K, S137F, A138S, R142G/K), three residues mapped to epitope B (T128A, T160K, and L194P), one residue mapped to epitope C (H311Q), four residues mapped to epitope D (N96S, N121K, N171K, and A212T), and three residues mapped to epitope E (E62G, K92R, and R261Q) (Figure 26B). Using A/Switzerland/9715293/2013 as a representative of A(H3N2) vaccine strain for subclade 3C.3a, which was the vaccine strain in 2015, four residue changes identified among the Thai strains were mapped onto the HA structure (S144K on site A, F193S on site B, N246E on site D, and S91N on site E) (Figure 26C). Five residues at positions 135, 137, 138, 144 and 194 varied on the RBS. Overall, most circulating A(H3N2) strains showed dominant diversity on epitope sites A, B, D and E.

On the HA structure of B/Brisbane/60/2008, circulating B/Victoria strains possessed substitutions at residues I117V, N129D, and K136E, which aggregate in the vicinity of the 120 loop region (Figure 265D). Meanwhile, D197N was mapped to the 190 helix region. In contrast, none of the residue changes identified among the circulating B/Yamagata strains occurred on the antigenic or the RBS (Figure 26E).

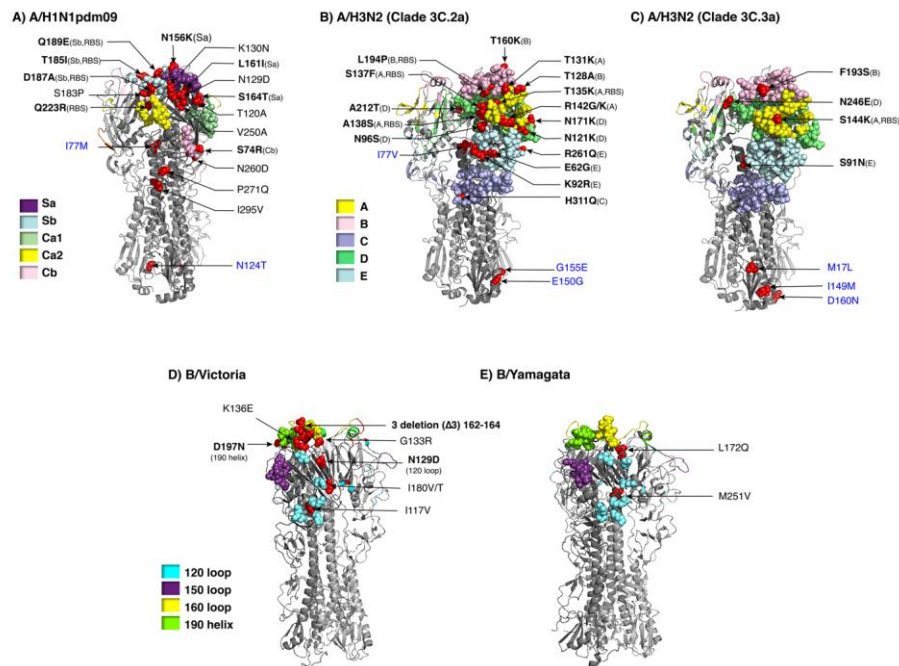


Figure 26 Placement of residue changes identified in influenza virus strains in this study.

Trimeric HA of influenza A and B virus for which three-dimensional structures were available from the Protein Data Bank served to illustrate differences in amino acids at various positions between the vaccine and the Thai strains identified in this study. A) The AA changes between A/Michigan/45/2015 and A(H1N1)pdm09 Thai strains were mapped onto HA structure of A/California/04/2009 (PDB:3LZG). Amino acid substitutions of A(H3N2) Thai strains compared with B) A/Hong Kong/4801/2014 (3C.2a) and C) A/Switzerland/9715293/2013 (3C.3a) were mapped on A/Victoria/361/2011 (PDB: 4WE9). D) Residue changes between B/Victoria Thai strains and vaccine strain, B/Brisbane/60/2008 (PDB: 4FQM) were shown. E) The AA changes of B/Yamagata Thai strains and B/Phuket/3073/2013 were mapped on B/Yamanashi/166/98 (PDB: 4M44). RBS and antigenic sites are color-coded. Residue of the vaccine strain, followed by the numerical position and the residue found in the Thai strains, are indicated with arrows pointing to the location (red). Bolded amino acid designations denote important antigenic and/or RBS, while blue designations are on HA2. Only one subunit comprising the trimeric HA is labeled for clarity.

Determination of the selection pressure on influenza virus

Amino acid changes on the HA often result from selective pressure being exerted on the virus by the host immunity during infection. We therefore evaluated the potential positive selection of these residues by examining their rate of change

(dN/dS) (Table S15). The relative rate of dN/dS for overall sites under positive selection on the HA1 region was 0.194 for A(H1N1)pdm09, 0.228 for A(H3N2), 0.657 for B/Victoria lineage, and 0.0525 for B/Yamagata lineage. These rates of <1 implied purifying selection. Site-by-site selection analysis showed that two residues at HA1 positions 120 and 233 in A(H1N1)pdm09 circulating strains were under positive selection. Meanwhile, HA1 residues 57, 131, 135, 144, and 193 were positively selected in A(H3N2). Although mixed effects model of evolution (MEME) algorithm yielded 10 positive sites in B/Victoria (76, 80, 87, 121, 126, 128, 136, 154, 160, and 238), only residue 238 was also identified by the fixed-effects likelihood (FEL) method. For B/Yamagata strains, only residue 227 was positively selected.

Implications on the influenza VE

We next evaluated how the evolving changes on the HA residues potentially affected VE (Figure 27). Given the genetic sequence of the A(H1N1)pdm09 strains identified in this study compared to the vaccine strain A/Michigan/45/2015 (which remained unchanged from 2017-2019), the predicted VE gradually decreased from 91.7% in 2017, 88.3% in 2018, and 74.2% in 2019. These findings suggest that the recent A(H1N1)pdm09 Thai strains identified in this study have significantly drifted from the vaccine sequence ($p < 0.001$). For the new 2020 season A(H1N1)pdm09 southern hemisphere vaccine strain A/Brisbane/02/2018, however, the predicted VE was 78.5% (Figure S9). Except for 2017, the vaccine component for southern hemisphere A(H3N2) has changed yearly. From 2017-2020, the predicted VE for A(H3N2) were 44.7%, 43.6%, 9.2%, and -18.9%. These values suggest that the A(H3N2) vaccine strain was a relatively poor match for the circulating strains in Thailand during the past four years ($p < 0.01$).

On the other hand, the predicted VE against the B/Victoria lineage strains for 2018 and 2019 were 94.9% and 85.8%, respectively ($p < 0.001$). For 2020, the chosen vaccine strain B/Washington/02/2019 demonstrated an improved predicted VE of 94.8%. Finally, the fact that VE remains relatively high for the B/Yamagata vaccine strain B/Phuket/3073/2013 (94.2%-100%), which has remained unchanged since 2015, suggests that the current vaccine strain remains appropriate. Taken together, VE estimates provided insight into the importance of the vaccine component match with the circulating influenza virus strains in the region.

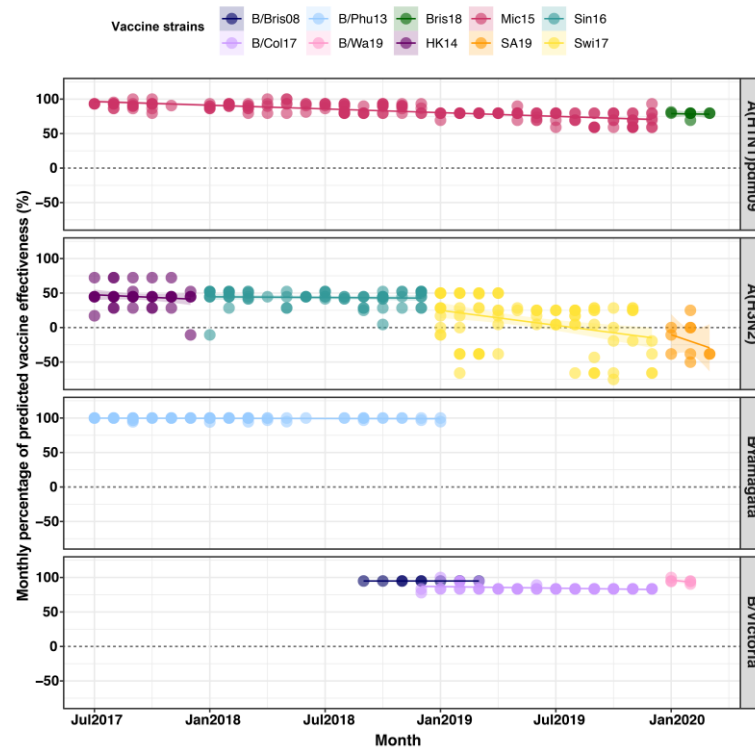


Figure 27 Estimation of the trend of predicted VE between July 2017 and March 2020. Vaccine effectiveness (VE) was derived using the $P_{epitope}$ model by comparing vaccine strains. Circulating A(H1N1)pdm09 viruses were compared with A/Michigan/45/2015 (Mic15) and B/Brisbane/02/2018 (Bris18). Circulating A(H3N2) viruses were compared with A/Hong Kong/4801/2014 (HK14), A/Singapore/INFIMH-16-0019/2016 (Sin16), A/Switzerland/8060/2017 (Swi17) and A/South Australia/34/2019 (SA19). The circulating B/Yamagata-like lineage was compared with B/Phuket/3073/2013 (B/Phu13) and the B/Victoria-like lineage was compared with B/Brisbane/60/2008 (B/Bris08), B/Colorado/06/2017 (B/Col17), B/Washington/02/2019 (B/Wa19) with the corresponding number of deletions. The colored circles of each panel represent individual predicted VE against the vaccine strain in that year.

Discussion

Year-round influenza activity in Thailand can give rise to antigenically drifted influenza virus strains, which are sufficiently different to be categorized into emerging new subclades. These strains sometimes differ significantly from the vaccine strains and are able to escape the host immunity elicited by the annual influenza vaccine. Consequently, the effectiveness of influenza immunization is substantially reduced [184, 209]. Our study aimed to characterize the predominantly circulating A(H1N1)pdm09 and A(H3N2), as well as both lineages of the influenza B virus and how residue changes can affect the predicted VE. Analysis of their HA gene sequence and deduced amino acids identified genetic heterogeneity, which were different from those found in the southern hemisphere vaccine strains for their respective years.

Among the influenza A(H1N1)pdm09 virus strains in this study, almost amino acid substitutions contributing to the phylogenetic cluster transitions were accumulated at the antigenic sites Sa and Sb, while A(H3N2) demonstrated greater diversity with most mutations dominantly located on epitopes A, B, D and E. Meanwhile, antigenic drifts of the influenza B virus occurred at the 120 loop and the 190 helix. Observed changes on the antigenic and the RBS can be important since even one residue substitution at these sites could potentially drive new antigenic variants [182, 199].

The predicted VE based on the HA of A(H1N1)pdm09 decreased significantly in 2019 from the previous year. This suggests that most circulating influenza strains were antigenically different from the A/Michigan/45/2015 vaccine component for 2019 and the A/Brisbane/02/2018 vaccine component for 2020. The A(H1N1)pdm09 strains predominant in Thailand from 2010 to 2015 season belonged primarily to clade 6B.1 [186], for which A/Michigan/45/2015 is a member and has served as the vaccine strain from 2017 to 2019. Since then, more recent A(H1N1)pdm09 strains have acquired S74R, S164T, and I295V, which have evolved into subclade 6B.1A [223]. Some strains with an additional S183P adjacent to the Sb antigenic site now form subclades 6B.1A1 to 6B.1A7 [213]. Several of the Thai A(H1N1)pdm09 circulating in 2018 are 6B.1A1 and 6B.1A6 strains, which is noteworthy since experimental studies have shown that serum from those immunized with the vaccine strain of clade 6B.1 was unable to efficiently neutralize influenza virus strain carrying S183P. This was why B/Brisbane/02/2018 (subclade 6B.1A1) was chosen for the 2020 flu season [218]. From 2019 onward, the majority of the A(H1N1)pdm09 Thai strains was 6B.1A5A, which was the predominant subclade in the 2018-19 influenza season in Europe [224]. Several studies of vaccine

estimates among all ages in 2018-19 influenza season revealed that the predominant newly subclade was associated with a relatively low VE (A/Michigan/45/2015) against influenza A(H1N1)pdm09, which found in Europe (40%–71%), USA(30%-58%), Canada (72%) [225]. Although B/Brisbane/02/2018 was used in the 2019-2020 influenza season for the northern hemisphere, low VE against A(H1N1)pdm09 has been observed in the USA (37%) and Europe (48%-75%) [226, 227]. Thus, 6B.1A5A strains in this study, however, possessed the additional D189E and either N156K or D187A. These changes, if continued, are expected to result in the introduction of a new strain component for the 2021 influenza vaccine.

The VE for A(H3N2) during this study period, on the other hand, performed worse than A(H1N1)pdm09. This was not surprising given that the evolutionary rate for A(H3N2) in the HA1 domain is considerably greater than that for A(H1N1)pdm09 [228]. Among several circulating A(H3N2), clade 3C.2a predominated since 2015 [186] and has now accumulated sufficient changes to be classified as 3C.2a1 and 3C.2a2 [223]. Since then, 3C.2a1b was established, which has gained additional substitutions (either T131K or T135K) in HA1 and these changes are located in the antigenic and the RBS region [213]. The 3C.2a1b virus was also reportedly the predominant subclade in Europe for 2017-18 winter month [224]. Due to multiple clades/subclades circulation, our study found the mismatch of the 2019 southern hemisphere vaccine (A/Switzerland/8060/2017 (subclade 3C.2a2)) and circulating strains in 2019 (3C.2a1b+T131K). Furthermore, although A/South Australia/34/2019 which is a 3C.2a1b+T131K strain was announced for the 2020 southern hemisphere vaccine strain [218], the predominate strains in the first three months of 2020 were subclade 3C.2a1b with additional T135K and T128A which slightly far away from their vaccine strain. T135K and T128A, which are located at antigenic sites A and B respectively, are predicted to cause a loss of potential glycosylation that might alter the HA antigenic properties and affect antibody recognition [229]. Further selective pressure analysis on the HA1 of A(H3N2) suggests that the residues changes at positions 131, 135, 144 and 193 were immune-escaped mutants. Detection of clade 3C.3a strains in 2020 has been less frequent so far. A previous report showed that antibodies generated against 3C.2a less neutralize 3C.3a virus, particularly when 3C.3a possesses an additional F193S. It also does not neutralize 3C.2a1 well compared to 3C.2a2 [229].

The A(H3N2) vaccine strain was not effective during the 2018-19 influenza season in Europe, and low VE (-58% to 57%) continues during 2019-20 season [227, 230]. Our study also found that the predicted VE against A(H3N2) was <50% between 2019 and 2020 due to the circulation of multiple clades/subclades. These data

suggested that the genetic diversity in A(H3N2) might hamper identification of a well-matched virus as a vaccine component in the 2014–2015 influenza season [231]. A meta-analysis indicated reduced protection and substantial variation of VE against A(H3N2). At the same time, the influenza vaccine provided moderate-to-high protection against A(H1N1)pdm09 and influenza B viruses³³. Alternatives to cell-based manufacturing should proceed since a negative impact of egg-induced mutations in the H3N2 vaccine strain has been found [232].

Newly emerging influenza B/Victoria strains are antigenically distinct and possess either double deletion at residues 162-163 or triple deletion at residues 162-164 within the HA1 domain. In this study, the triple deletion strains were more commonly found than the ancestor B/Brisbane-like strain during the 2019-2020 season. New B/Victoria lineages are actively circulating and warrant changing vaccine strain recommendations for this lineage since 2018 [213, 223]. Interim VE estimates of the 2019-20 influenza season in the U.S. against the predominant B/Victoria lineage was 39%-59% which showed a higher VE than influenza A virus [226]. This is consistent with a European study showing the VE of 62%-83% against the influenza B virus for all ages during 2019-20 season [227]. Our study also revealed a high predicted VE against the new B/Victoria virus.

Control measures to mitigate coronavirus disease 2019 (COVID-19) pandemic have resulted in a decrease of influenza activity in 2020 thus far compared to the corresponding period of the previous year [233-235]. Monitoring influenza virus genetic drift remains critical in tracking novel residue changes, which could potentially affect virulence and evasion of host immunity.

Our study had several limitations. First, there was no information on the vaccination status of the individuals with the samples sent to us for influenza virus testing. Second, the results for predicted VE, which was assessed using the accumulated substitutions on antigenic sites, ideally would require additional confirmatory antigenic characterization such as hemagglutinin inhibition or virus neutralization assay in order to complement and strengthen our existing data. Finally, we did not investigate the genetic changes in the neuraminidase gene, which encodes a surface glycoprotein that is also immunogenic.

By monitoring the genetic and antigenic changes of the influenza virus circulating in the tropics, data from this study suggests that new clades and subclades for both influenza A(H1N1)pdm09 and A(H3N2) viruses increasingly differ from those of the chosen vaccine strain, but not influenza B virus. These findings highlight the need for improved vaccine strain match particularly for A(H3N2).


CHAPTER V

EXTENDING THE STALK ENHANCES IMMUNOGENICITY OF THE
INFLUENZA VIRUS NEURAMINIDASE

(Part 5.4)

(Published in: Journal of virology. 2019 Aug;93(18):e00840-19.

DOI: 10.1128/JVI.00840-19)



Felix Broecker¹, Allen Zheng¹, Nungruthai Suntrongwong², Weina Sun¹, Mark J. Bailey¹,
Florian Krammer¹, Peter Palese^{1,3*}

¹Department of Microbiology, Icahn School of Medicine at Mount Sinai, New York,
New York, USA

²Center of Excellence in Clinical Virology, Department of Pediatrics, Faculty of
Medicine,
จุฬาลงกรณ์มหาวิทยาลัย
Chulalongkorn University, Bangkok, Thailand

³Division of Infectious Diseases, Department of Medicine, Icahn School of Medicine
at Mount Sinai, New York, New York, USA

CHAPTER V

Part 5.4: Extending the Stalk Enhances Immunogenicity of the Influenza Virus Neuraminidase

Summary

Influenza viruses express two surface glycoproteins, the hemagglutinin (HA) and the neuraminidase (NA). Anti-NA antibodies protect from lethal influenza virus challenge in the mouse model and correlate inversely with virus shedding and symptoms in humans. Consequently, the NA is a promising target for influenza virus vaccine design. Current seasonal vaccines, however, poorly induce anti-NA antibodies, partly because of the immunodominance of the HA over the NA when both glycoproteins are closely associated. To address this issue, we here investigated whether extending the stalk domain of the NA could render it more immunogenic on virus particles. Two recombinant influenza viruses based on the H1N1 strain A/Puerto Rico/8/1934 (PR8) were rescued with NA stalk domains extended by 15 or 30 amino acids. Formalin-inactivated viruses expressing wild type NA or the stalk-extended NA variants were used to vaccinate mice. Compared to the wild type PR8 virus, the virus with the 30 amino acid stalk extension induced significantly higher anti-NA IgG responses characterized by increased *in vitro* antibody-dependent cellular cytotoxicity (ADCC) activity, while anti-HA IgG levels were unaffected. Similarly, extending the stalk domain of the NA of a recent H3N2 virus enhanced the induction of anti-NA IgGs in mice. Based on these results we hypothesize that the subdominance of the NA can be modulated if the protein is modified such that it surpasses the height of the HA on the viral membrane. Extending the stalk domain of NA may help to enhance its immunogenicity in influenza virus vaccines without compromising antibody responses to HA.

Introduction

Influenza A and B viruses express two surface glycoproteins, hemagglutinin (HA) and neuraminidase (NA) [236]. Nine subtypes of the NA, N1-N9, are described for influenza A virus, two, N10 and N11, for bat influenza A-like viruses, and one for influenza B viruses [237]. Although the NA is recognized as a promising target for vaccines [237, 238], current seasonal influenza virus vaccines do not reliably induce robust anti-NA immunity [237-244]. Anti-NA antibodies have been shown to protect against lethal influenza virus challenge in mice [245-249], and human challenge studies revealed an inverse correlation between anti-NA titers and disease symptoms [250-253]. In humans, neuraminidase inhibiting (NI) antibody titers are a correlate of protection independent of anti-HA antibody titers [251, 254, 255]. The NA undergoes antigenic drift indicating that the NA is under immune pressure as well [244, 256, 257]. In contrast to anti-HA antibodies and despite the observed antigenic drift in the NA, anti-NA antibodies often cross-react within one subtype, such as N1 [249, 258-261] or N2 [249, 262, 263], or among influenza B virus NAs [249, 264, 265].

Many antibodies that target NA have been shown to inhibit its enzymatic activity, thereby preventing viral release from infected cells [237]. These antibodies typically exert *in vitro* NI activity. More recently, it has been shown that broadly protective anti-NA antibodies can also act by activating Fc receptor-mediated effector functions, such as antibody-dependent cellular cytotoxicity (ADCC) [265]. These antibodies potentially contribute to protection by mediating the killing of virus-infected cells. Future influenza virus vaccines designed to elicit strong anti-NA antibody responses, in addition to anti-HA antibodies, may be more effective than current vaccines, as immunity against the NA is often broad and viral escape is less likely if both glycoproteins are potentially targeted simultaneously [237, 238].

One reason for the poor induction of anti-NA antibodies upon infection or vaccination may be the immunodominance of the HA over the NA when both proteins are in close association, as is the case in virus particles and many seasonal vaccines [266-269]. However, when mice are immunized with purified HA and NA proteins that are administered separately, the NA becomes more immunogenic [270]. Consequently, supplementing seasonal vaccines with isolated NA proteins can enhance anti-NA responses in mice [271]. More recently, NA vaccine candidates based on recombinant tetrameric NA proteins [246, 247, 249, 272], DNA plasmids [248], virus-like or replicon particles [258, 259] and modified vaccinia virus Ankara vectors [273] have been shown to induce heterologous anti-NA immunity in mice. In humans, purified N2 protein has

been shown to induce heterologous antibody responses [262]. In addition, the NA is a validated drug target, as FDA-approved drugs such as oseltamivir and zanamivir are NA inhibitors which are broadly active against influenza A and B viruses [236]. Therefore, a promising approach to increase the breadth of protection afforded by seasonal influenza virus vaccines is to include an immunogenic NA component [77, 246, 249, 271]. Another path would be to modify the NA protein such that it becomes more immunogenic when expressed on the virus particle. If the modified NA remains functional and supports viral replication in eggs, it could be used in existing manufacturing processes for seasonal vaccines.

The NA protein is composed of the globular head domain that contains the enzymatically active site, and the stalk domain [236]. Truncations of various lengths in the hypervariable stalk have been identified in the NAs of subtypes N1-N3 and N5-N7 mostly from avian influenza viruses [274]. In addition, the stalk tolerates large artificially introduced insertions. For example, the NA stalk of the H1N1 A/WSN/1933 (WSN) virus has been shown to tolerate insertions of up to 28 amino acids without growth disadvantages in tissue culture or eggs [275]. Another study found that up to 41 amino acids could be inserted into the NA stalk of the WSN virus without affecting viral growth in tissue culture [276], and the NA stalk of the H1N1 A/Puerto Rico/8/1934 (PR8) virus tolerated an insertion of 20 amino acids [277]. It is presently unknown, however, whether extending the NA stalk influences the protein's immunogenicity. To answer this question, we generated variants of the PR8 virus that have the NA stalk domain extended by 15 or 30 amino acids. Vaccination studies in mice revealed that the virus with 30 amino acid-extended stalk induced significantly higher anti-NA IgG responses than the wild type PR8 virus, while anti-HA IgGs were induced to similar levels. No differences were observed in the NI activity of the antibody responses, but antisera raised with the 30 amino acid extended stalk exerted increased *in vitro* ADCC activity. Our results show that extending the stalk domain of the NA is a promising approach to enhance its immunogenicity and overcome the immunodominance of the HA, which may help in the design of improved influenza virus vaccines.

Material and Methods

Recombinant neuraminidase genes and cloning.

The recombinant NA segments were based on the NA gene of the PR8 virus or the NA gene of the HK14 virus [278]. The nucleotide sequences used for the 15 amino acid insertions were retrieved from the Influenza Research Database (<https://www.fludb.org>). They were derived from the NA sequences of the Cal09 (H1N1pdm09) virus (accession number FJ66084) and the A/New York/61/2012 (H3N2) virus (accession number KF90392). Sequences were aligned with Clustal X 2.0 [279]. DNA fragments encoding the NA gene segments that contained 15 base pair cloning sites specific for the pDZ vector at the 5' and 3' ends were obtained as synthetic double-stranded DNAs from Integrated DNA Technologies, using the gBlocks® Gene Fragments service. The NA DNAs were cloned using the In-Fusion HD Cloning Kit (Clontech) into the ambisense pDZ vector that was digested with the *SapI* restriction enzyme (New England Biolabs). Sequences were confirmed by Sanger sequencing (Macrogen). Sequencing primers *pDZ_forward* (TACAGCTCCTGGGCAACGTGCTGG) and *pDZ_reverse* (AGGTGTCCGTGTCGCGCGTCGCC) were obtained from Life Technologies.

Cell culture.

HEK 293T cells were cultured in Dulbecco's Modified Eagle Medium (DMEM; Gibco) with 10% (v/v) fetal bovine serum (FBS) (Hyclone), 100 units/mL penicillin and 100 µg/mL streptomycin (Pen-Strep; Gibco). MDCK cells were maintained in Minimum Essential Medium (MEM; Gibco) with 10% (v/v) FBS, Pen-Strep, 2 mM L-glutamine (Gibco), 0.15 % (w/v) sodium bicarbonate (Corning) and 20 mM 4-(2-hydroxyethyl)-1-piperazineethanesulfonic acid (HEPES, Gibco). Both cell lines were maintained at 37°C with 5% CO₂.

Rescue of recombinant influenza viruses.

Reassortant viruses were rescued by transfecting HEK 293T cells with 0.7 µg of NA-encoding pDZ plasmid, 0.7 µg of HA-encoding pDZ plasmid and 2.1 µg of a pRS-6 segment plasmid that drives ambisense expression of the six segments of PR8 virus except NA and HA and is described elsewhere [280], using the TransIT-LT1 transfection reagent (Mirus Bio). After 48 hours, cells were treated for 30 min with 1 µg per mL tosyl phenylalanyl chloromethyl ketone (TPCK)-treated trypsin at 37 °C. Supernatants were collected, clarified by low speed centrifugation, and injected into 8 to 10-day old specific pathogen-free embryonated chicken eggs (Charles River Laboratories) that were incubated at 37°C. After 48 hours, eggs were incubated at 4°C overnight, allantoic fluids were harvested and clarified by low speed centrifugation. The presence of

influenza virus in the allantoic fluids was determined by hemagglutination assays as described below. Positive virus cultures were plaque purified on confluent MDCK cell layers in the presence of TPCK-treated trypsin and expanded in embryonated chicken eggs. Sequences of the NA genes were confirmed by isolating viral RNA from allantoic fluids with the High Pure Viral RNA Kit (Roche) followed by reverse-transcription PCR using the SuperScript® III One-Step RT-PCR System with Platinum® Taq High Fidelity DNA Polymerase (Thermo Fisher) and primers *PR8_NA_for* (CGAAAGCAGGGGTTTAAAATG) and *PR8_NA_rev* (TTTTTGAACAGACTACTTGTCAATG) or *HK14_NA_for* (GGGAGCAAAGCAGGAGTAAAGATG) and *HK14_NA_rev* (TTATTAGTAGAAACAAGGAGTTTTTCTAAAATTGCG) obtained from Integrated DNA Technologies. The PCR products were purified from a 1% agarose gel with the NucleoSpin® Gel and PCR Clean-up kit (Macherey-Nagel) and submitted for Sanger sequencing (Genewiz) with the primers described above.

Preparation of formalin-inactivated viruses for vaccination.

Plaque-purified and sequenced influenza viruses were expanded in 8 to 10-day old embryonated chicken eggs. Pooled allantoic fluids of 10-20 eggs were added on top of 3 mL of a 20% (w/v) sucrose solution in 0.1 M NaCl, 1 mM ethylenediaminetetraacetic acid (EDTA) and 10 mM Tris-HCl, pH 7.4, in 38.5 mL ultracentrifuge tubes (Denville). Following centrifugation at 25,000 rpm for 2 hours at 4°C using an L7-65 ultracentrifuge (Beckman) equipped with an SW28 rotor, supernatants were carefully aspirated and pellets were recovered in 1 mL of PBS. After addition of 0.03% (v/v) formaldehyde, the virus suspensions were incubated for 48 hours at 4°C while shaking. To remove the formaldehyde, virus suspensions were diluted with PBS and subjected to ultracentrifugation as described above. Pellets were resuspended in sterile PBS and the total protein concentration was determined with the Pierce BCA Protein Assay Kit (Thermo Fisher).

Western blots.

Purified virus particles were lysed in NP-40 lysis buffer (1% (v/v) NP-40, 150 mM NaCl, 50 mM Tris-HCl, pH 8.0, protease inhibitors (Halt™ Protein and Phosphatase Inhibitor Cocktail; Thermo Fisher) and 1 mM dithiothreitol (DTT)). After incubation on ice for 30 min, samples were centrifuged for 10 min at 12,000 rpm in a table-top centrifuge. The supernatants were transferred to new microcentrifuge tubes and the protein concentrations after lysis were determined with the Pierce BCA Protein Assay Kit (Thermo Fisher). Proteins (1 or 2 µg) were separated on 12.5% polyacrylamide gels under denaturing conditions in the presence of sodium dodecyl sulfate (SDS) and then transferred onto polyvinylidene difluoride (PVDF) membranes. As protein size marker,

the ColorPlus™ Prestained Protein Ladder (New England Biolabs) was used. The membranes were blocked for 1 hour using PBS with 5% (w/v) skim milk powder and washed three times with PBS containing 0.05% (v/v) Tween-20. Primary antibodies were mouse anti-N1 4A5 [248], that was used at 1 µg per mL or rabbit anti-H1 (Thermo Fisher; cat.no. PA5-34929) that was used at a 1:5,000 dilution. Primary antibodies were diluted in PBS with 1% (w/v) bovine serum albumin (BSA) and incubated on the membranes for 1 hour. The membranes were washed three times with PBS containing 0.05% (v/v) Tween-20 and were incubated for 1 hour with secondary HRP-labeled antibodies (anti-mouse or anti-goat; GE Healthcare) diluted in PBS with 1% (w/v) BSA according to the manufacturer's recommendations. After washing three times with PBS containing 0.05% (v/v) Tween-20, developing solution (Western Lightning Plus-ECL; PerkinElmer) was added to the membranes that were subsequently developed in a ChemiDoc® MP Imaging System (Bio-Rad).

Immunization studies.

Animal experiments were performed with 6-8 weeks old female BALB/c mice (Charles River) in accordance with protocols approved by the Institutional Animal Care and Use Committee (IACUC) of the Icahn School of Medicine at Mount Sinai. Formalin-inactivated viruses were administered intramuscularly at a dose of 10 µg total protein per mouse diluted in a total volume of 100 µL sterile PBS. Four weeks after the final immunization, mice were euthanized and blood was collected by cardiac puncture. Sera were prepared by removing red blood cells by centrifugation and were stored at -20°C until use.

Enzyme-linked immunosorbent assays (ELISA).

The trimeric recombinant PR8 HA protein and the tetrameric recombinant PR8 and HK14 NA proteins were produced as described [281, 282]. Proteins were coated onto Immulon® 4 HBX 96-well microtiter plates (Thermo Scientific) at a concentration of 2 µg per mL in PBS (50 µL per well) for 16 hours at 4 °C. After washing once using PBS with 0.1% (v/v) Tween-20 (PBS-T), wells were blocked for 1 hour with 5% (w/v) skim milk powder in PBS and washed once with PBS-T. Mouse sera diluted in PBS (50 µL per well) were added and incubated on the plates for 1 hour. After washing with PBS-T three times, wells were incubated with HRP-conjugated anti-mouse IgG antibody (GE Healthcare) diluted 1:5,000 in 5% (w/v) skim milk powder in PBS for 1 hour, washed three times with PBS-T and developed with 100 µL per well of SigmaFast OPD substrate (Sigma-Aldrich) for 20 min. Reactions were stopped by adding 100 µL per well of 3 M hydrochloric acid (HCl) and absorbance at 490 nm was determined on a Synergy 4 plate reader (BioTek). For each ELISA plate, the average plus three standard deviations

of absorbance values of blank wells were used as a cutoff to calculate area under the curve (AUC) values in GraphPad Prism 5.03 (GraphPad Software).

Hemagglutination assays.

Using PBS, serial two-fold dilutions of allantoic fluids were prepared in 96 V-bottom well microtiter plates to a final volume of 50 μ L per well. To each well, 50 μ L of a 0.5% suspension of turkey red blood cells (Lampire) in PBS were added. Plates were incubated at 4 °C until red blood cells in PBS control samples settled to the bottom of the wells. The hemagglutination titer was defined as the reciprocal of the highest dilution of allantoic fluid that caused hemagglutination of red blood cells.

Enzyme-linked lectin assay (ELLA) to determine neuraminidase inhibition (NI).

This assay was performed as previously described [283, 284]. Microtiter 96-well plates (Immulon® 4 HBX; Thermo Fisher Scientific) were coated with 50 μ g per mL (150 μ L per well) of fetuin (Sigma) diluted in coating solution (SeraCare Life Sciences Inc.) and incubated overnight at 4°C. The next day, heat-inactivated (56°C, 30 min) serum samples were serially diluted 1:2 in PBS in separate 96-well plates (leaving the first column as virus only control and last column as the background), with a starting dilution of 1:20. The final volume of diluted serum samples was 75 μ L per well. A recombinant influenza virus expressing a chimeric HA protein, cH4/3 (containing the H4 globular head domain from A/duck/Czech/1956 (H4N6) virus in combination with the H3 stalk domain from A/Perth/16/2009 (H3N2) virus [282]) and the remaining proteins of PR8 virus was diluted to the 90% effective concentration (EC_{90}) in PBS containing 1% BSA, and 75 μ L per well were added to the serially diluted serum samples and virus only controls. Seventy-five microliters of PBS with 1% BSA were added to the background wells. The serum/virus plates were incubated for 2 hours at room temperature to allow for binding of antibodies to the virus particles. The fetuin-coated plates from the previous day were washed three times with PBS-T. One hundred microliters per well of the serum/virus mixtures were transferred to the washed fetuin-coated plates that were then incubated for 2 hours at 37 °C. The plates were washed three times with PBS-T and 100 μ L per well of peanut agglutinin-horseradish peroxidase conjugate (PNA-HRP; Sigma-Aldrich) diluted to 5 μ g per mL in PBS were added. The plates were incubated in the dark for 1 hour at room temperature. After washing three times with PBS-T, 100 μ L per well of SigmaFast OPD substrate (Sigma-Aldrich) were added and the plates were incubated for 10 min. Reactions were stopped by adding 100 μ L per well of 3 M HCl and absorbance at 490 nm was determined on a Synergy 4 plate reader (BioTek). Serum sample reactivity was determined by subtracting background absorbance values (no virus, no serum) from the raw absorbance values

of serum samples. The obtained values were divided by the average value from virus-only control wells and then multiplied by a factor of 100 to calculate the NA activity. Percent NI was determined by subtracting NA activity from 100%. Using GraphPad Prism, the percent NI was fitted to a nonlinear regression to determine the 50% inhibitory concentration (IC₅₀) of the serum samples.

Antibody-dependent cellular cytotoxicity (ADCC) reporter assays.

ADCC reporter assays were performed as described previously [285]. 96-well white flat-bottom plates (Costar Corning) were seeded with 2×10^4 MDCK cells per well. After 18 hours of incubation at 37°C, the MDCK cells were washed once with PBS and then infected with either wildtype PR8 virus or a 7:1 reassortant virus expressing the HA protein of A/Hong Kong/4801/2014 (H3N2) virus and the remaining proteins of PR8 virus [278] at a multiplicity of infection (MOI) of 5 for single cycle replication. Alternatively, HEK 293T cells were plated in 96-well white flat-bottom plates treated with poly-D-lysine (Sigma-Aldrich) at a density of 2×10^4 cells per well and, after incubation for 4 hours, were transfected with 100 ng per well of a pCAGGS plasmid expressing the NA of PR8 virus using the TransIT-LT1 transfection reagent (Mirus Bio). Infected MDCK cells or transfected HEK 293T cells were incubated for 16 hours at 37°C. Then, the culture medium was aspirated and 25 μL of assay buffer (RPMI 1640 supplemented with 4% low-IgG FBS) was added to each well. Pooled sera were added in a volume of 25 μL at a starting dilution of 1:60 and serial 2-fold dilutions prepared in assay buffer in triplicates. The sera were incubated with the cells for 30 min at 37°C. Genetically modified Jurkat cells expressing the murine Fc γ RIV with a luciferase reporter gene under control of the nuclear factor-activated T cells (NFAT) promoter (Promega) were added at 7.5×10^4 cells in 25 μL per well. After incubation for 6 hours at 37 °C, 75 μL per well of Bio-Glo Luciferase assay reagent (Promega) was added and luminescence was quantified using a Synergy 4 plate reader (BioTek). Fold induction was measured in relative light units and calculated by subtracting the background signal from wells without effector cells, then dividing signals of wells with antibody by those with no antibody added.

Immunofluorescence microscopy.

96-well tissue culture plates were seeded with 2×10^4 MDCK cells per well. After 24 hours of incubation at 37°C, the MDCK cells were washed once with PBS and then infected with either wild type PR8 virus, PR8 virus with N1-Ins15 NA, or PR8 virus with N1-Ins30 NA at an MOI of 5 for single cycle replication. Infected MDCK cells were incubated for 16 hours at 37°C. The culture medium was aspirated, the cells were washed twice with PBS and then fixed with a methanol-free 4% (v/v)

paraformaldehyde in PBS solution for 15 min. After washing twice with PBS, the wells were blocked with 5% (w/v) skim milk powder in PBS for 30 min. The cells were washed once with PBS and then incubated with the broadly N1-reactive mAb 4A5 (11) at 10 μ g per mL diluted in 5% (w/v) skim milk powder in PBS for 2 hours. After washing three times with PBS, the cells were incubated with fluorescence-labeled anti-mouse IgG Alexa Fluor 488 antibody (Life Technologies) diluted 1:2,000 in 5% (w/v) skim milk powder in PBS for 1 hour and then washed three times with PBS before pictures were taken on an EVOS fl inverted fluorescence microscope (AMG).

Statistics.

Statistical data was generated with GraphPad Prism. Statistical significance between groups was determined by performing one-way analysis of variance (ANOVA) tests with Bonferroni correction for multiple comparisons. Levels of significance are indicated as follows: * $P \leq 0.05$, ** $P \leq 0.01$, *** $P \leq 0.001$.



Results

Design, rescue and characterization of influenza viruses expressing NA proteins with extended stalk domains.

We selected PR8 as a model influenza virus to study whether the length of the stalk domain of NA influences its immunogenicity. We hypothesized that an extended stalk domain would increase the visibility of the NA protein on the surface of virus particles to the humoral immune system, thereby enhancing its immunogenicity.

Compared to circulating H1N1 strains (pre- and post-pandemic), the NA of the PR8 virus has a 15 amino acid deletion in the stalk domain [286]. It has been estimated by molecular dynamics calculations that the NA protein of the H1N1pdm09 A/California/04/2009 (Cal09) virus extends from the membrane by 149 Å, which is slightly shorter than the estimated height of the HA protein (154 Å) [287] (Figure 28A). It was also calculated that each amino acid in the stalk domain contributes to ~1.2 Å of the total height of the NA protein [287]. Consequently, the NA of PR8 virus has an estimated height of 131 Å. Adding 15 amino acids to the PR8 NA would increase its height to that of the Cal09 NA (149 Å) and inserting 30 amino acids would raise the height to 167 Å, which would be 13 Å taller than that of the HA protein (Figure 28A). Since unrelated sequences could perturb the structure of the PR8 NA protein, we selected to introduce stalk sequences of other NA proteins that, despite the variability of amino acid sequences, likely share structural features with those in the stalk of PR8 NA [275, 276].

Alignment of the NA protein sequences of the PR8 and Cal09 viruses revealed the position of the 15 amino acid deletion in the stalk of PR8 NA (Figure 28B). At that position, the corresponding 15 amino acids of the Cal09 NA were inserted into the PR8 NA (Figure 28C). This mutant was designated as N1-Ins15. An additional sequence of 15 amino acids was derived from the NA stalk domain of the H3N2 A/New York/61/2012 (NY12) virus. A mutant of the PR8 NA that contained both the 15 amino acids of Cal09 NA and the 15 amino acids of the NY12 NA was designated as N1-Ins30 (Figure 28C).

The nucleotide sequences of the NA gene segments from the Cal09 and NY12 viruses were used to create the recombinant RNAs encoding the N1-Ins15 and N1-Ins30 proteins. The modified segments were used to rescue viruses expressing these NAs in the PR8 backbone by reverse genetics. As a control, we also rescued the wild type PR8 virus in parallel, whose NA was designated as N1-wt. After growing for 48 hours in embryonated chicken eggs, the plaque-purified and sequence-confirmed viruses grew to comparable hemagglutination titers (Figure 28D). Thus, confirming previous reports

[275-277], there was no evidence that the stalk insertions significantly affected viral growth. Western blots with proteins isolated from virus particles revealed distinct size shifts of the extended NA proteins compared to the wild type NA (Figure 28E). NA and HA expression levels were comparable in the different viruses (Figure 28E). The three viruses were able to infect Madin-Darby canine kidney (MDCK) cells which resulted in expression of NA on the surface (Figure 28F).

In summary, we successfully rescued two viruses in the PR8 backbone with NA stalk domains extended by 15 or 30 amino acids that replicated in eggs and MDCK cells. On virus particles, the mutated NA proteins were expressed at comparable levels, and the levels of HA appeared to be unaffected by the mutations in the NA.

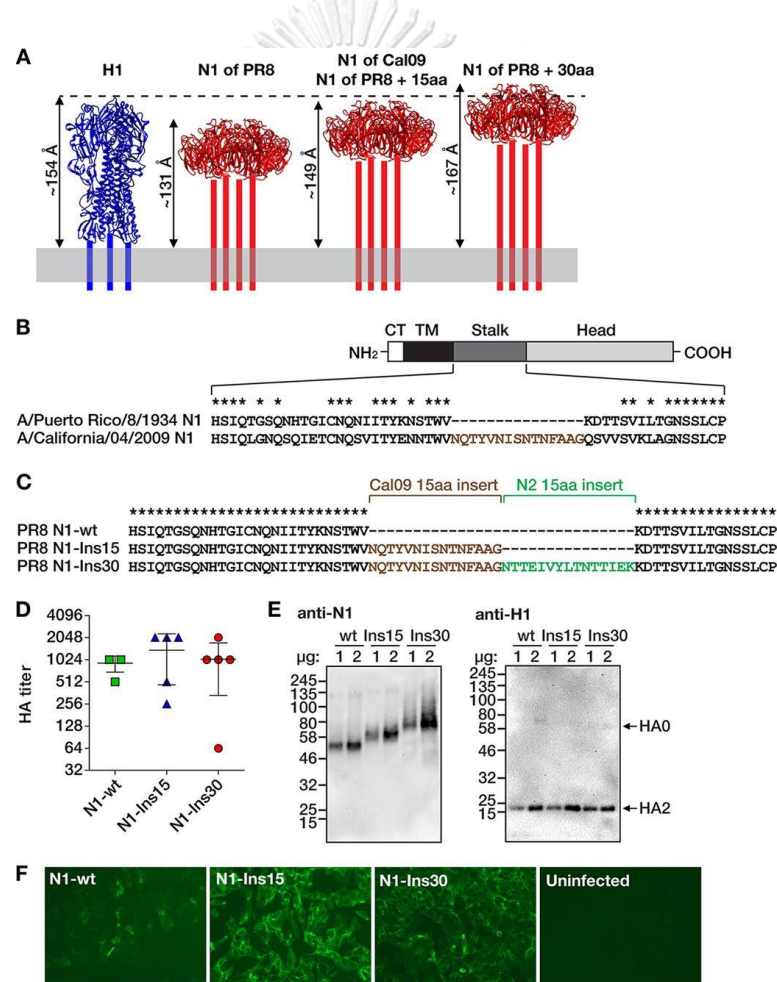


Figure 28 Design and rescue of influenza viruses with extended N1 neuraminidase stalk domains.

(A) Estimated lengths of the ectodomains of N1 proteins with different stalk lengths (red) compared with the ectodomain of H1 hemagglutinin (blue). The structure of the NA stalk has not been determined and is indicated by four bars. The lengths of the

ectodomains are estimates from molecular dynamics simulations, as reported before [287]. The depiction of H1 is based on the crystal structure of the PR8 HA (PDB number 1RU7 [284]), and the depictions of N1 are based on the crystal structure of the NA of A/California/04/2009 (Cal09) virus (PDB number 3TI3 [282]). The structures are not to scale and were visualized with UCSF Chimera. aa, amino acids. (B) The four domains of the NA protein are indicated (CT, cytoplasmic tail; TM, transmembrane domain). The diagram is not to scale. The amino acid sequences comprising the stalk region are defined as previously described [276]. Asterisks denote conserved amino acids. A 15-amino acid region of the Cal09 NA stalk that is not present in the PR8 NA is shown with brown letters. (C) Alignment of the three NA proteins with different stalk lengths. The 15-amino-acid N2 insertion is derived from the NA stalk domain of the A/New York/61/2012 (H3N2) virus. wt, wild type. (D) Hemagglutination (HA) titers of allantoic fluids from plaque-purified viruses. Data points represent individual plaques ($n = 5$ per virus). Horizontal bars show the mean values and whiskers the standard deviations. Phosphate-buffered saline (PBS) control wells showed no hemagglutination (not shown). (E) Western blots of proteins from concentrated viruses (left, anti-NA; right, anti-HA). One or two micrograms of total protein content of each virus preparation was analyzed, as indicated above the blots. Protein marker sizes (in kilodaltons) are indicated to the left of the blots. The bands corresponding to HA0 (uncleaved HA) and HA2 (cleavage product of HA0) are indicated with arrows (the antibody is specific to the C-terminal portion of the HA protein and therefore does not react with the HA1 polypeptide). (F) Immunofluorescence microscopy of MDCK cells infected with the indicated viruses and stained with anti-N1 monoclonal antibody 4A5 [249].

Extending the stalk domain by 30 amino acids enhances immunogenicity of the NA in mice.

Next, we assessed whether the length of the stalk domain influences the immunogenicity of the NA protein in the mouse model. Three groups of 10 BALB/c mice were immunized intramuscularly with formalin-inactivated viruses expressing the N1-wt, N1-Ins15 or N1-Ins30 proteins three times in three-week intervals with doses of 10 μ g total protein (Figure 29A). A fourth group of mice receiving phosphate-buffered saline (PBS) served as control. Four weeks after the third immunization, the mice were sacrificed and serum IgG responses were determined by enzyme-linked immunosorbent assays (ELISAs). Compared to the PBS controls, immunization with all three viruses induced significant IgG responses against recombinant NA protein from PR8 (Figure 29B). While the viruses with N1-wt and N1-Ins15 NAs induced comparable

levels of anti-NA IgG, the virus carrying the N1-Ins30 NA elicited significantly stronger (~2.5-fold) anti-NA IgG responses. By contrast, the three viruses induced comparable IgG responses against recombinant PR8 HA protein (Figure 29C). Thus, extending the stalk domain by 30 amino acid significantly enhanced the IgG responses against NA, without compromising anti-HA IgG levels.

Stalk extension enhances the induction of antibodies with *in vitro* effector functions.

We next sought to assess the functional properties of the antibodies elicited by the different viruses. In general, the majority of anti-NA antibodies are thought to prevent binding of the enzymatically active site to its substrate sialic acid [237]. As these types of antibodies typically exert *in vitro* NI activity, we performed NI assays with the sera obtained from the immunized mice. Although the N1-Ins30 expressing virus elicited higher total anti-NA IgG titers than the other two viruses, as measured by ELISA (Figure 29B), NI activities were similar between the groups of mice immunized with the three different viruses (Figure 30A).

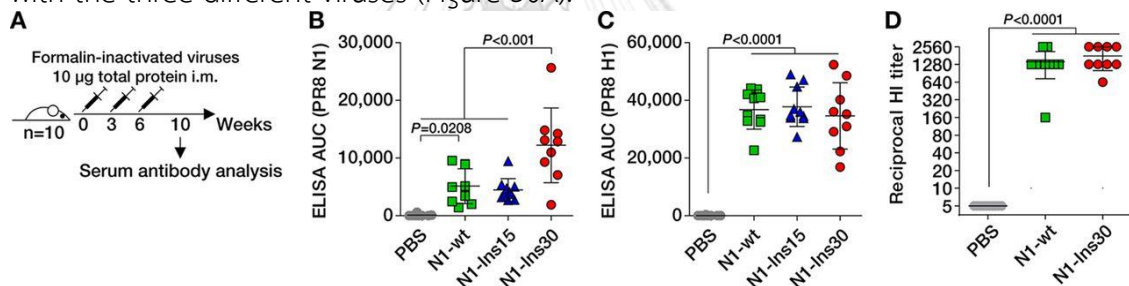


Figure 29 The extended stalk domain enhances IgG responses to the N1 neuraminidase.

(A) Immunization regime. Mice received three doses intramuscularly (i.m.) that contained 10 µg of formalin-inactivated viruses. Serum obtained 4 weeks after the third immunization was analyzed for antibodies against N1 neuraminidase and H1 hemagglutinin proteins. (B and C) Serum IgG levels corresponding to recombinant tetrameric N1 neuraminidase (B) and recombinant trimeric H1 hemagglutinin (C) from PR8 virus, as measured by ELISA. AUC, area under the curve. (D) Hemagglutination inhibition (HI) titers against wild-type PR8 virus. Statistical significance was inferred by one-way ANOVA with Bonferroni correction and P values are indicated in the graphs. Note that the Ins30 group comprised only 9 sera, as one animal in that group died from causes unrelated to the experiment.

Another previously described function of anti-NA antibodies is the induction of Fc receptor-mediated effector functions, such as ADCC [265]. To assess whether the induction of antibodies with effector functions was influenced by the stalk length of NA, we subjected the murine immune sera to an *in vitro* ADCC reporter assay [285]. Using human embryonic kidney (HEK) 293T cells expressing the PR8 NA protein, sera raised with the N1-Ins30 expressing virus showed substantially higher ADCC activity than sera induced with viruses carrying N1-wt or N1-Ins15 (Figure 30B). Similar results were obtained using MDCK cells that were infected either with wild type PR8 virus or an H3N1 virus expressing the PR8 NA and the HA of the HK14 H3N2 virus [278] (Figure 30B). In summary, extending the stalk domain of the NA enhanced antibody responses with *in vitro* ADCC activity, but not the induction of NI active antibodies.

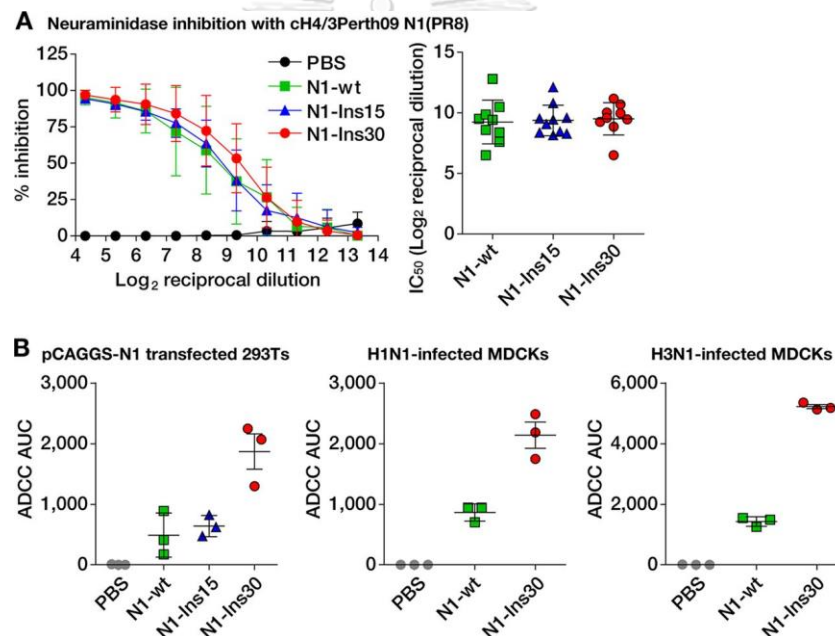


Figure 30 The extended stalk domain enhances ADCC active antibody responses to the N1 neuraminidase.

(A) Results of the neuraminidase inhibition assay. The two subpanels show the same data. The left subpanel shows percent inhibition relative to the serum dilution with data points representing mean values corresponding to 9 (Ins30 group) or 10 (all other groups) individual mice \pm standard deviations. The right subpanel shows the 50% inhibitory concentrations (IC_{50} values) calculated from the curves in the left subpanel.

(B) Results from antibody-dependent cellular cytotoxicity (ADCC) reporter assays. From left to right, the subpanels show assays performed with HEK 293T cells transfected with a pCAGGS expression plasmid for the N1 protein of the PR8 virus (left) and MDCK cells infected with either an H1N1 virus (PR8) (middle) or an H3N1 virus

(right) (H3 was from A/Hong Kong/4801/2014; all other proteins were from PR8). Data points represent pooled sera measured in triplicate; horizontal bars show the mean values, and the whiskers indicate the standard deviations.



Discussion

Although other reasons for the poor immunogenicity of the NA of current seasonal vaccines are recognized, such as varying and unreliable amounts of NA proteins [269] and their inconsistent stability [288], it is established that anti-NA antibody responses are suppressed in current vaccines due to the immunodominance of the HA [266-269]. Here, we demonstrate that a simple extension of the NA stalk can significantly enhance the anti-NA immune response without compromising the immunogenicity of the HA. Consistent with previous studies [275-277], mutant viruses in the PR8 backbone carrying NA proteins with 15 or 30 amino acid extended NA stalk domains replicate in eggs and MDCK cells without any apparent growth disadvantages compared to wild type PR8 virus. In mice, immunization studies with formalin-inactivated virus particles reveal that a 30 amino acid extension to PR8 NA, but not a 15 amino acid extension, significantly enhance total anti-NA IgG responses without affecting IgG responses to the HA. Based on published molecular dynamics simulations [287], a 30 amino acid extension in PR8 (but not a 15 amino acid extension) is predicted to increase the height of the NA such that it surpasses the height of the HA, suggesting that the improvement in immunogenicity is dependent on the visibility of the NA relative to the HA.

We found that stalk extension of PR8 NA did not affect the induction of NI reactive antibodies, but substantially increased the production of antibodies with *in vitro* ADCC activity. This suggests that the longer stalk makes novel epitopes accessible that are targeted by ADCC active antibodies but not by NI active antibodies, while the immunogenicity of regions recognized by NI reactive antibodies is preserved. Of note, it has been shown that ADCC active IgGs recognizing the stalk domain of the HA [289] or the NA protein [290]) can protect against lethal influenza virus infection in mice, in an Fc gamma receptor-dependent manner. A recent study also showed that ADCC-active and NI inactive anti-NA mAbs targeting the lateral surface of the head domain could confer protection in mice [291]. We hypothesize that our approach of extending the stalk may enhance the exposure of epitopes below the head domain and/or on the lateral surface of the head domain, thereby increasing the induced antibody repertoire. Moreover, broadly reactive anti-NA antibodies that target conserved epitopes are often ADCC active [265]. Therefore, extending the NA stalk domain may not only increase the immunogenicity of the NA on virus particles, but also enhance the breadth of protection afforded by the induced anti-NA antibodies.

Unlike other pursued approaches to enhance anti-NA immunity that are based on isolated or recombinant NA proteins [246, 247, 249, 265], DNA plasmids [248], virus-like and replicon particles [258, 259] or virus-vectored vaccines [273], the NA stalk extension described here could be implemented in existing manufacturing processes for seasonal influenza virus vaccines, as the mutated NAs can be expressed on virus particles that efficiently replicate in eggs. Moreover, we provide evidence that the length of the NA stalk contributes to the subdominance of the NA relative to the HA. We hypothesize that immunodominance is associated with viral epitopes being most distal from the surface of the virus or the infected cell and that immunodominance may simply be a question of being more easily recognized by B-cell receptors of the infected host.



CHAPTER VI

Conclusion and Discussion

The fluctuation of seasonal influenza activity is typically different depending on the geographical locations [24]. The triggering of seasonal influenza epidemic results from a complex interplay between viral factors, host factors and external factors such as climate and social factors [102, 137, 159, 212]. For the external factors, we only focused on the climate factors. Here, we observed increased influenza activity in Thailand appears biannually which peaks in the rainy (June-August) and cold (December-February) seasons. A long-term study indicated that the lowest peak of influenza activity typically occurs following the hot and dry months of April and May. The distribution of influenza (sub)type occurred as an annual cyclical pattern. Influenza A(H1N1)pdm09 commonly appeared in the first wave with a lesser extent of influenza B virus, both of which peaked in February and again in August-September. Whereas influenza A(H3N2) is primarily detected in the second wave of influenza activity that is a major peak occurs around August-September in which all influenza viruses co-circulate. The observation that influenza A(H1N1)pdm09 activity increases during the periods of low (February-May) and high (August-October) relative humidity has previously been reported and suggests that humidity extremes along with temperatures influence influenza virus survival and/or transmission in a complex way [102, 137-139]. Our findings showed that overall influenza positively correlated with relative humidity (up to lag 1) and rainfall (lag 1) similar to an earlier report in the tropics including a previous Thai study with data from 2009-2014 [110, 123]. One of the most significant findings from this study was that temperature, relative humidity, and rainfall were all associated with influenza A(H3N2) activity in Bangkok. Moreover, the temperature was positively correlated with overall influenza activity at 4 months lag, which happens to coincide with the period of increased rainfall and humidity. Using time series analysis, the relationship between all influenza incidence and climate factors enabled a forecast model with significant prediction. SARIMA model showed that after comparing the model with (multivariate model) and without (univariate model) climate factors effect, the best-fit model could be found when incorporating climate factor parameters. Furthermore, the SARIMA of the overall influenza model provided higher accuracy than models of individual influenza sub(type).

For the host factor such as the pre-existing immunity, the previous study suggest that the lack of pre-existing immunity or cross reactive antibodies to influenza

virus likely contribute to the high attract rate and rapid spread of influenza virus. To gain insight into influenza immunity among the population, we determine the prevalence of cross-reactive antibodies in the elderly population who are at high risk of infection. In Thailand, the prevalence of cross-reactive antibodies to A(H1N1)pdm09, A(H3N2) were account for 50% and 65% whereas the prevalence of antibodies against the influenza B virus was lower than influenza A virus which account for 14%, 21% and 25% for B/Yamagata2, B/Yamagata3, and B/Victoria, respectively. Moreover, only 5% of this population presented the antibodies against both the influenza A and B viruses, this suggests that a low proportion of individuals provided broadly protective antibodies against the seasonal influenza virus.

Besides, viral genomic diversity also influences the increase in influenza activity. As we known influenza viruses constantly evolve over time. Such evolution can occur through the acquisition of point mutations, accumulate the faulty nucleotide in significant positions can lead to emerging the new influenza strain. In this study, we assess the genetic change of both non-antigenic and antigenic gene of circulating influenza virus in Thailand. For non-antigenic genes, the polymerase gene was selected to study the genetic changes and evolution patterns. The viral polymerase complex consists of PB1, PB2, and PA proteins that assembly and responsible for viral replication, are considered as a further antiviral drug target. Mutations in the polymerase gene showed a significant relation with the efficacy of viral replication, transmission, and virulence. The pattern of evolutionary dynamics of A(H3N2) and B/Victoria has considerably changed over time, while A(H1N1)pdm09 slightly stable and B/Yamagata was increasing in 2017. All polymerase genes for individual (sub)type exhibited in a similar pattern. The polymerase gene of the recent influenza A(H3N2), B/Victoria, and B/Yamagata are evolving at a faster rate than in the previous decades. Our data reveal adaptive acquired mutations relatively occur as high genetic diversity in the polymerase gene. The substitution rate of influenza A virus was higher than the influenza B virus with consistent the previous study [169]. Besides, all PA gene has shown a higher evolution rate than PB2 and PB1, except A(H3N2).

Although the influenza vaccine has been a primary tool to prevent influenza infection, the reduction of vaccine effectiveness, and the high incidence of influenza infection have continually observed. Therefore, the influenza vaccine needs to reformulate every year. Several factors affect the influenza vaccine effectiveness including the type of vaccine administrated, host factors such as the health and age of the vaccinated individual, host pre-existing immunity, and the degree of similarity between circulating strain and vaccine strain [145]. As we known influenza typically

evolves with a high mutation rate undergone the antigenic variation mechanisms and selective pressure, particularly hemagglutinin (HA) which is the surface glycoprotein that has high immunogenicity to induce the host immune [200]. Such constantly evolving, the viral variants were produced leading to escape the pre-existing immunity against the previously circulating strain. In Thailand during the 2016-17 season, influenza A(H3N2) diverged from the A/Hong Kong/4801/2014 vaccine strain and emerged newly 5 subclades (designated I to V) within the 3C.2a clade. Such emergence of multiple subclades collectively contributed to the declining predicted vaccine effectiveness (VE) from 74% in 2016 down to 48% in 2017. During 2017-2020, multiple clades/subclades of influenza A(H1N1)pdm09 and A(H3N2) were co-circulating contemporaneous and diverged from their vaccine strain, but not the influenza B virus. The predominant circulating strains of A(H1N1)pdm09 belonged to 6B.1A1 (2017–18) and 6B.1A5 (2019–20) with additional AA substitutions. Clade 3C.2a1b and 3C.2a2 viruses co-circulated in A(H3N2) and clade 3C.3a virus was found in 2020. The B/Victoria-like lineage predominated since 2019 with an additional three AA deletions. Antigenic drift was dominantly facilitated at epitopes Sa and Sb of A(H1N1)pdm09, epitopes A, B, D, and E of A(H3N2), and the 120 loop and 190 helix of influenza B virus. Moderate predicted VE was observed in A(H1N1)pdm09. The predicted VE of A(H3N2) indicated a significant decline in 2019 (9.17%) and 2020 (-18.94%) whereas the circulating influenza B virus was antigenically similar (94.81%) with its vaccine strain. Furthermore, newly subclade of influenza B/Victoria strains are antigenically distinct and possess either double deletion at residues 162-163 or triple deletion at residues 162-164 within the HA1 domain have been emerged since 2019 and shown the close relation with the changing vaccine strain recommendations for this lineage since 2018. The high genetic diversity among influenza virus and reducing of VE annually, the universal vaccine is an ideal target to resolve this problem.

It is striking to develop the influenza vaccine that presented the broadly protective against influenza virus. Several studies support that neuraminidase (NA) is recognized as a promising target of vaccines [238] and can produce broadly protective antibodies. However, current seasonal influenza virus vaccines do not reliably induce robust anti-NA immunity. These findings suggest that the recombinant virus with the 30 amino acid stalk extension induced significantly higher anti-NA IgG responses characterized by increased *in vitro* antibody-dependent cellular cytotoxicity (ADCC) activity, while anti-HA IgG levels were unaffected. In the mouse model, extending the stalk domain of the NA protein can enhance its immunogenicity on virus particles and

overcome the immunodominance of the HA without affecting antibody responses to the HA.

In conclusion, our results suggest that certain climate factors do influence influenza activity and further support the existing schedule for influenza vaccination prior to the rainy season. The time series analysis of the influenza virus could potentially supplement more accurate forecasting of future seasonal influenza activity when combined with active epidemiological surveillance. Insights into the host pre-existing immunity in the population, viral population dynamic and the genetic divergence from vaccine strains, which could aid antiviral drug development and vaccine updating. Extending the stalk domain of the NA is a promising approach to enhance its immunogenicity and overcome the immunodominance of the HA, which may help in the design of improved influenza virus vaccines. Continue monitoring genetic variation and evolution dynamic will assist the public health for effective control and prevention against the influenza virus.

APPENDIX

APPENDIX A

Table S1. Comparison of the mean meteorological variables between no influenza activity month and influenza activity month.

Meteorological variables	Mean Rank		p-value
	No influenza activity month ^a	Influenza activity month ^b	
Mean Temperature (°C)	57.31	47.52	0.141
Relative humidity (%)	47.10	72.89	<0.001***
Rainfall (cm ³)	51.78	61.26	0.154

Asterisk denotes significance: *** p<0.001.

^a Defined as a monthly case proportion of <10%.

^b Defined as a monthly case proportion of ≥10%.

Table S2. Cross-correlation between individual and all influenza viruses with climate factors at different lag times.

Influenza A(H1N1)pdm09 virus					
	Lag0	Lag1	Lag2	Lag3	Lag4
Temp	0.158	0.069	0.023	0.111	0.166
p-value	0.185	0.672	0.242	0.836	0.113
RH	0.118	-0.050	-0.182	-0.190	-0.198
p-value	0.630	0.513	0.108	0.103	0.055
RF	0.167	0.025	-0.069	0.011	-0.054
p-value	0.106	0.772	0.391	0.945	0.635
H3	0.196	0.040	-0.124	-0.210	-0.264
p-value	0.054	0.434	0.450	0.053	0.018*
B	0.633	0.526	0.294	0.130	0.099
p-value	<0.001***	<0.001***	0.024*	0.511	0.566
Influenza A(H3N2) virus					
	Lag0	Lag1	Lag2	Lag3	Lag4
Temp	-0.228	-0.021	0.306	0.576	0.646
p-value	0.083	0.567	0.038*	<0.001***	<0.001***
RH	0.502	0.471	0.349	0.197	0.015
p-value	<0.001***	<0.001***	0.002**	0.093	0.865
RF	0.311	0.436	0.459	0.467	0.287

p-value	0.036*	<0.001***	0.001**	<0.001***	0.058
H1	0.196	0.210	0.158	0.176	0.213
p-value	0.054	0.095	0.249	0.180	0.055
B	0.292	0.194	0.088	-0.006	-0.006
p-value	0.011*	0.125	0.602	0.829	0.990
Influenza B virus					
	Lag0	Lag1	Lag2	Lag3	Lag4
Temp	-0.021	-0.046	0.074	0.253	0.374
p-value	0.666	0.365	0.613	0.295	0.013*
RH	0.152	0.110	-0.030	-0.085	-0.096
p-value	0.535	0.656	0.576	0.365	0.406
RF	0.067	0.132	0.094	0.127	0.137
p-value	0.391	0.181	0.353	0.245	0.389
H1	0.633	0.585	0.417	0.219	0.100
p-value	<0.001***	<0.001***	<0.001***	0.049*	0.449
H3	0.292	0.184	-0.002	-0.115	-0.100
p-value	0.011*	0.114	0.976	0.296	0.370
all influenza viruses					
	Lag0	Lag1	Lag2	Lag3	Lag4
Temp	-0.132	-0.082	0.162	0.473	0.617
p-value	0.936	0.417	0.796	0.005**	<0.001***
RH	0.392	0.323	0.128	0.030	-0.045
p-value	0.002**	0.006**	0.324	0.970	0.470
RF	0.232	0.296	0.277	0.337	0.222
p-value	0.050	0.014*	0.081	0.023*	0.215

RH, Relative Humidity; RF, Rainfall; Temp, Temperature.

Asterisk denotes significance; * $p < 0.05$, ** $p < 0.01$, *** $p < 0.001$.

Table S3. Parameters estimated by ARIMA(X) model with RMSE, AICc, MAPE, and coefficient values.

Influenza virus	Univariate Analysis					Multivariate Analysis						
	Model	Fit		Pred.		Model	Fit		Pred.		Vars.	Coef.
		RM SE	AICc	RM SE	MA PE		RM SE	AICc	RM SE	MA PE		
A(H1N1)pdm09	SARIMA(2,1,1)(0,1,1) ₁₂	0.74	209.06	1.10	28.63	SARIMA(2,1,1)(0,1,1) ₁₂	0.68	196.84	0.89	22.99	H1N1 (lag 1)* H3N2 (lag 4) B (lag 1)	- 0.1021 - 0.4088 - 0.0197
A(H3N2)	SARIMA(1,0,2)(1,1,0) ₁₂	0.73	187.99	1.33	40.54	SARIMA(1,0,2)(1,1,0) ₁₂	0.65	176.89	0.77	22.47	Temp (lag 4) RH (lag 1) RF (lag 1) H3N2 (lag 1)*	- 0.0214 - 0.0095 0.0286 0.9029
B	SARIMA(1,0,0)(1,0,1) ₁₂	0.82	222.38	1.41	60.88	ARIMA(3,0,3) ₁₂	0.71	203.04	1.14	46.09	Temp (lag 4) H1N1 (lag 1) B(lag 1)*	0.1536 0.3318 0.2352
All	SARIMA(2,0,1)(1,0,0) ₁₂	0.67	191.25	0.61	10.93	SARIMA(2,0,1)(1,0,0) ₁₂	0.65	186.27	0.15	2.81	Temp (lag 4) RH (lag 1) RF(lag 1) All Flu (lag 1)*	0.0090 - 0.0222 0.0236 0.8726

Temp=Temperature, RH= Relative humidity, RF=Rainfall, All= influenza A(H1N1)pdm09+A(H3N2)+B, RMSE= Root Mean Square Error, AICc= corrected Akaike Information Criterion, MAPE= mean absolute percentage error, Pred=prediction, Coef=coefficient. Asterisk indicates the auto-lag for each model by using the previous one month incidence to predict the next month incidence.

Table S4. Hemagglutination inhibition titers (HI titers) against the individual seasonal influenza (sub)type among elderly in Khon Kaen, Thailand.

ID	Age	A(H1N1)pdm09	A(H3N2)	B/Vic	B/Yam2	B/Yam3
		A/Thailand/ CU-CN364/2017	A/Thailand/ CU-B36461/2018	B/Thailand/ CU-B31196/2019	B/Massachusetts /02/2012	B/Thailand/ CU-B26097/2018
1	69	20	40	20	10	10
2	70	40	40	20	10	10
3	68	<10	20	20	10	10
4	67	<10	10	<10	<10	10
5	69	80	<10	20	20	10
6	62	80	160	20	40	40
7	73	80	<10	20	20	20
8	63	10	<10	20	<10	10
9	74	40	20	40	20	40
10	70	80	40	80	<10	20
11	72	80	10	160	80	40
12	67	40	40	<10	20	20
13	81	80	10	20	20	10
14	65	80	80	20	80	20
15	66	40	20	20	40	20
16	80	80	20	40	<10	10
17	63	160	10	40	10	10
18	63	80	20	20	<10	10
19	69	80	10	20	10	10
20	71	10	20	20	10	10
21	71	10	10	40	10	20
22	72	40	10	20	20	10
23	68	40	10	20	10	20
24	62	80	80	20	20	40
25	61	80	10	20	<10	10
26	78	40	20	20	<10	10
27	66	40	10	20	<10	10
28	64	80	20	20	<10	10
29	61	320	20	20	10	20
30	63	40	10	20	20	20
31	64	40	80	40	<10	10
32	67	80	40	20	20	10
33	69	40	10	<10	<10	10
34	76	80	160	<10	80	160
35	68	40	10	20	40	40
36	60	80	40	20	20	40
37	63	80	160	20	<10	10
38	79	40	80	80	20	10

ID	Age	A(H1N1)pdm09 A/Thailand/ CU-CN364/2017	A(H3N2) A/Thailand/ CU-B36461/2018	B/Vic B/Thailand/ CU-B31196/2019	B/Yam2 B/Massachusetts /02/2012	B/Yam3 B/Thailand/ CU-B26097/2018
39	66	40	10	40	10	40
40	69	80	20	20	20	10
41	61	80	10	40	10	10
42	62	20	40	20	10	20
43	66	40	20	40	40	20
44	70	80	20	20	20	20
45	65	320	10	20	20	80
46	70	80	10	20	<10	10
47	65	80	20	10	<10	10
48	69	<10	10	<10	<10	10
49	65	160	160	20	80	80
50	71	20	10	10	<10	20
51	68	<10	80	10	<10	10
52	73	<10	10	10	10	10
53	71	20	10	10	<10	10
54	66	40	80	40	10	40
55	61	80	20	20	<10	10
56	84	10	40	10	<10	10
57	68	160	20	10	<10	20
58	86	40	10	10	<10	10
59	65	20	10	10	<10	20
60	78	20	10	10	<10	10
61	80	20	10	40	<10	10
62	78	<10	10	<10	<10	20
63	83	80	10	80	10	20
64	70	<10	10	40	20	40
65	75	320	320	80	20	160
66	67	320	160	40	<10	20
67	70	<10	80	<10	<10	20
68	65	20	160	10	<10	10
69	77	<10	160	<10	<10	20
70	65	80	160	80	20	20
71	95	20	160	10	<10	20
72	81	<10	160	10	<10	160
73	68	40	160	20	80	10
74	60	<10	160	20	<10	10
75	62	<10	160	10	<10	20
76	63	<10	160	10	<10	20
77	61	10	160	10	10	40
78	61	160	160	10	<10	20
79	89	160	160	10	<10	20
80	72	<10	160	<10	<10	20

ID	Age	A(H1N1)pdm09 A/Thailand/ CU-CN364/2017	A(H3N2) A/Thailand/ CU-B36461/2018	B/Vic B/Thailand/ CU-B31196/2019	B/Yam2 B/Massachusetts /02/2012	B/Yam3 B/Thailand/ CU-B26097/2018
81	77	40	160	40	10	20
82	62	<10	160	20	20	40
83	63	40	160	80	20	80
84	66	80	160	10	<10	10
85	64	40	160	10	<10	20
86	69	80	160	160	80	20
87	66	<10	20	10	<10	10
88	77	640	640	40	40	160
89	69	80	80	10	<10	20
90	61	<10	160	80	40	160
91	87	80	40	20	20	10
92	80	<10	80	80	40	20
93	78	<10	80	20	40	40
94	65	<10	80	20	10	10
95	81	<10	80	<10	<10	10
96	69	<10	160	20	<10	10
97	61	<10	80	20	<10	10
98	68	<10	80	<10	<10	10
99	81	320	320	20	40	10
100	65	<10	40	20	40	10
101	75	10	80	40	20	10
102	68	<10	80	20	10	10
103	61	<10	80	20	10	80
104	77	80	160	40	40	160
105	65	<10	80	20	20	10
106	65	<10	80	80	<10	80
107	73	40	80	20	80	160
108	76	<10	80	20	40	10
109	71	<10	160	20	10	10
110	71	40	160	40	20	80
111	83	40	80	160	20	20
112	81	40	160	20	20	40
113	64	20	80	20	20	20
114	67	80	160	10	20	20
115	73	<10	80	10	<10	20
116	73	1280	80	20	<10	10
117	61	<10	80	10	<10	10
118	66	80	80	10	<10	20
119	69	20	160	20	40	20
120	65	160	80	160	80	40
121	64	40	80	20	20	40
122	70	40	80	10	10	40

ID	Age	A(H1N1)pdm09 A/Thailand/ CU-CN364/2017	A(H3N2) A/Thailand/ CU-B36461/2018	B/Vic B/Thailand/ CU-B31196/2019	B/Yam2 B/Massachusetts /02/2012	B/Yam3 B/Thailand/ CU-B26097/2018
123	78	<10	1280	80	<10	10
124	60	<10	40	20	<10	20
125	76	<10	40	10	<10	20
126	61	40	160	40	10	20
127	67	20	40	20	10	20
128	61	<10	80	20	<10	20
129	69	20	80	10	<10	10
130	73	20	160	20	20	40
131	70	<10	20	10	<10	10
132	69	320	160	<10	<10	20
133	74	<10	80	40	<10	10
134	71	<10	40	10	<10	10
135	62	40	80	40	20	80
136	81	40	40	40	40	20
137	78	<10	320	10	<10	10
138	83	<10	40	20	<10	10
139	83	20	40	20	20	20
140	71	20	40	40	20	80
141	80	<10	40	20	<10	10
142	70	<10	20	<10	<10	10
143	75	<10	160	10	<10	10
144	73	<10	20	10	<10	10
145	61	<10	80	20	10	10
146	73	<10	80	20	<10	10
147	61	40	40	20	20	40
148	74	80	20	80	20	20
149	70	<10	80	20	<10	<10
150	67	<10	40	10	<10	<10
151	82	20	20	40	20	20
152	76	<10	80	20	<10	<10
153	61	<10	20	10	<10	<10
154	85	40	80	20	<10	<10
155	63	20	320	160	80	160
156	88	80	20	20	10	20
157	67	40	40	20	<10	10
158	63	<10	20	10	<10	10
159	84	<10	40	40	10	10
160	66	<10	20	10	<10	10
161	72	<10	80	20	20	10
162	60	80	40	20	10	20
163	71	<10	320	<10	<10	10
164	74	10	40	80	<10	20

ID	Age	A(H1N1)pdm09 A/Thailand/ CU-CN364/2017	A(H3N2) A/Thailand/ CU-B36461/2018	B/Vic B/Thailand/ CU-B31196/2019	B/Yam2 B/Massachusetts /02/2012	B/Yam3 B/Thailand/ CU-B26097/2018
165	71	10	20	10	<10	20
166	80	40	40	20	20	10
167	79	40	80	10	<10	10
168	78	<10	<10	<10	<10	10
169	68	80	80	40	10	20
170	60	20	40	10	<10	10
171	80	80	80	20	10	20
172	74	<10	40	10	10	10
173	67	<10	20	20	40	40
174	63	80	80	40	40	80
175	78	80	80	10	20	40
176	83	10	20	160	20	10



จุฬาลงกรณ์มหาวิทยาลัย
CHULALONGKORN UNIVERSITY

Table S5. Comparison the seropositivity (HI titers ≥ 40) to seasonal influenza viruses among different aged groups.

Virus	Age group	HI ≥ 40		GMT			Kruskal-Wallis test p-value
		Number/ Total	%	Mean	Lower 95% CI	Upper 95% CI	
A(H1N1)Pdm09	60-69	52/92	56.5 2 37.9	29.37	22.83	37.79	0.51
	70-79	22/58	3 53.8	19.79	14.22	27.56	
	≥ 80	14/26	5 66.3	35.52	23.56	53.54	
A(H3N2)	60-69	61/92	0 63.7	47.93	38.58	59.54	0.885
	70-79	37/58	9 69.2	49.01	35.39	67.88	
	≥ 80	18/26	3 19.5	44.5	30.02	65.96	
B/Victoria	60-69	18/92	7 29.3	19.12	16.45	22.21	0.845
	70-79	17/58	1 34.6	18.39	14.63	23.13	
	≥ 80	9/26	2 16.3	24.75	17.57	34.89	
B/Yamagata 2	60-69	15/92	0 12.0	10.95	9.124	13.13	0.298
	70-79	7/58	7 11.5	10.24	8.188	12.81	
	≥ 80	3/26	4 22.8	10.83	7.945	14.77	
B/Yamagata 3	60-69	21/92	3 24.1	18.27	15.67	21.31	0.495
	70-79	14/58	4	18.84	14.9	23.82	
	≥ 80	2/26	7.69	14.92	11.45	19.44	

Table S6. Primers used for conventional PCR amplification of the whole genome of influenza A(H1N1)pdm09 strains circulating in Thailand.

Target Gene	Primer	Sequence (5'-3')
PB2	PB2-F5'	AGCAAAAGCAGGTCAATTATATTC
	PB2_H1_F529	TTCCTAATGAAGTGGGAGC
	PB2_H1_R626	GGGGAAATTTTGCAATCCTG
	PB2_H1_F1099	GAGGGATATGAAGAGTTCAC
	PB2_H1_R1217	GCTTCGACTATTGACTGTTC
	PB2_H1_F1721	CTCAGAACCCTACAATGCTAT
	PB2_H1_R1850	CCAAGCACATCCCTCATTTG
	PB2-R3'	AGTAGAAACAAGGTCGTTTTTAAA
PB1	PB1-F5'	AGCAAAAGCAGGCAAACCATTTG
	PB1_H1_F506	GGAGGCTAATAGACTTCCTTA
	PB1_H1_R701	GTGTTCAAGGTTAATGCCT
	PB1_H1_F1232	TGAGTCCTGGAATGATGATG
	PB1_H1_R1319	GTGTATCTCTTTTGCCCAAGA
	PB1_H3_F1705	TGCCACAGAGGTGACACAC
	PB1_H1_R1863	CCATTTCAAGCAGACTTCAG
	PB1-R3'	AGTAGAAACAAGGCATTTTTTCA
	PA	PA-F5'
PA_H1_F481		GAAGAAATGGCCACAAGGC
PA_H1_R613		CTCTTTCGGACTGACGAAAG
PA_H1_F1246		CAGAAATGAGTTCAACAAGGC
PA_H1_R1383		GCAATGGGACACCTCAGCT
PA_H1_R1921		TGGAACCTTCTTCCACTCCT
PA-R3'		AGTAGAAACAAGGTAATTTTTTGG

Table S7. Primers used for conventional PCR amplification of the whole genome of influenza A(H3N2) strains circulating in Thailand.

Target Gene	Primer	Sequence (5'-3')
PB2	PB2-F5'	AGCAAAAGCAGGTCAATTATATTC
	PB2_H3_F493	GCCAAGGAGGCACAAGATG
	PB2_H3_R642	GTATGCAACCATCAAGGGAG
	PB2_H3_F1059	GCTTACAGGCAATCTCCAAAC
	PB2_H3_R1189	CACTCACTATGAGCTGAACC
	PB2_H3_F1637	GGGAGATTAACGGTCCTGA
	PB2_H3_R1851	CCCAAGTACATCTCTCATTTG
	PB2-R3'	AGTAGAAACAAGGTCGTTTTTAAA
PB1	PB1-F5'	AGCAAAAGCAGGCAAACCATTTG
	PB1_H3_F491	CAGCTAATGAATCAGGAAGGC
	PB1_H3_R762	CATCCCGGGTGTGCAATAG
	PB1_H3_F1116	CCGAACACAAATACCCGCAG
	PB1_H3_R1225	GTGCCATCTATTAGAAGAGG
	PB1_H3_F1704	GTGCCATAGAGGAGACACAC
	PB1_H3_R1867	GCTCCCACTTTAAGCAGACT
	PB1-R3'	AGTAGAAACAAGGCATTTTTTCA
PA	PA-F5'	AGCAAAAGCAGGTAAGTATCCG
	PA_H3_F472	TTCACTGGGGAGGAAATGGCC
	PA_H3_R681	GAGACTTTGGTCGGCAAGCC
	PA_H3_F1129	GCTCTTGGTGAAAACATGGC
	PA_H3_R1247	CTGTATCCAGCTTGAAAGTGA
	PA_H3_F1585	GTGAGCATGGAGTTTTCTCTC
	PA_H3_R1778	AGGCAACGTCTCATCTCCAT
	PA-R3'	AGTAGAAACAAGGTAAGTTTTTGG

Table S8. Primers used for conventional PCR amplification of the whole genome of influenza B strains circulating in Thailand.

Target gene	Primer	Nucleotide Sequences (5'-3')
PB2	PB2-F5'	AGC AGA AGC GGA GCC TTT TCA AG
	PB2-R1082	CCG TCC CAT ATT CCA ATC TTC TG
	PB2-F902	CAG CCA TAG ACG GAG GTG ATG T
	PB2-R1907	TGA TAA GGC TCC CCA TTG CTC CTT
	PB2-F1716	GTT CCA ATG GGA TGC ATT TGA AG
	PB2-R3	ATG ACC AGT AGA AAC ACG AGC A
PB1	PB1-F5'	AGC AGA AGC GGA GCC TTT AAG ATG
	PB1-R1024	CCG GTG CTA TAC TAC AAA AAT CCC
	PB1-F896	GCA TGA CAG TAA CAG GAG ACA AT
	PB1-R1946	CCA TGT GCT GGG GTT ATA TCT GC
	PB1-F1667	ACA CCT ACA AAT GCC ACA GGG GAG
	PB1-R3'	TGA CCA GTA GAA ACA CGA GCC TTT
PA	PA-F5'	AGC AGA AGC GGT GCG TTT GAT TTG
	PA-R1114	ATG TTA ATC CAT CCC CTG TGG CCC
	PA-F1010	GGA AGC TTT GGA GAG ACT GTG TAA A
	PA-R1836	GGG GCT ATT TAC TCT GTC TCC C
	PA-F1622	TTG GCT CCC TAT TTG TGA GTG GG
	PA-R3'	AGT AGA AAC ACG TGC ATT TTT GAT TC

Table S9. The accession number of PB2, PB1 and PA nucleotide sequences of influenza A(H1N1)pdm09, A(H3N2), influenza B virus and the details of patients for individual sequences that collected in this study.

Influenza A(H1N1)pdm09 virus

Sequence ID	Age	Gender	collection-date	PB2	PB1	PA
A/Thailand/CU-B4656/2011	3	female	24-Mar-11	MW126812	MW127282	MW127886
A/Thailand/CU-B4662/2011	49	female	30-Mar-11	MW126813	MW127283	MW127887
A/Thailand/CU-B4717/2011	19	female	20-May-11	MW126814	MW127284	MW127888
A/Thailand/CU-B4773/2011	25	male	17-Jun-11	MW126815	MW127285	MW127889
A/Thailand/CU-B5356/2011	36	male	18-Aug-11	MW126816	MW127286	MW127890
A/Thailand/CU-B5515/2011	28	male	27-Aug-11	MW126817	MW127287	MW127891
A/Thailand/CU-B6475/2012	38	female	28-Jun-12	MW126818	MW127288	MW127892
A/Thailand/CU-B6609/2012	13	female	10-Aug-12	MW126819	MW127289	MW127893
A/Thailand/CU-B6801/2012	47	female	1-Sep-12	MW126820	MW127290	MW127894
A/Thailand/CU-B8091/2013	29	male	28-Jun-13	MW126821	MW127291	MW127895
A/Thailand/CU-B8571/2013	42	female	15-Oct-13	MW126822	MW127292	MW127896
A/Thailand/CU-B8573/2013	31	female	16-Oct-13	MW126823	MW127293	MW127897
A/Thailand/CU-B8906/2014	51	female	31-Jan-14	MW126824	MW127294	MW127898
A/Thailand/CU-B8981/2014	51	female	30-Jan-14	MW126825	MW127295	MW127899
A/Thailand/CU-B9024/2014	12	male	4-Feb-14	MW126826	MW127296	MW127900
A/Thailand/CU-B9225/2014	48	male	24-Feb-14	MW126827	MW127297	MW127901
A/Thailand/CU-H3628/2014	1	male	15-Mar-14	MW126828	MW127298	MW127902
A/Thailand/CU-B10032/2014	56	female	18-Apr-14	MW126829	MW127299	MW127903
A/Thailand/CU-B10044/2014	25	female	25-Apr-14	MW126830	MW127300	MW127904
A/Thailand/CU-B10126/2014	25	male	6-May-14	MW126831	MW127301	MW127905
A/Thailand/CU-B10174/2014	30	female	27-May-14	MW126832	MW127302	MW127906
A/Thailand/CU-A1058/2014	14	male	25-Jun-14	MW126833	MW127303	MW127907
A/Thailand/CU-B10405/2014	27	female	23-Jul-14	MW126834	MW127304	MW127908
A/Thailand/CU-B10909/2014	43	female	22-Sep-14	MW126835	MW127305	MW127909
A/Thailand/CU-H3658/2014	55	female	15-Sep-14	MW126836	MW127306	MW127910
A/Thailand/CU-C5149/2014	1	male	1-Oct-14	MW126837	MW127307	MW127911
A/Thailand/CU-C5169/2014	5	female	8-Oct-14	MW126838	MW127308	MW127912
A/Thailand/CU-B11291/2014	51	male	19-Nov-14	MW126839	MW127309	MW127913
A/Thailand/CU-C5263/2014	14	female	19-Nov-14	MW126840	MW127310	MW127914
A/Thailand/CU-B11363/2014	24	female	3-Dec-14	MW126841	MW127311	MW127915
A/Thailand/CU-B11422/2014	34	female	18-Dec-14	MW126842	MW127312	MW127916
A/Thailand/CU-B11495/2015	54	female	10-Jan-15	MW126843	MW127313	MW127917
A/Thailand/CU-B11556/2015	27	female	29-Jan-15	MW126844	MW127314	MW127918
A/Thailand/CU-B11606/2015	42	male	16-Feb-15	MW126845	MW127315	MW127919

Sequence ID	Age	Gender	collection-date	PB2	PB1	PA
A/Thailand/CU-B11669/2015	3	female	2-Mar-15	MW126846	MW127316	MW127920
A/Thailand/CU-B11699/2015	28	female	11-Mar-15	MW126847	MW127317	MW127921
A/Thailand/CU-B11841/2015	24	female	23-Apr-15	MW126848	MW127318	MW127922
A/Thailand/CU-B11877/2015	69	female	9-May-15	MW126849	MW127319	MW127923
A/Thailand/CU-C5866/2015	1	female	2-Jul-15	MW126850	MW127320	MW127924
A/Thailand/CU-B12167/2015	22	female	1-Aug-15	MW126851	MW127321	MW127925
A/Thailand/CU-B12591/2015	46	male	28-Aug-15	MW126852	MW127322	MW127926
A/Thailand/CU-B12604/2015	24	female	3-Aug-15	MW126853	MW127323	MW127927
A/Thailand/CU-B12974/2015	37	male	24-Sep-15	MW126854	MW127324	MW127928
A/Thailand/CU-B13202/2015	55	female	14-Oct-15	MW126855	MW127325	MW127929
A/Thailand/CU-B13274/2015	3	female	20-Oct-15	MW126856	MW127326	MW127930
A/Thailand/CU-B14522/2015	1	female	22-Dec-15	MW126857	MW127327	MW127931
A/Thailand/CU-B14936/2016	32	male	29-Jan-16	MW126858	MW127328	MW127932
A/Thailand/CU-B14943/2016	64	female	30-Jan-16	MW126859	MW127329	MW127933
A/Thailand/CU-B15134/2016	48	male	11-Feb-16	MW126860	MW127330	MW127934
A/Thailand/CU-B15328/2016	39	male	24-Feb-16	MW126861	MW127331	MW127935
A/Thailand/CU-B15497/2016	34	male	1-Mar-16	MW126862	MW127332	MW127936
A/Thailand/CU-C6558/2016	1	female	18-May-16	MW126863	MW127333	MW127937
A/Thailand/CU-B16399/2016	35	female	2-May-16	MW126864	MW127334	MW127938
A/Thailand/CU-B16575/2016	31	male	1-Jun-16	MW126865	MW127335	MW127939
A/Thailand/CU-B16576/2016	40	female	1-Jun-16	MW126866	MW127336	MW127940
A/Thailand/CU-B17578/2016	39	female	10-Aug-16	MW126867	MW127337	MW127941
A/Thailand/CU-B17584/2016	31	male	11-Aug-16	MW126868	MW127338	MW127942
A/Thailand/CU-B17739/2016	72	male	19-Aug-16	MW126869	MW127339	MW127943
A/Thailand/CU-B17794/2016	55	female	27-Aug-16	MW126870	MW127340	MW127944
A/Thailand/CU-B18022/2016	44	male	1-Sep-16	MW126871	MW127341	MW127945
A/Thailand/CU-B18043/2016	4	female	3-Sep-16	MW126872	MW127342	MW127946
A/Thailand/CU-B18062/2016	69	male	6-Sep-16	MW126873	MW127343	MW127947
A/Thailand/CU-B18280/2016	62	male	8-Sep-16	MW126874	MW127344	MW127948
A/Thailand/CU-B18306/2016	45	female	12-Sep-16	MW126875	MW127345	MW127949
A/Thailand/CU-B18484/2016	33	female	13-Sep-16	MW126876	MW127346	MW127950
A/Thailand/CU-B19243/2016	38	female	13-Oct-16	MW126877	MW127347	MW127951
A/Thailand/CU-B19888/2016	5	male	8-Nov-16	MW126878	MW127348	MW127952
A/Thailand/CU-B19954/2016	12	female	12-Nov-16	MW126879	MW127349	MW127953
A/Thailand/CU-B19715/2016	8	male	7-Nov-16	MW126880	MW127350	MW127954
A/Thailand/CU-B20025/2016	15	male	21-Nov-16	MW126881	MW127351	MW127955
A/Thailand/CU-B21395/2017	25	female	28-Feb-17	MW126882	MW127352	MW127956
A/Thailand/CU-B21586/2017	6	male	3-Apr-17	MW126883	MW127353	MW127957
A/Thailand/CU-B21677/2017	56	male	18-Apr-17	MW126884	MW127354	MW127958
A/Thailand/CU-B21877/2017	27	male	17-May-17	MW126885	MW127355	MW127959

Sequence ID	Age	Gender	collection-date	PB2	PB1	PA
A/Thailand/CU-B21984/2017	4	male	30-May-17	MW126886	MW127356	MW127960
A/Thailand/CU-B22092/2017	58	male	7-Jun-17	MW126887	MW127357	MW127961
A/Thailand/CU-B22395/2017	35	male	28-Jun-17	MW126888	MW127358	MW127962
A/Thailand/CU-B22514/2017	51	female	5-Jul-17	MW126889	MW127359	MW127963
A/Thailand/CU-B22532/2017	38	male	7-Jul-17	MW126890	MW127360	MW127964
A/Thailand/CU-B22888/2017	34	female	24-Jul-17	MW126891	MW127361	MW127965
A/Thailand/CU-B23198/2017	78	male	1-Aug-17	MW126892	MW127362	MW127966
A/Thailand/CU-B23241/2017	29	female	4-Aug-17	MW126893	MW127363	MW127967
A/Thailand/CU-B24083/2017	36	female	1-Sep-17	MW126894	MW127364	MW127968
A/Thailand/CU-B24386/2017	17	female	7-Sep-17	MW126895	MW127365	MW127969
A/Thailand/CU-B25124/2017	3	male	2-Oct-17	MW126896	MW127366	MW127970
A/Thailand/CU-B25276/2017	9	male	4-Oct-17	MW126897	MW127367	MW127971
A/Thailand/CU-B25494/2017	19	male	14-Oct-17	MW126898	MW127368	MW127972
A/Thailand/CU-B26815/2018	43	female	3-Jan-18	MW126899	MW127369	MW127973
A/Thailand/CU-B26827/2018	33	female	5-Jan-18	MW126900	MW127370	MW127974
A/Thailand/CU-B27073/2018	32	male	19-Jan-18	MW126901	MW127371	MW127975
A/Thailand/CU-B27082/2018	56	female	22-Jan-18	MW126902	MW127372	MW127976
A/Thailand/CU-B27420/2018	8	male	10-Feb-18	MW126903	MW127373	MW127977
A/Thailand/CU-B27534/2018	31	female	17-Feb-18	MW126904	MW127374	MW127978
A/Thailand/CU-B27898/2018	50	female	8-Mar-18	MW126905	MW127375	MW127979
A/Thailand/CU-B27943/2018	10	female	7-Mar-18	MW126906	MW127376	MW127980
A/Thailand/CU-B28162/2018	53	male	3-Apr-18	MW126907	MW127377	MW127981
A/Thailand/CU-B28420/2018	30	female	4-May-18	MW126908	MW127378	MW127982
A/Thailand/CU-B29061/2018	6	male	26-Jun-18	MW126909	MW127379	MW127983
A/Thailand/CU-B29280/2018	43	male	4-Jul-18	MW126910	MW127380	MW127984
A/Thailand/CU-E995/2018	95	female	4-Sep-18	MW126911	MW127381	MW127985
A/Thailand/CU-E1099/2018	3	female	11-Oct-18	MW126912	MW127382	MW127986
A/Thailand/CU-B30149/2018	47	female	25-Sep-18	MW126913	MW127383	MW127987
A/Thailand/CU-B31088/2019	38	male	2-Jan-19	MW126914	MW127384	MW127988
A/Thailand/CU-B32110/2019	46	female	20-Feb-19	MW126915	MW127385	MW127989
A/Thailand/CU-H3938/2019	2	female	19-Mar-19	MW126916	MW127386	MW127990
A/Thailand/CU-B33041/2019	3	female	7-May-19	MW126917	MW127387	MW127991
A/Thailand/CU-B33247/2019	31	male	12-Jun-19	MW126918	MW127388	MW127992
A/Thailand/CU-B33254/2019	40	female	14-May-19	MW126919	MW127389	MW127993
A/Thailand/CU-B33583/2019	45	male	19-Jul-19	MW126920	MW127390	MW127994
A/Thailand/CU-B33692/2019	54	female	8-Aug-19	MW126921	MW127391	MW127995
A/Thailand/CU-B33699/2019	39	female	10-Aug-19	MW126922	MW127392	MW127996
A/Thailand/CU-B34081/2019	36	female	3-Sep-19	MW126923	MW127393	MW127997
A/Thailand/CU-B34351/2019	51	female	23-Sep-19	MW126924	MW127394	MW127998
A/Thailand/CU-B34831/2019	37	female	8-Oct-19	MW126925	MW127395	MW127999

A/Thailand/CU-B35002/2019	42	male	19-Oct-19	MW126926	MW127396	MW128000
A/Thailand/CU-B35253/2019	55	female	11-Nov-19	MW126927	MW127397	MW128001
A/Thailand/CU-B35326/2019	19	male	15-Nov-19	MW126928	MW127398	MW128002
A/Thailand/CU-B35599/2019	38	male	4-Dec-19	MW126929	MW127399	MW128003
A/Thailand/CU-B35519/2019	62	male	27-Nov-19	MW126930	MW127400	MW128004



Influenza A(H3N2) virus

Sequence ID	Age	Gender	collection-date	PB2	PB1	PA
A/Thailand/CU-H1285/2010	-	male	21-Jan-10	CY074947	CY074948	CY074949
A/Thailand/CU-H1443/2010	-	male	04-Feb-10	CY074955	CY074956	CY074957
A/Thailand/CU-B4929/2011	37	female	18-Jul-11	KP335691	KP335749	KP335807
A/Thailand/CU-B5105/2011	-	female	03-Aug-11	KP335692	KP335750	KP335808
A/Thailand/CU-H3020/2011	4	female	15-Aug-11	KP335701	KP335759	KP335817
A/Thailand/CU-B5614/2011	33	male	05-Sep-11	KP335693	KP335751	KP335809
A/Thailand/CU-B5848/2011	30	male	17-Oct-11	KP335695	KP335753	KP335811
A/Thailand/CU-B5873/2011	35	male	24-Oct-11	KP335696	KP335754	KP335812
A/Thailand/CU-B5909/2011	4m	male	03-Nov-11	GQ902814	GQ902815	GQ902816
A/Thailand/CU-B5928/2011	-	female	15-Nov-11	KP335698	KP335756	KP335814
A/Thailand/CU-C2417/2011	3	female	08-Dec-11	KP335699	KP335757	KP335815
A/Thailand/CU-H3141/2012	60	male	09-Jan-12	KP335709	KP335767	KP335825
A/Thailand/CU-B6091/2012	35	female	23-Feb-12	KP335702	KP335760	KP335818
A/Thailand/CU-B6251/2012	36	male	06-Jun-12	KP335703	KP335761	KP335819
A/Thailand/CU-B6274/2012	9	male	22-Jun-12	KP335704	KP335762	KP335820
A/Thailand/CU-B6309/2012	31	female	02-Jul-12	KP335705	KP335763	KP335821
A/Thailand/CU-H3368/2012	12	male	31-Aug-12	KP335710	KP335768	KP335826
A/Thailand/CU-B6936/2012	36	female	13-Sep-12	KP335706	KP335764	KP335822
A/Thailand/CU-H3453/2012	1	male	16-Oct-12	KP335711	KP335769	KP335827
A/Thailand/CU-B7235/2012	36	male	26-Nov-12	KP335707	KP335765	KP335823
A/Thailand/CU-B7367/2012	9	male	22-Dec-12	KP335708	KP335766	KP335824
A/Thailand/CU-B7536/2013	29	male	28-Jan-13	KP335712	KP335770	KP335828
A/Thailand/CU-B7585/2013	90	male	02-Feb-13	KP335713		
A/Thailand/CU-B7765/2013	67	female	18-Mar-13	KP335714	KP335772	KP335830
A/Thailand/CU-B7885/2013	23	female	22-Apr-13	KP335721	KP335779	KP335837
A/Thailand/CU-B7937/2013	3	female	01-May-13	KP335722	KP335780	KP335838
A/Thailand/CU-A114/2013	57	male	04-Jun-13	KP335715	KP335773	KP335831
A/Thailand/CU-A134/2013	33	male	20-Jun-13	KP335716	KP335774	KP335832
A/Thailand/CU-A166/2013	26	male	10-Jul-13	KP335717	KP335775	KP335833
A/Thailand/CU-B8121/2013	45	male	02-Aug-13	KP335723	KP335781	KP335839
A/Thailand/CU-B8127/2013	35	female	05-Aug-13	KP335724	KP335782	KP335840
A/Thailand/CU-A305/2013	15	male	29-Aug-13	KP335719	KP335777	KP335835
A/Thailand/CU-C4087/2013	14	female	04-Sep-13	KP335729	KP335787	KP335845
A/Thailand/CU-B8364/2013	38	male	23-Sep-13	KP335725	KP335783	KP335841
A/Thailand/CU-B8518/2013	3	female	02-Oct-13	KP335726	KP335784	KP335842
A/Thailand/CU-H3567/2013	-	female	10-Oct-13	KP335731	KP335789	KP335847
A/Thailand/CU-A459/2013	19	male	29-Oct-13	KP335720	KP335778	KP335836

Sequence ID	Age	Gender	collection-date	PB2	PB1	PA
A/Thailand/CU-B8736/2013	26	male	14-Nov-13	KP335727	KP335785	KP335843
A/Thailand/CU-B8772/2013	26	female	11-Dec-13	KP335728	KP335786	KP335844
A/Thailand/CU-C4364/2013	9	male	18-Dec-13	KP335730	KP335788	KP335846
A/Thailand/CU-B8849/2014	20	female	07-Jan-14	KP335732	KP335790	KP335848
A/Thailand/CU-C4406/2014	10	female	07-Jan-14	KP335738		
A/Thailand/CU-H3595/2014	40	female	04-Feb-14	KP335741	KP335799	KP335857
A/Thailand/CU-C4546/2014	2	female	12-Feb-14	KP335739	KP335797	
A/Thailand/CU-H3626/2014	6	male	07-Mar-14	KP335742	KP335800	KP335858
A/Thailand/CU-CB166/2014	9	female	01-Apr-14	KP335740		KP335856
A/Thailand/CU-B10282/2014	15	male	16-Jun-14	KP335733	KP335791	KP335849
A/Thailand/CU-H3649/2014	8	male	09-Jul-14	KP335743	KP335801	KP335859
A/Thailand/CU-B10509/2014	42	male	04-Aug-14	KP335735	KP335793	KP335851
A/Thailand/CU-B10521/2014	9	male	05-Aug-14	KP335736	KP335794	KP335852
A/Thailand/CU-H3656/2014	8	male	02-Sep-14	KP335744	KP335802	KP335860
A/Thailand/CU-B10828/2014	23	female	10-Sep-14	KP335737	KP335795	KP335853
A/Thailand/CU-B10975/2014	35	male	06-Oct-14	KP335745	KP335803	KP335861
A/Thailand/CU-B11202/2014	6	male	01-Nov-14	KP335747	KP335805	KP335863
A/Thailand/CU-H3680/2014	-	-	13-Nov-14	KP335748		KP335864
A/Thailand/CU-B11461/2015	29	male	03-Jan-15	MW127401	MW127188	MW127014
A/Thailand/CU-B11507/2015	13	male	15-Jan-15	MW127402	MW127189	MW127015
A/Thailand/CU-B11566/2015	41	female	03-Feb-15	MW127403	MW127190	MW127016
A/Thailand/CU-C5500/2015	8	female	11-Feb-15	MW127404	MW127191	MW127017
A/Thailand/CU-B11686/2015	39	female	06-Mar-15	MW127405	MW127192	MW127018
A/Thailand/CU-H3689/2015	7	male	02-Jun-15	MW127406	MW127193	MW127019
A/Thailand/CU-B11807/2015	28	female	08-Apr-15	MW127407	MW127194	MW127020
A/Thailand/CU-B11820/2015	35	male	16-Apr-15	MW127408	MW127195	MW127021
A/Thailand/CU-B11870/2015	1	female	07-May-15	MW127409	MW127196	MW127022
A/Thailand/CU-B11889/2015	65	female	14-May-15	MW127410	MW127197	MW127023
A/Thailand/CU-B12006/2015	83	male	15-Jun-15	MW127411	MW127198	MW127024
A/Thailand/CU-H3700/2015	55	female	12-Jun-15	MW127412	MW127199	MW127025
A/Thailand/CU-B12139/2015	25	female	22-Jul-15	MW127413	MW127200	MW127026
A/Thailand/CU-H3708/2015		female	29-Jul-15	MW127414	MW127201	MW127027
A/Thailand/CU-12191/2015	48	female	07-Aug-15	MW127415	MW127202	MW127028
A/Thailand/CU-B12589/2015	45	female	27-Aug-15	MW127416	MW127203	MW127029
A/Thailand/CU-B12788/2015	30	female	17-Sep-15	MW127417	MW127204	MW127030
A/Thailand/CU-C6062/2015	12	male	15-Sep-15	MW127418	MW127205	MW127031
A/Thailand/CU-B13425/2015	41	female	27-Oct-15	MW127419	MW127206	MW127032
A/Thailand/CU-C6193/2015	5	female	21-Oct-15	MW127420	MW127207	MW127033
A/Thailand/CU-B13893/2015	21	male	19-Nov-15	MW127421	MW127208	MW127034

Sequence ID	Age	Gender	collection-date	PB2	PB1	PA
A/Thailand/CU-C6246/2015	12	male	19-Nov-15	MW127422	MW127209	MW127035
A/Thailand/CU-B14354/2015	64	female	11-Dec-15	MW127423	MW127210	MW127036
A/Thailand/CU-A2137/2016	87	male	07-Jan-16	MW127424	MW127211	MW127037
A/Thailand/CU-B14944/2016	25	female	01-Feb-16	MW127425	MW127212	MW127038
A/Thailand/CU-B15149/2016	12	female	15-Feb-16	MW127426	MW127213	MW127039
A/Thailand/CU-B15712/2016	18	male	15-Mar-16	MW127427	MW127214	MW127040
A/Thailand/CU-B15894/2016	70	female	25-Mar-16	MW127428	MW127215	MW127041
A/Thailand/CU-C6513/2016	7	female	21-Apr-16	MW127429	MW127216	MW127042
A/Thailand/CU-A2407/2016	80	male	18-May-16	MW127430	MW127217	MW127043
A/Thailand/CU-B16712/2016	53	male	16-Jun-16	MW127431	MW127218	MW127044
A/Thailand/CU-B16949/2016	70	female	09-Jul-16	MW127432	MW127219	MW127045
A/Thailand/CU-B17573/2016	102	female	10-Aug-16	MW127433	MW127220	MW127046
A/Thailand/CU-B17583/2016	28	female	11-Aug-16	MW127434	MW127221	MW127047
A/Thailand/CU-B18031/2016	38	female	02-Sep-16	MW127435	MW127222	MW127048
A/Thailand/CU-B18308/2016	13	male	12-Sep-16	MW127436	MW127223	MW127049
A/Thailand/CU-B18515/2016	4	female	19-Sep-16	MW127437	MW127224	MW127050
A/Thailand/CU-B19263/2016	4	male	15-Oct-16	MW127438	MW127225	MW127051
A/Thailand/CU-B19401/2016	50	female	19-Oct-16	MW127439	MW127226	MW127052
A/Thailand/CU-B19855/2016	1	female	12-Nov-16	MW127440	MW127227	MW127053
A/Thailand/CU-B20004/2016	61	female	17-Nov-16	MW127441	MW127228	MW127054
A/Thailand/CU-B20273/2016	10	female	03-Dec-16	MW127442	MW127229	MW127055
A/Thailand/CU-B20489/2016	37	male	20-Dec-16	MW127443	MW127230	MW127056
A/Thailand/CU-B20852/2017	11	female	18-Jan-17	MW127444	MW127231	MW127057
A/Thailand/CU-B20929/2017	64	female	26-Jan-17	MW127445	MW127232	MW127058
A/Thailand/CU-C7086/2017	1	female	01-Feb-17	MW127446	MW127233	MW127059
A/Thailand/CU-B20992/2017	8	male	04-Feb-17	MW127447	MW127234	MW127060
A/Thailand/CU-B21369/2017	31	female	01-Mar-17	MW127448	MW127235	MW127061
A/Thailand/CU-B21378/2017	5	female	04-Mar-17	MW127449	MW127236	MW127062
A/Thailand/CU-CN148/2017	1	male	26-Apr-17	MW127450	MW127237	MW127063
A/Thailand/CU-B21760/2017	54	female	19-Apr-17	MW127451	MW127238	MW127064
A/Thailand/CU-E379/2017	12	female	30-May-17	MW127452	MW127239	MW127065
A/Thailand/CU-B22183/2017	63	female	19-Jun-17	MW127453	MW127240	MW127066
A/Thailand/CU-B22342/2017	24	female	22-Jun-17	MW127454	MW127241	MW127067
A/Thailand/CU-B22413/2017	63	female	03-Jul-17	MW127455	MW127242	MW127068
A/Thailand/CU-B22867/2017	37	female	19-Jul-17	MW127456	MW127243	MW127069
A/Thailand/CU-B23240/2017	10	male	04-Aug-17	MW127457	MW127244	MW127070
A/Thailand/CU-B23866/2017	19	female	26-Aug-17	MW127458	MW127245	MW127071
A/Thailand/CU-B24415/2017	4	male	11-Sep-17	MW127459	MW127246	MW127072
A/Thailand/CU-B24679/2017	21	female	16-Sep-17	MW127460	MW127247	MW127073

Sequence ID	Age	Gender	collection-date	PB2	PB1	PA
A/Thailand/CU-B25464/2017	35	female	10-Oct-17	MW127461	MW127248	MW127074
A/Thailand/CU-B25698/2017	60	female	21-Oct-17	MW127462	MW127249	MW127075
A/Thailand/CU-B26075/2017	8	male	05-Nov-17	MW127463	MW127250	MW127076
A/Thailand/CU-B26185/2017	43	female	03-Jan-18	MW127464	MW127251	MW127077
A/Thailand/CU-B26618/2017	43	female	03-Jan-18	MW127465	MW127252	MW127078
A/Thailand/CU-B26734/2017	48	female	21-Dec-17	MW127466	MW127253	MW127079
A/Thailand/CU-B27083/2018	55	female	22-Jan-18	MW127467	MW127254	MW127080
A/Thailand/CU-B27093/2018	65	male	16-Jan-18	MW127468	MW127255	MW127081
A/Thailand/CU-B27503/2018	72	female	10-Feb-18	MW127469	MW127256	MW127082
A/Thailand/CU-B27591/2018	45	male	15-Feb-18	MW127470	MW127257	MW127083
A/Thailand/CU-B28536/2018	69	male	08-May-18	MW127471	MW127258	MW127084
A/Thailand/CU-B28861/2018	12	male	14-Jun-18	MW127472	MW127259	MW127085
A/Thailand/CU-B29307/2018	15	male	14-Jul-18	MW127473	MW127260	MW127086
A/Thailand/CU-H3900/2018		female	06-Sep-18	MW127474	MW127261	MW127087
A/Thailand/CU-B30632/2018	53	male	31-Oct-18	MW127475	MW127262	MW127088
A/Thailand/CU-B31119/2018	10	male	21-Dec-18	MW127476	MW127263	MW127089
A/Thailand/CU-H3914/2019	10	male	14-Jan-19	MW127477	MW127264	MW127090
A/Thailand/CU-B31931/2019	56	male	04-Feb-19	MW127478	MW127265	MW127091
A/Thailand/CU-B32345/2019	19	male	09-Mar-19	MW127479	MW127266	MW127092
A/Thailand/CU-E1501/2019	15	male	19-Apr-19	MW127480	MW127267	MW127093
A/Thailand/CU-B33021/2019	5	female	06-May-19	MW127481	MW127268	MW127094
A/Thailand/CU-B33261/2019	4	male	17-Jun-19	MW127482	MW127269	MW127095
A/Thailand/CU-B33444/2019	37	male	04-Jul-19	MW127483	MW127270	MW127096
A/Thailand/CU-B33676/2019	9	female	29-Jul-19	MW127484	MW127271	MW127097
A/Thailand/CU-B33700/2019	58	female	13-Aug-19	MW127485	MW127272	MW127098
A/Thailand/CU-B34006/2019	86	female	30-Aug-19	MW127486	MW127273	MW127099
A/Thailand/CU-B34085/2019	46	female	05-Sep-19	MW127487	MW127274	MW127100
A/Thailand/CU-B34340/2019	49	female	19-Sep-19	MW127488	MW127275	MW127101
A/Thailand/CU-B34698/2019	35	male	02-Oct-19	MW127489	MW127276	MW127102
A/Thailand/CU-B35321/2019	11	male	13-Nov-19	MW127490	MW127277	MW127103
A/Thailand/CU-B35397/2019	6	male	17-Nov-19	MW127491	MW127278	MW127104
A/Thailand/CU-B35502/2019	7	male	23-Nov-19	MW127492	MW127279	MW127105

Influenza B virus

Sequence ID	Age	Gender	collection-date	PB2	PB1	PA
B/Thailand/CU-B11464/2015	56	female	5-Jan-15	MW126636	MW126704	MW126931
B/Thailand/CU-B11517/2015	58	male	19-Jan-15	MW126637	MW126705	MW126932
B/Thailand/CU-B11603/2015	33	female	13-Feb-15	MW126638	MW126706	MW126933
B/Thailand/CU-B13917/2015	36	female	23-Nov-15	MW126639	MW126707	MW126934
B/Thailand/CU-B14525/2015	29	female	23-Dec-15	MW126640	MW126708	MW126935
B/Thailand/CU-B14831/2016	33	male	21-Jan-16	MW126641	MW126709	MW126936
B/Thailand/CU-B14972/2016	37	male	5-Feb-16	MW126642	MW126710	MW126937
B/Thailand/CU-B14986/2016	35	female	8-Feb-16	MW126643	MW126711	MW126938
B/Thailand/CU-B15585/2016	9	female	22-Feb-16	MW126644	MW126712	MW126939
B/Thailand/CU-B16416/2016	35	female	10-May-16	MW126645	MW126713	MW126940
B/Thailand/CU-B17180/2016	45	male	25-Jul-16	MW126646	MW126714	MW126941
B/Thailand/CU-B19872/2016	23	female	15-Nov-16	MW126647	MW126715	MW126942
B/Thailand/CU-B20298/2017	25	female	30-Nov-16	MW126648	MW126716	MW126943
B/Thailand/CU-B21093/2017	5	male	10-Feb-17	MW126649	MW126717	MW126944
B/Thailand/CU-B21469/2017	32	female	21-Mar-17	MW126650	MW126718	MW126945
B/Thailand/CU-CN133/2017	6	male	20-Apr-17	MW126651	MW126719	
B/Thailand/CU-B21762/2017	7	male	20-Apr-17	MW126652	MW126720	MW126946
B/Thailand/CU-B21998/2017	5	male	1-Jun-17	MW126653	MW126721	MW126947
B/Thailand/CU-B22512/2017	16	female	4-Jul-17	MW126654	MW126722	MW126948
B/Thailand/CU-B27737/2017	56	male	13-Jul-17	MW126655	MW126723	MW126949
B/Thailand/CU-B24367/2017	33	female	6-Sep-17	MW126656	MW126724	MW126950
B/Thailand/CU-B24631/2017	46	female	12-Sep-17	MW126657	MW126725	MW126951
B/Thailand/CU-B25308/2017	53	male	7-Oct-17	MW126658	MW126726	MW126952
B/Thailand/CU-B25670/2017	88	female	17-Oct-17	MW126659	MW126727	MW126953
B/Thailand/CU-B26338/2017	59	male	27-Nov-17	MW126660	MW126728	MW126954
B/Thailand/CU-B26467/2017	9	female	12-Dec-17	MW126661	MW126729	MW126955
B/Thailand/CU-B26647/2017	10	male	14-Dec-17	MW126662	MW126730	MW126956
B/Thailand/CU-B26977/2017	59	male	11-Jan-18	MW126663	MW126731	MW126957
B/Thailand/CU-B27406/2018	9	male	6-Feb-18	MW126664	MW126732	MW126958
B/Thailand/CU-B27905/2018	28	female	12-Mar-18	MW126665	MW126733	MW126959
B/Thailand/CU-B28017/2018	45	female	16-Mar-18	MW126666	MW126734	MW126960
B/Thailand/CU-B29948/2018	4	male	1-Sep-18	MW126667	MW126735	MW126961
B/Thailand/CU-H3906/2018		female	24-Oct-18	MW126668	MW126736	MW126962
B/Thailand/CU-B30897/2018	16	female	25-Nov-18	MW126669	MW126737	MW126963
B/Thailand/CU-E1271/2018	5	male	18-Dec-18	MW126670	MW126738	MW126964
B/Thailand/CU-B31196/2019	25	female	3-Jan-19	MW126671	MW126739	MW126965

Sequence ID	Age	Gender	collection-date	PB2	PB1	PA
B/Thailand/CU-B31974/2019	25	female	9-Feb-19	MW126672	MW126740	MW126966
B/Thailand/CU-B32499/2019	35	male	19-Mar-19	MW126673	MW126741	MW126967
B/Thailand/CU-B32772/2019	32	female	18-Apr-19	MW126674	MW126742	MW126968
B/Thailand/CU-H3948/2019	33	male	15-May-19	MW126675	MW126743	MW126969
B/Thailand/CU-B33344/2019	13	male	20-Jun-19	MW126676	MW126744	MW126970
B/Thailand/CU-B33492/2019	25	female	19-Jul-19	MW126677	MW126745	MW126971
B/Thailand/CU-B33686/2019	6	female	3-Aug-19	MW126678	MW126746	MW126972
B/Thailand/CU-B33757/2019	6	female	4-Aug-19	MW126679	MW126747	MW126973
B/Thailand/CU-B34094/2019	59	female	7-Sep-19	MW126680	MW126748	MW126974
B/Thailand/CU-B34270/2019	43	female	12-Sep-19	MW126681	MW126749	MW126975
B/Thailand/CU-B34381/2019	38	male	17-Sep-19	MW126682	MW126750	MW126976
B/Thailand/CU-B34528/2019	77	female	28-Sep-19	MW126683	MW126751	MW126977
B/Thailand/CU-B35320/2019	57	female	13-Nov-19	MW126684	MW126752	MW126978
B/Thailand/CU-E1993/2019	7	male	27-Nov-19	MW126685	MW126753	MW126979
B/Thailand/CU-B35796/2019	28	female	19-Dec-19	MW126686	MW126754	MW126980
B/Thailand/CU-B35721/2019	20	female	12-Dec-19	MW126687	MW126755	MW126981

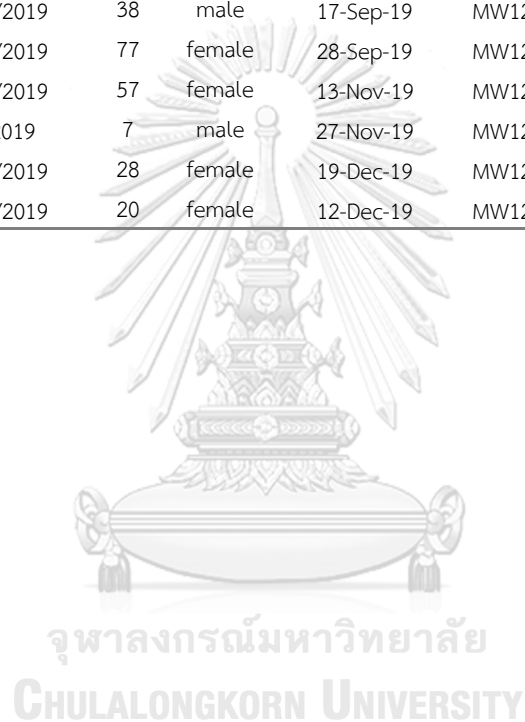


Table S10. *Influenza A(H3N2) virus strains sequenced in this study.*

Strains	Collection-date (DD-MM-YYYY)	Location	Age(yr)	Sex	Accession numbers (HA gene)
A/Thailand/CU-A2137/2016	7-Jan-2016	Khon Kaen	87	Male	MF673231
A/Thailand/CU-A2144/2016	7-Jan-2016	Khon Kaen	63	Female	MF673232
A/Thailand/CU-A2160/2016	7-Jan-2016	Khon Kaen	45	Female	MF673233
A/Thailand/CU-B14944/2016	1-Feb-2016	Bangkok	25	Female	MF673234
A/Thailand/CU-B15149/2016	15-Feb-2016	Bangkok	12	Female	MF673235
A/Thailand/CU-B15317/2016	23-Feb-2016	Bangkok	54	Female	MF673236
A/Thailand/CU-B15712/2016	15-Mar-2016	Bangkok	18	Male	MF673237
A/Thailand/CU-B15894/2016	25-Mar-2016	Bangkok	70	Female	MF673238
A/Thailand/CU-B16161/2016	7-Apr-2016	Bangkok	53	Female	MF673239
A/Thailand/CU-C6513/2016	21-Apr-2016	Khon Kaen	7	Female	MF673240
A/Thailand/CU-A2407/2016	18-May-2016	Khon Kaen	80	Male	MF673241
A/Thailand/CU-B16712/2016	16-Jun-2016	Bangkok	53	Male	MF673242
A/Thailand/CU-B16720/2016	20-Jun-2016	Bangkok	16	Male	MF673243
A/Thailand/CU-B16825/2016	5-Jul-2016	Bangkok	57	Female	MF673244
A/Thailand/CU-B16949/2016	9-Jul-2016	Bangkok	70	Female	MF673245
A/Thailand/CU-B17008/2016	21-Jul-2016	Bangkok	35	Male	MF673246
A/Thailand/CU-B17183/2016	25-Jul-2016	Bangkok	33	Female	MF673247
A/Thailand/CU-H3742/2016	28-Jul-2016	Bangkok	4	Female	MF673248
A/Thailand/CU-B17430/2016	9-Aug-2016	Bangkok	50	Male	MF673249
A/Thailand/CU-B17573/2016	10-Aug-2016	Bangkok	102	Female	MF673250
A/Thailand/CU-B17583/2016	11-Aug-2016	Bangkok	28	Female	MF673251
A/Thailand/CU-B18031/2016	2-Sep-2016	Bangkok	38	Female	MF673252
A/Thailand/CU-B18041/2016	3-Sep-2016	Bangkok	28	Female	MF673253
A/Thailand/CU-B18053/2016	5-Sep-2016	Bangkok	59	Female	MF673254
A/Thailand/CU-B18308/2016	12-Sep-2016	Bangkok	13	Male	MF673255
A/Thailand/CU-B18515/2016	19-Sep-2016	Bangkok	4	Female	MF673256
A/Thailand/CU-H3756/2016	13-Sep-2016	Bangkok	66	Female	MF673257
A/Thailand/CU-H3763/2016	26-Sep-2016	Bangkok	13	Male	MF673258
A/Thailand/CU-B18950/2016	4-Oct-2016	Bangkok	81	Female	MF673259
A/Thailand/CU-B19094/2016	7-Oct-2016	Bangkok	51	Male	MF673260
A/Thailand/CU-B19263/2016	15-Oct-2016	Bangkok	4	Male	MF673261
A/Thailand/CU-B19401/2016	19-Oct-2016	Bangkok	50	Female	MF673262
A/Thailand/CU-B19835/2016	10-Nov-2016	Bangkok	52	Male	MF673263
A/Thailand/CU-B19855/2016	12-Nov-2016	Bangkok	1	Female	MF673264
A/Thailand/CU-B19865/2016	15-Nov-2016	Bangkok	60	Female	MF673265
A/Thailand/CU-B20273/2016	3-Dec-2016	Bangkok	10	Female	MF673266
A/Thailand/CU-B20276/2016	6-Dec-2016	Bangkok	10	Male	MF673267
A/Thailand/CU-B20369/2016	9-Dec-2016	Bangkok	17	Female	MF673268
A/Thailand/CU-B20489/2016	20-Dec-2016	Bangkok	37	Male	MF673269
A/Thailand/CU-B20712/2017	5-Jan-2017	Bangkok	19	Female	MF673270

Strains	Collection-date (DD-MM-YYYY)	Location	Age(yr)	Sex	Accession numbers (HA gene)
A/Thailand/CU-B20791/2017	14-Jan-2017	Bangkok	39	Male	MF673271
A/Thailand/CU-B20852/2017	18-Jan-2017	Bangkok	11	Female	MF673272
A/Thailand/CU-B20929/2017	26-Jan-2017	Bangkok	64	Female	MF673273
A/Thailand/CU-B20992/2017	4-Feb-2017	Bangkok	8	Male	MF673274
A/Thailand/CU-C7086/2017	1-Feb-2017	Khon Kaen	1	Female	MF673275
A/Thailand/CU-H3780/2017	7-Feb-2017	Bangkok	9	Male	MF673276
A/Thailand/CU-B21369/2017	1-Mar-2017	Bangkok	31	Female	MF673277
A/Thailand/CU-B21378/2017	4-Mar-2017	Bangkok	5	Female	MF673278
A/Thailand/CU-B21451/2017	5-Mar-2017	Bangkok	72	Male	MF673279
A/Thailand/CU-B21458/2017	11-Mar-2017	Bangkok	1	Male	MF673280
A/Thailand/CU-B21690/2017	6-Apr-2017	Bangkok	29	Male	MF673281
A/Thailand/CU-B21722/2017	12-Apr-2017	Bangkok	38	Male	MF673282
A/Thailand/CU-B21760/2017	19-Apr-2017	Bangkok	54	Female	MF673283
A/Thailand/CU-CN148/2017	26-Apr-2017	Khon Kaen	1	Male	MF673284
A/Thailand/CU-B21873/2017	15-May-2017	Bangkok	52	Female	MF673285
A/Thailand/CU-CN209/2017	30-May-2017	Khon Kaen	27	Male	MF673286
A/Thailand/CU-CN220/2017	30-May-2017	Khon Kaen	7	Female	MF673287
A/Thailand/CU-E372/2017	30-May-2017	Khon Kaen	69	Female	MF673288
A/Thailand/CU-E379/2017	30-May-2017	Khon Kaen	12	Male	MF673289
A/Thailand/CU-B21988/2017	1-Jun-2017	Bangkok	5	Male	MF673290
A/Thailand/CU-E386/2017	22-Jun-2017	Khon Kaen	29	Male	MF673291
A/Thailand/CU-E396/2017	22-Jun-2017	Khon Kaen	34	Female	MF673292

Table S11. Accession numbers in GenBank and GISAID of HA influenza A(H3N2) and gene sequences used for phylogenetic tree analysis.

Name	Accession Numbers			
A/H3N2 reference and vaccine strains	EPI545333	EPI467994	EPI513286	EPI630781
	EPI577972	EPI460558	EPI1015612	EPI641435
	EPI547993	EPI814528	EPI326139	EPI831633
	EPI574644	EPI769485	EPI346607	EPI831759
	EPI984070	EPI426061	EPI1026711	EPI699750
	EPI551882	EPI746057	EPI550842	EPI831876
A/H3N2-TH strains (2016)	EPI919303	EPI813825	EPI925087	EPI836924
	EPI919249	EPI813865	EPI925071	EPI919402
	EPI919405	EPI813857	EPI825071	EPI925111
	EPI919411	EPI925047		
Name	Accession Numbers			
A/H3N2-TH strains (2017)	EPI1044759	EPI1058585	EPI1058593	EPI1058213
	EPI1045321	EPI1058173	EPI1058221	EPI1058165
	EPI1058561	EPI1044762	EPI1058523	EPI1044765
	EPI1058569	EPI1058157	EPI1058553	
A/H3N2-Canada strains (2016-17)	EPI953884	EPI953827	EPI953856	EPI1033751
	EPI953911	EPI953908	EPI953698	
A/H3N2-Greece strains (2016-17)	EPI884614	EPI901680		
A/H3N2-Denmark strains (2016-17)	EPI879358	EPI879380	EPI879349	
A/H3N2-Israel strains (2016-17)	EPI942316	EPI942315		
A/H3N2-London strains (2016-17)	From (198).			

Table S12. Positive selected sites on coding sequences of HA among influenza A(H3N2) circulating in Thailand between January 2016 and June 2017.

Codon	SLAC		FEL		MEME	
	dN/dS	p-value	dN/dS	p-value	ω^+	p-value
131					>100	0.001
142			56.21	0.07		
144					>100	0.036
171			52	0.06	>100	0.089
261			46.76	0.07	>100	0.095
406			41.34	0.08		
416					>100	0.074

dN/dS or ω is the ratio of non-synonymous to synonymous substitutions.

p-value from the SLAC, FEL, and MEME results for positive selection sites.

The statistically significant values are shown in bold.

Table S13. Calculated vaccine efficacy using $P_{epitope}$ model and number of mutations in dominant epitope of influenza A(H3N2) circulating in Thailand during January, 2016 to June, 2017.

Vaccine strain	Year	Dominant epitope	No. mutation	No. of strain	$P_{epitope}$	vaccine efficacy(%)
A/Hong Kong/4801/2014	2016 (n=53)	A	1	30	0.053	72.34
			2	4	0.105	44.68
		B	1	2	0.048	74.97
			1	2	0.037	80.54
		D	1	13	0.024	87.18
			3	1	0.073	61.55
		E	1	1	0.046	76.11
	Mean				0.049	74.17
A/Hong Kong/4801/2014	2017 (n=38)	A	1	7	0.053	72.34
			2	21	0.105	44.68
			3	2	0.158	17.02
		B	2	1	0.095	49.94
			3	1	0.143	24.92
		E	1	1	0.046	76.11
			2	2	0.091	52.22
		3	3	0.136	28.34	
	Mean				0.099	47.87

Table S14. Accession numbers of HA sequences of circulating influenza A(H1N1)pdm09, A(H3N2) and B virus strains in this study.

Influenza A(H1N1)pdm09

Accession No.	Sequence ID	Accession No.	Sequence ID
MT803149	A/Thailand/CU-B28541/2018	MT803194	A/Thailand/CU-B33041/2019
MT803150	A/Thailand/CU-B28297/2018	MT803195	A/Thailand/CU-B33058/2019
MT803151	A/Thailand/CU-B25494/2017	MT803196	A/Thailand/CU-B32333/2019
MT803152	A/Thailand/CU-B24689/2017	MT803197	A/Thailand/CU-B33247/2019
MT803153	A/Thailand/CU-B23453/2017	MT803198	A/Thailand/CU-B32110/2019
MT803154	A/Thailand/CU-B23241/2017	MT803199	A/Thailand/CU-B31995/2019
MT803155	A/Thailand/CU-B22888/2017	MT803200	A/Thailand/CU-B31366/2019
MT803156	A/Thailand/CU-B25506/2017	MT803201	A/Thailand/CU-B27932/2018
MT803157	A/Thailand/CU-B31088/2019	MT803202	A/Thailand/CU-B28803/2018
MT803158	A/Thailand/CU-B28420/2018	MT803203	A/Thailand/CU-B26903/2018
MT803159	A/Thailand/CU-E1099/2018	MT803204	A/Thailand/CU-B27534/2018
MT803160	A/Thailand/CU-B36824/2020	MT803205	A/Thailand/CU-B29642/2018
MT803161	A/Thailand/CU-B37035/2020	MT803206	A/Thailand/CU-H3896/2018
MT803162	A/Thailand/CU-B36559/2020	MT803207	A/Thailand/CU-B29280/2018
MT803163	A/Thailand/CU-B36313/2020	MT803208	A/Thailand/CU-B28162/2018
MT803164	A/Thailand/CU-B36543/2020	MT803209	A/Thailand/CU-B25276/2017
MT803165	A/Thailand/CU-B37406/2020	MT803210	A/Thailand/CU-B26079/2017
MT803166	A/Thailand/CU-B33254/2019	MT803211	A/Thailand/CU-B26815/2018
MT803167	A/Thailand/CU-B36101/2020	MT803212	A/Thailand/CU-B26827/2018
MT803168	A/Thailand/CU-B33657/2019	MT803213	A/Thailand/CU-B27179/2018
MT803169	A/Thailand/CU-B33961/2019	MT803214	A/Thailand/CU-B29765/2018
MT803170	A/Thailand/CU-B32495/2019	MT803215	A/Thailand/CU-B29061/2018

Influenza A(H1N1)pdm09 (continued)

Accession No.	Sequence ID	Accession No.	Sequence ID
MT803171	A/Thailand/CU-B33264/2019	MT803216	A/Thailand/CU-E995/2018
MT803172	A/Thailand/CU-B35405/2019	MT803217	A/Thailand/CU-B29290/2018
MT803173	A/Thailand/CU-B34831/2019	MT803218	A/Thailand/CU-B27420/2018
MT803174	A/Thailand/CU-B34351/2019	MT803219	A/Thailand/CU-A3166/2018
MT803175	A/Thailand/CU-B35002/2019	MT803220	A/Thailand/CU-B25124/2017
MT803176	A/Thailand/CU-B34081/2019	MT803221	A/Thailand/CU-B30149/2018
MT803177	A/Thailand/CU-B34082/2019	MT803222	A/Thailand/CU-B30542/2018
MT803178	A/Thailand/CU-B35519/2019	MT803223	A/Thailand/CU-B30621/2018
MT803179	A/Thailand/CU-B36840/2020	MT803224	A/Thailand/CU-B30112/2018
MT803180	A/Thailand/CU-B35253/2019	MT803225	A/Thailand/CU-B27943/2018
MT803181	A/Thailand/CU-B33609/2019	MT803226	A/Thailand/CU-B27082/2018
MT803182	A/Thailand/CU-B33269/2019	MT803227	A/Thailand/CU-B27898/2018
MT803183	A/Thailand/CU-B35326/2019	MT803228	A/Thailand/CU-B24386/2017
MT803184	A/Thailand/CU-B34836/2019	MT803229	A/Thailand/CU-H3898/2018
MT803185	A/Thailand/CU-B35599/2019	MT803230	A/Thailand/CU-B28019/2018
MT803186	A/Thailand/CU-B33692/2019	MT803231	A/Thailand/CU-B27073/2018
MT803187	A/Thailand/CU-B33972/2019	MT803232	A/Thailand/CU-B22514/2017
MT803188	A/Thailand/CU-B33649/2019	MT803233	A/Thailand/CU-B23198/2017
MT803189	A/Thailand/CU-B33583/2019	MT803234	A/Thailand/CU-B25092/2017
MT803190	A/Thailand/CU-B33616/2019	MT803235	A/Thailand/CU-B22532/2017
MT803191	A/Thailand/CU-B32938/2019	MT803236	A/Thailand/CU-B27410/2018
MT803192	A/Thailand/CU-B33699/2019	MT803237	A/Thailand/CU-B27490/2018
MT803193	A/Thailand/CU-B31081/2019	MT803238	A/Thailand/CU-B24083/2017

Influenza A(H3N2) virus

Accession No.	Sequence ID	Accession No.	Sequence ID
MT803239	A/Thailand/CU-B36536/2020	MT803284	A/Thailand/CU-B24398/2017
MT803240	A/Thailand/CU-B36023/2020	MT803285	A/Thailand/CU-B27414/2018
MT803241	A/Thailand/CU-B36542/2020	MT803286	A/Thailand/CU-B25961/2017
MT803242	A/Thailand/CU-B35602/2019	MT803287	A/Thailand/CU-B31991/2019
MT803243	A/Thailand/CU-CN846/2019	MT803288	A/Thailand/CU-B25464/2017
MT803244	A/Thailand/CU-E1482/2019	MT803289	A/Thailand/CU-B33398/2019
MT803245	A/Thailand/CU-E1426/2019	MT803290	A/Thailand/CU-B33996/2019
MT803246	A/Thailand/CU-E1421/2019	MT803291	A/Thailand/CU-B34006/2019
MT803247	A/Thailand/CU-E1422/2019	MT803292	A/Thailand/CU-B31893/2019
MT803248	A/Thailand/CU-B36095/2020	MT803293	A/Thailand/CU-B26867/2017
MT803249	A/Thailand/CU-B32225/2019	MT803294	A/Thailand/CU-B26053/2017
MT803250	A/Thailand/CU-B36392/2020	MT803295	A/Thailand/CU-B26815/2018
MT803251	A/Thailand/CU-B37010/2020	MT803296	A/Thailand/CU-B27086/2018
MT803252	A/Thailand/CU-B36805/2020	MT803297	A/Thailand/CU-B27083/2018
MT803253	A/Thailand/CU-B37058/2020	MT803298	A/Thailand/CU-B23250/2017
MT803254	A/Thailand/CU-B34078/2019	MT803299	A/Thailand/CU-B23240/2017
MT803255	A/Thailand/CU-B33013/2019	MT803300	A/Thailand/CU-B25287/2017
MT803256	A/Thailand/CU-B31078/2018	MT803301	A/Thailand/CU-B26075/2017
MT803257	A/Thailand/CU-B34085/2019	MT803302	A/Thailand/CU-B25502/2017
MT803258	A/Thailand/CU-B34928/2019	MT803303	A/Thailand/CU-B23448/2017
MT803259	A/Thailand/CU-B34789/2019	MT803304	A/Thailand/CU-B23053/2017
MT803260	A/Thailand/CU-B36553/2020	MT803305	A/Thailand/CU-B26734/2017
MT803261	A/Thailand/CU-B31931/2019	MT803306	A/Thailand/CU-B27093/2018
MT803262	A/Thailand/CU-B30914/2018	MT803307	A/Thailand/CU-B31119/2018
MT803263	A/Thailand/CU-B31216/2019	MT803308	A/Thailand/CU-B31714/2019
MT803264	A/Thailand/CU-B35270/2019	MT803309	A/Thailand/CU-B32345/2019
MT803265	A/Thailand/CU-B35397/2019	MT803310	A/Thailand/CU-B31593/2019
MT803266	A/Thailand/CU-B34340/2019	MT803311	A/Thailand/CU-B29296/2018
MT803267	A/Thailand/CU-B32786/2019	MT803312	A/Thailand/CU-B30632/2018
MT803268	A/Thailand/CU-B33665/2019	MT803313	A/Thailand/CU-B28861/2018
MT803269	A/Thailand/CU-H3957/2019	MT803314	A/Thailand/CU-E1501/2019
MT803270	A/Thailand/CU-B33676/2019	MT803315	A/Thailand/CU-H3900/2018
MT803271	A/Thailand/CU-B33912/2019	MT803316	A/Thailand/CU-B30672/2018
MT803272	A/Thailand/CU-B33421/2019	MT803317	A/Thailand/CU-H3914/2019

Influenza A(H3N2) virus (Continued)

Accession No.	Sequence ID	Accession No.	Sequence ID
MT803273	A/Thailand/CU-B33444/2019	MT803318	A/Thailand/CU-B28696/2018
MT803274	A/Thailand/CU-B33261/2019	MT803319	A/Thailand/CU-B28847/2018
MT803275	A/Thailand/CU-B33143/2019	MT803320	A/Thailand/CU-B27591/2018
MT803276	A/Thailand/CU-B33021/2019	MT803321	A/Thailand/CU-B30421/2018
MT803277	A/Thailand/CU-B33700/2019	MT803322	A/Thailand/CU-B27503/2018
MT803278	A/Thailand/CU-B33224/2019	MT803323	A/Thailand/CU-B28536/2018
MT803279	A/Thailand/CU-B34698/2019	MT803324	A/Thailand/CU-B24679/2017
MT803280	A/Thailand/CU-B25698/2017	MT803325	A/Thailand/CU-B22867/2017
MT803281	A/Thailand/CU-B36847/2020	MT803326	A/Thailand/CU-B22539/2017
MT803282	A/Thailand/CU-B24415/2017	MT803327	A/Thailand/CU-B22742/2017
MT803283	A/Thailand/CU-B23866/2017	MT803328	A/Thailand/CU-B22413/2017

Influenza B virus

Accession No.	Sequence ID	Accession No.	Sequence ID
MT803397	B/Thailand/CU-H3906/2018	MT803438	B/Thailand/CU-B31196/2019
MT803398	B/Thailand/CU-B30897/2018	MT803439	B/Thailand/CU-B33467/2019
MT803399	B/Thailand/CU-B29948/2018	MT803440	B/Thailand/CU-B34528/2019
MT803400	B/Thailand/CU-B31984/2019	MT803441	B/Thailand/CU-B35712/2019
MT803401	B/Thailand/CU-B36630/2020	MT803442	B/Thailand/CU-B23834/2017
MT803402	B/Thailand/CU-B36616/2020	MT803443	B/Thailand/CU-B22512/2017
MT803403	B/Thailand/CU-B35426/2019	MT803444	B/Thailand/CU-B22891/2017
MT803404	B/Thailand/CU-B35796/2019	MT803445	B/Thailand/CU-B25303/2017
MT803405	B/Thailand/CU-B34172/2019	MT803446	B/Thailand/CU-B26338/2017
MT803406	B/Thailand/CU-B34270/2019	MT803447	B/Thailand/CU-B24631/2017
MT803407	B/Thailand/CU-E1993/2019	MT803448	B/Thailand/CU-B22889/2017
MT803408	B/Thailand/CU-WC06/2020	MT803449	B/Thailand/CU-B24918/2017
MT803409	B/Thailand/CU-B35320/2019	MT803450	B/Thailand/CU-B26097/2017
MT803410	B/Thailand/CU-B34269/2019	MT803451	B/Thailand/CU-B27905/2018
MT803411	B/Thailand/CU-B32496/2019	MT803452	B/Thailand/CU-B27783/2018
MT803412	B/Thailand/CU-B33492/2019	MT803453	B/Thailand/CU-B27406/2018
MT803413	B/Thailand/CU-E1825/2019	MT803454	B/Thailand/CU-B27774/2018
MT803414	B/Thailand/CU-B33997/2019	MT803455	B/Thailand/CU-B27416/2018
MT803415	B/Thailand/CU-B34094/2019	MT803456	B/Thailand/CU-B30062/2018
MT803416	B/Thailand/CU-B31974/2019	MT803457	B/Thailand/CU-B27293/2018

Influenza B virus (Continued)

Accession No.	Sequence ID	Accession No.	Sequence ID
MT803417	B/Thailand/CU-B33686/2019	MT803458	B/Thailand/CU-B30789/2018
MT803418	B/Thailand/CU-B33757/2019	MT803459	B/Thailand/CU-E1271/2018
MT803419	B/Thailand/CU-B36464/2020	MT803460	B/Thailand/CU-B28017/2018
MT803420	B/Thailand/CU-B34980/2019	MT803461	B/Thailand/CU-B30027/2018
MT803421	B/Thailand/CU-B36369/2020	MT803462	B/Thailand/CU-B26467/2017
MT803422	B/Thailand/CU-B36643/2020	MT803463	B/Thailand/CU-B24367/2017
MT803423	B/Thailand/CU-B34381/2019	MT803464	B/Thailand/CU-B27287/2018
MT803424	B/Thailand/CU-E1983/2019	MT803465	B/Thailand/CU-B27301/2018
MT803425	B/Thailand/CU-B33344/2019	MT803466	B/Thailand/CU-B26732/2017
MT803426	B/Thailand/CU-H3948/2019	MT803467	B/Thailand/CU-B25966/2017
MT803427	B/Thailand/CU-B33517/2019	MT803468	B/Thailand/CU-B26096/2017
MT803428	B/Thailand/CU-B32499/2019	MT803469	B/Thailand/CU-B25697/2017
MT803429	B/Thailand/CU-B35644/2019	MT803470	B/Thailand/CU-B24933/2017
MT803430	B/Thailand/CU-B32772/2019	MT803471	B/Thailand/CU-B25090/2017
MT803431	B/Thailand/CU-B34486/2019	MT803472	B/Thailand/CU-B26809/2018
MT803432	B/Thailand/CU-B33518/2019	MT803473	B/Thailand/CU-B26647/2017
MT803433	B/Thailand/CU-B33235/2019	MT803474	B/Thailand/CU-B22737/2017
MT803434	B/Thailand/CU-B32961/2019	MT803475	B/Thailand/CU-B25670/2017
MT803435	B/Thailand/CU-B31194/2019	MT803476	B/Thailand/CU-B26746/2017
MT803436	B/Thailand/CU-H3934/2019	MT803477	B/Thailand/CU-B26977/2018
MT803437	B/Thailand/CU-B31046/2018		

Table S15. Positive selected sites on the HA coding sequences of influenza A and B viruses identified in Thailand between July 2017 and March 2020.

Subtype	Mixed Effects Model of Evolution				Fixed effects likelihood			
	dN/dS ^a	HA regions	position	β ⁺	P-value ^b	position	omega	P-value ^b
A/H1N1(pdm09)	0.194	HA1	120	3.77	0.05	120	Infinity	0.033
			233	1.76	0.09	233	Infinity	0.069
		HA2	213	3963.97	<0.001			
A/H3N2	0.228	HA1	57	12.75	0.06	57	Infinity	0.049
			131	1574.54	<0.001	135	Infinity	0.034
			135	7.49	0.05	193	Infinity	0.058
			144	53.68	0.07			
			193	3.21	0.08			
		HA2	18	1.94	0.09	18	Infinity	0.071
		200	3.25	0.06	200	Infinity	0.043	
		201	2.43	0.1	201	Infinity	0.075	
B/Victoria	0.657	HA1	76	168.8	0.03	238	Infinity	0.058
			80	150.56	0.05			
			87	96.25	<0.001			
			121	255.22	<0.001			
			126	32.72	0.04			
			128	247.49	0.04			
			136	37.85	0.04			
			154	154.28	0.03			
			160	44.19	0.03			
			238	1.8	0.08			
B/Yamagata	0.0525	HA1	227	3659.33	0.01	N/D	N/D	N/D

N/D defined as not detected.

^a dN/dS is the ratio of synonymous/non-synonymous substitutions.

^b P-value from the MEME and FEL result for a positive selection level.

β ⁺ is the non-synonymous substitution rate at a site for the positive/neutral evolution component.

Bold text denotes an amino-acid substitution associated with a clade/subclade transition.

APPENDIX B

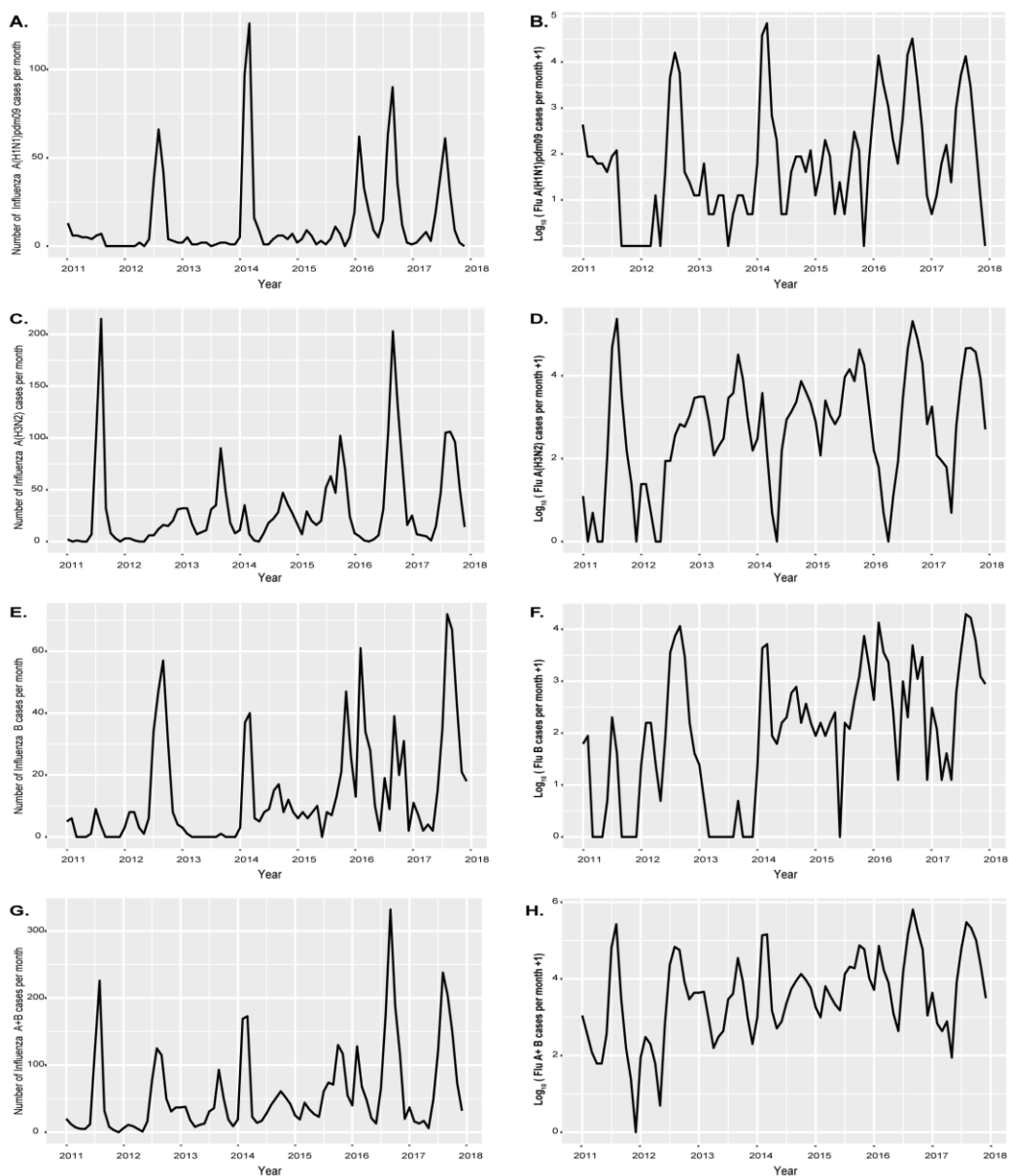


Figure S1. The original and \log_{10} transformed time series plots of the monthly confirmed influenza-positive cases. Original time series (left panels) and transformed time series (right panels) are shown for influenza A(H1N1)pdm09 (A and B), influenza A(H3N2) (C and D), influenza B (E and F), and all influenza viruses (G and H).

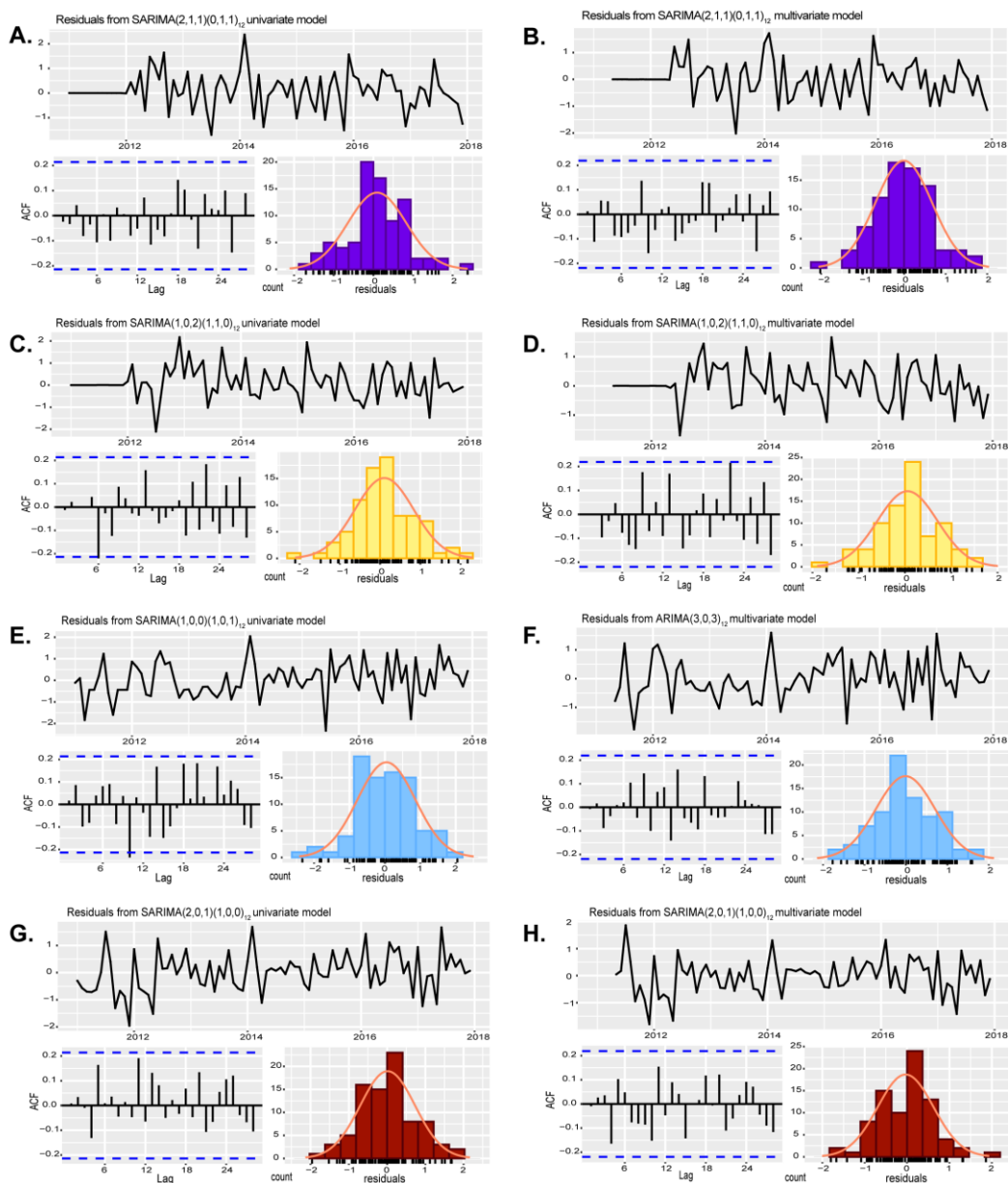


Figure S2. Plots of residuals of selected forecasting model, autocorrelation function (ACF), and the normal distribution of the residuals. The left column represents the residuals of univariate models, while the right column represents the residuals of multivariate models. (A and B) influenza A(H1N1)pdm09, (C and D) influenza A(H3N2), (E and F) influenza B, (G and H) all influenza viruses.

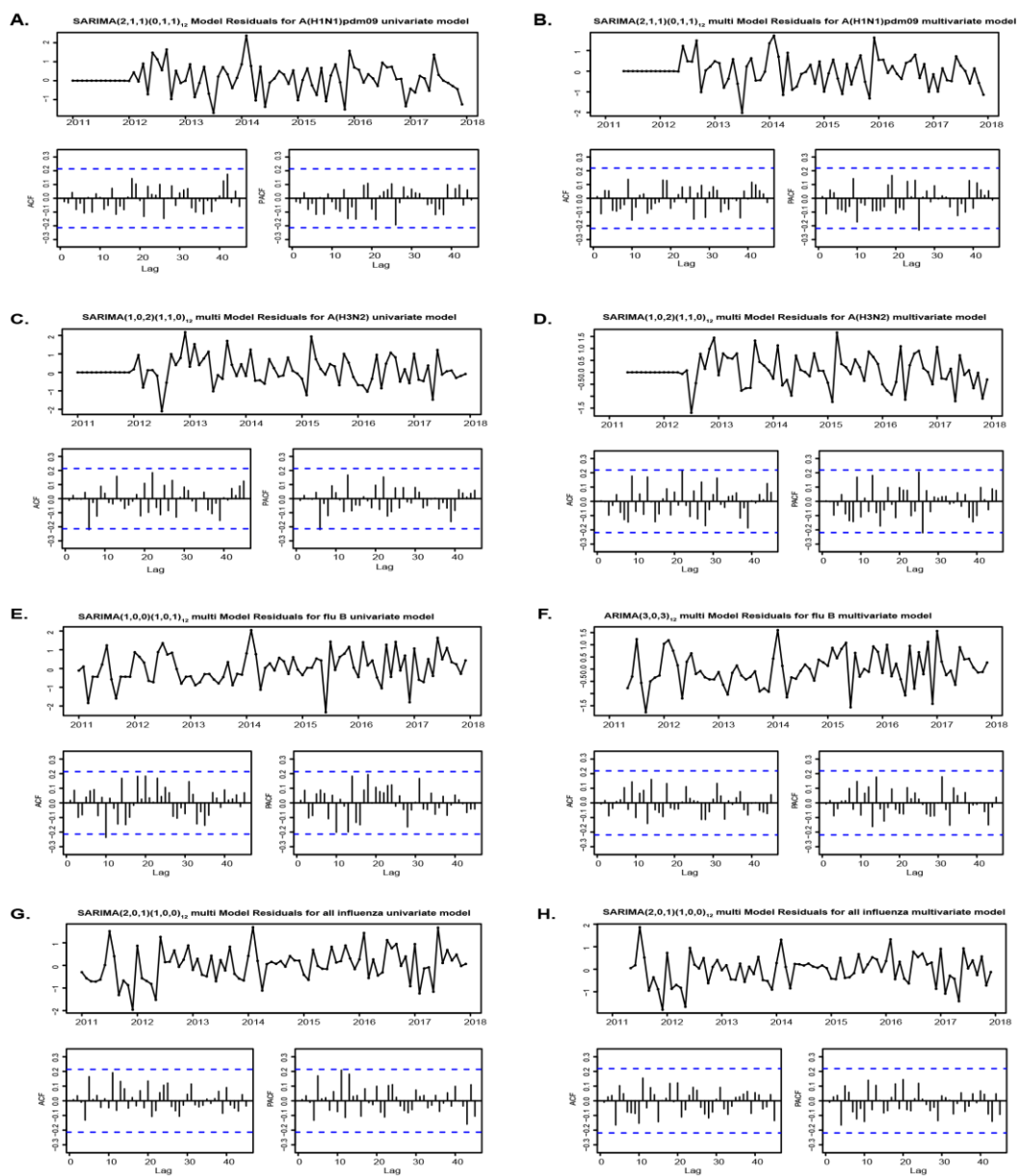


Figure S3. Plots of residuals of a selected forecasting model, autocorrelation function (ACF), and partial autocorrelation function (PACF). The left column represents the residuals of univariate models, while the right column represents the residuals of multivariate models. (A and B) Influenza A(H1N1)pdm09 virus. (C and D) Influenza A(H3N2) virus. (E and F) Influenza B virus. (G and H) All influenza viruses.

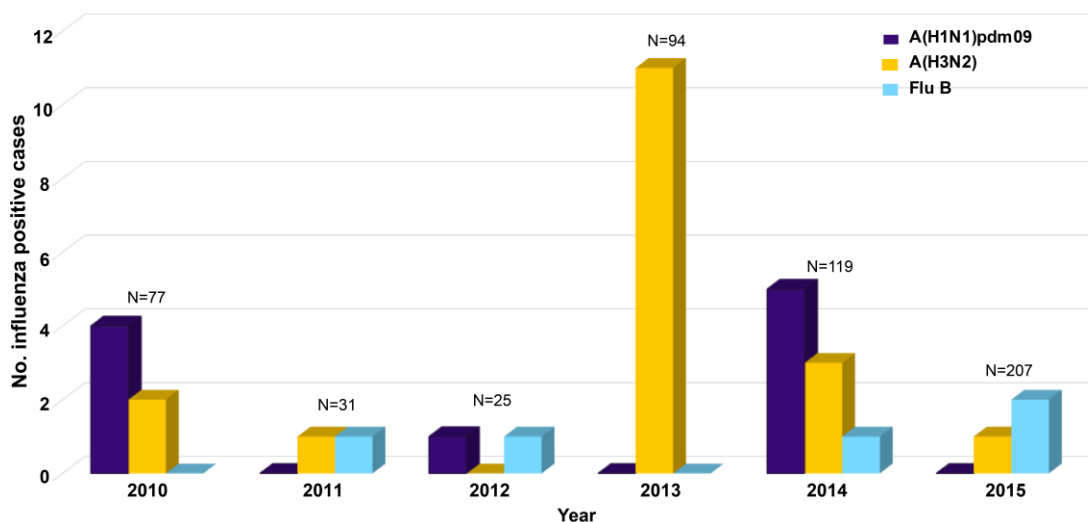


Figure S4. Distribution of influenza (sub)type among the elderly population that collected in Khon Kean, Thailand between 2010 and 2015.

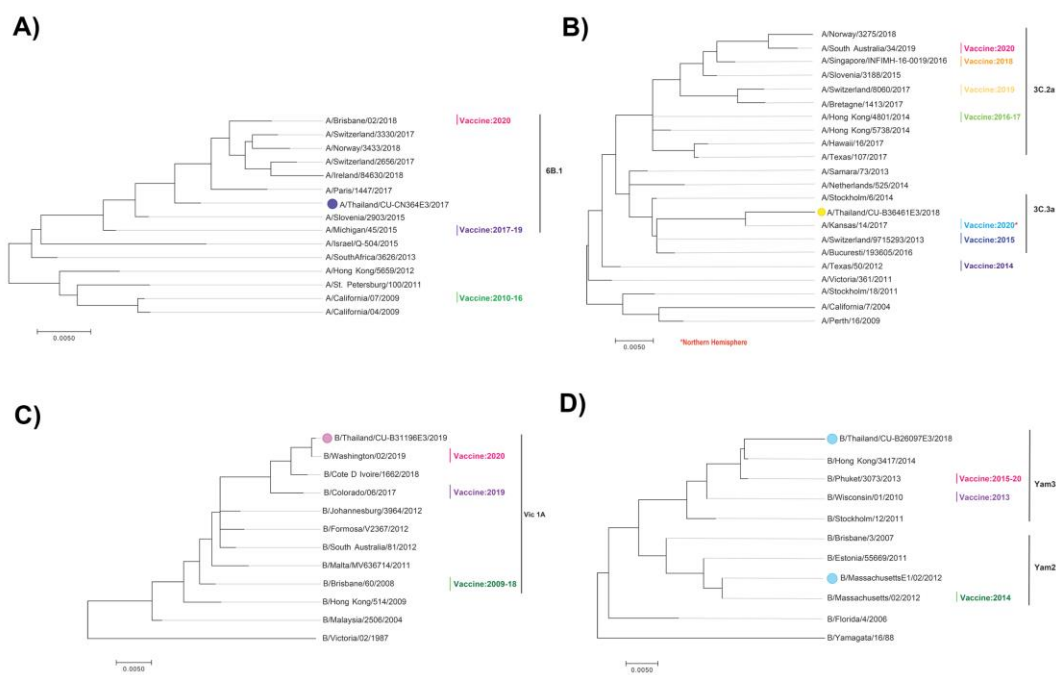


Figure S5. Schematic showed the phylogenetic trees of representative tested virus compared with the vaccine strain.

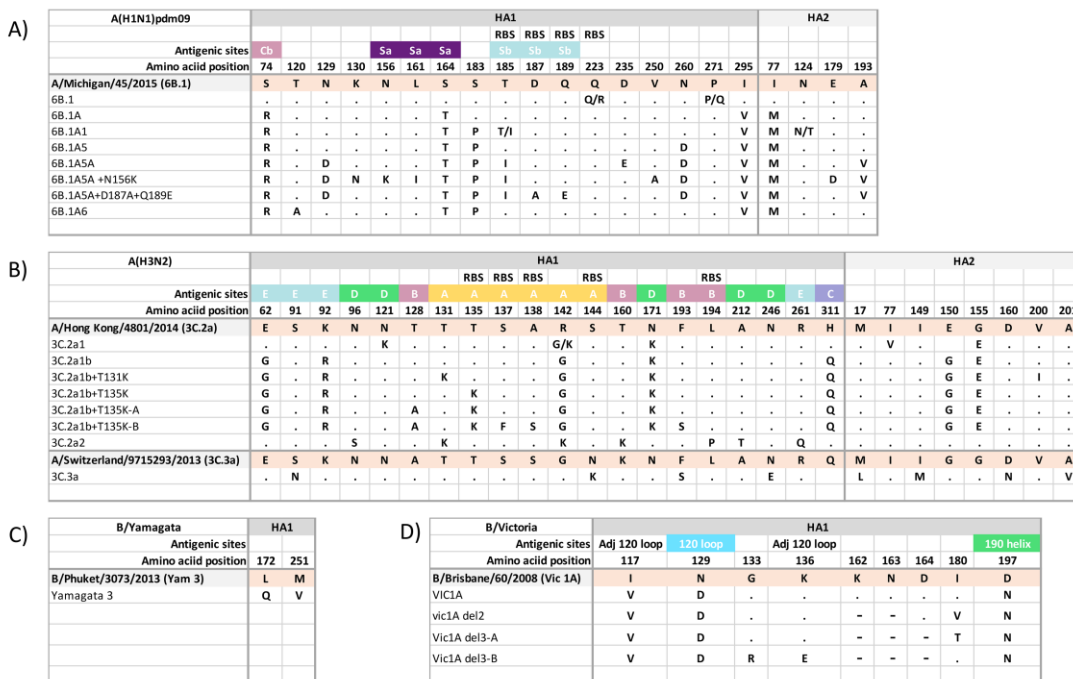


Figure S7. Sequences Alignment of individual clade/subclade was found in Thai strains. Residue changes between vaccine strains (shown in bold) and the subclade of Thai circulating strains were observed in A) A(H1N1)pdm09, B) A(H3N2), C) B/Yamagata-like lineage and D) B/Victoria-like lineage. Adj defined as AA position located adjacent antigenic site.

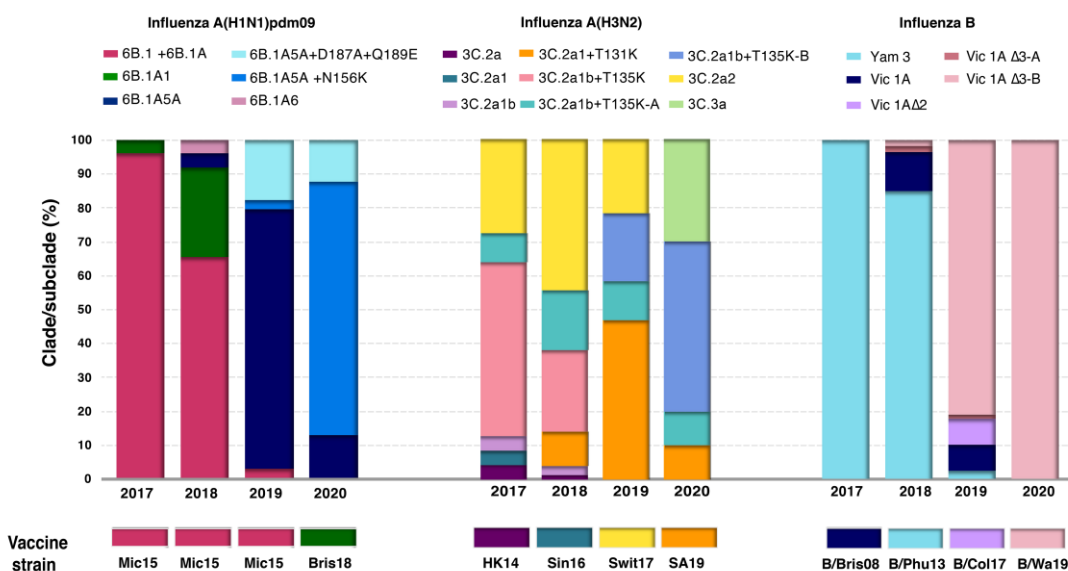


Figure S8. Distribution of clades/subclades of circulating influenza viruses in Thailand and their vaccine strain.

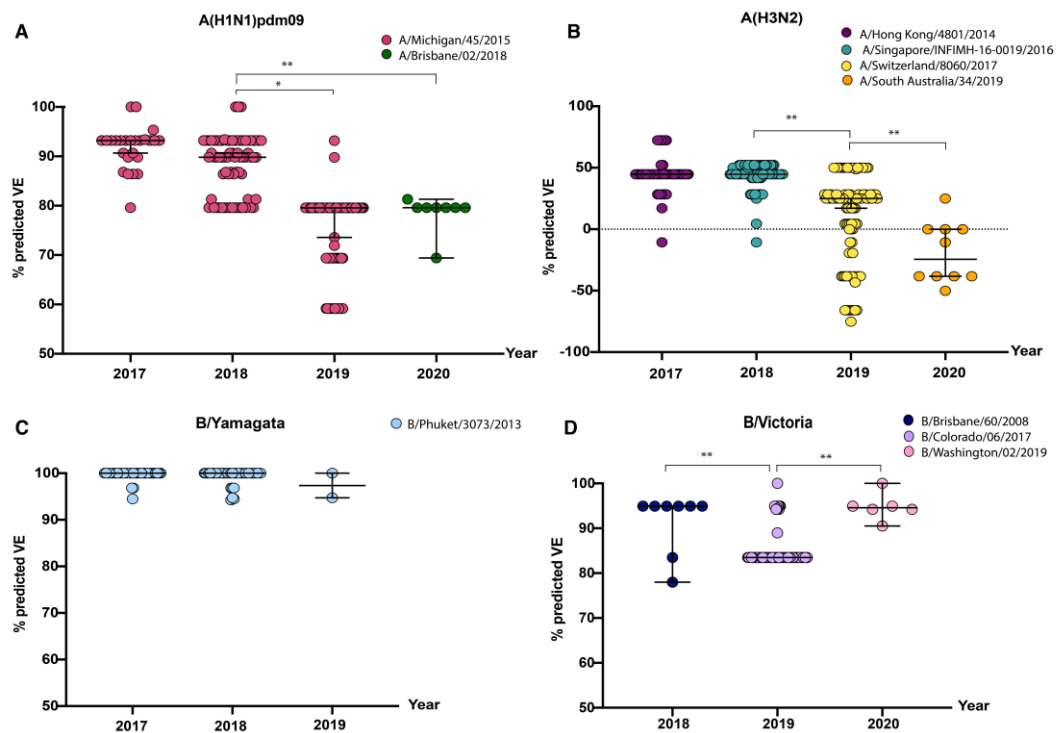


Figure S9. Comparison of the yearly predicted vaccine effectiveness between July 2017 and March 2020. Colored circles indicate the predicted VE for A(H1N1)pdm09 (A), A(H3N2) (B), B/Yamagata-like lineage (C), and B/Victoria-like lineage (D) compared with their vaccine. For each year, the middle bar represents the median value with 95%CI. P-values were calculated using one-way ANOVA. * $p < 0.01$, ** $p < 0.001$.

REFERENCES

1. Iuliano, A.D., et al., *Estimates of global seasonal influenza-associated respiratory mortality: a modelling study*. The Lancet, 2018. **391**(10127): p. 1285-1300.
2. CDC, *What You Should Know and Do this Flu Season If You Are 65 Years and Older [Online]*. Available from: <https://www.cdc.gov/flu/about/disease/65over.html>. Cited 2017, November 7.
3. Brankston, G., et al., *Transmission of influenza A in human beings*. The Lancet infectious diseases, 2007. **7**(4): p. 257-265.
4. Hutchinson, E.C., *Influenza virus*. Trends in microbiology, 2018. **26**(9): p. 809-810.
5. Centers for Disease Control and Prevention, N.C.f.l.a.R.D.N., *Flu Symptoms & Complications [Online]*. Available from: <https://www.cdc.gov/flu/consumer/symptoms.html>. Cited 2020, November 6.
6. Kwong, J.C., et al., *Acute myocardial infarction after laboratory-confirmed influenza infection*. New England Journal of Medicine, 2018. **378**(4): p. 345-353.
7. Sellers, S.A., et al., *The hidden burden of influenza: a review of the extra-pulmonary complications of influenza infection*. Influenza and other respiratory viruses, 2017. **11**(5): p. 372-393.
8. Webster, R.G., et al., *Evolution and ecology of influenza A viruses*. Microbiological reviews, 1992. **56**(1): p. 152-179.
9. Ohishi, K., et al., *Serological evidence of transmission of human influenza A and B viruses to Caspian seals (*Phoca caspica*)*. Microbiology and immunology, 2002. **46**(9): p. 639-644.
10. Matsuzaki, Y., et al., *Clinical features of influenza C virus infection in children*. The Journal of infectious diseases, 2006. **193**(9): p. 1229-1235.
11. Hause, B.M., et al., *Characterization of a novel influenza virus in cattle and swine: proposal for a new genus in the Orthomyxoviridae family*. MBio, 2014. **5**(2).

12. Ma, W., A. García-Sastre, and M. Schwemmler, *Expected and unexpected features of the newly discovered bat influenza A-like viruses*. PLoS Pathog, 2015. **11**(6): p. e1004819.
13. Tong, S., et al., *A distinct lineage of influenza A virus from bats*. Proceedings of the National Academy of Sciences, 2012. **109**(11): p. 4269-4274.
14. Tong, S., et al., *New world bats harbor diverse influenza A viruses*. PLoS pathogens, 2013. **9**(10): p. e1003657.
15. Palese, P. and M. Shaw, *Orthomyxoviridae: the viruses and their replication* In: *Knipe DM, Howley PM, eds. Fields' Virology [monograph on the internet]*. 2007, Philadelphia: Lippincott, Williams, & Wilkins.
16. Chen, J.-M., et al., *Exploration of the emergence of the Victoria lineage of influenza B virus*. Archives of virology, 2007. **152**(2): p. 415-422.
17. Shaw, M.W., et al., *Reappearance and global spread of variants of influenza B/Victoria/2/87 lineage viruses in the 2000–2001 and 2001–2002 seasons*. Virology, 2002. **303**(1): p. 1-8.
18. Horsfall, F.L., et al., *The Nomenclature of Influenza*. Lancet, 1940. **239**: p. 413-414.
19. Palese, P., T.M. Tumpey, and A. Garcia-Sastre, *What can we learn from reconstructing the extinct 1918 pandemic influenza virus?* Immunity, 2006. **24**(2): p. 121-124.
20. Nicoll, A., *A new decade, a new seasonal influenza: the Council of the European Union Recommendation on seasonal influenza vaccination*. Eurosurveillance, 2010. **15**(1): p. 19458.
21. Taubenberger, J.K. and J.C. Kash, *Influenza virus evolution, host adaptation, and pandemic formation*. Cell host & microbe, 2010. **7**(6): p. 440-451.
22. Russell, C.A., et al., *The global circulation of seasonal influenza A (H3N2) viruses*. Science, 2008. **320**(5874): p. 340-346.
23. Bahl, J., et al., *Temporally structured metapopulation dynamics and persistence of influenza A H3N2 virus in humans*. Proceedings of the National Academy of Sciences, 2011. **108**(48): p. 19359-19364.

24. Li, Y., et al., *Global patterns in monthly activity of influenza virus, respiratory syncytial virus, parainfluenza virus, and metapneumovirus: a systematic analysis*. *Lancet Glob Health*, 2019. **7**(8): p. e1031-e1045.
25. Jayasundara, K., et al., *Natural attack rate of influenza in unvaccinated children and adults: a meta-regression analysis*. *BMC infectious diseases*, 2014. **14**(1): p. 670.
26. Tokars, J.I., S.J. Olsen, and C. Reed, *Seasonal incidence of symptomatic influenza in the United States*. *Clinical Infectious Diseases*, 2018. **66**(10): p. 1511-1518.
27. CDC, *Burden of influenza [Online]*. Available from: <https://www.cdc.gov/flu/about/burden/index.html>. Cited 2020, October 5.
28. McCAULEY, J.W. and B. Mahy, *Structure and function of the influenza virus genome*. *Biochemical Journal*, 1983. **211**(2): p. 281.
29. Noda, T., et al., *Three-dimensional analysis of ribonucleoprotein complexes in influenza A virus*. *Nature communications*, 2012. **3**(1): p. 1-6.
30. Boulo, S., et al., *Nuclear traffic of influenza virus proteins and ribonucleoprotein complexes*. *Virus research*, 2007. **124**(1): p. 12-21.
31. Dou, D., et al., *Influenza A virus cell entry, replication, virion assembly and movement*. *Frontiers in immunology*, 2018. **9**: p. 1581.
32. Medina, R.A. and A. García-Sastre, *Influenza A viruses: new research developments*. *Nature Reviews Microbiology*, 2011. **9**(8): p. 590-603.
33. Ghanem, A., et al., *Peptide-mediated interference with influenza A virus polymerase*. *Journal of virology*, 2007. **81**(14): p. 7801-7804.
34. Subbarao, E.K. and B. Murphy, *A single amino acid in the PB2 gene of influenza A virus is a determinant of host range*. *Journal of virology*, 1993. **67**(4): p. 1761-1764.
35. Gabriel, G., A. Herwig, and H.-D. Klenk, *Interaction of polymerase subunit PB2 and NP with importin α 1 is a determinant of host range of influenza A virus*. *PLoS pathogens*, 2008. **4**(2): p. e11.

36. Reeves, A.B. and H.S. Ip, *H9N2 influenza A virus isolated from a greater white-fronted wild goose (Anser albifrons) in Alaska has a mutation in the PB2 gene, which is associated with pathogenicity in human pandemic 2009 H1N1*. Genome announcements, 2016. **4**(5): p. e00869-16.
37. Hayashi, T., et al., *Identification of influenza A virus PB2 residues involved in enhanced polymerase activity and virus growth in mammalian cells at low temperatures*. Journal of virology, 2015. **89**(15): p. 8042-8049.
38. Vasin, A., et al., *Molecular mechanisms enhancing the proteome of influenza A viruses: an overview of recently discovered proteins*. Virus research, 2014. **185**: p. 53-63.
39. Wise, H.M., et al., *Overlapping signals for translational regulation and packaging of influenza A virus segment 2*. Nucleic acids research, 2011. **39**(17): p. 7775-7790.
40. Reich, S., et al., *Structural insight into cap-snatching and RNA synthesis by influenza polymerase*. Nature, 2014. **516**(7531): p. 361-366.
41. Ozawa, M., et al., *Impact of amino acid mutations in PB2, PB1-F2, and NS1 on the replication and pathogenicity of pandemic (H1N1) 2009 influenza viruses*. Journal of virology, 2011. **85**(9): p. 4596-4601.
42. Yu, Z., et al., *A PB1 T296R substitution enhance polymerase activity and confer a virulent phenotype to a 2009 pandemic H1N1 influenza virus in mice*. Virology, 2015. **486**: p. 180-186.
43. Chen, Y., et al., *Probing nucleocytoplasmic transport by two-photon activation of PA-GFP*. Microscopy research and technique, 2006. **69**(3): p. 220-226.
44. Jagger, B., et al., *An overlapping protein-coding region in influenza A virus segment 3 modulates the host response*. Science, 2012. **337**(6091): p. 199-204.
45. Yuan, P., et al., *Crystal structure of an avian influenza polymerase PA N reveals an endonuclease active site*. Nature, 2009. **458**(7240): p. 909-913.
46. Matsuoka, Y., et al., *A comprehensive map of the influenza A virus replication cycle*. BMC systems biology, 2013. **7**(1): p. 97.

47. Chen, J., J.J. Skehel, and D.C. Wiley, *A polar octapeptide fused to the N-terminal fusion peptide solubilizes the influenza virus HA2 subunit ectodomain*. *Biochemistry*, 1998. **37**(39): p. 13643-13649.
48. Nelson, M.I. and E.C. Holmes, *The evolution of epidemic influenza*. *Nature reviews genetics*, 2007. **8**(3): p. 196-205.
49. Wu, W.W., Y.-H.B. Sun, and N. Panté, *Nuclear import of influenza A viral ribonucleoprotein complexes is mediated by two nuclear localization sequences on viral nucleoprotein*. *Virology journal*, 2007. **4**(1): p. 49.
50. Berkhoff, E., et al., *The loss of immunodominant epitopes affects interferon- γ production and lytic activity of the human influenza virus-specific cytotoxic T lymphocyte response in vitro*. *Clinical & Experimental Immunology*, 2007. **148**(2): p. 296-306.
51. Danzy, S., et al., *Mutations to PB2 and NP proteins of an avian influenza virus combine to confer efficient growth in primary human respiratory cells*. *Journal of virology*, 2014. **88**(22): p. 13436-13446.
52. Gamblin, S.J. and J.J. Skehel, *Influenza hemagglutinin and neuraminidase membrane glycoproteins*. *Journal of Biological Chemistry*, 2010. **285**(37): p. 28403-28409.
53. Palese, P. and J. Schulman, *Isolation and characterization of influenza virus recombinants with high and low neuraminidase activity: Use of 2-(3'-methoxyphenyl)-N-acetylneuraminic acid to identify cloned populations*. *Virology*, 1974. **57**(1): p. 227-237.
54. McKimm-Breschkin, J.L., *Influenza neuraminidase inhibitors: antiviral action and mechanisms of resistance*. *Influenza and other respiratory viruses*, 2013. **7**(s1): p. 25-36.
55. Wise, H.M., et al., *Identification of a novel splice variant form of the influenza A virus M2 ion channel with an antigenically distinct ectodomain*. *PLoS pathogens*, 2012. **8**(11): p. e1002998.

56. Astrahan, P., et al., *A novel method of resistance for influenza against a channel -blocking antiviral drug*. *Proteins: Structure, Function, and Bioinformatics*, 2004. **55**(2): p. 251-257.
57. Wang, X., et al., *Functional replacement of the carboxy-terminal two-thirds of the influenza A virus NS1 protein with short heterologous dimerization domains*. *Journal of virology*, 2002. **76**(24): p. 12951-12962.
58. Robb, N.C., et al., *NS2/NEP protein regulates transcription and replication of the influenza virus RNA genome*. *Journal of general virology*, 2009. **90**(6): p. 1398-1407.
59. Lamb, R.A., et al., *Mapping of the two overlapping genes for polypeptides NS1 and NS2 on RNA segment 8 of influenza virus genome*. *Proceedings of the National Academy of Sciences*, 1980. **77**(4): p. 1857-1861.
60. Wu, N.C., et al., *High-throughput identification of loss-of-function mutations for anti-interferon activity in the influenza A virus NS segment*. *Journal of virology*, 2014. **88**(17): p. 10157-10164.
61. Kim, I.-H., et al., *Effects of different NS genes of avian influenza viruses and amino acid changes on pathogenicity of recombinant A/Puerto Rico/8/34 viruses*. *Veterinary microbiology*, 2015. **175**(1): p. 17-25.
62. Clark, A.M., et al., *Functional Evolution of Influenza Virus NS1 Protein in Currently Circulating Human 2009 Pandemic H1N1 Viruses*. *Journal of Virology*, 2017. **91**(17): p. e00721-17.
63. Brown, E., et al., *Pattern of mutation in the genome of influenza A virus on adaptation to increased virulence in the mouse lung: identification of functional themes*. *Proceedings of the National Academy of Sciences*, 2001. **98**(12): p. 6883-6888.
64. Muramoto, Y., et al., *Identification of novel influenza A virus proteins translated from PA mRNA*. *Journal of virology*, 2013. **87**(5): p. 2455-2462.
65. de Graaf, M. and R.A. Fouchier, *Role of receptor binding specificity in influenza A virus transmission and pathogenesis*. *The EMBO journal*, 2014. **33**(8): p. 823-841.

66. Skehel, J.J. and D.C. Wiley, *Receptor binding and membrane fusion in virus entry: the influenza hemagglutinin*. Annual review of biochemistry, 2000. **69**(1): p. 531-569.
67. Hutchinson, E.C. and E. Fodor, *Transport of the influenza virus genome from nucleus to nucleus*. Viruses, 2013. **5**(10): p. 2424-2446.
68. S, P., *Chapter 23 - Family Orthomyxoviridae*. Viruses, 2017: p. 197-208.
69. Glezen, W.P., *Prevention and treatment of seasonal influenza*. New England Journal of Medicine, 2008. **359**(24): p. 2579-2585.
70. Gu, R.-X., L.A. Liu, and D.-Q. Wei, *Structural and energetic analysis of drug inhibition of the influenza A M2 proton channel*. Trends in pharmacological sciences, 2013. **34**(10): p. 571-580.
71. Moscona, A., *Neuraminidase inhibitors for influenza*. New England Journal of Medicine, 2005. **353**(13): p. 1363-1373.
72. WHO, *Antiviral Drugs Treatment for Influenza [Online]*. Available from: <https://www.cdc.gov/flu/professionals/antivirals/links.html>. Cited 2017, December 6.
73. Hayden, F.G., et al., *Baloxavir marboxil for uncomplicated influenza in adults and adolescents*. New England Journal of Medicine, 2018. **379**(10): p. 913-923.
74. Ison, M.G., et al., *Early treatment with baloxavir marboxil in high-risk adolescent and adult outpatients with uncomplicated influenza (CAPSTONE-2): a randomised, placebo-controlled, phase 3 trial*. The Lancet Infectious Diseases, 2020.
75. WHO, *WHO recommendations on the composition of influenza virus vaccines*. Available from: <http://www.who.int/influenza/vaccines/virus/recommendations/en/>. Cited 2019, January 20.
76. Prachayangprecha, S., et al., *Influenza activity in Thailand and occurrence in different climates*. SpringerPlus, 2015. **4**(1): p. 356.
77. Krammer, F. and P. Palese, *Advances in the development of influenza virus vaccines*. Nature reviews Drug discovery, 2015. **14**(3): p. 167-182.

78. Soema, P.C., et al., *Current and next generation influenza vaccines: formulation and production strategies*. European Journal of Pharmaceutics and Biopharmaceutics, 2015. **94**: p. 251-263.
79. Grohskopf, L.A., et al., *Prevention and control of seasonal influenza with vaccines: recommendations of the Advisory Committee on Immunization Practices—United States, 2020–21 influenza season*. MMWR Recommendations and Reports, 2020. **69**(8): p. 1.
80. CDC, *Who is at high risk for Flu complications [Online]*. Available from: <https://www.cdc.gov/flu/highrisk/index.html>. Cited 2020, November 6.
81. Simmerman, J.M., et al., *Influenza in Thailand: a case study for middle income countries*. Vaccine, 2004. **23**(2): p. 182-187.
82. Haq, K. and J.E. McElhaney, *Immunosenescence: influenza vaccination and the elderly*. Current opinion in immunology, 2014. **29**: p. 38-42.
83. Matsuzaki, Y., et al., *Epitope mapping of the hemagglutinin molecule of A(H1N1) pdm09 influenza virus by using monoclonal antibody escape mutants*. Journal of virology, 2014. **88**(21): p. 12364-12373.
84. Caton, A.J., et al., *The antigenic structure of the influenza virus A/PR/8/34 hemagglutinin (H1 subtype)*. 1982. **31**(2): p. 417-427.
85. Koel, B.F., et al., *Substitutions near the receptor binding site determine major antigenic change during influenza virus evolution*. Science, 2013. **342**(6161): p. 976-979.
86. Bush, R.M., et al., *Positive selection on the H3 hemagglutinin gene of human influenza virus A*. Molecular biology and evolution, 1999. **16**(11): p. 1457-1465.
87. Shih, A.C.-C., et al., *Simultaneous amino acid substitutions at antigenic sites drive influenza A hemagglutinin evolution*. Proceedings of the National Academy of Sciences, 2007. **104**(15): p. 6283-6288.
88. Wang, Q., et al., *Crystal structure of unliganded influenza B virus hemagglutinin*. Journal of virology, 2008. **82**(6): p. 3011-3020.
89. Wang, Q., et al., *Structural basis for receptor specificity of influenza B virus hemagglutinin*. Proceedings of the National Academy of Sciences, 2007. **104**(43): p. 16874-16879.

90. Chen, R. and E.C. Holmes, *Avian influenza virus exhibits rapid evolutionary dynamics*. *Molecular biology and evolution*, 2006. **23**(12): p. 2336-2341.
91. Carrat, F. and A. Flahault, *Influenza vaccine: the challenge of antigenic drift*. *Vaccine*, 2007. **25**(39-40): p. 6852-6862.
92. Tewawong, N., et al., *Evolution of the neuraminidase gene of seasonal influenza A and B viruses in Thailand between 2010 and 2015*. 2017. **12**(4).
93. Drummond, A.J., et al., *Bayesian phylogenetics with BEAUti and the BEAST 1.7*. *Molecular biology and evolution*, 2012. **29**(8): p. 1969-1973.
94. Mehle, A. and J.A. Doudna, *Adaptive strategies of the influenza virus polymerase for replication in humans*. *Proceedings of the National Academy of Sciences*, 2009. **106**(50): p. 21312-21316.
95. Trifonov, V., H. Khiabani, and R. Rabadan, *Geographic dependence, surveillance, and origins of the 2009 influenza A (H1N1) virus*. *New England journal of medicine*, 2009. **361**(2): p. 115-119.
96. Landolt, G.A. and C.W. Olsen, *Up to new tricks-a review of cross-species transmission of influenza A viruses*. *Animal Health Research Reviews*, 2007. **8**(1): p. 1.
97. Suarez, D.L., et al., *Recombination resulting in virulence shift in avian influenza outbreak, Chile*. *Emerging infectious diseases*, 2004. **10**(4): p. 693.
98. Troeger, C.E., et al., *Mortality, morbidity, and hospitalisations due to influenza lower respiratory tract infections, 2017: an analysis for the Global Burden of Disease Study 2017*. *Lancet Respir Med*, 2019. **7**(1): p. 69-89.
99. Kamigaki, T., et al., *Seasonality of Influenza and Respiratory Syncytial Viruses and the Effect of Climate Factors in Subtropical–Tropical Asia Using Influenza-Like Illness Surveillance Data, 2010–2012*. *PLoS One*, 2016. **11**(12): p. e0167712.
100. Lowen, A.C., et al., *Influenza virus transmission is dependent on relative humidity and temperature*. *PLoS Pathog*, 2007. **3**(10): p. e151.
101. Lowen, A.C., et al., *High temperature (30 C) blocks aerosol but not contact transmission of influenza virus*. *J Virol*, 2008. **82**(11): p. 5650-5652.
102. Lowen, A.C. and J.J.J.o.v. Steel, *Roles of humidity and temperature in shaping influenza seasonality*. *J Virol*, 2014. **88**(14): p. 7692-7695.

103. Mubareka, S., et al., *Transmission of influenza virus via aerosols and fomites in the guinea pig model*. 2009. **199**(6): p. 858-865.
104. Shiu, E.Y., N.H. Leung, and B.J.J.C.o.i.i.d. Cowling, *Controversy around airborne versus droplet transmission of respiratory viruses: implication for infection prevention*. 2019. **32**(4): p. 372-379.
105. Tamerius, J.D., et al., *Environmental predictors of seasonal influenza epidemics across temperate and tropical climates*. PLoS Pathog, 2013. **9**(3): p. e1003194.
106. Caini, S., et al., *Temporal patterns of influenza A and B in tropical and temperate countries: what are the lessons for influenza vaccination?* PLoS One, 2016. **11**(3): p. e0152310.
107. Newman, L.P., et al., *Global influenza seasonality to inform country-level vaccine programs: an analysis of WHO FluNet influenza surveillance data between 2011 and 2016*. PLoS One, 2018. **13**(2): p. e0193263.
108. Price, R.H.M., C. Graham, and S.J.S.r. Ramalingam, *Association between viral seasonality and meteorological factors*. Sci Rep, 2019. **9**(1): p. 929.
109. Pica, N. and N.M.J.C.o.i.v. Bouvier, *Environmental factors affecting the transmission of respiratory viruses*. Curr Opin Virol, 2012. **2**(1): p. 90-95.
110. N'gattia, A., et al., *Effects of climatological parameters in modeling and forecasting seasonal influenza transmission in Abidjan, Cote d'Ivoire*. BMC Public Health, 2016. **16**(1): p. 972.
111. Yang, W., et al., *Dynamics of influenza in tropical Africa: Temperature, humidity, and co-circulating (sub) types*. 2018. **12**(4): p. 446-456.
112. Soebiyanto, R.P., et al., *The role of temperature and humidity on seasonal influenza in tropical areas: Guatemala, El Salvador and Panama, 2008–2013*. PLoS One, 2014. **9**(6): p. e100659.
113. Dapat, C., et al., *Epidemiology of human influenza A and B viruses in Myanmar from 2005 to 2007*. 2009. **52**(6): p. 310-320.
114. Hirve, S., et al., *Influenza seasonality in the tropics and subtropics—when to vaccinate?* PLoS One, 2016. **11**(4): p. e0153003.

115. Horwood, P.F., et al., *Circulation and characterization of seasonal influenza viruses in Cambodia, 2012-2015*. 2019. **13**(5): p. 465-476.
116. Phommasack, B., et al., *Capacity building in response to pandemic influenza threats: Lao PDR case study*. 2012. **87**(6): p. 965-971.
117. Chittaganpitch, M., et al., *Influenza viruses in Thailand: 7 years of sentinel surveillance data, 2004-2010*. 2012. **6**(4): p. 276-283.
118. Adisasmito, W., et al., *Surveillance and characterisation of influenza viruses among patients with influenza-like illness in Bali, Indonesia, July 2010-June 2014*. 2019. **19**(1): p. 231.
119. Ang, L.W., et al., *Characterization of influenza activity based on virological surveillance of influenza-like illness in tropical Singapore, 2010-2014*. 2016. **88**(12): p. 2069-2077.
120. Suntronwong, N., et al., *Genetic and antigenic divergence in the influenza A (H3N2) virus circulating between 2016 and 2017 in Thailand*. PloS one, 2017. **12**(12): p. e0189511.
121. Thai, P.Q., et al., *Seasonality of absolute humidity explains seasonality of influenza-like illness in Vietnam*. 2015. **13**: p. 65-73.
122. Tang, J.W., et al., *Comparison of the incidence of influenza in relation to climate factors during 2000-2007 in five countries*. 2010. **82**(11): p. 1958-1965.
123. Chadsuthi, S., et al., *Modeling seasonal influenza transmission and its association with climate factors in Thailand using time-series and ARIMAX analyses*. Comput Math Methods Med, 2015. **2015**.
124. Wolfram Research, I., *Climate of Thailand; 2019*. Database: Wolframalpha [Online]. Available from : <https://www.wolframalpha.com/input/?i=climate+of+Thailand>. Cited 2019, May 10.
125. Tewawong, N., et al., *Molecular epidemiology and phylogenetic analyses of influenza B virus in Thailand during 2010 to 2014*. PloS one, 2015. **10**(1): p. e0116302.

126. Suwannakarn, K., et al., *Typing (A/B) and subtyping (H1/H3/H5) of influenza A viruses by multiplex real-time RT-PCR assays*. Journal of virological methods, 2008. **152**(1): p. 25-31.
127. Tay, E.L., et al., *Exploring a proposed WHO method to determine thresholds for seasonal influenza surveillance*. PLoS One, 2013. **8**(10): p. e77244.
128. Naumova, E.N. and I.B. MacNeill, *Seasonality assessment for biosurveillance systems*, in *Advances in Statistical Methods for the Health Sciences*. 2007, Springer. p. 437-450.
129. Naumova, E.N., et al., *Seasonality in six enterically transmitted diseases and ambient temperature*. Epidemiol Infect, 2007. **135**(2): p. 281-292.
130. Liu, L., et al., *Predicting the incidence of hand, foot and mouth disease in Sichuan province, China using the ARIMA model*. Epidemiol Infect, 2016. **144**(1): p. 144-151.
131. Brockwell, P.J. and R.A. Davis, *Introduction to time series and forecasting*. 2016: springer.
132. Ljung, G.M. and G.E.J.B. Box, *On a measure of lack of fit in time series models*. 1978. **65**(2): p. 297-303.
133. Hyndman, R.J. and G. Athanasopoulos, *Forecasting: principles and practice*. 2018: OTexts.
134. Wangdi, K., et al., *Development of temporal modelling for forecasting and prediction of malaria infections using time-series and ARIMAX analyses: a case study in endemic districts of Bhutan*. Malar J, 2010. **9**(1): p. 251.
135. Hyndman, R.J. and Y. Khandakar, *Automatic time series for forecasting: the forecast package for R*. Vol. 27. 2007; 27(1), 1–22: Journal of Statistical Software.
136. Saha, S., et al., *Influenza seasonality and vaccination timing in tropical and subtropical areas of southern and south-eastern Asia*. Bull World Health Organ, 2014. **92**: p. 318-330.
137. Bloom-Feshbach, K., et al., *Latitudinal variations in seasonal activity of influenza and respiratory syncytial virus (RSV): a global comparative review*. PLoS One, 2013. **8**(2): p. e54445.

138. Deyle, E.R., et al., *Global environmental drivers of influenza*. 2016. **113**(46): p. 13081-13086.
139. Schaffer, F., M. Soergel, and D.J.A.o.v. Straube, *Survival of airborne influenza virus: effects of propagating host, relative humidity, and composition of spray fluids*. 1976. **51**(4): p. 263-273.
140. Kieffer, A., et al., *2009 A (H1N1) seroconversion rates and risk factors among the general population in Vientiane Capital, Laos*. 2013. **8**(4): p. e61909.
141. Saha, S., et al., *Divergent seasonal patterns of influenza types A and B across latitude gradient in Tropical Asia*. *Influenza Other Respir Viruses*, 2016. **10**(3): p. 176-184.
142. Paynter, S.J.E. and *Infection*, *Humidity and respiratory virus transmission in tropical and temperate settings*. 2015. **143**(6): p. 1110-1118.
143. Tamerius, J., et al., *Influenza transmission during extreme indoor conditions in a low-resource tropical setting*. *Int J Biometeorol*, 2017. **61**(4): p. 613-622.
144. WHO, *Up to 650 000 people die of respiratory diseases linked to seasonal flu each year [Online]*. Available from: <https://www.who.int/news-room/detail/14-12-2017-up-to-650-000-people-die-of-respiratory-diseases-linked-to-seasonal-flu-each-year>, 2017. Cited 2020, September 25.
145. CDC, *Vaccine Benefits [Online]*. Available from: <https://www.cdc.gov/flu/prevent/vaccine-benefits.html>. Cited 2020, September 25.
146. MMWR, *Prevention and Control of Seasonal Influenza with Vaccines: Recommendations of the Advisory Committee on Immunization Practices — United States, 2020-21 Influenza Season*. 2020. **69**(RR-8): p. 1-24.
147. Thompson, W.W., et al., *Influenza-associated hospitalizations in the United States*. *Jama*, 2004. **292**(11): p. 1333-1340.
148. Beyer, W.E., et al., *Cochrane re-arranged: support for policies to vaccinate elderly people against influenza*. *Vaccine*, 2013. **31**(50): p. 6030-6033.
149. Demicheli, V., et al., *Vaccines for preventing influenza in the elderly*. *Cochrane Database of Systematic Reviews*, 2018(2).

150. Knodel, J., et al., *The situation of Thailand's older population: An update based on the 2014 Survey of Older Persons in Thailand*. 2015.
151. Wilson, S.E., et al., *The role of seroepidemiology in the comprehensive surveillance of vaccine-preventable diseases*. *Cmaj*, 2012. **184**(1): p. E70-E76.
152. Muangchana, C., P. Thamapornpilas, and O. Karnkawinpong, *Immunization policy development in Thailand: the role of the Advisory Committee on Immunization Practice*. *Vaccine*, 2010. **28**: p. A104-A109.
153. Surichan, S., et al., *Development of influenza vaccine production capacity by the Government Pharmaceutical Organization of Thailand: addressing the threat of an influenza pandemic*. *Vaccine*, 2011. **29**: p. A29-A33.
154. Chokephaibulkit, K., et al., *Seroprevalence of 2009 H1N1 virus infection and self-reported infection control practices among healthcare professionals following the first outbreak in bangkok, Thailand*. *Influenza and other respiratory viruses*, 2013. **7**(3): p. 359-363.
155. Organization, W.H., *WHO Global Influenza Surveillance Network. Manual for the laboratory diagnosis and virological surveillance of influenza*. World Health Organization, 2011. **252**.
156. Cox, R., *Correlates of protection to influenza virus, where do we go from here? Human vaccines & immunotherapeutics*, 2013. **9**(2): p. 405-408.
157. Tsang, T.K., et al., *Association between antibody titers and protection against influenza virus infection within households*. *The Journal of infectious diseases*, 2014. **210**(5): p. 684-692.
158. Stephenson, I., et al., *Reproducibility of serologic assays for influenza virus A (H5N1)*. *Emerging infectious diseases*, 2009. **15**(8): p. 1250.
159. Tewawong, N., et al., *Genetic and antigenic characterization of hemagglutinin of influenza A/H3N2 virus from the 2015 season in Thailand*. 2016. **52**(5): p. 711-715.
160. Tewawong, N., et al., *Evidence for influenza B virus lineage shifts and reassortants circulating in Thailand in 2014–2016*. *Infection, Genetics and Evolution*, 2017. **47**: p. 35-40.

161. Nobusawa, E. and K. Sato, *Comparison of the mutation rates of human influenza A and B viruses*. Journal of virology, 2006. **80**(7): p. 3675-3678.
162. Severson, J.J., et al., *Persistence of influenza vaccine-induced antibody in lung transplant patients and healthy individuals beyond the season*. Human vaccines & immunotherapeutics, 2012. **8**(12): p. 1850-1853.
163. Mantel, C., et al., *Seasonal influenza vaccination in middle-income countries: Assessment of immunization practices in Belarus, Morocco, and Thailand*. Vaccine, 2020. **38**(2): p. 212-219.
164. Owusu, J.T., et al., *Seasonal influenza vaccine coverage among high-risk populations in Thailand, 2010–2012*. Vaccine, 2015. **33**(5): p. 742-747.
165. Cohen, S.A., Chui, K. K. & Naumova, E. N., *Influenza vaccination in young children reduces influenza-associated hospitalizations in older adults, 2002–2006*. J. Am. Geriatr. Soc, 2011. **59**: p. 327–332.
166. Omoto, S., et al., *Characterization of influenza virus variants induced by treatment with the endonuclease inhibitor baloxavir marboxil*. Scientific reports, 2018. **8**(1): p. 1-15.
167. Tewawong, N., et al., *Lineage-specific detection of influenza B virus using real-time polymerase chain reaction with melting curve analysis*. Archives of virology, 2016. **161**(6): p. 1425-1435.
168. Makkoch, J., et al., *Whole genome characterization, phylogenetic and genome signature analysis of human pandemic H1N1 virus in Thailand, 2009–2012*. PLoS One, 2012. **7**(12): p. e51275.
169. Lindstrom, S.E., et al., *Comparative analysis of evolutionary mechanisms of the hemagglutinin and three internal protein genes of influenza B virus: multiple cocirculating lineages and frequent reassortment of the NP, M, and NS genes*. Journal of virology, 1999. **73**(5): p. 4413-4426.
170. Virk, R.K., et al., *Divergent evolutionary trajectories of influenza B viruses underlie their contemporaneous epidemic activity*. 2020. **117**(1): p. 619-628.
171. Gorman, O.T., et al., *Evolution of influenza A virus PB2 genes: implications for evolution of the ribonucleoprotein complex and origin of human influenza A virus*. Journal of virology, 1990. **64**(10): p. 4893-4902.

172. Rambaut, A., et al., *The genomic and epidemiological dynamics of human influenza A virus*. Nature, 2008. **453**(7195): p. 615-619.
173. Nair, H., et al., *Global burden of respiratory infections due to seasonal influenza in young children: a systematic review and meta-analysis*. The Lancet, 2011. **378**(9807): p. 1917-1930.
174. Osterholm, M.T., et al., *Efficacy and effectiveness of influenza vaccines: a systematic review and meta-analysis*. The Lancet infectious diseases, 2012. **12**(1): p. 36-44.
175. Grohskopf, L., et al., *Prevention and Control of Seasonal Influenza with Vaccines*. MMWR Recomm Rep 2016, 2016. **65**(No. RR-5): p. 1-54.
176. Ndifon, W., N.S. Wingreen, and S.A. Levin, *Differential neutralization efficiency of hemagglutinin epitopes, antibody interference, and the design of influenza vaccines*. Proceedings of the National Academy of Sciences, 2009. **106**(21): p. 8701-8706.
177. Isin, B., P. Doruker, and I. Bahar, *Functional motions of influenza virus hemagglutinin: a structure-based analytical approach*. Biophysical journal, 2002. **82**(2): p. 569-581.
178. Nakajima, S., E. Nobusawa, and K. Nakajima, *Variation in response among individuals to antigenic sites on the HA protein of human influenza virus may be responsible for the emergence of drift strains in the human population*. Virology, 2000. **274**(1): p. 220-231.
179. Krystal, M., et al., *Evolution of influenza A and B viruses: conservation of structural features in the hemagglutinin genes*. Proceedings of the National Academy of Sciences, 1982. **79**(15): p. 4800-4804.
180. Skehel, J., et al., *A carbohydrate side chain on hemagglutinins of Hong Kong influenza viruses inhibits recognition by a monoclonal antibody*. Proceedings of the National Academy of Sciences, 1984. **81**(6): p. 1779-1783.
181. Webster, R. and W. Laver, *Determination of the number of nonoverlapping antigenic areas on Hong Kong (H3N2) influenza virus hemagglutinin with monoclonal antibodies and the selection of variants with potential epidemiological significance*. Virology, 1980. **104**(1): p. 139-148.

182. Wiley, D., I. Wilson, and J. Skehel, *Structural identification of the antibody-binding sites of Hong Kong influenza haemagglutinin and their involvement in antigenic variation*. *Nature*, 1981. **289**(5796): p. 373-378.
183. Huang, R.T., R. Rott, and H.-D. Klenk, *Influenza viruses cause hemolysis and fusion of cells*. *Virology*, 1981. **110**(1): p. 243-247.
184. Belongia, E.A., et al., *Variable influenza vaccine effectiveness by subtype: a systematic review and meta-analysis of test-negative design studies*. *The Lancet Infectious Diseases*, 2016. **16**(8): p. 942-951.
185. Bhatt, S., E.C. Holmes, and O.G. Pybus, *The genomic rate of molecular adaptation of the human influenza A virus*. *Molecular biology and evolution*, 2011. **28**(9): p. 2443-2451.
186. Tewawong, N., et al., *Assessing antigenic drift of seasonal influenza A (H3N2) and A (H1N1) pdm09 viruses*. *PloS one*, 2015. **10**(10): p. e0139958.
187. Schweiger, B., I. Zadow, and R. Heckler, *Antigenic drift and variability of influenza viruses*. *Medical microbiology and immunology*, 2002. **191**(3): p. 133-138.
188. Stray, S.J. and L.B. Pittman, *Subtype-and antigenic site-specific differences in biophysical influences on evolution of influenza virus hemagglutinin*. *Virology journal*, 2012. **9**(1): p. 91.
189. Berton, M.T., C.W. Naeve, and R.G. Webster, *Antigenic structure of the influenza B virus hemagglutinin: nucleotide sequence analysis of antigenic variants selected with monoclonal antibodies*. *Journal of virology*, 1984. **52**(3): p. 919-927.
190. *WHO information for molecular diagnosis of influenza virus - update. Revision May 2017*. Available from: http://www.who.int/influenza/gisrs_laboratory/molecular_diagnosis/en/. Cited **2017, September 12**.
191. Hoffmann, E., et al., *Universal primer set for the full-length amplification of all influenza A viruses*. *Archives of virology*, 2001. **146**(12): p. 2275-2289.
192. Tamura, K., et al., *MEGA6: molecular evolutionary genetics analysis version 6.0*. *Molecular biology and evolution*, 2013. **30**(12): p. 2725-2729.

193. Gupta R and Jung E and Brunak S, *Prediction of N-glycosylation sites in human proteins*. Database: NtNGlyc 1.0[Internet] . Available from: <http://www.cbs.dtu.dk/services/NetNGlyc/>, 2004.
194. Delpont, W., et al., *Datamonkey 2010: a suite of phylogenetic analysis tools for evolutionary biology*. Bioinformatics, 2010. **26**(19): p. 2455-2457.
195. Humphrey, W., A. Dalke, and K. Schulten, *VMD: visual molecular dynamics*. Journal of molecular graphics, 1996. **14**(1): p. 33-38.
196. Gupta, V., D.J. Earl, and M.W. Deem, *Quantifying influenza vaccine efficacy and antigenic distance*. Vaccine, 2006. **24**(18): p. 3881-3888.
197. Glatman-Freedman, A., et al., *Genetic divergence of Influenza A (H3N2) amino acid substitutions mark the beginning of the 2016–2017 winter season in Israel*. Journal of Clinical Virology, 2017.
198. Harvala, H., et al., *Emergence of a novel subclade of influenza A (H3N2) virus in London, December 2016 to January 2017*. Eurosurveillance, 2017. **22**(8).
199. Yang, H., et al., *Structure and receptor binding preferences of recombinant human A (H3N2) virus hemagglutinins*. Virology, 2015. **477**: p. 18-31.
200. Ferguson, N.M., A.P. Galvani, and R.M. Bush, *Ecological and immunological determinants of influenza evolution*. Nature, 2003. **422**(6930): p. 428.
201. Vigerust, D.J. and V.L. Shepherd, *Virus glycosylation: role in virulence and immune interactions*. Trends in microbiology, 2007. **15**(5): p. 211-218.
202. Hergens, M.-P., et al., *Mid-season real-time estimates of seasonal influenza vaccine effectiveness in persons 65 years and older in register-based surveillance, Stockholm County, Sweden, and Finland, January 2017*. Eurosurveillance, 2017. **22**(8).
203. Skowronski, D.M., et al., *Interim estimates of 2016/17 vaccine effectiveness against influenza A (H3N2), Canada, January 2017*. Eurosurveillance, 2017. **22**(6).
204. Castilla, J., et al., *Combined effectiveness of prior and current season influenza vaccination in northern Spain: 2016/17 mid-season analysis*. Eurosurveillance, 2017. **22**(7).

205. Kissling, E. and M. Rindy, *Early 2016/17 vaccine effectiveness estimates against influenza A (H3N2): I-MOVE multicentre case control studies at primary care and hospital levels in Europe*. *Eurosurveillance*, 2017. **22**(7).
206. Melidou, A., et al., *Influenza A (H3N2) genetic variants in vaccinated patients in northern Greece*. *Journal of Clinical Virology*, 2017.
207. Wang, X., et al., *Global burden of respiratory infections associated with seasonal influenza in children under 5 years in 2018: a systematic review and modelling study*. 2020. **8**(4): p. e497-e510.
208. Cox, N.J. and K.J.A.r.o.m. Subbarao, *Global epidemiology of influenza: past and present*. 2000. **51**(1): p. 407-421.
209. Tricco, A.C., et al., *Comparing influenza vaccine efficacy against mismatched and matched strains: a systematic review and meta-analysis*. 2013. **11**(1): p. 153.
210. Skowronski, D.M., et al., *Serial vaccination and the antigenic distance hypothesis: effects on influenza vaccine effectiveness during A (H3N2) epidemics in Canada, 2010–2011 to 2014–2015*. 2017. **215**(7): p. 1059-1099.
211. Skowronski, D.M., et al., *A perfect storm: impact of genomic variation and serial vaccination on low influenza vaccine effectiveness during the 2014–2015 season*. 2016. **63**(1): p. 21-32.
212. Broberg, E., et al., *Predominance of influenza A (H1N1) pdm09 virus genetic subclade 6B. 1 and influenza B/Victoria lineage viruses at the start of the 2015/16 influenza season in Europe*. 2016. **21**(13): p. 30184.
213. *World Health Organization Collaborating Centre for Reference and Research on Influenza. Report prepared for the WHO annual consultation on the composition of influenza vaccine for the Northern Hemisphere 2019-2020*; 2019. Available from: https://www.crick.ac.uk/sites/default/files/2019-04/Crick%20VCMFeb2019%20report_toPost.pdf.

214. Wilson, I.A., J.J. Skehel, and D.J.N. Wiley, *Structure of the haemagglutinin membrane glycoprotein of influenza virus at 3 Å resolution*. 1981. **289**(5796): p. 366-373.
215. Wu, N.C. and I.A.J.J.o.m.b. Wilson, *A perspective on the structural and functional constraints for immune evasion: insights from influenza virus*. 2017. **429**(17): p. 2694-2709.
216. Doud, M.B., S.E. Hensley, and J.D.J.P.p. Bloom, *Complete mapping of viral escape from neutralizing antibodies*. 2017. **13**(3): p. e1006271.
217. Alonso, W.J., et al., *A global map of hemispheric influenza vaccine recommendations based on local patterns of viral circulation*. 2015. **5**(1): p. 1-6.
218. Epperson, S., et al., *Update: influenza activity—United States and worldwide, May 19–September 28, 2019, and composition of the 2020 southern hemisphere influenza vaccine*. 2019. **68**(40): p. 880.
219. Richard, S.A., C. Viboud, and M.A.J.V. Miller, *Evaluation of Southern Hemisphere influenza vaccine recommendations*. 2010. **28**(15): p. 2693-2699.
220. Kumar, S., et al., *MEGA X: molecular evolutionary genetics analysis across computing platforms*. 2018. **35**(6): p. 1547-1549.
221. Deem, M.W., K.J.P.E. Pan, Design, and Selection, *The epitope regions of H1-subtype influenza A, with application to vaccine efficacy*. 2009. **22**(9): p. 543-546.
222. Pan, Y. and M.W. Deem, *Prediction of influenza B vaccine effectiveness from sequence data*. *Vaccine*, 2016. **34**(38): p. 4610-4617.
223. *World Health Organization Collaborating Centre for Reference and Research on Influenza. Report prepared for the WHO annual consultation on the composition of influenza vaccines for the Southern Hemisphere 2020; 2019. Available from: https://www.crick.ac.uk/sites/default/files/2019-10/CrickSH2019VCMreport_v2.pdf*
224. Melidou, A., et al., *Predominance of influenza virus A (H3N2) 3C. 2a1b and A (H1N1) pdm09 6B. 1A5A genetic subclades in the WHO European Region, 2018–2019*. 2020.

225. Skowronski, D.M., et al., *Interim estimates of 2018/19 vaccine effectiveness against influenza A (H1N1) pdm09, Canada, January 2019*. 2019. **24**(4): p. 1900055.
226. Dawood, F.S., et al., *Interim estimates of 2019–20 seasonal influenza vaccine effectiveness—United States, February 2020*. 2020. **69**(7): p. 177.
227. Rose, A., et al., *Interim 2019/20 influenza vaccine effectiveness: six European studies, September 2019 to January 2020*. 2020. **25**(10): p. 2000153.
228. Kirkpatrick, E., et al., *The influenza virus hemagglutinin head evolves faster than the stalk domain*. 2018. **8**(1): p. 1-14.
229. Zost, S.J., et al., *Contemporary H3N2 influenza viruses have a glycosylation site that alters binding of antibodies elicited by egg-adapted vaccine strains*. Proceedings of the National Academy of Sciences, 2017. **114**(47): p. 12578-12583.
230. Kissling, E., et al., *Interim 2018/19 influenza vaccine effectiveness: six European studies, October 2018 to January 2019*. 2019. **24**(8).
231. Flannery, B., et al., *Enhanced genetic characterization of influenza A (H3N2) viruses and vaccine effectiveness by genetic group, 2014–2015*. 2016. **214**(7): p. 1010-1019.
232. Barr, I.G., et al., *Cell culture-derived influenza vaccines in the severe 2017–2018 epidemic season: a step towards improved influenza vaccine effectiveness*. 2018. **3**(1): p. 1-5.
233. Kuo, S.-C., et al., *Collateral Benefit of COVID-19 Control Measures on Influenza Activity, Taiwan*. 2020. **26**(8).
234. Soo, R.J., et al., *Decreased Influenza Incidence under COVID-19 Control Measures, Singapore*. 2020. **26**(8).
235. Suntronwong, N., et al., *Impact of COVID-19 public health interventions on influenza incidence in Thailand*. 2020: p. 1-3.
236. Krammer, F., et al., *Influenza (Primer)*. Nature Reviews: Disease Primers, 2018.
237. Krammer, F., et al., *NAction! How can neuraminidase-based immunity contribute to better influenza virus vaccines?* MBio, 2018. **9**(2).

238. Marcelin, G., M.R. Sandbulte, and R.J. Webby, *Contribution of antibody production against neuraminidase to the protection afforded by influenza vaccines*. *Reviews in medical virology*, 2012. **22**(4): p. 267-279.
239. Couch, R.B., et al., *Randomized comparative study of the serum antihemagglutinin and antineuraminidase antibody responses to six licensed trivalent influenza vaccines*. *Vaccine*, 2012. **31**(1): p. 190-195.
240. Kilbourne, E.D., *Comparative efficacy of neuraminidase-specific and conventional influenza virus vaccines in induction of antibody to neuraminidase in humans*. *Journal of infectious diseases*, 1976. **134**(4): p. 384-394.
241. Krammer, F., *The human antibody response to influenza A virus infection and vaccination*. *Nature Reviews Immunology*, 2019. **19**(6): p. 383-397.
242. Laguio-Vila, M.R., et al. *Comparison of serum hemagglutinin and neuraminidase inhibition antibodies after 2010–2011 trivalent inactivated influenza vaccination in healthcare personnel*. in *Open forum infectious diseases*. 2015. Oxford University Press.
243. Powers, D.C., E.D. Kilbourne, and B.E. Johansson, *Neuraminidase-specific antibody responses to inactivated influenza virus vaccine in young and elderly adults*. *Clinical and diagnostic laboratory immunology*, 1996. **3**(5): p. 511-516.
244. Sandbulte, M.R., et al., *Discordant antigenic drift of neuraminidase and hemagglutinin in H1N1 and H3N2 influenza viruses*. *Proceedings of the National Academy of Sciences*, 2011. **108**(51): p. 20748-20753.
245. Chen, Y.-Q., et al., *Influenza infection in humans induces broadly cross-reactive and protective neuraminidase-reactive antibodies*. *Cell*, 2018. **173**(2): p. 417-429. e10.
246. Job, E., et al., *Broadened immunity against influenza by vaccination with computationally designed influenza virus N1 neuraminidase constructs*. *NPJ vaccines*, 2018. **3**(1): p. 1-11.
247. Liu, W.-C., et al., *Cross-reactive neuraminidase-inhibiting antibodies elicited by immunization with recombinant neuraminidase proteins of H5N1 and*

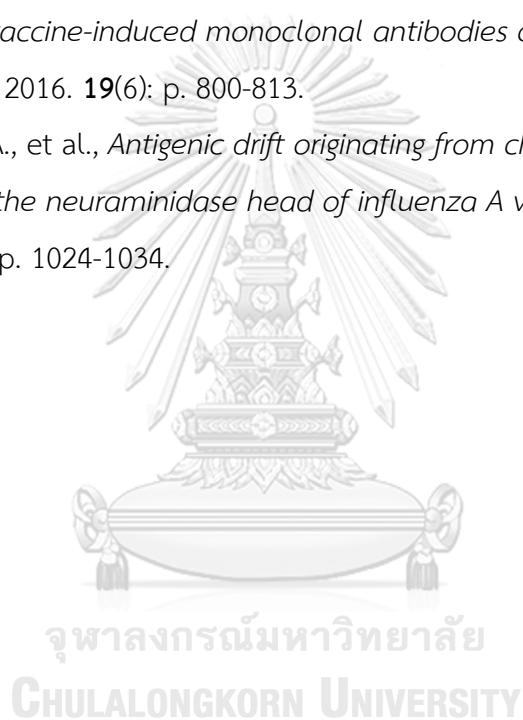
- pandemic H1N1 influenza A viruses*. Journal of virology, 2015. **89**(14): p. 7224-7234.
248. Sandbulte, M.R., et al., *Cross-reactive neuraminidase antibodies afford partial protection against H5N1 in mice and are present in unexposed humans*. PLoS Med, 2007. **4**(2): p. e59.
249. Wohlbold, T.J., et al., *Vaccination with adjuvanted recombinant neuraminidase induces broad heterologous, but not heterosubtypic, cross-protection against influenza virus infection in mice*. MBio, 2015. **6**(2).
250. Clements, M., et al., *Serum and nasal wash antibodies associated with resistance to experimental challenge with influenza A wild-type virus*. Journal of clinical microbiology, 1986. **24**(1): p. 157-160.
251. Couch, R.B., et al., *Induction of partial immunity to influenza by a neuraminidase-specific vaccine*. Journal of Infectious Diseases, 1974. **129**(4): p. 411-420.
252. Memoli, M.J., et al., *Evaluation of antihemagglutinin and antineuraminidase antibodies as correlates of protection in an influenza A/H1N1 virus healthy human challenge model*. MBio, 2016. **7**(2).
253. Murphy, B.R., J.A. Kasel, and R.M. Chanock, *Association of serum anti-neuraminidase antibody with resistance to influenza in man*. New England Journal of Medicine, 1972. **286**(25): p. 1329-1332.
254. Couch, R.B., et al., *Antibody correlates and predictors of immunity to naturally occurring influenza in humans and the importance of antibody to the neuraminidase*. The Journal of infectious diseases, 2013. **207**(6): p. 974-981.
255. Monto, A.S., et al., *Antibody to influenza virus neuraminidase: an independent correlate of protection*. The Journal of infectious diseases, 2015. **212**(8): p. 1191-1199.
256. Gao, J., et al., *Antigenic drift of the influenza A (H1N1) pdm09 virus neuraminidase results in reduced effectiveness of A/California/7/2009 (H1N1pdm09)-specific antibodies*. Mbio, 2019. **10**(2).
257. Kilbourne, E.D., B.E. Johansson, and B. Grajower, *Independent and disparate evolution in nature of influenza A virus hemagglutinin and neuraminidase*

- glycoproteins*. Proceedings of the National Academy of Sciences, 1990. **87**(2): p. 786-790.
258. Easterbrook, J.D., et al., *Protection against a lethal H5N1 influenza challenge by intranasal immunization with virus-like particles containing 2009 pandemic H1N1 neuraminidase in mice*. Virology, 2012. **432**(1): p. 39-44.
259. Halbherr, S.J., et al., *Biological and protective properties of immune sera directed to the influenza virus neuraminidase*. Journal of virology, 2015. **89**(3): p. 1550-1563.
260. Mendez-Legaza, J.M., R. Ortiz de Lejarazu, and I. Sanz, *Heterotypic neuraminidase antibodies against different A (H1N1) strains are elicited after seasonal influenza vaccination*. Vaccines, 2019. **7**(1): p. 30.
261. Wan, H., et al., *Molecular basis for broad neuraminidase immunity: conserved epitopes in seasonal and pandemic H1N1 as well as H5N1 influenza viruses*. Journal of virology, 2013. **87**(16): p. 9290-9300.
262. Kilbourne, E.D., et al., *Purified influenza A virus N2 neuraminidase vaccine is immunogenic and non-toxic in humans*. Vaccine, 1995. **13**(18): p. 1799-1803.
263. Schulman, J.L., *The role of antineuraminidase antibody in immunity to influenza virus infection*. Bulletin of the World Health Organization, 1969. **41**(3-4-5): p. 647.
264. Piepenbrink, M.S., et al., *Broad and protective influenza B virus neuraminidase antibodies in humans after vaccination and their clonal persistence as plasma cells*. MBio, 2019. **10**(2).
265. Wohlbold, T.J., et al., *Broadly protective murine monoclonal antibodies against influenza B virus target highly conserved neuraminidase epitopes*. Nature microbiology, 2017. **2**(10): p. 1415-1424.
266. Johansson, B. and E. Kilbourne, *Dissociation of influenza virus hemagglutinin and neuraminidase eliminates their intravirionic antigenic competition*. Journal of virology, 1993. **67**(10): p. 5721-5723.
267. Johansson, B., et al., *Immunologic response to influenza virus neuraminidase is influenced by prior experience with the associated viral hemagglutinin. II*.

- Sequential infection of mice simulates human experience.* The Journal of Immunology, 1987. **139**(6): p. 2010-2014.
268. Johansson, B.E., T.M. Moran, and E.D. Kilbourne, *Antigen-presenting B cells and helper T cells cooperatively mediate intravirionic antigenic competition between influenza A virus surface glycoproteins.* Proceedings of the National Academy of Sciences, 1987. **84**(19): p. 6869-6873.
269. Wohlbold, T.J. and F. Krammer, *In the shadow of hemagglutinin: a growing interest in influenza viral neuraminidase and its role as a vaccine antigen.* Viruses, 2014. **6**(6): p. 2465-2494.
270. Johansson, B., D. Bucher, and E. Kilbourne, *Purified influenza virus hemagglutinin and neuraminidase are equivalent in stimulation of antibody response but induce contrasting types of immunity to infection.* Journal of virology, 1989. **63**(3): p. 1239-1246.
271. Johansson, B.E., J.T. Matthews, and E.D. Kilbourne, *Supplementation of conventional influenza A vaccine with purified viral neuraminidase results in a balanced and broadened immune response.* Vaccine, 1998. **16**(9-10): p. 1009-1015.
272. Wohlbold, T.J., A. Hirsh, and F. Krammer, *An H10N8 influenza virus vaccine strain and mouse challenge model based on the human isolate A/Jiangxi-Donghu/346/13.* Vaccine, 2015. **33**(9): p. 1102-1106.
273. Meseda, C.A., et al., *Immunogenicity and protection against influenza H7N3 in mice by modified vaccinia virus Ankara vectors expressing influenza virus hemagglutinin or neuraminidase.* Scientific reports, 2018. **8**(1): p. 1-14.
274. Li, J., et al., *Emergence and genetic variation of neuraminidase stalk deletions in avian influenza viruses.* PloS one, 2011. **6**(2): p. e14722.
275. Castrucci, M.R. and Y. Kawaoka, *Biologic importance of neuraminidase stalk length in influenza A virus.* Journal of virology, 1993. **67**(2): p. 759-764.
276. Guangxiang, L., C. Jeffrey, and P. Palese, *Alterations of the stalk of the influenza virus neuraminidase: deletions and insertions.* Virus research, 1993. **29**(2): p. 141-153.

277. Kosik, I., et al., *Neuraminidase inhibition contributes to influenza A virus neutralization by anti-hemagglutinin stem antibodies*. *Journal of Experimental Medicine*, 2019. **216**(2): p. 304-316.
278. Broecker, F., et al., *Immunodominance of antigenic site B in the hemagglutinin of the current H3N2 influenza virus in humans and mice*. *Journal of virology*, 2018. **92**(20).
279. Larkin, M.A., et al., *Clustal W and Clustal X version 2.0*. *bioinformatics*, 2007. **23**(21): p. 2947-2948.
280. Fulton, B.O., et al., *The influenza B virus hemagglutinin head domain is less tolerant to transposon mutagenesis than that of the influenza A virus*. *Journal of virology*, 2018. **92**(16).
281. Krammer, F., et al., *A carboxy-terminal trimerization domain stabilizes conformational epitopes on the stalk domain of soluble recombinant hemagglutinin substrates*. *PloS one*, 2012. **7**(8): p. e43603.
282. Margine, I., et al., *Hemagglutinin stalk-based universal vaccine constructs protect against group 2 influenza A viruses*. *Journal of virology*, 2013. **87**(19): p. 10435-10446.
283. Gao, J., L. Couzens, and M.C. Eichelberger, *Measuring influenza neuraminidase inhibition antibody titers by enzyme-linked lectin assay*. *JoVE (Journal of Visualized Experiments)*, 2016(115): p. e54573.
284. Rajendran, M., et al., *Analysis of anti-influenza virus neuraminidase antibodies in children, adults, and the elderly by ELISA and enzyme inhibition: evidence for original antigenic sin*. *MBio*, 2017. **8**(2).
285. Bailey, M.J., et al., *A method to assess Fc-mediated effector functions induced by influenza hemagglutinin specific antibodies*. *JoVE (Journal of Visualized Experiments)*, 2018(132): p. e56256.
286. Steuler, H., W. Rohde, and C. Scholtissek, *Sequence of the neuraminidase gene of an avian influenza A virus (A/parrot/ulster/73, H7N1)*. *Virology*, 1984. **135**(1): p. 118-124.
287. Durrant, J.D., R.M. Bush, and R.E. Amaro, *Microsecond Molecular Dynamics Simulations of Influenza Neuraminidase Suggest a Mechanism for the Increased*

- Virulence of Stalk-Deletion Mutants*. The Journal of Physical Chemistry B, 2016. **120**(33): p. 8590-8599.
288. Sultana, I., et al., *Stability of neuraminidase in inactivated influenza vaccines*. Vaccine, 2014. **32**(19): p. 2225-2230.
289. DiLillo, D.J., et al., *Broadly neutralizing hemagglutinin stalk-specific antibodies require FcγR interactions for protection against influenza virus in vivo*. Nature medicine, 2014. **20**(2): p. 143-151.
290. Dunand, C.J.H., et al., *Both neutralizing and non-neutralizing human H7N9 influenza vaccine-induced monoclonal antibodies confer protection*. Cell host & microbe, 2016. **19**(6): p. 800-813.
291. Yasuhara, A., et al., *Antigenic drift originating from changes to the lateral surface of the neuraminidase head of influenza A virus*. Nature Microbiology, 2019. **4**(6): p. 1024-1034.





จุฬาลงกรณ์มหาวิทยาลัย
CHULALONGKORN UNIVERSITY

VITA

NAME	Nungruthai Suntronwong
DATE OF BIRTH	12 December 1992
PLACE OF BIRTH	Chonburi
INSTITUTIONS ATTENDED	Faculty of Medicine, Chulalongkorn University
HOME ADDRESS	5 Moo 2, Bua Ngam, Damnoen Saduak District, Ratchaburi.
PUBLICATION	<ol style="list-style-type: none"> 1. Suntronwong N, Vichaiwattana P, Klinfueng S, Korkong S, Thongmee T, Vongpunsawad S, et al. Climate factors influence seasonal influenza activity in Bangkok, Thailand. <i>PLoS one</i>. 2020;15(9):e0239729. 2. Suntronwong N, Thongpan I, Chuchaona W, Budi Lestari F, Vichaiwattana P, Yorsaeng R, et al. Impact of COVID-19 public health interventions on influenza incidence in Thailand. <i>Pathogens and Global Health</i>. 2020:1-3. 3. Suntronwong N, Klinfueng S, Vichaiwattana P, Korkong S, Thongmee T, Vongpunsawad S, et al. Genetic and antigenic divergence in the influenza A (H3N2) virus circulating between 2016 and 2017 in Thailand. <i>PLoS one</i>. 2017;12(12):e0189511. 4. Broecker F, Zheng A, Suntronwong N, Sun W, Bailey MJ, Krammer F, et al. Extending the stalk enhances immunogenicity of the influenza virus neuraminidase. <i>Journal of virology</i>. 2019;93(18):e00840-19. 5. Broecker F, Liu ST, Suntronwong N, Sun W, Bailey MJ, Nachbagauer R, et al. A mosaic hemagglutinin-based influenza virus vaccine candidate protects mice from challenge with divergent H3N2 strains. <i>NPJ vaccines</i>. 2019;4(1):1-9. 6. Thongpan I, Suntronwong N, Vichaiwattana P, Wanlapakorn N, Vongpunsawad S, Poovorawan Y. Respiratory syncytial virus, human metapneumovirus, and influenza virus infection in Bangkok, 2016-2017. <i>PeerJ</i>. 2019;7:e6748. 7. Tewawong N, Vichaiwattana P, Korkong S, Klinfueng S, Suntronwong N, Thongmee T, et al. Evolution of the neuraminidase gene of seasonal influenza A and B viruses in Thailand between 2010 and 2015. <i>PLoS one</i>. 2017;12(4):e0175655. 8. Tewawong N, Suntronwong N, Korkong S, Theamboonlers A, Vongpunsawad S, Poovorawan Y. Evidence for influenza B virus lineage shifts and reassortants circulating in Thailand in 2014-2016. <i>Infection, Genetics and</i>

Evolution. 2017;47:35-40.

9. Tewawong N, Suntronwong N, Vichiwattana P, Vongpunsawad S, Theamboonlers A, Poovorawan Y. Genetic and antigenic characterization of hemagglutinin of influenza A/H3N2 virus from the 2015 season in Thailand. Virus genes. 2016;52(5):711-5.

AWARD RECEIVED

Suntronwong N, et al. "Molecular Evolution of Influenza B Viruses by Time Dependence in Thailand between 2010 and 2015". The 2016 Pediatric Research Day, Chulalongkorn University (1st Place Student Award).

